Development of materials for construction with low environmental Impact made with low content of cement and with natural fibers

Riana Herlina Lumingkewas

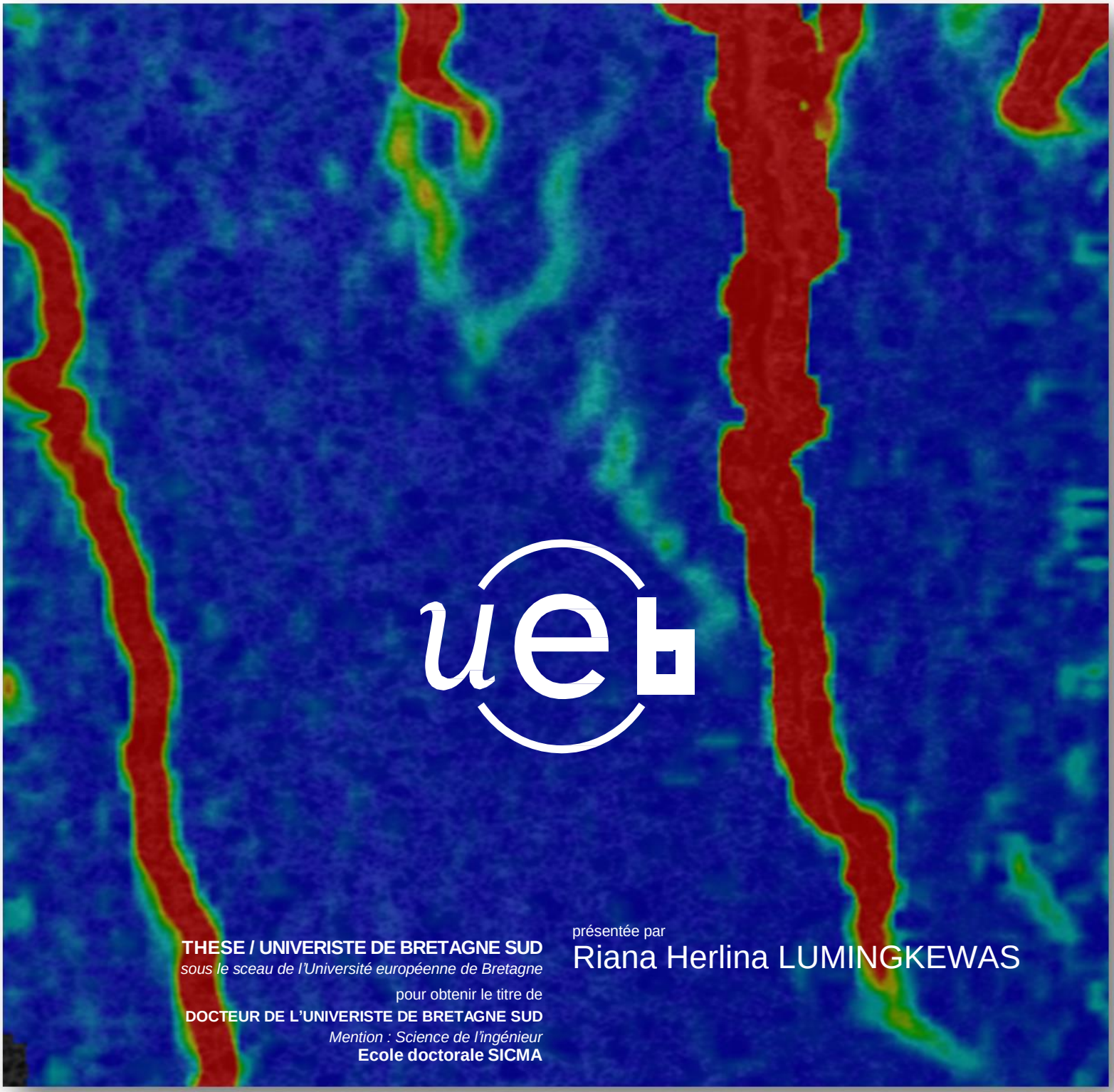

THESE / UNIVERISTE DE BRETAGNE SUD
sous le sceau de l'Université européenne de Bretagne
pour obtenir le titre de
DOCTEUR DE L'UNIVERISTE DE BRETAGNE SUD
Mention : Science de l'ingénieur
Ecole doctorale SICMA

présentée par
Riana Herlina LUMINGKEWAS

Development of Materials for Construction with Low Environmental Impact Made with Low Content of Cement and With Natural Fibers

Thèse soutenue le //2015
devant le jury composé de :

M. Dedi PRIADI
Professeur, Universitas Indonesia / Examinateur
M. Irwan KATILI
Professeur, Universitas Indonesia ./ Directrice de thèse
M. Heru PURNOMO
Maître de conférences HDR, Universitas Indonesia / Co-directrice de thèse
M. Yannick MELINGE
Professeur, Université de Cergy- Pontoise / Examinateur
M. TAVIO
Professeur, Institut Teknologi Surabaya / Examinateur
M. Gilles AUSIAS
Maître de conférences HDR, Université de Bretagne Sud / Directrice de thèse
M. Thibaut LECOMPTE
Maître de conférences HDR, Université de Bretagne Sud / Co-directrice de thèse
M. Arnaud PERROT
Maître de conférences HDR, Université de Bretagne Sud / Co-directrice de thèse

ACKNOWLEDGEMENTS

The research reported in this dissertation was a part of cooperation between Université de Bretagne Sud, UBS France and Universitas Indonesia, UI Indonesia.

I would like to express my sincere gratitude to my supervisors **Assoc. Prof. Gilles AUSIAS** and **Prof. Irwan KATILI**, who gave me the chance to work with this collaboration on this interesting project. I would also like to thank my co-supervisors **Assoc. Prof**. **Thibaut LECOMPTE**, **Assoc. Prof**. **Arnaud PERROT** and **Assoc. Prof. Heru PURNOMO**, who provided me an excellent source of help and support for the present work in France and Indonesia. Without their invaluable guidance and support, this dissertation work would have never been accomplished. They have not only been advisors, but also mentors and friends to me. Their mentorship was and will be paramount in providing a well-rounded experience for both the academic part of my career and another aspect of my life.

I would like to thanks, **Prof. Yannick Melinge**, **Prof. Tavio**, and **Prof. Dedi Priadi** for giving me the honor to accept being part of my thesis jury. Their careful reading of my dissertation report and their comments were relevant and contributed to improving the dissertation report.

I would like to thanks and appreciate for the scholarship provided by **Indonesian Government (DIKTI)** during my study. As well as **France Government (BGF)** for the scholarship during my study in France, that made my Ph.D. work possible. I am very grateful to **Université de Bretagne Sud (UBS)**, **Universitas Indonesia(UI),** and **Institut Teknologi Indonesia (ITI)** for their continuous support my study.

I would like to thanks particularly: **Prof. Sébastien LEFEVRE** Directeur-Adjoint de l'école doctorale ED SICMA UBS. **Prof. Pierre-Yves MANACH** Directeur Laboratories d'Ingenierie des Matériaux de Bretagne (LIMATB), Université de Bretagne Sud (UBS) and **Prof. Sandrine THUILLIER** for their participation in the realization of this dissertation.

I offer my sincere regards to those friends and colleagues in Laboratories d'Ingenierie des Matériaux de Bretagne (LIMATB), Université de Bretagne Sud (UBS), Université de Bretagne Européenne (EA 4250). **Hervé Bellegou, Francoise Peresse, Séverine Georgin, Jean Costa, Anthony Magueresse, Anthony Jegat, Pierre Tronet, Khelifi Hamid, Thanh Hung Pham, Alice Youssef, Anaële**, they help my life to be easier in France. Moreover, also my colleagues in Universitas Indonesia, my very heartfelt thanks go to my friends who shared much laughter, debates, ideas, but which, above all, proved their support and understanding.

My deepest gratitude to **My Parents** in heaven, for their endless love and unending encouragement and prayers to me. Last, but not least, the high words. I would like to dedicate this dissertation to my dear husband, **Prof. Sigit P Hadiwardoyo,** and my lovely children, **Rietsi Arvitricia Hadiwardoyo, SE, MM; Seilendria Ardityarama Hadiwardoyo, ST, MSc; Finno Ariandiyudha Hadiwardoyo; Graidy Arianugraha Hadiwardoyo** for their love, understanding, and support in every aspect.

(Riana Herlina Lumingkewas-Hadiwardoyo)

CONTENTS

LIST OF FIGURES

Page

LIST OF TABLES

Page

CHAPTER.1.
GENERAL INTRODUCTION

1.1. Research background

Recently, researchers are extremely focused toward the global warming. Environmental damage currently is a major concern for people. The study and design of materials now are more geared toward preventing environmental damage. According to CDIAC, the global production of cement contributed about 3.4% of the total carbon dioxide (CO2) into the earth's atmosphere in 2003 [1]. Now represent 4.9% of total CO2 [2]. Furthermore, the global emissions of CO2, the main cause of global warming increased by 3% in 2011.[3]. In total, cement production accounts for roughly 9.5% of global CO2 emissions in 2013. According to estimates by USGS (2014), cement production increased in 2013 in most countries among which Indonesia, Iran, the Russian Federation, Turkey and Vietnam by 5% to 10%[Olivier et al, 2014].
In the construction industry, a major component of the common materials such as steel or cement comes from natural resources and requires much energy. Cement production continues increased along with the increasing demand for the construction sector. Therefore, the construction industry handles the depletion of a large number of resources that are not renewable. This activity generates millions of tons of mineral waste and millions of tons of carbon dioxide emissions. From the total greenhouse gasses emitted by this sector, half is directly generated from the transportation, manufacturing and use of materials in the construction phase [4].
The motivates researchers to develop alternative materials to reduce the amount of CO2 emissions and other toxic gasses that released into the environment. Use of supplementary cementitious materials or valorization of local raw materials such as soils is common options to limit environmental impacts of building materials. It is also interesting to limit the steel reinforcement in concrete by adding bio-based fibers that are locally available.

Use of natural fibers in cementitious composites is an alternative in construction materials that can reduce the price, energy cost, and environmental impact. Natural fibers are renewable and sustainable resources. It can found in a large amount worldwide including in Indonesia. For example, the fiber of the coconut husk is now wasted and has not been widely used as composite materials in civil engineering. Coconut husk constituted of 30 wt. % coir fiber and of 70 wt. % pith [Jan et al., 2004] [5], [Rodrígueza et al., 2011]. Also, coconut husk is another significant source of cellulose. Cellulose is a classic example where the reinforcing elements and deposited in a continuous manner. The coir fiber is natural fiber extracted from coconut husk.

Currently in Indonesia use coir fiber limited to the results of the housing industry that produces equipment household appliances such as doormats, brushes, vases of plants, ropes, and textiles. There is still much waste from coconut copra industry as raw material that mostly exported and not used optimally. Indonesia is one of the countries with the largest potential of coconut natural resources in the world. About 87% of coconuts lands located in the countries member of the Asian and Pacific Coconut Community (APCC). The coconut acreage is Indonesia 32.4% and the Philippines 27.5% in the world [CAPPI, 2008].

It is worth to note that coir fiber presents ductile properties [Munawar SS et al., 2007]. Utilization of coir fiber into cementitious matrices is very suitable for earthquake-resistant construction materials. Therefore, fiber reinforced cementitious composites are fascinating for Indonesia, which located in an area with risk of intense earthquakes. That surrounded by the three Indo - Australian, Eurasian and Pacific tectonic plates where colliding can produce heaps of energy).

A study of the properties of coir fiber still limited to the countries of India, Brazil, Malaysia, and Vietnam. [Kulkarni et al. 1981], [Satyanarayana. KG et al. 1982], [Noguera P et al. 2003], [Munawar SS et al, 2007], [MM Rahman and MA Khan, 2007], [Jústiz-Smith CA et al, 2008], [Defoirdt N et al, 2010], [Muensri P et al, 2011], [Ezekiela N et al, 2011], [Saw SK et al, 2011].

The material ingredients of the cementitious composite are similar to that of fiber reinforced concrete, including cement, sand, water, fiber, and a few chemical additives. The mixing procedure of cementitious composites is similar to that employed for the normal concrete.

Making cementitious composites reinforced with natural fibers represent one way of recycling waste that is of economic interest for developing countries. The cementitious composite is a material with exciting potential. The price of the material could be 30% cheaper than standard construction materials, and the mechanical properties of cementitious reinforced composites can equal conventional building materials.

Moreover, conventional cement products are characterized by a brittle behavior, with low tensile strength [Balaguru & Shah, 1992], [Kuder & Shah, 2010]. Hence, fibers incorporated into cement matrix is likely to overcome this weakness, producing materials with increased tensile strength, ductility, therefore, improved durability (cracks limitation). Natural fiber reinforcement has good effects on fracture toughness behavior, durability, environmental-induced damage and aging [Savastano Jr. et al., 2003], [Tolêdo Filho et al., 2003].

The incorporation of such natural fibers as cement and/or earth-based materials offers significant potential for the development of low-cost and local construction materials for affordable housing. However, there are significant challenges that must overcome before natural fibers can optimally incorporated into building materials. In the field of construction materials, the industry can take part in creating and

manufacturing environmentally in a friendly building materials made from local environmental waste and natural raw materials. It can lead to useful material for developing countries. Therefore, to build with local materials reinforced with natural fibers is one way to achieve sustainable development. Hence, the need for sustainable, energy efficient construction materials has oriented extensive research on alternative materials that can reduce the cost and environmental impact of building processes. In either case, it reduces CO2 emissions by a lower cement proportion in concrete mixes.
In this work, studied coir fiber reinforced mixes of sand, clay, and cement are considered cement stabilized soil to design extruded. It has been shown, that for mixes containing more clay than cement, mechanical strength can be close to common concrete blocks for housing [Khelifi et al. 2012].

Processing can substantially influence fiber dispersion and orientation, material compactness, quality of the composite performance and cost of production. The relationship between processing and composite performance is of great importance and relatively little studied. Extrusion usually used for the forming process of food, fertilizers, pharmaceuticals, clay, polymers, and metal can also use in cement materials processing. It is an efficient forming process that induces high productivity and reduced void content. Extrusion should be a valuable method to decrease the porosity and improve mechanical strength; these are being principal characteristics of building materials [Qian et al. 2003], [Perrot et al. 2009a].
However, use of extrusion of cement-based construction materials is still very limited. Precast industries are interested in extrusion. Because it is a continuous process that allows for the production of high-resistance engineered cementitious composites [Peled & Shah, 2003], [Qian et al. 2003], [Perrot et al. 2009b]. Also, the precast concrete plant is one solution to reducing air content by compacting concrete mixes by pressure and vibration. It is crucial because it well known that the concrete resistance directly linked to porosity [De Larrard & Sedran, 2002].
The cost of extruded fiber reinforced cementitious composites were significantly reduced using alternate clay binders [Kuder & Shah, 2010]. Availability of new building materials ready to use is still extremely limited. Extrusion use for the production of construction materials in civil engineering is limited. On the other hand, these tools can accelerate the productivity of the forming process. There are still obstacles to density, mechanical strength performance, fiber-matrix adhesion and surface appearance. However, the extrusion of cement based materials seems to be very promising in the scope of high the mechanical performance precast concrete.

Overview of the state of the art in natural fiber cement-based composites research highlights the need to develop alternative and sustainable new materials, using local, energy-efficient, low-cost materials with low environmental impact. Many attempts to develop locally optimized materials presented in the literature. However, very limited data on the rheology, the mechanical and micromechanical properties of coir fiber

reinforced cementitious composites shown. The research approach has been carried out, on low cement content stabilized soils (reducing emissions associated with cement production and material transportation) and reinforced with coir fiber. Furthermore, the coir fiber cementitious composites are processed using extrusion to limit the material porosity. This research starts with the preparation and the performances of the coir fiber. Then the design, processing, the performances and microstructural analysis of the composites are presented. The physical structures, mechanical, thermal and morphological characteristics of coir fibers studied. Mix design, rheological behavior, extrusion, and mechanical characteristics of the coir fiber reinforced cementitious composites are studied and propose rheology and micromechanical model.

1.2. Research Question

Currently, developments of new building material products focused on environmental issues. How to develop new materials for industry construction with the low environmental impact made with a low content of cement, and coir fibers using extrusion?

This study will answer some of the new challenges and find solutions for the following response:

1. How to improve the characteristic of coir fiber to reinforce cement based materials?
2. How to determine formulations of productivity extrudate of coir fiber reinforced cementitious composite?
3. What is the rheology model of the coir fiber reinforced cementitious composite?
4. What is the mechanical model of the coir fiber reinforced cementitious composite of extrusion products?
5. What is the micromechanical model of the coir fiber cementitious composites of extrusion products?

1.3. Objective of research

The goals of this research are to develop new environmentally friendly materials for construction made with local raw and renewable materials such as natural fiber. To be used for industry, these raw materials must be optimized and well characterized. All the components studied must add into the mix at the optimized content.

Screw Extrusion will process materials and samples characterized using Scanning Electronic Microscope (SEM), mechanical test using destructive testing, Mechanical Testing System (MTS) and non-destructive testing Digital Image Correlation (DIC). Coir fiber studied the physical structure, mechanical, and microstructure. Fiber cementitious composite materials studied formulation, rheological

model, fabrication process, mechanical characteristics, microstructure, and micromechanical model.
The outputs are to obtain:

1. The physical, mechanical, microstructure and thermal properties of coconut/coir fiber with and without treatment.
2. The formulation of extrudate coir fibers reinforced cementitious composites.
3. The rheology model of the extrudate coir fiber reinforced cementitious composite.
4. The mechanical behaviour and models of screw extruded of the coir fiber reinforced cementitious composite.
5. The micromechanical model of screw extruded of the coir fiber reinforced cementitious composites.

The long-term goal of this research is to produce new green building materials with low cement content and high amount of local raw materials. Such as clay, sand, and reinforced coir fibers on concrete technology for industry construction.

1.4. Limitation of Research.

Based on the above background, there is an urgency to develop new building materials that are environmentally friendly. The use of local materials and natural materials can replace environmentally harmful materials. New building materials and renewable energy will reduce harmful emissions. The exploitation of the abundant natural resources will drive the growth of the green building materials industry. This work aims to focus on rheology, mechanical and micromechanical of new low cement content materials reinforced with coconut/coir fiber and formed by extrusion.

1.5. Contribution of Research

The aim is to contribute to the field of civil engineering and materials science by developing and creating environmental friendly building materials. The incorporation of natural fibers with cement and basic materials of the Earth offers significant potential for the development of cheap construction materials for affordable housing. Generate new materials that applied to increase the production of readymade materials in the construction industry. Developing local materials and waste natural fiber materials, giving added value to agriculture, accelerating the development of environmentally friendly building materials industry and the promotion of social economy are long-term goals.
Also, based on the results of state of the art, advances these researchers are:

1. The characteristics of the coir fiber.
2. The method of assessing formulation of mix design for extrusion of the fiber cementitious composite materials.
3. The rheology models for prediction yield stress of the fiber reinforced cementitious composite.
4. The macro-mechanical model for prediction tensile strength and compressive strength of extruded of the fiber reinforced cementitious composite.
5. The micromechanical models prediction tensile strength and compressive strength of extruded of the fiber reinforced cementitious composite.

1.6. Overview of Dissertation

This dissertation is divided into eight chapters, as follows:

The first chapter contains an introduction describing the background and presents recent topics and focus natural fiber cementitious composite on the concrete technology of building materials for industry construction. Then the most current issues that need to be solved are listed. Those issues orient our work from start to end.

The second chapter consists of a literature review, including the state of the art of current research on the performance of fiber-reinforced cement-stabilized soils. Use of natural fibers of coconut on building materials also investigated. Then, the review on the extrusion of cement-based materials is done. To conclude, this chapter reviews the issue of environmental impacts of building materials.

In the third chapter, the research methodology to achieve the research objectives is presented. It contains a flow chart of research and implementation of experiments on coir fibers, and coir fiber reinforced cementitious composites. Studied materials are listed. Then, the experimental devices and protocols used to obtain the physical, mechanical, thermal and microstructural properties are presented.

In the fourth chapter, an analysis of the performance of natural fibers from coconut husks is performed from experimental observations and measurements. A review conducted on the physical, mechanical, thermal, and microstructure properties of coir fibers. Deeper observations are carried out by the influence of fiber length and diameter of the fibers in its use as reinforced concrete.

The fifth chapter presents the composition and formulation of coir fiber reinforced cement stabilized soil composites designed for extrusion. The influence of the fiber content and aspect ratio on the fiber composites rheological properties and rheology model were assessed to keep an extrudate material.

The sixth chapter presents the analysis of the experimental results of mechanical tests performed on fiber reinforced cementitious composite materials processed by screw extrusion. The effect of fiber length and fiber content on the material properties is a highlight. Similarly, the processing (extrusion and molding) influence on the material mechanical and physical properties are also studied.

The seventh chapter consists in the development of a micromechanical model that describes the fiber-reinforced ductile cementitious composite behavior. Then, the evolution of damage is observation. The modeling used to predict the evolution of micromechanical is compare to experimental data provided using destructive method by mechanical testing system and non-destructive method by digital image correlation

Finally, in the eighth chapter, the conclusions of the research and the future work that needs are presented.

CHAPTER.2.
LITERATURE REVIEW

2.1. Introduction

The literature review and state of the art in this chapter aim to provide a comprehensive and detailed overview of the results of recent research conducted on environmentally friendly building materials.

This state of the art on construction materials focused on the properties and performance characteristics of natural fibers cement, clay and fiber cementitious composite materials. Also mix design and method of extrusion processes for fiber reinforced cement-based composites is studied.

The mechanical performances of such composites studied at micro and macro scales. Finally, the environmental impacts of the cement-based fiber reinforced composites investigated, and the life cycle analysis method presented.

2.2. Natural Fiber

Natural fibers can obtain from natural resources such as plants (vegetable, leaves and wood), animals, and geological processes. There are six basic types of natural plant fibers. They classified as follows: 1. bast fibers (jute, flax, hemp, ramie and kenaf), 2. leaf fibers (abaca, sisal and pineapple), 3. seed fibers (coir and cotton), 4. core fibers (kenaf, and jute, reed fibers (wheat, corn and rice), and all other types (wood and roots) [Faruk 2012].

Natural fibers represent a renewable resource that is available almost all over the world [Brandt 2008]. Some of the most popular natural fiber that often used are flax, hemp, jute, sisal, hemp, and kenaf fibers. They have been extensively studied and used in different applications. Nowadays, abaca, pineapple leaf, coir, oil palm, bagasse, and rice husk fibers are gaining interest and importance to both researchers and industrial applications.

This focus is due to their properties and availability. It should mention that there are also shortcomings: lack of consistency of fiber qualities, and conditions of the processing; high levels of variability in fiber properties related to the location and time of harvest; sensitivity to moisture, and UV radiation. A multi-

step manufacturing process is required to produce high-quality natural fibers, which contributes to the cost of high-performance natural fibers as well as, the improved mechanical properties of the composites.

Furthermore, due to cancer health risks [Azuma 2009], it is now forbidden to cementitious product products containing silicates fiber (asbestos). Researchers used natural fibers as an alternative source of steel and/or artificial fibers to used in cement- based composites (cement paste, mortar, and concrete) to improve the mechanical behavior. Among some emerging natural fibers: coir, sisal, jute, ramie bast, pineapple leaf, bamboo, palm, banana, hemp, flax, cotton, and sugarcane are targeted to used as reinforcement in engineered cementitious composites. [Ramakrishna 2005; Li et al., 2007; Asasutjarita 2007; Toledo Filho 2005; Munawar 2007; Rao 2007; Li 2006; Fernandez 2002; Reis 2006; Corradini 2006].

Natural fiber reinforced cementitious composites can use for many civil engineering applications. Examples including roofing tiles [Agopyan 2005], corrugated slabs [Paramasivam 1984], simple slab panels [Ramakrishna, 2005], boards [Li 2007]; [Asasutjarita 2007]; and mortar [Toledo Filho 2005] are reported in the literature.

2.2.1. Structure and chemical composition.

The principal components of the fiber cell walls are cellulose, hemicellulose and lignin with pectin typically considered being the primary binder. Cellulose is a polymer containing glucose units. It is a strong, linear (crystalline) molecule with no branching. Cellulose has good resistance to hydrolysis although chemical and solution treatments will degrade it to some extent. [Heinze, 2005]. Hemicellulose is a polysaccharide polymer that consists of low molecular weight, copolymer glucose, mannose, glucuronic acid, arabinose, and xylose. Besides, it presents in the form of random, amorphous structure with a small force branching. Dilute acid or base hydrolyzes the hemicellulose. This enzyme is commercially important because they open the bound structure of cellulosic materials [Summerscales 2010].

Lignin is an amorphous and heterogeneous mixture of polymer and monomer aromatic phenyl-propane [John 2005] [Mohanty 2000]. The lignin is formed by removing water from the sugar (mainly xylose) to create aromatic structures. Lignifications occur in the mature plant. Lignin becomes more rigid, far from the surface of the lumen, and creates a porous area that maintains the strength of the walls and helps to transport water. Lignin is not sensitive to microorganisms as their aromatic rings are resistant to anaerobic processes while the aerobic breakdown of lignin is very slow. [Summerscales 2010].

Table 2.1 shows the average amount of chemical constituents for a broad range of fiber types. The important structural component of nearly all green plant cell walls is cellulose, especially on many natural fibers.

Climatic conditions, age and degradation process influence not only the structure of fibers but also the chemical composition. Water is an important chemical component of a living tree. However, on a dry basis, all plant cell walls consist mainly of sugar-based polymers (cellulose, hemicellulose) that combined with lignin with a lesser amount of extractives, protein, starch and inorganics. The chemical components distributed throughout the cell wall, which are composed of primary and secondary wall layers.

Table 2.1 **Chemical composition of some natural fibers**

Fiber	Cellulose (wt. %)	Hemicellulose (wt. %)	Lignin (wt. %)	Waxes (wt. %)
Bagasse	55.2	16.8	25.3	–
Bamboo	26–43	30	21–31	–
Flax	71	18.6–20.6	2.2	1.5
Kenaf	72	20.3	9	–
Jute	61–71	14–20	12–13	0.5
Hemp	68	15	10	0.8
Ramie	68.6–76.2	13–16	0.6–0.7	0.3
Abaca	56–63	20–25	7–9	3
Sisal	65	12	9.9	2
Coir	32–43	0.15–0.25	40–45	–
Oil palm	65	–	29	–
Pineapple	81	–	12.7	–
Curaua	73.6	9.9	7.5	–
Wheat straw	38–45	15–31	12–20	–
Rice husk	35–45	19–25	20	14–17
Rice straw	41–57	33	8–19	8–38

Source: [Faruk 2012]. It has been reprocessed.

The chemical composition varies from one fiber type to another, and within different parts of the same plant. It also varies in plants from various geographical regions, ages, and climate and soil conditions. The chemical properties are influenced by the fiber growth time (days after planting), the botanical classification of fiber and the stalk height. The chemical composition

can also vary within the same part of a plant. Both the root and stalk core have a higher lignin content than that of the fibers.

2.2.2. Physical and mechanical properties

The natural fibers properties differ in all cited works because of the differences in the fiber structure due to the overall environment conditions during growth and stock but also due to different testing methods. However, to expand the use of natural fibers in composites and improved their performance, it is essential to know fiber characteristics.

Many factors can influence mechanical properties of natural fibers. First, it is required to know if the sample consists of fiber bundles or ultimate fiber tested. Table.2.2 presents the important physical-mechanical properties of commonly used natural fibers collected by different authors [Faruk 2012], [Hattallia 2002], [Hoareau 2004].

Table 2.2 **Physical-mechanical properties of natural fiber**

Fiber	Tensile strength (MPa)	Young's modulus (GPa)	Elongation at break (%)	Density (g/cm^3)
Abaca	400	12	3–10	1.5
Bagasse	290	17	–	1.25
Bamboo	140–230	11–17	–	0.6–1.1
Flax	345–1035	27.6	2.7–3.2	1.5
Hemp	690	70	1.6	1.48
Jute	393–773	26.5	1.5–1.8	1.3
Kenaf	930	53	1.6	–
Sisal	511–635	9.4–22	2.0–2.5	1.5
Ramie	560	24.5	2.5	1.5
Oil palm	248	3.2	25	0.7–1.55
Pineapple	400–627	1.44	14.5	0.8–1.6
Coir	175	4–6	30	1.2
Curaua	500–1150	11.8	3.7–4.3	1.4

Source: [Faruk 2012]. Has been reprocessed

The physical properties of each natural fiber are critical and include the fiber dimensions, defects, strengths, and structure. It is crucial to estimate physical properties of each natural fiber to optimize its efficiency in a given composite. Fiber dimensions, defects, strength, variability, crystallinity, and structure must be taken into consideration. Moreover, the hydrophilic nature of natural fibers influences the mechanical properties. The moisture content at a given relative humidity has a high effect on the performance of a composite made of natural fibers. The equilibrium moisture content of different natural fibers at 65% relative humidity and 21^{o}C [Rowell, 2008] given in Table 2.3.

Natural fibers have high tensile strength, comparing to they are the relatively low modulus of elasticity (Table 2.4). Even though, their tensile performance can stand in a favorable manner with synthetic ones. The disadvantages of using natural fibers are that they have a high variation in their properties that could lead to unpredictable concrete properties [Li 2006], [Pacheco, 2011].

Table 2.3 **The equilibrium moisture content of natural fiber.**

Fiber	Moisture Content (%)
Sisal	11
Hemp	9
Jute	12
Flax	7
Abaca	15
Ramie	9
Pineapple	13
Coir	10
Bagasse	8.8
Bamboo	8.9

Source: [Rowell 2008]. Has been reprocessed

To improve the performance of fiber reinforced cementitious composite, it is possible to treat the fibers industrially before their incorporation into the matrix. For example to the treatment fiber that improves the adhesion of fiber cement matrix and also resistance to alkali attack is pulping [Savastano, 2003b]. The latest research results provide results that fibers treatment show an improvement in the properties of the fibers, the better rheological behavior of the cement

mixtures, and an increase of the mechanical strength of the composites, [Sawsen et al., 2015]. It is also important to consider the effect of treatment on the fracture toughness, durability, environmental-induced damage and aging of both the fiber and the composite [Savastano, 2003a; Tolêdo Filho, 2003].

The correlation between some mechanical properties of natural fibers is shown in Figure 2.1[Rao 2007] and Figure 2.2. [Munawar 2007]. These figures show the stress-strain relationship for different fibers. It appears that the coir fiber behavior is very different in both cases. It highlights the dispersion of such natural fibers properties. Emphasis should be made to develop typical curves, not only for a stress-strain relationship but also for other relationships. The variation of tensile strength and Young's modulus with fiber diameter is shown in Figure 2.3 and Figure 2.4, respectively. It can be observed that both decreases when the fiber diameter increase.

Table 2.4 **Properties of natural and synthetic fibers**

Properties	**Specific gravity (kg/m^3)**	**Water absorption (%)**	**Tensile strength (MPa)**	**Modulus of elasticity (GPa)**
Sisal	1370	110	347–378	15.2
Coconut	1177	93.8	95–118	2.8
Bamboo	1158	145	73–505	10–40
Hemp	1500	85–105	900	34
Caesar weed	1409	182	300–500	10–40
Banana	1031	407	384	20–51
Piassava palm	1054	34–108	143	5.6
Date palm	1300–1450	60–84	70–170	2.5–4
Polypropylene	913	–	250	2.0
PVA F45	1300	–	900	23

Source: [Pacheco 2011]. Has been reprocessed

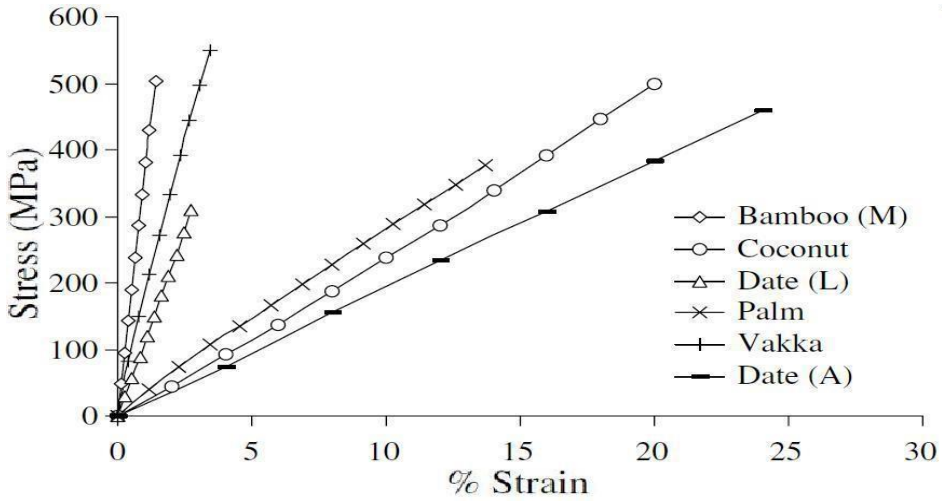

Figure 2.1. Stress versus percentage strains of various fibers [Rao 2007]

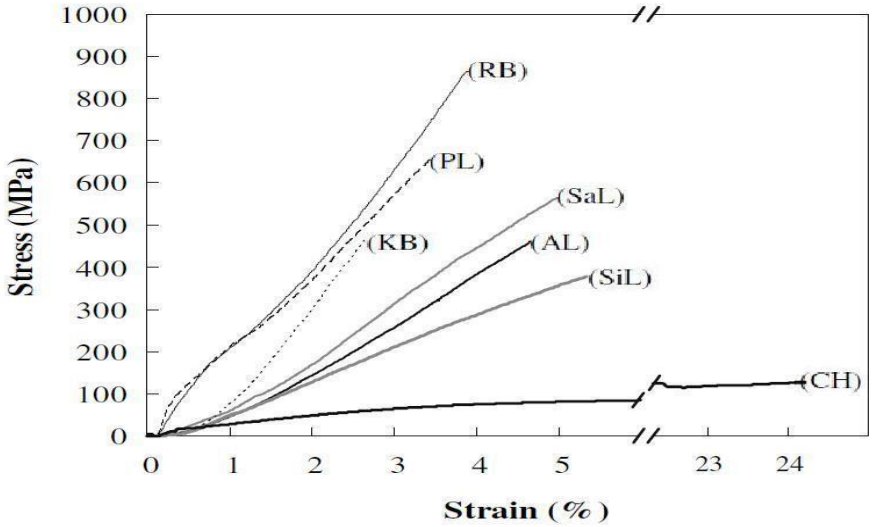

Figure 2.2. Typical stress-strain curves for the non-wood plant fiber bundles [Munawar 2007]. (Note: RB, Ramie bast fiber; PL, pineapple leaf fiber; KB, kenaf bast fiber; SaL, Sansevieria leaf fiber; CH, coconut husk fiber; AL, abaca leaf fiber; SiL, sisal leaf fiber).

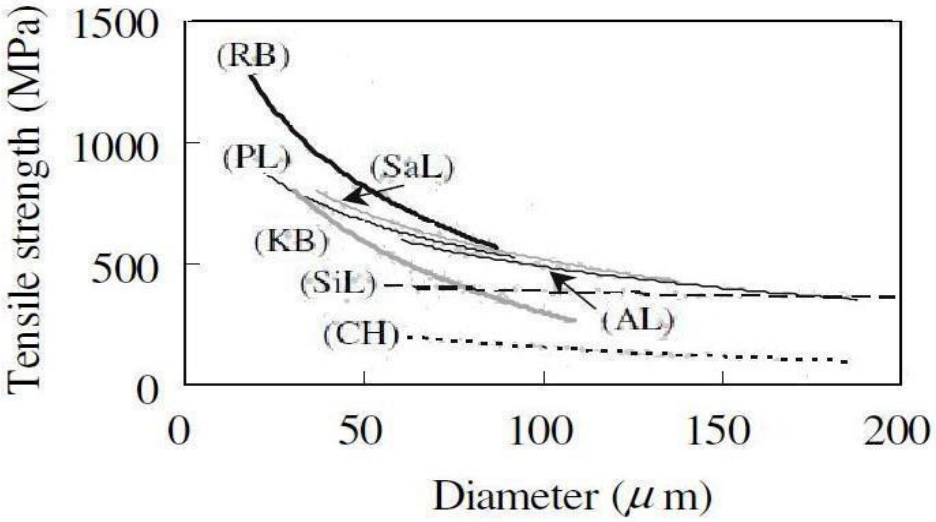

Figure.2.3. **Relationship between diameter and tensile strength of non-wood plant fiber bundles**

Source: [Munawar 2007]

(Note: RB, Ramie bast fiber; PL, pineapple leaf fiber; KB, kenaf bast fiber; SaL, Sansevieria leaf fiber; CH, coconut husk fiber; AL, abaca leaf fiber; SiL, sisal leaf fiber),

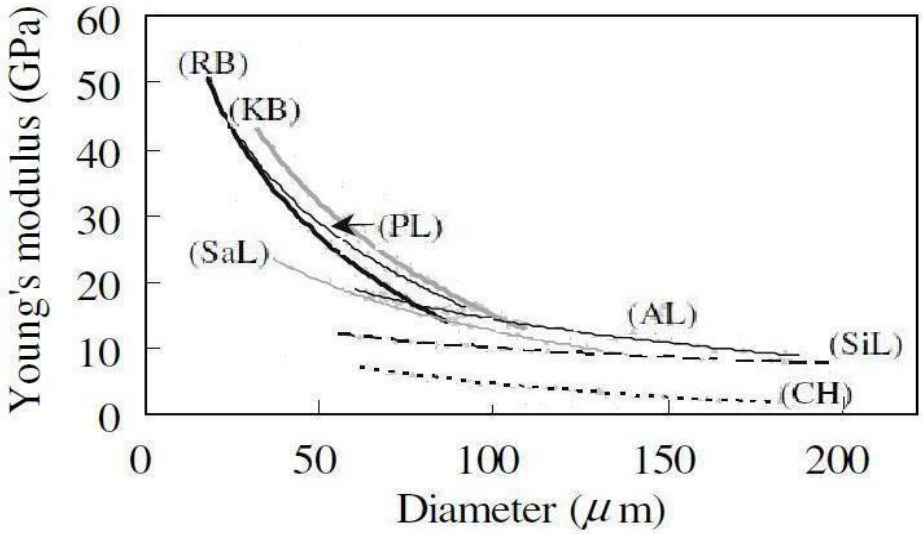

Figure.2.4. **Relationship between diameter and Young's modulus of non-wood plant fiber bundles**

Source: [Munawar 2007]

(Note: RB, Ramie bast fiber; PL, pineapple leaf fiber; KB, kenaf bast fiber; SaL, Sansevieria leaf fiber; CH, coconut husk fiber; AL, abaca leaf fiber; SiL, sisal leaf fiber)

Munawar et al. characterized the morphological, physical and mechanical properties of the non-wood plant fiber bundles (ramie, pineapple, kenaf, abaca, sisal and coconut fiber) [Munawar 2007]. The larger the diameter of the fiber bundles is the lesser will be the density, tensile strength, and the Young's modulus.

2.2.3. Microstructure

Micrographs of fibers along the longitudinal axis showed residue on the surfaces of the fibers [Justiz-Smith 2008]. In the case of bagasse, the residue was mostly pith. From the microstructure of the vertical cross-sectional area (Figure.2.5), it is observed that the single strand of the coconut fiber had a hollow section. It suggests that the 'single' strand is a series of microfibers, called a fiber bundle.

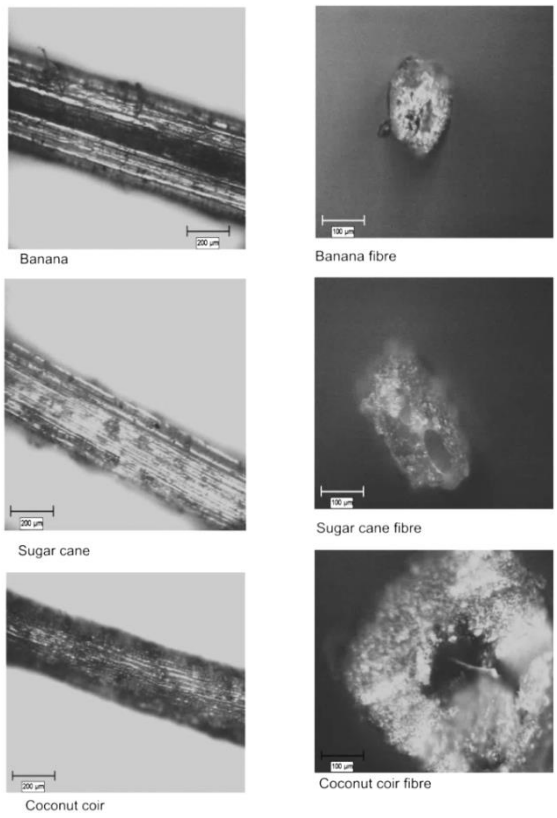

Figure.2.5. **The SEM micrographs of the longitudinal section and cross-sectional area of fiber strands.**
Source: [Jústiz-Smith 2008]

2.3. Coir fibers

In the recent past, coir was considered as a low-quality, low-value natural fiber that can be used for spinning of yarn, cordage, door mats, matting, carpets, rugs, brushes, and brooms. Even though, man-made synthetic fibers have taken over the market for natural fibers. Natural fibers have some advantages over synthetics fibers as they possess properties that cannot be a match or copied easily. The current trends in enhanced utilization of ecologically friendly bio-products have paved the way for more diversified applications for coir and value-added products, providing greater potential for improving the rural economy in major coir producing countries. Coir is an eco-friendly, natural, biodegradable, durable, renewable, low-cost and sustainable product.

Coir is a versatile, non-abrasive, porous, hygroscopic, viscoelastic, biodegradable, combustible and compostable natural product. Compared with other natural fibers, coir fiber bundles have medium strength but interesting elongation properties, which makes them attractive for certain technical applications.

Coir husk fibers are located between the husk and the outer shell of the coconut. The coconut demand mainly determined coir production. The coconut husks are available in abundant quantities. It implies that coir producers can adjust relatively rapidly to market conditions. It can be noted that the coir fibers are also commercially available at relatively high cost when prepared for special purposes like brushes, mats, and pedestal seats. This cost can be reduced if fibers are mechanically processed at large scales. Until now there has been no commercial product that provides fiber-based uniform size and fiber size below 100 mm. The numbers of coconuts harvested annually in the world are about 55 billion, but only 15% of the husk fibers are recovered for use [Wang 2009]. Most husks are abandoned in nature, constituting a waste of natural resources and causing environmental pollution.

2.3.1. Production coir fibers

Coir fibers are extracted from the outer shell of a coconut. There are two types of coir fibers, brown type fibers that are extracted from matured coconuts and white type fibers that are extracted from immature coconuts. Brown fibers are thick, strong and have high abrasion resistance. White fibers are smoother and finer but also weaker.

The total exported amounts of unfinished coir and coir products from producing countries in 2003 and 2004 were 172,928 million ton and 194,926 million ton respectively [APCC 2006]. The Philippines are the principal coconut producer in the world. Indonesia, India, and Sri Lanka are the followers. India is the major coir producer in the world while Sri Lanka and Thailand maintain second and third positions respectively. In 2007, 90% of the production came from the Asia and Pacific region [APCC 2007]. Philippines, Indonesia, China, Vietnam, Mexico, Venezuela, and Tanzania are the other coir-producing countries in the world. The major importing countries of coir and coir products are United States, European Union, Canada, Australia, Japan, the Middle East and Korea.

Nevertheless, the use of coconut husk for coir extraction is still limited to a few developing countries while the others use coconut mainly for its kernel products, such as copra, oil or desiccated coconut. Major coconut producing countries like the Philippines, Indonesia or Pacific countries like Papua New Guinea and Fiji use coconut husks and shells as an energy source for the manufacture of copra. Because of it is the importance economic versatility (i.e. coconut can produce food, oil, fiber and timber crop) and moreover for its, aesthetic value. The coconut tree is popularly known as the tree of life or tree of heaven.

Traditionally, coconut coir fiber is processed into various products such as carpets, mats, ropes, nets, bristles, brooms, brushes, and for domestic uses with a mattress and as coatings industry. However, only a fraction of available coir fibers is currently used for construction materials. In recent years, the use of natural fibers decreases due to intense competition from synthetic products. However, there is a tendency of companies in industrialized countries to use more environmentally friendly products and systems. This trend can help to reduce the ecological impacts of current production methods. The effects of the chemical industry on atmospheric degradation, global warming, declining of natural resources, deforestation, waste production, pollution and global issues have increased demand for environmentally friendly products.

In most areas, coir is considered as a byproduct of the production of copra and the remaining husk at best used as fertilizer. Husk is composed of pith for 70 percent and fiber for 30 percent on a dry weight ratio [Jorg Mussig 2005]. The ratio of long, medium and short fibers stands for the average weight ratio of respectively 60%, 30%, and 10%. Major production areas of palm trees are found along the coastal regions in the wet tropics of Asia in India, Sri Lanka, Indonesia, Philippines, and Malaysia.

Productivity is defined as of coconut lands in the world of Nuts/ha [APCC 2008]. It appears that Brazil presents the best coconut land productivity followed by Mexico. Indonesia has amounted to 4273 nuts/ha as shown in Figure.2.6. The maximum total world production of coir fiber including short fiber can estimate at 5-6 million tons per year and less than 10 percent of this potential into the commercial trade [Dam 2002].

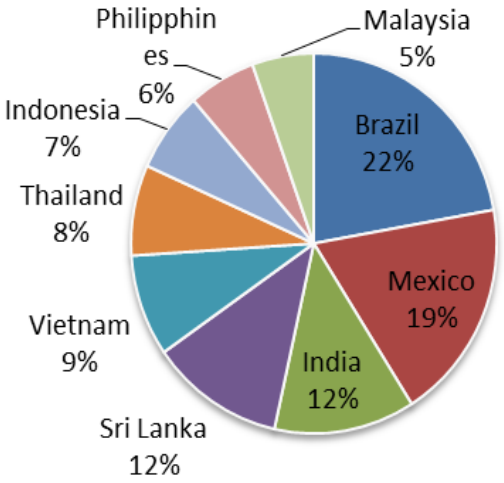

Mexico	11,725
India	7,748
Sri Lanka	7,365
Vietnam	5,390
Thailand	4,802
Indonesia	4,273
Philippines	3,720
Malaysia	3,391

Figure.2.6. **Productivity of coconut lands in the world in Nuts/ha**
Source: Coconut Statistical Year Book, APCC, 2008.
It has reprocessed.

2.3.2. Extraction of coir fibers

The coconut fibers are taken from a mature coconut that is covered by fibrous material. This part of the coconut fruit called the coconut husk, consists of hard skin and a large number of fibers embedded in a soft material. The fibers can be extracted only by soaking the husk in water to decompose the soft material surrounding the fibers. This process, called retting, is widely used in developing countries. Alternately, a mechanical process can be used to separate the fibers.

The best-quality of coir fiber is extracted from the husk of ripe-harvested before the husk has completely dried. In general, extra carried in bulk and commercial is as follows:

1. The extraction of coir involves the breakdown and the separation of the coir fiber bundles from the connecting tissues or pith in between the fiber bundles. The extraction of coir fiber is done manually by beating the retted husks. The bristle coir or long fiber bundles have a smaller amount of

residual pith. Therefore, bristled fiber bundles are cleaned by combing through a set of steel spikes. The coir fibers are sometimes, but not always, washed with clean water and dried to give a better appearance.

2. Another way to extract fiber bundles from the machine and mattress coir (medium and short fiber bundles) is to use the traditional drum pairs consisting of a cone-shaped revolving screen sifter. By gravitational action, fiber bundles are separated from the pith tissues. The coir is then fed into a turbo cleaner, which consists of radially fixed iron rods rotating at high speed, for further cleaning. By centrifugal action, remaining pith tissues and other debris attached to the fiber bundles are removed by this mechanical process. Moreover, better quality of coir is obtained.

There are four different types of coir fiber, which are produced commercially as well as bristle fiber bundles, omat fiber bundles, mattress fiber bundles and mixed fiber bundles. [Jorg Mussig 2010]

1. Bristle Coir: long, parallel, clean fiber bundles produced from retted coir husks on the traditional needle drum or the deferring machine. Bristle coir has unique features and is still competitive with other coir fiber types produced in other countries. They are mostly used in the manufacture of brushes, rubberized coir fibers, nettings, and high-strength twine.
2. Omat Coir: medium-length fiber bundles produced on the traditional needle drum and the deferring machine with length ranging between 70 and 135 mm.
3. Mattress Coir: short fiber bundle fraction collected on the traditional needle drum or the deferring machine and give length ranging between 30 and 69 mm. Those small fibers are considered as waste and are just valorized as a plant fertilizer.
4. Mixed Coir: fiber bundles extracted from matured green husk or brown husks, with lengths ranging between 36 and 119 mm.

Asasutjarita et al. have already studied pretreatments of coir fiber by washing and boiling them to remove the impurities on the coir surface. [Asasutjarita, 2009]**.** Regarding surface topology, pretreatments can create voids and produce fiber fibrillation, leading to a better fiber/matrix adhesion, and, therefore, better mechanical properties of coir fiber reinforced cement composite.

2.3.3. Physical and chemical properties

Coir fiber obtained from coconut husk is a mostly under vaporized raw materials. It is composed of cellulose nanofiber that constitutes 32–43% of its dry

weight [Ayrilmis, 2011]. The coir husk is another significant source of cellulose. The coir fiber comprises mainly of cellulose, lignin, and hemicellulose.

The color of coir fibers varies from pale yellow to dark brown. It mainly depends on the coconut variety, the maturity of the fruit, time lapsing between husking and retting, quality of water used for retting and the duration of retting. Coir fiber is a coarse fiber bundle. In comparison with other natural fibers, they have high lignin content. As consequence, coir fibers are highly resistant to microbial attacks and sea water.

The length of coir fiber bundles varies considerably within a sample. The size of a coconut varies with the coconut variety, with the location in which it grows and also with the environmental conditions. As for all natural fibers, it is statistically more accurate to express the length of coir fiber bundles within a range. There is a significant variation in length distribution with the type of extraction technology used and fiber grade produced. Coir fiber bundles are coarser for a natural fiber, and their diameters vary from 50 to 200 μm [Leson 2002]. Weighted average diameter at the mid-point of a coir fiber strand also varies with coconut type.

The capacity to absorb moisture from the surroundings is a noticeable characteristic of all natural fibers. The absorption of moisture changes the properties of coir such as tensile strength, elastic recovery, electrical resistance, and rigidity. Due to absorption of water, the fibers and the fiber bundles tend to swell leading to increasing dimensions. As a consequence size, shape, stiffness and permeability of products such as yarn or ropes can also vary. When a dry fiber or fiber bundles exposed to the atmosphere, they will take up moisture from the surroundings and reach equilibrium. Similarly, when they are exposed to a dry climate, moisture is lost on the surroundings to establish a new equilibrium. The amount of water in coir fiber could be expressed regarding humidity or moisture regained. Nawaratne et al. found that the moisture content of fresh-water-retted fiber samples was 10.20% with moisture regain of 11.31% when they are sea-water-retted. The coir was 7.92% with moisture regain of 8.60% [Nawaratne 2002]. Thus, retting methods have some effects on the moisture absorption of coir fiber bundles. Physical properties of coir fiber are given in Table 2.5.

As with other vegetable fibers, the main chemical components of coconut fiber bundles are cellulose, hemicellulose, pectin, and lignin. In most plant fibers, more than 70% consists of cellulose. In contrast, coir has high lignin content and a lower amount of cellulose [Dam, 2002]. Cellulose is a metabolically inactive structural carbohydrate, a polysaccharide consisting of a linear chain. Hemicellulose is another polysaccharide with a random, amorphous structure,

contained many different sugar monomers and associated with cellulose. The combination of cellulose and hemicellulose is known as holo-cellulose. Lignin is a polymer of phenylpropanoid units. Lignins are formed from three other phenyl propane's, alcohols (monolingual monomers) called coumarin alcohol, coniferyl alcohol, and sinapic alcohol.

However, these compounds can vary with the maturity of the fruit, as well as with the coconut variety. Lignin in the cell walls gives rigidity and color. It also reduces the permeation of water through the cell walls. Lignin also plays a significant role in the transport of water, nutrients and metabolites in the vascular system of plants. Furthermore, lignin in plant cells helps to maintain rigidity of the cell wall and gives resistance towards compression and bending, as well as protection against attack by microorganisms.

Table 2.5 **The physical properties of coir fibers.**

Reference	Diameter	Length	Density	Moisture Content	Water Absorption Saturation *
Ramakrishna& Sundararaja 2005b	0.40 - 0.10 mm	60 -250 mm	-	-	-
Agopyan et al. 2005 c	210 µm	-	-	-	93.8 –161 %
Paramasivam et al. 1984	0.3 mm	-	-	-	-
Ramakrishna& Sundararaja 2005a	-	-	-	-	180 %
LI et al. 2007	270 ± 73 µm	50 ± 10 mm	-	10% m	24 % l
Toledo Filho at al. 2005	0.11 – 0.53 mm	-	0.67 –10 g/cm3	-	85.0 –135 %
Munawar at al. 2007	121.3 ± 4.9 µm	-	0.87 g/cm3	-	-
Rao and Rao et al. 2007	-	-	1150 Kg/m3	11.36%	-
Fernandez 2002	-	-	1.2 g/cm3	-	-
Reis 2006	0.1 - 0.4 mm	-	-	-	-

Aggarwal 1992	0.1 - 0.4 mm	50 -250 mm	145-280 Kg/m3	-	130 - 180 %
Satyanarayana et al. 1990	100 - 450 µm	-	1150 Kg/m3	-	-

Source: [Majid Ali 2012]. Has been reprocessed

[Satyanarayana 1982] found that cellulose content varies from 33 to 43%, lignin from 41 to 46%, hemicellulose from 0.15 to 0.25% and pectins from 2 to 4%. The property of resistance of coir to degradation, when attributed to its high content of lignin (30% or more) compared with other plant fibers such as cotton and jute [Rao 2002].

Coconut coir fiber is on average composed of 46% of lignin (weight basis); it is one of the natural fibers containing the higher lignin content [Khedari 2004]. Lignin can be extracted selectively and progressively by treating the fibers with an alkaline aqueous solution or an organic solvent [Le Digable 2006]. It is thus a medium to conduct a systematic study on the effect of lignin on bio-composites properties.

2.3.4. Mechanical properties

Ramakrishna and Sandararajan investigated the effect of variation in chemical composition of tensile strength of four natural fibers (coir, sisal, jute and cannabinus fibers) when subjected to alternate wetting and drying, and continuous immersion for 60 days in three mediums (water, saturated lime and sodium hydroxide) [Ramakrishna and Sandararajan 2005b]. Chemical compositions of all fibers are affected by the immersion conditions.

Table 2.6 **Mechanical properties of coir fibers**.

Reference	Tensile strength	Elongation	Young's Modulus
Ramakrishna& Sundararaja 2005b	15 - 327 N/mm2	0.75%	-
Agopyan et al. 2005 c	107 MPa	37.7 %	2.8 GPa
Paramasivam et al. 1984	69.3 N/mm2	-	2.0×10^3 N/mm2
Ramakrishna& Sundararaja 2005a	50.89 MPa	17.6 mm	-
LI et al. 2007	142 ± 36 MPa	24 ± 10 %	2.0 ± 0.3 GPa

Toledo Filho at al. 2005	108.26 –251.90 MPa	13.70 –41 %	2.50-4.50 GPa
Munawar at al. 2007	137 ± 11 MPa	-	3.7 ±0.6 GPa
Rao and Rao et al. 2007	500 MPa	-	-
Fernandez 2002	175 MPa	30%	4.0 - 6 GPa
Reis 2006	174 MPa	10-25 %	16 - 26 GPa
Aggarwal 1992	100-130 N/mm2	10-26 %	19 -26 N/mm2
Satyanarayana et al. 1990	106 - 175 MPa	17 - 47 %	4.0 -6 GPa

Source: [Majid Ali 2012]. Has been reprocessed

Continuous immersion is found to be critical, and fibers lost their strength. However, coir fibers were reported to present the best tensile strength retaining the ability for all tested immersion conditions.

Munawar et al. characterized the morphological, physical and mechanical properties of the non-wood plant fiber bundles (ramie, pineapple, sansevieria, kenaf, abaca, sisal and coconut fiber) [Munawar 2007]. The larger the diameter of the fiber bundles, the lesser will be the density, tensile strength, and the Young's modulus.

2.3.5. Thermal properties

The Energy conversion of coir is little [Rowell 2002]. With its high percentage of lignin, coir fiber possesses natural resistance to soiling and dampness. In hot climates, it gives cool comfort and in cold weather it retains warmth. It also has good stretching and shrinking ability. Because of these favorable properties, it is widely used for floor covering all over the world. Coir fiber can be dyed and printed easily to get the desired colors and designs with lasting finish. It can also absorb sound waves, and because of its superior acoustic qualities it frequently used for wall paneling and floor covering in auditoria and concert

The presence of lignin–cellulose compound in the raw coir fiber plays a significant role in its structural and thermal properties of the fiber. [Abraham 2013] The extracted lignin is also a suitable source for renewable energy production.

2.3.6. Microstructure

The SEM micrographs of the coir fiber at different processing stages are shown in Figure.2.7. The SEM micrograph of the natural raw coir fiber is shown in Figure.2.7 (A). The fiber surface appears to be smooth due to the presence of waxes and oil. However, the presence of pores could be observed on the surface. Though coir fiber has high lignin content (49.2%), the moisture absorption capability is comparable (9.2%) with the other fibers (Table.2.6). Figure.2.7 (B) is the SEM micrograph of an alkali treated fiber. The arrangement of cellulose fibers within the matrix of lignin is clearly seen in this picture. The removal of cementing materials, primarily lignin, from the surface of the natural fiber, occurs during this step.

Table 2.7 **The chemical properties of coir fibers.**

	Cellulose (%)	Lignin (%)	Hemicellulose (%)	Moisture Content (%)
Raw coir fiber	39.3 (±4)	49.2 (±5)	2 (±0.5)	9.8 (±1)
Alkali treated fiber	50.5 (±3)	38.8 (±4)	<1	10.3(±1

Source: [Abraham, 2012]. Has been reprocessed

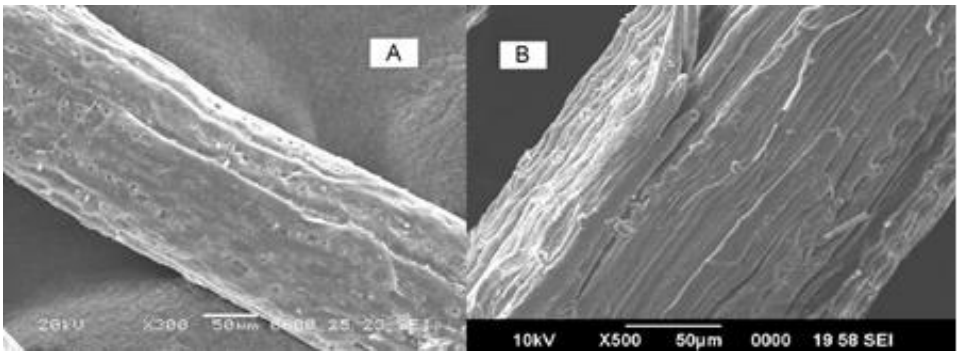

Figure.2.7. **SEM pictures: (A) raw coir fiber, (B) alkali treated coir fiber**
Source: [Abraham 2012].

2.4. Natural fiber reinforced cementitious composites.

Applications of natural fibers in composites used for building purpose have been performed for centuries. Examples, in the Egypt of Pharaohs, Israel or China show the reinforcement of clay bricks by natural straw. Fiber reinforced cement-based composites can use for many applications in civil engineering. For example, fiber reinforced cementitious tiles [Agopyan 2005], corrugated roofing sheets [Paramasivam 1984], simple slab panels [Ramakrishna, 2005], wallboard [Li 2007] [Asasutjarita 2007], and mortar [Toledo Filho 2005]. There have reported in the recent literature. Currently, the construction is the largest are of application of fiber composites (in volume).

Natural fibers have a low environmental impact comparing to synthetic or steel ones. As a result, they are suitable to design eco-friendly building materials. Fiber reinforced concrete can absorb seismic waves like a massive stone. Concrete made with flexible fiber reinforcements can withstand earthquakes [Shelly 2006].

Since ancient time, fibers are added to brittle materials to give them more tensile strength and more ductile properties. Since 1910, steel wire is attached to cement-based materials. Later studies using glass fibers in cement took place in the50's. In the 60's, the synthetic fiber was also examined as concrete reinforcement. Since 1970, the study of natural fibers, to replace relatively expensive synthetic fibers, began. Gradually since 1980, research has been conducted on the characteristics of coconut fiber from tropical countries such as India, Brazil, Malaysia, Thailand, Vietnam, Sri Lanka, Bangladesh, and Tanzania.

The applications of materials made of natural and local resources have increased worldwide. Their significant variation in properties and characteristics is the greatest challenge in working with natural fiber reinforced composites. Some variables, including the fiber type, environmental conditions where the plant fibers sourced, processing methods, and any modification of the fiber influence composite properties. Products processed with Portland cement blended with natural fibers such as coconut, sisal, bagasse, bamboo, hemp, wood and vegetable fibers. It has shown to be suitable to add to construction materials [Aziz 1981], [Paramasivan 1984]. Although the results are encouraging, there are some drawbacks especially some durability issues. It seems that the interface between fiber and cement paste is affected by the fiber swelling in the presence of moisture. For that reason, some researchers are now investigating remedial measures for improving durability. Accordingly, natural fiber-reinforced cement composites are most suitable. It is for earthquake resistant construction, foundation floor for machinery in factories, fabrication of lightweight cement-based roofing and ceiling boards, wall plaster, and building materials for low-cost

housing [Aziz 1981]. The use of natural fibers in the construction industry will help to achieve sustainable patterns of consumption of building materials.

Natural fibers used as reinforcement in concrete is a cost-effective replacement for expensive, high energy consumed and non-renewable fibers [Pacheco 2011]. Recently, the use of natural fibers to replace carbon/glass fibers as reinforcement in fiber-reinforced polymer composites has gained popularity due to increasing environmental concern. Natural fibers are low-cost fibers with low density. They are Biodegradable, non-abrasive, renewable, recyclable, required reduced energy consumption and present less health risk. Also, they are readily available, and their specific mechanical properties are comparable to those of glass fibers used as reinforcement [Malkapuram 2008]. Therefore, natural fibers represent a highly "sustainable" material. The use of natural fibers in fiber reinforced concrete composites as building materials will promote the "sustainable" development in the construction industry

The natural fibers are used for a long time in many developing countries in cement composites because of their availability and low cost [Ghavami 1999] [Savastano 2000]. Also, for low-cost building construction in developing countries, natural fiber-reinforced cement composites are found attractive [Ramakrishna 2005]. Un-reinforced cement concrete has low tensile strength and low strain capacity at fracture. Then researchers began looking for other alternatives for concrete reinforcement. Along with an increase in the environmental awareness in the world, researchers have focused their work on the valorization of bio-based high-performance materials such as natural fibers. Natural fibers are locally available in many countries. So their uses as a construction material for increasing properties of composites at a very little cost (almost nothing when compared to the total cost of the composites) are very promising. Moreover, their use can lead to having sustainable development [Ramakrishna 2005].

The researchers have used plant fibers as an alternative to steel fibers in the manufacture of fiber composites such as cement paste, mortar, and concrete. For example, natural fibers blended cements include coir, sisal, jute, hemp bast, pineapple leaves, kenaf bast, leaf abaca, bamboo, banana, flax, cotton and sugarcane [Ramakrishna 2005] [Agopyan 2005] [Li et al., 2007] [Asasutjarita 2007] [Toledo Filho 2005] [Munawar 2007] [Rao 2007] [Li 2006] [Fernandez 2002] [Reis 2006] [Corradini 2006].

A problem of workability arises when a high percentage of fibers is incorporated into a fresh mix, as in the case of steel fibers [Martinie 2010]. Volume fraction and fiber content are two terminologies used for expressing the quantities of fibers in a given composites [Ramakrishna 2005] [Agopyan 2005]

[Paramasivam 1984] [Li 2007] [Asasutjarita 2007] [Toledo Filho 2005] [Li 2006] [Fernandez 2002] [Reis 2006] [Aggarwal 1992] [Corradini 2006] [Toledo Filho 1999]. The various researcher has already studied uses of coconut coir as reinforcement in cement. Among them, a study on the feasibility of cement board [Asasutjarita 2009] or the durability of coir cement composites [Toledo Filho 2000] is reported.

Natural fibers are a valuable renewable resource materials; the substitution of steel fibers by coconut vegetal fibers presents many advantages because the coir is an abundant, versatile, renewable, cheap, and biodegradable lignocellulosic material.

2.4.1. Rheological behavior

In the building industry, fresh concrete flowability is required to ensure a smooth casting and to keep the mix homogeneously. This property is defined as workability. The workability of concrete depends on their rheological properties. Concrete or more cement-based materials are mainly considered to behave as Bingham materials. The Bingham behavior is modeled using two parameters: the yield stress and the plastic viscosity.

Fibers have a very positive influence on the mechanical properties of cementations materials in the hardened state. This impact depends primarily on the fibers (shape, constitutive material, volume fraction) but also on the casting process. Indeed, contrary to traditional aggregates, flow, in the case of fiber-reinforced materials. It can induce a preferred orientation of the fibers, which actively modify both fresh and hardened material properties as presented by [Martinie 2010].

The yield stress, plastic viscosity, and thixotropy are important rheological parameters to analyzes fresh concrete. Newtonian liquids, such as water and oil, show a linear relationship between shear stress (τ) and shear rate $(\dot{\gamma})$ as shown in Figure 2.8 as:

$$\tau = \eta\, \dot{\gamma} \qquad \ldots\ldots\ldots\ldots\ldots\ldots (2.1)$$

Where: η is the viscosity. There is considerable evidence that the cement-based materials behave as a Bingham material. The Bingham model can be modeled as follow:

$$\tau = \tau o + \mu\, \dot{\gamma} \quad \text{If} \quad \tau \geq . \tau o \qquad \ldots\ldots\ldots\ldots\ldots\ldots\ldots (2.2)$$

$$\dot{\gamma} = 0 \qquad \text{If} \quad \tau < \tau o \qquad \text{.....(2.3)}$$

Where: τ is shear stress (Pa), $\dot{\gamma}$ Is the shear rate (1/s), τo is the yield stress (Pa), and μ is a plastic viscosity (Pa-s) respectively. If the shear stress is lower than the yield stress, the material behaves as an elastic solid but when the yield stress was exceeded, the material start to flow. Yield stress is the critical shear stress required to initiate flow deformation and is directly linked to entering particular forces. As shown in Figure 2.8, the plastic viscosity is the slope angle of the shear stress vs. shear rate relationship.

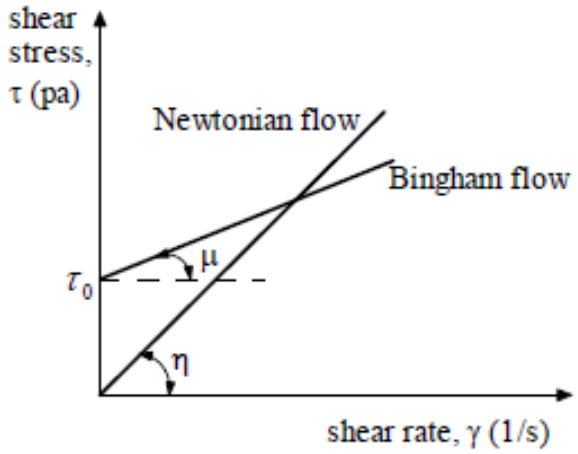

Figure 2.8. **Newtonian and Bingham flow, models**

Thixotropy is also an important rheological term to describe fresh concrete. Thixotropy is a decrease of apparent viscosity under shear stress, followed by a gradual recovery when the pressure removed. The effect is time-dependent [Barnes 1997]. Thus, after the concrete casting into the form, a structural build-up occurs, and both yield stress and viscosity increase. To some extent the concrete, supports its weight that results in little pressure on formwork and a high casting rate [Koehler 2005a]. The thixotropic property reduces the risk of segregation after placing.

Figure 2.9 taken from Newman and Choo shows the effects of different materials on the rheological properties for concretes, in general [Newman 2003]. Incorporation of super plasticizers dramatically decreases the yield stress but has only little effect on viscosity. Compared with superplasticizers, water decreases both the yield stress and the viscosity (however, it also drastically decreases concrete strength).. The side effect of the change in water content in concrete is that it may induce bleeding or segregation. Viscosity modifying admixtures can be added to prevent any segregation risk by increasing the viscosity without affecting the yield stress. The paste is another important factor on the Bingham parameters.

The addition of paste will result in a decrease in yield stress and increase in viscosity. Using supplementary cementitious material such as fly ash leads to a decrease in the yield stress of concrete.

It is worth to note that the rheology of cement-based materials influences the orientation of the fibers during casting or extrusion.

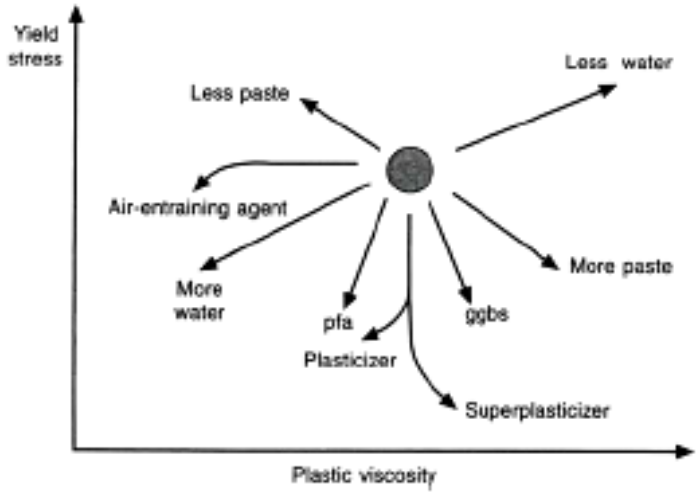

Figure 2.9. **General effects of concrete constituents on the Bingham parameter**
Source: [Newman 2003]

2.4.2. Physical properties

Sugar components of fiber such as hemicellulose and lignin may interfere with cement hydration. Savastano mentioned that acid compounds released from natural fibers increase the setting time of the cement matrix [Savastano 2003a].

According to Sedan, fiber inclusion can increase the delay of setting by 45 min. It relies on the fact that fibers pectin can fix calcium preventing the formation of CSH structures [Sedan 2007].

2.4.3. Mechanical properties

Fiber characteristics such as tensile strength, elastic modulus, diameter or length affect the mechanical properties of fiber-reinforced composites. Fibers dispersion and orientation within the matrix play also an important role. The bond strength of the fiber-matrix interface is essential to reach high mechanical properties. Also, factors like processing conditions/techniques have a significant influence on the mechanical properties of the fiber reinforced composites. The

most important characteristic of the composites is their strength. Their high mechanical strength combines with they're a relatively low weight for optimized use in engineered structures such as ships, cars or buildings. Composites tensile strength can be four to six times greater than that of steel or aluminum [Biswas 2002]. Structures made of composites are 30-40% lighter than similar ones made of aluminum.

Environmental interactions influence the strength of composites. A recent study shows that the tensile strength of composite resins presents lower values after storage and test in water as compared to the dry condition due to its water absorption [Tani 2002]. Tensile strength expressed as the breaking load per unit cross-sectional area of the test specimen is an important physical property of fibers. 34% can increase the fiber tensile strength, fiber toughness and fiber–concrete bond strength, 55%, and 184%, respectively when fibers are boiled and washed [Ali 2013].

The flexural strength can be slightly increased by using only coconut fiber. Natural fibers such as coconut are reported to improve the compressive and tensile strength of cement based composites [Asasutjarit 2007]. Likewise, fracture toughness and fracture energy of polymer concrete can be increased by using chopped coconut fiber and sugarcane bagasse fiber [Reis 2006].

The use of natural fibers in the cement matrix leads to lightweight materials with excellent tensile behavior. Previous researchers on fiber reinforced concrete have shown that short natural fibers can modify tensile and flexural strength, toughness, impact resistance and fracture energy of cementitious materials [Pacheco 2011].

Pacheco-Torgal and Jalali reviewed the mechanical impact of several vegetable fibers (i.e. sisal, hemp, coir, banana and sugar cane bagasse) as reinforcement in cementitious building materials. Among those natural fibers, coir fiber presents some advantages to being used as reinforcement. Its highest toughness among natural fibers, it's extremely low cost, as well as its availability [Baruah 2007] makes coir fiber very interesting. Li et al. stated that flexural toughness and flexural toughness index of cementitious composites with coir fiber are increased by more than ten times due to coir fiber bridging effect [Li 2004].

Reis also reported that coir fiber increases concrete composite fracture toughness. Moreover, the use of coir fibers shows even better flexural properties than synthetic fibers (glass and carbon) [Reis 2006]. Therefore, the inclusion of coir fiber might be useful to increase the flexural performance of concrete composites, particularly in changing the brittle failure pattern of the concrete core.

Meanwhile, according to Filhoa et al. [Filho 2000], cementitious composites made with coconut fiber present a significant decrease in toughness after six months out of aging or submitted to cycles of wetting and drying.

Majid Ali et al, show that fibers have the maximum bond strength with concrete when (i) embedment length is 30 mm, (ii) fibers are thick, (iii) fibres are treated with boiling water, and (iv) concrete are mix designed with ratio of one mass of cement; 3 masses of sand; 3 masses of gravel [Majid Ali 2013].

Single fiber pull-out tests have been carried out to determine load–slippage curves with the help of an Instron tensile machine fitted with a load cell. Bond strength and energy required for fiber pullout are computed from experimental data [Majid Ali 2013].

The use of natural fibers in concrete is not only useful to improve the mechanical properties of concrete, but also promote the sustainable development of green concrete and thus conserve natural resources [Awwad 2012].

2.4.4. Thermal properties

Measurements of the thermal properties have been performed by [Khedari 2002] and [Asautjarit 2007] on cement-based composites containing coconut coir fibers. Coir fiber is an interesting product because it has low thermal conductivity and bulk density. The development of composite materials for buildings using natural fibers such as coconut coir can then help to improve the energetical efficiency of the building.

Asasutjarita et al. determined the physical, mechanical and thermal properties of coir fiber-based light weight cement boards after 28 days of curing [Asasutjarita 2007]. The parameters studied were fiber length, coir pre-treatment, and mixture ratio. After being boiled and washed, 6 cm long fibers gave better results. On the other hand, optimum mixture ratio by weight of cement; fiber; water was 2:1:2. Also, the tested boards had a lower thermal conductivity than that of commercial flake board composites.

Assessment of thermal characteristics of coconut fiber and its use to modulate the temperature of concrete slabs in the construction industry are presented by Rodriguez [Rodriguez 2011]. This study indicates that fiber located on the outer surface of the concrete allows the room temperature to be in the range of comfort.

2.4.5. The fiber–matrix interface

There are several factors related to natural fibers that influence the performance of the composites such as an interfacial bond, fiber orientation, tensile strength and, chemical fiber properties. The reinforcements are the solid part of the composites, which reinforced into the matrix. They determine the strength and stiffness of the composites. In terms of reinforcing effects, lignin removal has no significant impact on composite mechanical properties but slightly reduces the water absorption of samples.

The mechanical efficiency of the fiber-reinforced cement composites depends on the fiber–matrix interface and the ability to transfer stress from the matrix to the fiber as reported by many researchers.

The fiber composition depends on the plant from which it has been extracted, and the agricultural conditions. It is mainly composed three compounds. There are cellulose, hemicellulose, and lignin. Moreover, the local repartition of the compounds is not homogeneous. In general, lignin mainly located at the surface of the fiber while the backbone is mainly composed of cellulose. Adhesion between matrix and fiber is an important parameter affecting the mechanical properties. A composite with excellent adhesion ensures a good stress transfer from the matrix to the fiber [Riande 2000].

The realization of the mechanical performance of the reinforcement is critically dependent on the effective load transfer by shear over the critical half-length at each fiber end. These are a function of the chemical -physical bonds between the fiber and the matrix. The main approaches to enhance the interaction between the fiber and the matrix are surface modification of the fiber (grafting or other chemical/physical treatments), application of coupling agents to the fiber surface and/or the use of compatibilizers in the matrix. George et al. have critically reviewed the physical and chemical treatments that may improve the fiber–matrix adhesion [George 2001].

Single fiber pullout tests are performed to determine the bond strength and the energy required for fiber pullout. The experiments on fiber tensile and fiber–concrete bond strength reveal that, thick (0.30–0.35 mm diameter) boiled fibers have higher tensile strength compared to the thin (0.15–0.20 mm diameter), medium (0.20–0.30 mm diameter), soaked and chemically treated fibers. The bond strength increases with embedment length and has the highest value at 30 mm embedment. Furthermore, Ali present that pullout energy increases with a rise in embedment length. Thin fibers in concrete with a 1:3:3 mix design ratio. The medium fibers in concrete with a 1:2:2 mix design ratio break because the pullout

load is higher than the fiber tensile strength. The thick fibers have the bond strength and tensile strength of 37 and 82 MPa, respectively [Majid Ali 2013].

2.5. Extrusion of cementitious composites

In recent years, the processing and production technologies for cement-based composites have also advanced. To date, injection molding, extrusion, compression molding, sheet molding and self-consolidating paste are the primary manufacturing processes for natural fiber-reinforced cement-based precast composites. Hence, new downstream and auxiliary equipment has been designed.

Cement-based materials can be classified as cement paste (cement + water), mortar (cement paste + sand) and concrete (mortar + gravel). They are used as materials for the building industry. Cement-based materials were commonly cast in place. However, new engineering composites are now precast in dedicated factories. Then the use of extrusion is intended to optimize the manufacturing process of precast elements.

Extrusion of cement-based materials can be a high productivity forming process. The extrusion process can form hardened cement composite with higher mechanical properties compared with traditional casting process [Mu 1999] [Peled 1999].

Hence, it is expected to improve the mechanical properties of the processed materials. However, it has not yet become a common way to form cement-based material in an industrial setting. The mechanism that regulates the flow of mortar or cement paste extrusion is an important point for the development of viable industrial extrusion process for cement-based materials. The material becomes softer and plug flow zone in which the material becomes more difficult on part of the liquid phase can flow through the die and creating a shared zone. Such phenomenon has to be avoided to ensure extrusion success [Perrot 2009]. Then, extruders must be optimized to provide homogeneous extrudates at high speeds to ensure the industrial processing of the material.

This process is developed and used since a long time for the perfect and homogeneous plastic and viscoplastic materials. In this case, the stress distribution and the material flow have been well described. It is not the case of more complex materials such as cement-based pastes. For these saturated and concentrated suspensions which present high solid volume content, extrusion should be an interesting way to decrease their porosity and improve their mechanical strengths, which are the main characteristics of building materials. However, it has been

observed that very concentrated suspensions are likely to undergo liquid filtration during their extrusion [Perrot 2007] [Perrot 2009] [Khelifi 2013].

According to Toutou et al., a granular paste must have an internal yield stress around 20 kPa to be suitable for extrusion [Toutou 2006]. This critical value corresponds to a paste firm enough to keep its shape at the extruder outlet and sufficiently "soft" to limit extrusion force due to plastic deformation and internal friction. Several recent studies suggest that cement-based materials are likely to undergo drainage during extrusion. Authors have proposed criterions based on filtration velocity linked to paste permeability. Stress distribution, internal friction, and wall friction remain constant if extrusion process is largely faster than the filtration. In this case, the material remains homogeneous, its behavior remains viscoplastic, and the process corresponds to a proper extrusion. On the contrary, if filtration is allowed by a low speed of extrusion, solid volume fraction increases and particles may percolate.

If the percolation threshold was reached, the material behavior becomes frictional. As a result, shear and friction stresses largely increase [Lecompte 2012]. In this case, normal forces due to shearing appear and induce an internal friction increase [Khelifi 2013]. It was also shown that drainage appears for low extrusion velocity when viscous effects may be neglected. A growing consolidated area located at the ram may appear. In this case, extrudates contain more liquid than the initial mixture. This material heterogeneity leads to an increase of the extrusion load and unsuitable extrudate quality. In the worst case, it can lead to a process blockage (Figure 2.10). Filtration occurs; the material becomes heterogeneous in the extruder

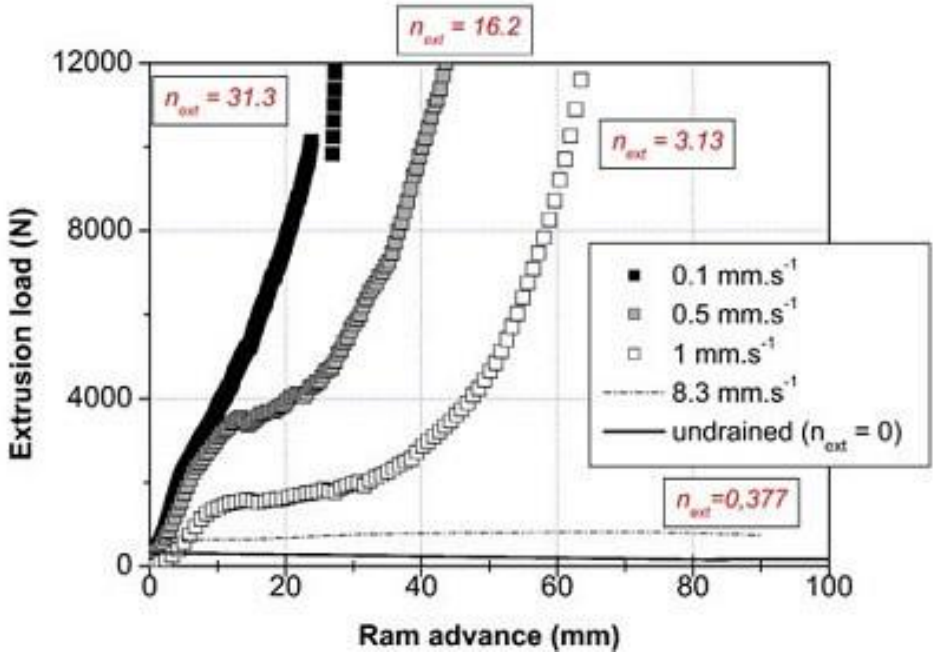

Figure 2.10. **Evolution of the extrusion according to the ram advance for different speeds of extrusion effort.**
Source: [Perrot 2009].

The surface quality of the extrudate is also an important characteristic of the extrudates. The periodic appearance of defects on the surface of the material studied is shown in Figure 2.11. The period of occurrence of defects seems to depend on the extrusion speed and appears to disappear for sufficiently high speeds [Lanos 2004]. The periodic appearance of the defect seems too related to the friction conditions at the wall. The authors conclude that the phenomenon of speed dependency is due to the phenomenon of drainage and reorganization of pore pressures during extrusion at slow speed. It is confirmed by the study of the extrusion type flow [Perrot 2009].

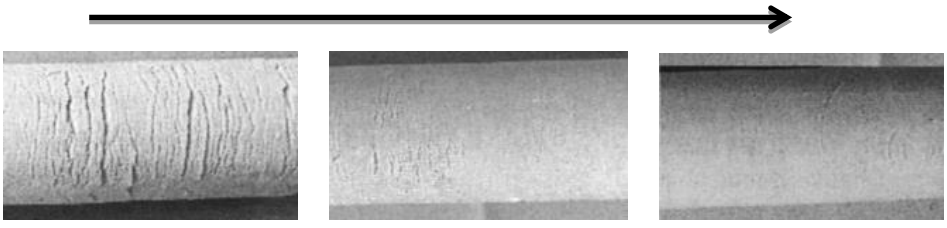

Figure.2.11. **The appearance of the surface defects according to the extrusion speed**.
Source: [Lanos 2004] has reprocessed

During the process of shaping material, the conditions of contact between the surfaces of the forming tools and the material may change significantly. The knowledge of the type of tribological behavior at interfaces is, therefore, necessary to understand and optimize the flow conditions during processing. Furthermore, the tribological behavior near the die may have a significant influence on the appearance of the extrudate defects in the particular case of materials with a very marked plastic behavior.

2.5.1. Extrudability of cementitious materials.

Pates must meet some criteria to be extrudate. During extrusion, the problem of drainage and consolidation of paste flow has to be taken into account in order to optimize extrusion conditions. Heterogeneities can occur and affect the quality of the extrudate [Perrot 2006]. On the other hand, Toutou develops a method for optimizing the composition of mortars and cement pastes from the use of simple compression test (also called squeeze flow). As an identifier of the rheological behavior and the field of extrudability. A criterion of the surface appearance and dimensional stability of the extrudate fresh is then defined to describe an entire extrudability field (Figure 2.12) [Toutou 2005]. In order to sustain gravity and handling, the paste has to present a minimum yield stress value. The author sets this parameter to 20 kPa.

Other criteria related to the homogeneity of the material during extrusion established; they seek to avoid surface defects and heterogeneity of the extrudate induced by the phenomenon of drainage [Perrot 2009]. In this study, the author performs an analysis based on the mechanisms of filtration of the fluid through the granular skeleton, leading to the definition of a criterion based on the extrusion rate. It to avoid the appearance of heterogeneities. Concepts of soil mechanics (consolidation theory, Darcy's law) are related to the concept of rheology and used to describe the permeability of the granular skeleton and the kinetics of drainage. A dimensionless number, defined as the ratio of extrusion time to the time needed to double the yield stress of the paste during the flow as the reference criterion for filtration effects.

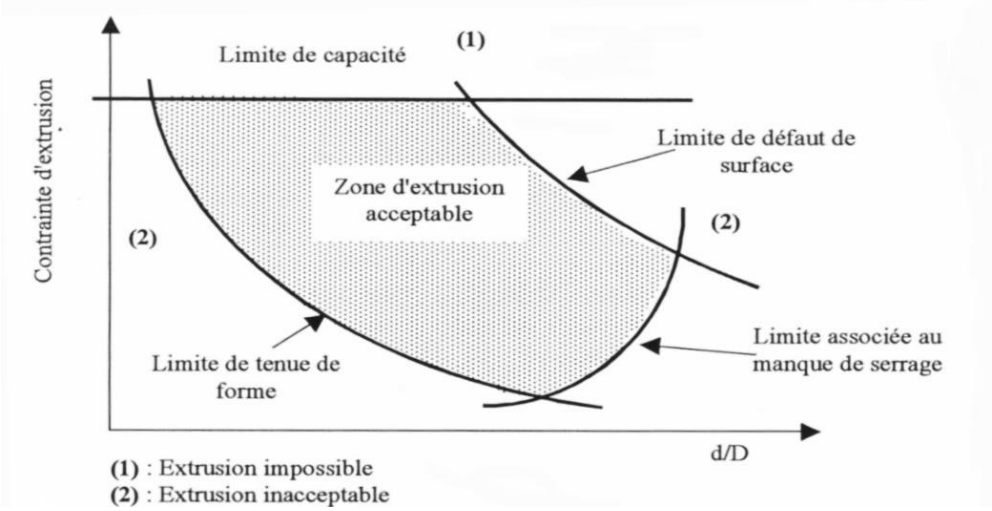

Figure.2.12. **Border field of extrusion of plastic material - no effect - speed according**
Source: [Toutou 2002]

2.5.2. Extrudability of fibers cementitious materials.

Extrusion technology has been used for the production of cement boards with unbleached kraft pulps. Extrusion was found to be a suitable process for cement boards with up to 8% pulp by weight. Higher pulp content increases the toughness of the material but does not enhance the flexural strength due to higher water content required for extrudability. Hardwood pulps, cheaper and more available than the softwood ones, were found to be more suitable for extrusion production in terms of extrudability [Shao 2002]. Extrusion allows incorporating both hydrophilic and hydrophobic fibers into fiberboard production. It found that sand content had a significant effect on toughness. The more the sand added, the less the toughness is. In this study, fiber dispersion seems not to be critical. Fiberboard made by non-dispersive mixing exhibited acceptable performance. Accordingly, the mixing time and energy in extrusion production could, therefore, be reduced.

Shao presents a comparative study of cementitious sheets extruded fibers of polyethylene terephthalate (PET), glass, polyolefin (PO) and PVA. The flexural strength of the plates with glass fiber presents the highest deformation at failure. SEM analysis shows that the plates of PVA exhibit good fiber - matrix adhesion and thus a larger energy are consumed for the tear in the fiber matrix [Shao et al. 2001].

The use of hybrid glass/carbon fiber reinforcement has shown efficiency. The fiber is a very convenient solution for strengthening reinforced concrete structures [Qian 2003]. The hybrid compound, a mixture of two or more types of fibers is a very advantageous solution for strengthening cementitious materials. Also, a hybrid combination of appropriate fibers can potentially improve global concrete properties. This concept has also been tested on extruded cementitious materials. While glass fiber reinforcement primarily improves the tensile strength, reinforcing PVA fibers improve the ductility. The use of a hybrid combination of glass and PVA fiber induces improvements brought by the large deformability of PVA fibers and the glass strength. However, the tensile strength is lower than that of glass fiber reinforced composites [Mu 2000], [Li 2001].

The analysis of the state of the art on cementitious extruded material shows that extrudates are denser and has better bonding between fibers and matrix. [Akkaya 2000c], [Akkaya 2001], [Shao 2001], [Qian 2003]. Akkaya et al. compared the material properties of extruded and molded cement containing PVA fiber reinforcement of different lengths (2, 4 and 6 mm for extruded materials, 2 and 4 mm for cast materials). The tensile strength, the flexural strength of the extruded material decreases with the length of the fiber while it increased with the fiber length when the material was cast. This contradiction is associated with differences in failure mechanisms and the change in fiber dispersion and orientation [Akkaya 2000b]. Peled and Shah studied the effect of fiber length (3% by volume of PVA and acrylic fibers 2 and 6 mm). Moreover, the substitution of cement by fly ash on the mechanical characteristics of extrudates confirm the results obtained by Akkaya [Akkaya 2000b] and show using microscopic observations that extrusion improves fiber-matrix bond [Peled 2003].

2.6. Environmental impact

Many researchers have conducted studies to assess if plants can provide interesting raw materials for composites to reduce their environmental impacts. The use of composites has reduced the impacts on the environment as it has reduced the use of various toxic compounds. Houses may be built in earthquake zones using lightweight composites and may help in reducing the impact on human life when disaster strikes. Lightweight composite structures have increased fuel efficiency in cars, buses, ships.

During construction design, one of the important things to consider is insulation nowadays. It helps reducing energy losses and to retain the internal temperature. The construction industry is a major consumer of natural resources and energy, have a strong impact on the environment. Cement production process

produces CO2 emissions that give a high environmental impact. From the total greenhouse gasses emitted by this sector, 50% are directly resulting from transportation, manufacturing and use of materials in the construction phase [Habert 2009]. It is necessary to evaluate the environmental impact of the product. It can be mass using Life Cycle Assessment (LCA) method.

2.6.1. Life cycle assessment methodology

Today the world is working towards a sustainable environment. People tend to be aware of their environment and want to know more. Many tools are designed to study the impacts on the environment and to help producers, decision-makers, and consumers to decide what to choose as an environmentally friendly product and bring it into use. Similarly, Life Cycle Assessment (LCA) is a tool use to assess the present and future impacts of any construction.

LCA is now a part of the International Organization for Standardization ISO 14040-14044 which issued in 2006. The term 'lifecycle' refers to the notion that holistic assessment the raw material production; Manufacturer; distribution; use and disposal (including all intervening transportation steps). These inputs and outputs are then converted into their effects on the environment to assess, their environmental impacts [ISO 14040, 2006].

LCA is used now for the past 10-15 years. It has helped to provide grounds for decision makers, political bodies and consumers to make the right choice, which is more sustainable and safe for the environment, in the long run.

Boundaries for the study were set. The functional unit has to be defined. For e.g. functional unit can be the impact per liter of packaged beverage. In this phase, the impact categories and methods that will be used to study the impacts are also discussed.

In the inventory analysis phase, it is defined where the data was collected. The impact assessment phase includes three steps: classification of parameters according to the impact categories they contribute to, characterization of the potential contribution to each impact studied, and the last step is weighting. The total impact over the lifecycle is usually an optional step. It can also be known as the combination of the above two mentioned steps of classification and characterization.

Interpretation is the last phase where all the results of the impact assessment were discussed, keeping in mind the functional unit. It is the final step in an LCA where we can analyze all data and come to a conclusion. It should be

used as a tool to find the best choice when considering different products (comparative LCA). In the present work, LCA is used to study environmental impacts of fiber reinforced composites for a given application (functional unit).

The construction and operation of a building cause the consumption of a large amount of energy; they also induce a high demand for physical resources and significant impact on the environment. The building also significantly influences the energy consumption of future generations and the deconstruction, recycling or disposal of the buildings will take place about 80– 100 years after the construction. Thus, the construction sector can significantly contribute to a more sustainable development [Zimmermann 2005]. Heavy materials and long transportation distance will affect the outcome of transportation on Environmental life cycle assessment (LCA). Another issue is cement production; authors have assessed the environmental impacts associated with three alternative technologies for the cement manufacturing process [Huntzinger 2009].

Environmental LCA is a valuable tool to understand the environmental hazards of products. It is also used to optimize the manufacturing process to reduce adverse environmental impacts. However, there are limitations to the study, and it should note that data aggregation problems associated with secondary information sources might cause variation in impact values for replication studies. However, the results of LCA show that blended fibers cement may provide considerable environmental savings.

2.6.2. CO2 emissions

Over the year's emissions from industries, car, fuel combustion, deforestation has led to the phenomena called as the global warming. It is due to the greenhouse effect of gasses as carbon dioxide, NOX, SOX, and methane cause the heat to be trapped within the earth atmosphere and stop it from moving into space. It has led to increased temperature of the land and has resulted in climate change.

In conclusion, the available data indicate that natural fibers have a tremendous potential as a mean not only to save nonrenewable resources but also to control greenhouse gas emissions [Zini 2011]. The five following sectors are the most significant contributors to CO2 emissions:

1. Fossil fuel combustion (including international transport 'bunkers', marine and aviation),
2. Fugitive is emissions from fuels,
3. Cement production and other carbonate use,
4. Feedstock and

5. Other non-energy uses of fossil fuels.

Global CO2 emissions have declined by 1% in 2009 and have known an unprecedented increase of 5% in 2010 followed by a novel increase of 3% in 2011. C02 emissions have reached an all-time high of 34 billion tons, as shown in Figure 2.14 [Olivier 2012].

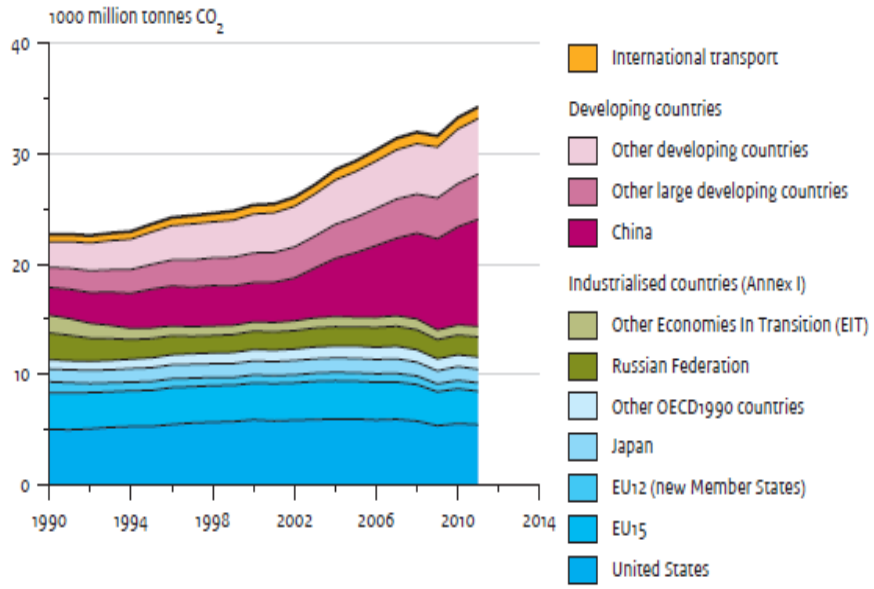

Figure.2.13. **Global CO2 emissions per region from fossil fuel use and cement production.**
Source: [Olivier 2012]

Globally, cement production is an indicator of national construction activity. Cement was mainly used in building and road construction. The carbonate oxidation in the cement clinker production process generated CO2 emissions. This principal constituent of cement is the largest non-combustion sources of CO2 from industrial manufacturing contributed about 4% to total global emissions [Lucinda 2012].

In total, cement production accounts for roughly 8% of global CO2 emissions [Olivier 2012]. It is especially severe in the current context of climate change caused by carbon dioxide emissions worldwide, leading to a rise in the sea level [Pacheco 2011].

The biggest emitters are in 2011: China 29%, United States 16%, European Union (EU27) 11%, India 6%, the Russian Federation 5% and Japan 4% [Olivier 2012]. The CO2 emissions from fossil fuel used and cement production shown in Figure 2.15.

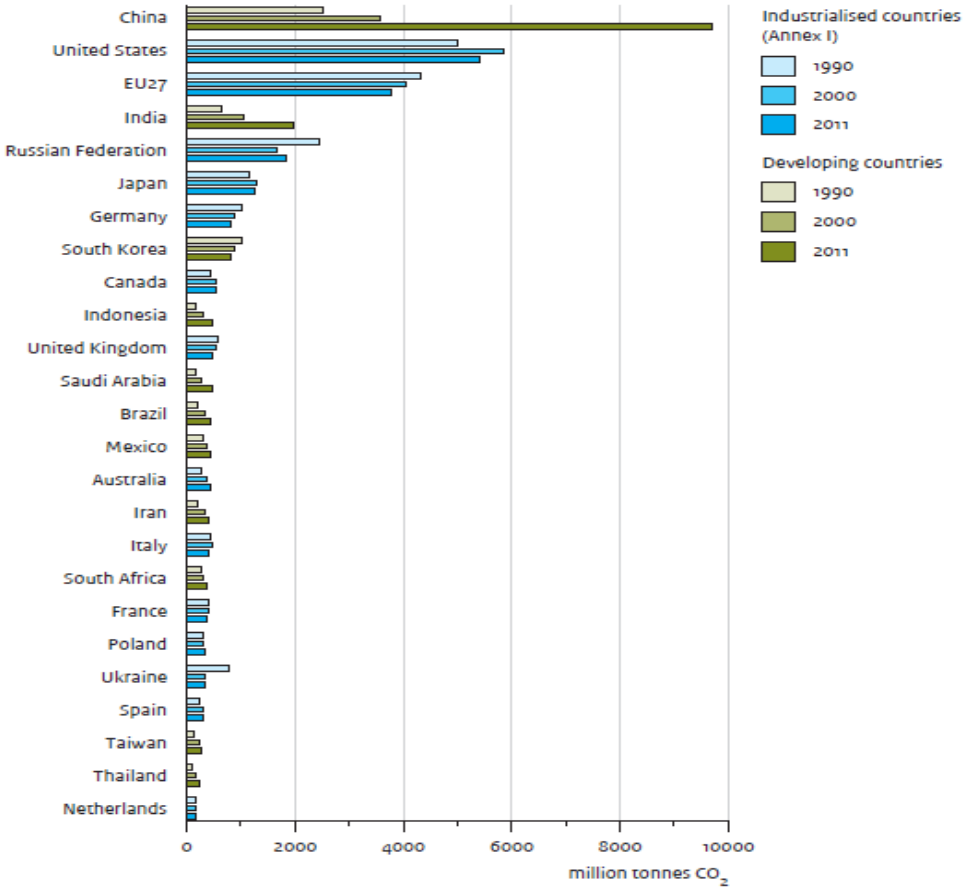

Figure.2.14. **CO_2 emissions per country from fossil fuel utilization and cement production**
Source: [Olivier 2012]

2.7. Conclusions of chapter

Natural fiber is a renewable, sustainable material, with low environmental impact. However, there are still problems that need attention. They were used as reinforcement material in composites, but fiber properties are much dispersed and water sensitive. Fibers have an irregular cross section with a central void (lumen) which makes the determination of their mechanical properties more complicated than for stable circular glass fibers. Cellulose is a hydrophilic molecule, so the fibers have properties that are dependent on the water content. Fibers degrade over time at temperatures of 200 ^{0}C or higher. Historically many fibers have been used to reinforce various building materials. Recently scientific efforts have been devoted to the use of natural fibers for reinforcement in cement-based building materials.

Environmental conditions that occurred most recently led researchers to try to get renewable materials that have a low environment impact. Utilization of natural fibers as reinforcement in the design of building materials is an opportunity to gain new and renewable construction materials. The use of fibers in the material will reduce the impact on the environment. It will be highly beneficial to the development of research on renewable building materials that do not affect the environment and has reduced economic value.

Indonesia as a tropical country land has a significant amount of improving coconut husk. It creates problems for the environment. Researchers are required to describe the performance of coir fiber and its influence on the cement paste. Reduction in the use of transport for materials will reduce the impact of environmental emission. That condition inspired to use local materials. It needs research to improve production and quality of local ingredients. Reduction of greenhouse gas emissions and energy consumption required a decrease in the use of cement and using natural and local materials. In the manufacture of building materials establishment needs to get reliable results, quality, and quantity. The use of extrusion technology is expected to overcome it. Literature review highlights that there is a gap that needs to be filled by further research to provide mix design methods for low cement content – natural fiber reinforced composites. Recent developments published in the literature deals with the development of building materials with low environmental impact. It can be done using reduced cement content and natural fiber, especially the coconut fiber.

This research is a step to have profound insight to investigate the strength of the bond between the coconut fiber and cement-based material because it then contributes to a better behavior of the composite. The result of this work is helpful in selecting the optimum fiber properties and pre-treatment to enhance the bond

between fiber and cement-based materials, ultimately resulting in increasing strength of composites. The results of the state of the art, it is clear that research has to be conducted to develop more of the characteristics and treatment of coconut coir fiber in cement-based composites.

The construction industry is one of the major and most active. This industry is also responsible for the depletion of large amounts of nonrenewable resources and 30% of carbon dioxide gas emissions. The use of renewable resources by the construction industry will help to achieve sustainable consumption pattern of building materials. Development of building materials for the construction, from the state of the renewable art research, should be continued the formulation of materials with a low content of cement, improved local materials and natural fibers as reinforcement. The formulation has a thermal resistance as well as having a low environmental impact.

Furthermore, the process and production of the material can be evaluated by using LCA software Simaphro. It has intended to assess the extent of the environmental impact caused by the material. In this case, the result of the evaluation is conducted on advanced research.

CHAPTER.3.
RESEARCH DESIGN AND METHODOLOGY

3.1. Introduction

The aim of this chapter is to describe the tested materials and the followed experimental procedure. All tests are performed to evaluate the behavior of coir fibers and both the rheological properties at the fresh state and the mechanical properties at the hardened state of extruded coir fiber reinforced cement-based composites. The first step consists in defining the materials used in the experimental investigation and the testing devices. Methods and procedures are explained in details. Experiments are conducted with the four following steps: 1. The measurement of coir fiber strength; 2. The design of the fiber reinforced cement-based composite; 3. Rheological characterization of the paste in the fresh state; 4. Mechanical performance of the extruded composites at the hardened state.

Furthermore, based on the results of the experiments, we can expect to develop an analytical model able to describe the stress-strain of fiber cement mortar composites

3.2. Flow chart of the experimental approach

This chapter describes the experimental approach and test procedures. The raw materials used in this work are coir fiber and cement-sand-clay mixes. This research design is summarized in Figure 3.1. The chart of the research work is divided into three successive stages. The first one is the preparation research carried out in the UI, Indonesia and continued at UBS, France. Then, the phase of materials preparation and characterization is done in the laboratory at UBS, France. This work performed in the laboratory that starts with the preparation of materials consists of materials design and processing, followed by the physical, mechanical and microstructural characterization. The last stage is analysis, discussion and final conclusions held at UBS, France and UI, Indonesia.

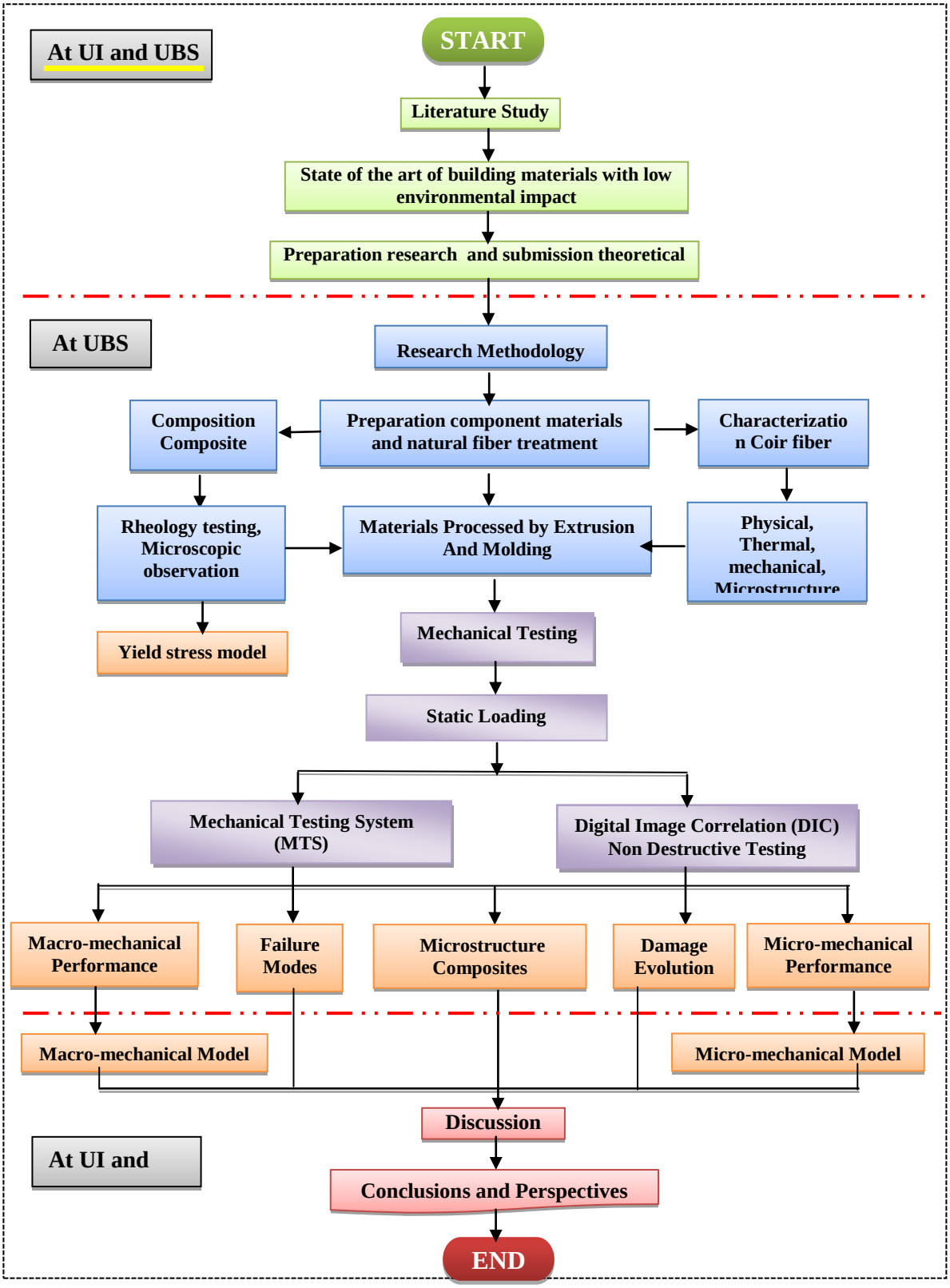

Figure.3.1. **The flow chart of the research design**

As shown in the flow chart of research in Figure 3.1, the design and development of material are organized as follows:

1. A selection of natural fiber and description of its extraction process.
2. The design of an extrudate mix of cement, sand and clay, reinforced by natural fibers.
3. Effect of the fibers on the behavior of the cement paste at the fresh state.
4. Study of the physical properties of the material components using morphological microstructure observations such as surface morphology, shape, dimension using scanning electron microscopy (SEM).
5. Fabrication of extruded natural fiber reinforced cement pastes.
6. Measurement of splitting tensile strength and compressive strength of the extrudates at the hardened state carried out simultaneously with microstructure analysis by SEM observation

3.3. Fibers

3.3.1. Preparation of fibers

The used fiber is coir, which is a product from the coconut (Cocos nucifera). The coconut trees are extensively grown in tropical countries. The coir fiber of the present work comes from the island of Java Indonesia as shown in Figure.3.3. Fiber has been extracted from coconut husks. In the present work, Coir fibers are extracted manually from the coconut shell and outer membrane.

Cleaning and sieving steps are needed to obtain the fibers manually as shown in Figure 3.2. After the coconut fibers are separated from the coconut shell as shown in Figure 3.2.a, they are separated and released from peat that stacked up into fibers (Fig. 3.2.b). Then fibers are sieved by length (3.2.c.d.e.f.). Residual dust and peat are partially removed from fibers.

Two types of fibers are studied: fibers that are cleaned and thermally treated and fibers that are untreated. Treatment of fibers is done manually without any chemical additive. The cleaning consists in a washing of fibers with tap water to obtain a smooth surface and to remove the rest of peat and dust that still exist on the surface after sieving. Fibers are dived in clean water during 1-2 hours. Then dirty water, loaded with peat and dust, is removed, and the operation is renewed with clean tap water, to separate fibers. Some peats and dust are then extracted manually from fibers skin and fibers are placed on a paper, so that it can absorb water. Finally, fibers are combed and sieved, to release the residual peat and dust.

Those treated fibers are stored in a chamber at a 20°±1°C room temperature before being put in the oven at 50˚ C for two days. The treated coir fibers are shown in Figure 3.5. Untreated fibers are just left in an air-conditioned room (temperature 20°±1°C and relative humidity of 50%), before tests. The untreated fibers are shown in Figure 3.4.

Figure.3.2. **Extracted Coconut Fiber**

The Fibers are carefully cut to the required length. After the drying of the fibers room temperature, the long fibers were firstly separated from short fibers and peat. Then three ranges of length were selected: 1 to 10 mm; 10 to 50 mm; 50 to 250 mm. All the fibers are then combed and finally cut to the required length with scissors. Three lengths are studied: 5 mm, 10mm, and 15mm.

It must be noted that the coir fibers are also commercially available at relatively high cost, as they are prepared for special purposes like brushes, mats, and pedestal seats. This cost can be reduced if fibers are mechanically prepared at a larger scale. Until now there has been no commercial product that provides fiber-based uniform size and fiber size below 100 mm.

Figure 3.3. **Coconut fibers.**

Figure 3.4. **Untreated coconut fibers.**

Figure.3.5. **Treated coir fiber**

3.3.2. Water absorption

The water absorption coefficient was measured following the ASTM 127/88 standard. The untreated and treated fibers samples are weighed after drying at 50 ^{o}C (until a constant weight is obtained). Then, the samples are immersed in distilled water at a room temperature of 20 ^{o} C. The samples are removed from the water after different immersion times and weighed with a high precision balance and then dived again in water. A minimum of three samples was tested.

The weight difference provides the content of water. The absorption percentage is calculated using Eq. (3.1).

$$\%\ \text{Water absorption} = \frac{\text{Weight of wet fibers} - \text{Weight of oven dry fibers}}{\text{Weight of oven dry fibers}} \text{x} 100\% \quad \text{.. (3.1)}$$

3.3.3. Density tests

The density determinations for coconut fiber and coconut powder were obtained by using the Archimedes principle. This principle states that any solid object immersed in a fluid will lose weight an amount equal the fluid it displaces. The laboratory METTLER TOLEDO balance is equipped for this experiment. At first, the coconut fiber and coconut powder must be in a compacted form with the diameter of 23.00 mm and thickness of 4.00 mm. After all the compacted specimens have been prepared for both coconut fiber and coconut powder, the second step was to measure the density of the compacted specimens by using the balances. This device can calculate and give the density value automatically when the specimens are put into the balances according to the setting that has been set up. However, Equation 3.2 has also been used to calculate the density of the specimens to compare the result of theory and experiment.

$$\rho = \frac{A}{A-B}\left(\rho_{\circ} - \rho L\right) + \rho L \quad \text{…….. (3.2)}$$

Where: ρ is the density of sample, A is the weight of sample in air, B is weight of sample in the auxiliary liquid, $\rho_{\circ}$ is the density of the auxiliary liquid, and ρ_{L} is air density (0.0012g/cm3). Figure 3.6 shows the steps for density measurement using Mettler Toledo balance device for porous solid. Procedure of density measurements is as follow:

a. Setup the porous solid in the device,
b. Put the sample in the pan,

c. Dive the sample in oil and put it back in the pan,
d. Put sample in basket,
e. Compute the density value.

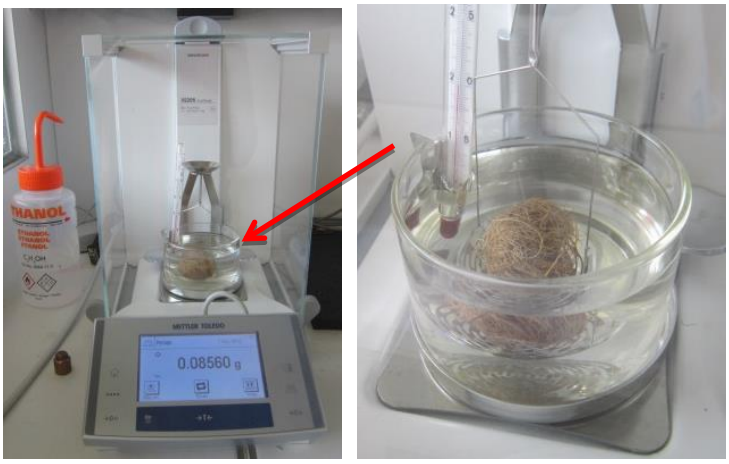

Figure 3.6. **Density measurement using balances device.**

3.3.4. Optical microscopy

An optical microscope is used for coconut fiber diameter measurements before the mechanical tests (Figure 3.7). The average diameter is obtained after the measurement of at least five measurements throughout the length of the fiber.

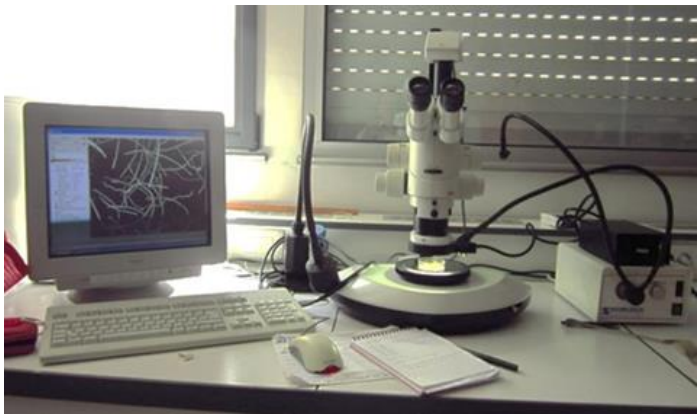

Figure.3.7. **Optical Microscopy**

3.3.5. Mechanical testing

The mechanical properties are an ultimate tensile strength, failure strain and Young's modulus of single coir fibers. Those were determined using a universal MTS tensile testing machine equipped with a 10 N capacity load cell. The device used is the MTS Synergies RT/100 from the LIMATB laboratory. Bundle fibers tensile strength is determined by applying a constant rate of displacement of 1 mm/min on a fiber length of 10 mm as shown in Figure. 3.8.

The tensile properties of the coir fibers were determined according to ASTM D 638. Single fibers are manually separated from the bundles. Fibers are cut into 40 mm length ones, and their diameters are determined used micro-optic. Before testing, the fiber was glued to the paper frame. Its diameter is determined by the average of optical measurements in minimal three different spots. Then, the frame is clamped on the MTS machine. While mounting, the specimens were handled using the paper frame. After the clamping of the ends of the paper frame in the test machine, the paper frame sides were carefully cut in the middle, before the start of the tensile test as shown in Figure. 3.9. The tests were displacement-controlled with a loading rate of 1 mm/min at 20^{o} C±1^{o}C and 50% relative humidity. The test was repeated 4 to 5 times, and the average values are reported.

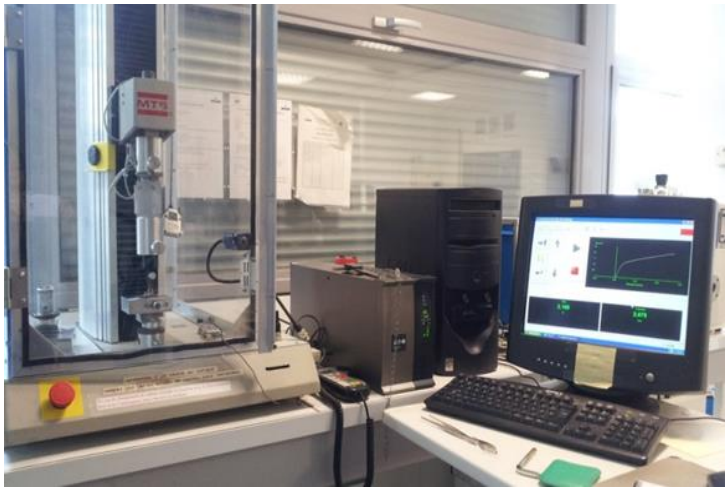

Figure.3.8. **Set up of the tensile test**

Figure.3.9. **Preparation of specimen for the tensile test**

The MTS testing machine is used to determine the tensile strength of fibers. This machine can plot automatic load versus extension graph. The fiber breaks down automatically when it reaches its ultimate expansion. The point where the fiber breaks down is known as the breaking point. From given data, stress and strain can be calculated at breaking point from the load-extension data as follows:

$$\text{Stress} = \frac{\text{Load}}{\text{Original section area}} \quad \text{..... (3.3)}$$

$$\text{Strain} = \frac{\text{Displacement}}{\text{Original length}} \quad \text{..... .....(3.4)}$$

The stress values (MPa) is calculated by dividing measured force values (N) by the original cross-sectional area of the sample (mm^2). Strain values were the elongating part of the specimen in the percentage of the original length (L_0 = 10 mm) while, young's modulus is determined as the slope of the linear part of the stress–strain curve.

3.3.6. Scanning electron microscopy

To identify surface morphology of single fiber bundle samples and fracture surfaces in the sample, a scanning electron microscope (SEM), type JEOL model JSM-6460LV, was used (Figure 3.11). SEM produces high-resolution images of a sample surface. It can resolve smaller feature, down to nearly 2 nm than a standard microscope. The electrons lose energy by repeated scattering when the primary electron interacts with the specimen. So absorption within a shaped volume of the specimen known as the interaction volume extends from less than 100 nm to 5 nm into the surface.

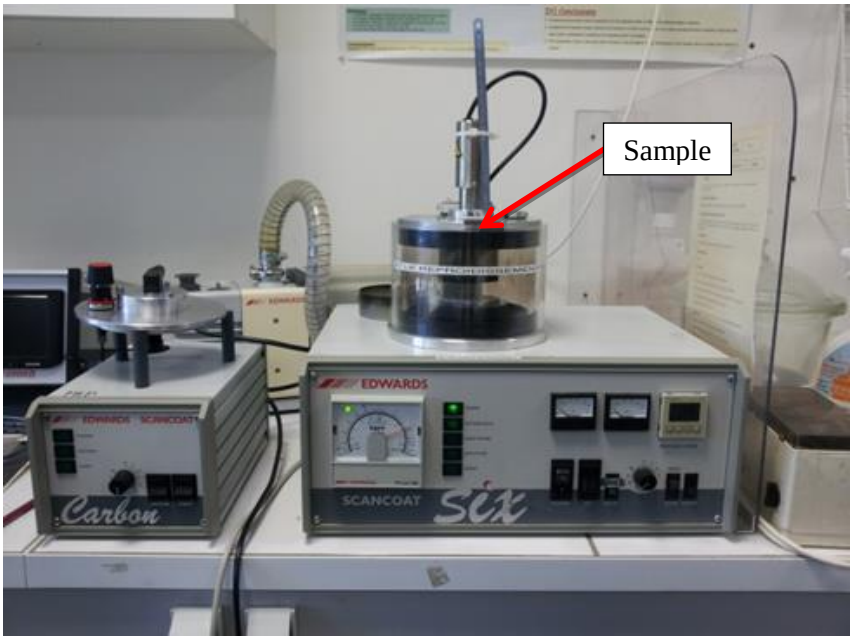

Figure.3.10. **Vacuum-system**

Figure.3.11**. Set up of Scanning Electron Microscope**

The scanning electron microscope was used. The surfaces of the treated single fibers and untreated individual coir fiber samples are examined and observed at the acceleration voltage of 20 kV. The individual coir fiber samples are mounted on stubs with silver paste. A thin film of platinum is vacuum evaporated (Figure 3.10) to enhance the conductivity of the samples before the photomicrographs taken with backscattered electron image and energy dispersive spectroscopy (EDS). SEM images were realized to characterize the coir fiber, and fracture surface made on samples tested in the tensile stress test.

3.3.7. Thermal gravimetric analysis

Thermo Gravimetric Analyses (TGA) were carried out using Mettler Toledo equipment; Model TGA-50 attached to a Mettler TC 11 4000 thermal analyzer as shown in Figure 3.12. The samples (10–20 mg) placed in platinum pans and heated from 20^{o} C to 1000 ^{o}C at the heating rate of 20 ^{o}C /min as shown in Figure 3.13. The thermal analyzes were done in a nitrogen atmosphere at a flow rate of 20ml/min. The synthetic air atmosphere was used to simulate the usual conditions of the end use of this material. It yielded the onset temperature of decomposition, mass loss, and maximum decomposition peak.

Figure.3.12. **Thermogravimetric analyses device.**

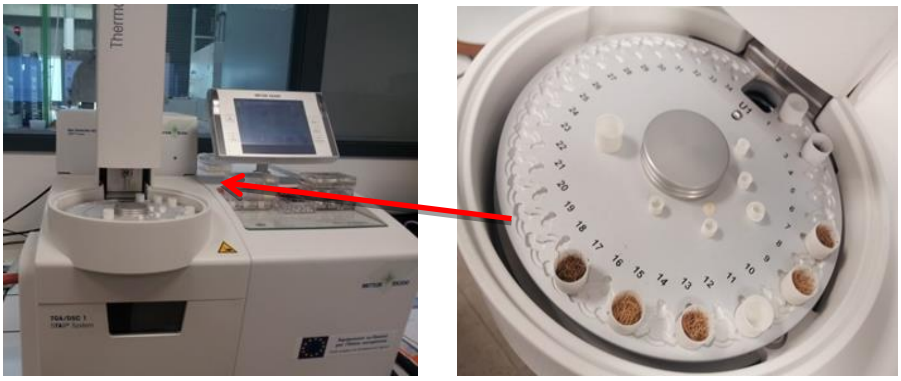

Figure.3.13. **Thermo Gravimetric Analyses (TGA)**

3.4. Fiber reinforced cement mortars, at fresh state.

3.4.1. Materials are tested.

3.4.1.1. Cement

The cement was a Portland cement CEM I/52.5 N CE CP2, from Lafarge plant of Saint Pierre la Cour, France.

This cement was without any addition of mineral admixture or filler. The cement size distribution, measured using a laser granulometry in ethanol, ranged between 1 μm and 100 μm. The specific surface measured using a Blaine was 3,390 cm^2 / g, and its density are 3,150 kg/m^3. The chemical composition of cement CEM I /52.5 N used as specified in the French Standard. It given in Table 3.1.

Table 3.1 **Chemical composition of cement**

Oxidations	Proportion (weight %)
SiO2	22,40
Al2O3	2,85
Fe2O3	2,25
CaO	66,70
MgO	0,83
K2O	0,19
Na2O	0,17
SO3	2,20
CO2	1,30
CaO free	0,55
Insoluble	0,30
Alkaline	0,32

3.4.1.2. Sand

A graded river sand is used as fine aggregates. The raw sand used was a Loire river sand, France. The river sand was used to mix the mortar according to the ASTM standard C128, with a density of 2,600 kg/m3 and sand absorption

capacity of 2 %. The particle size distribution of the raw sand as shown in Figure.3.14.

For extrusion formulations, sand particles were sieved under 2mm and then ranged from 20 µm to 2 mm. Sand was stored in the laboratory and exposed to fluctuating temperatures and relative humidity instability. Before mixing, Sand was dried at 105 ° C for 24 hours.

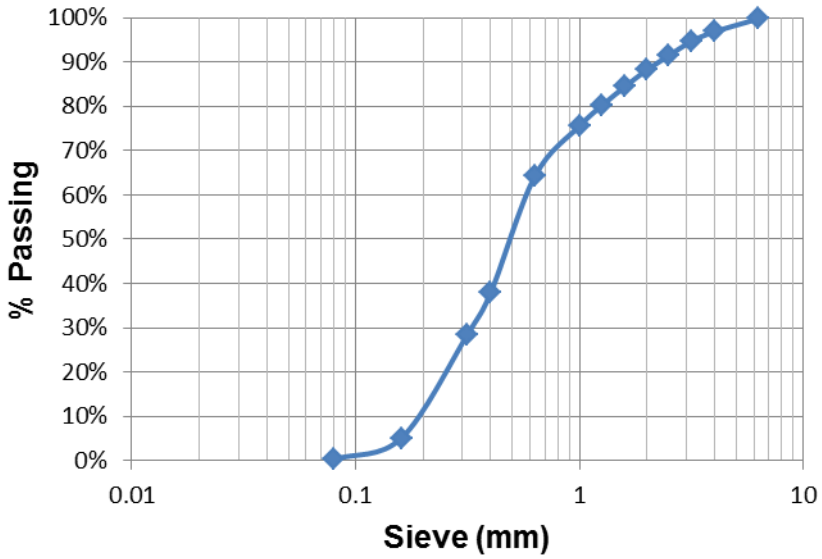

Figure.3.14. **Particle size distribution of sand**

3.4.1.3. Water

The water used in this study was tap water, not subjected to any particular preparation. Water was taken from the laboratory civil engineering LIMATB-UBS in France.

3.4.1.4. Clay

The Clay/Kaolin used comes from the IMERYS quarry, located in Ploemeur, France. It presents a density of 2,600 kg/m^3. The chemical composition of clay/kaolin is shown in Table 3.2. The SEM analysis of kaolin particles arises in a laminated structure. Kaolin has a grain size ranging between 5 and 50 µm.

Table 3.2 **Chemical Composition of Kaolin**

Oxide	Proportion (% mass)
Al2O3	48.15
Fe2O3	37.0
TiO2	0.8
CaO	0.1
MgO	0.2
K2O	1.1
Na2O	0.1
Li2O	Traces

3.4.1.5. Super-plasticizer

Super-plasticizer was a High Range Water Reducing Admixture (HRWRA) CHRYSO Fluid Optima 206. The HRWRA is a polycarboxylic type polymer. It is in liquid form containing 20 % of the dry material. It recommended dosage ranges from 0.3 to 3 % per weight of cement. In this study, dosage was fixed at 1.5 %. Mixtures with an HRWRA were tested to estimate its efficiency to reduce water content in fresh mixtures and to increase the strength of hardened mortars.

Table 3.3 **Characteristics of CHRYSO Fluid Optima 206**

HRWRA, CHRYSO Fluid Optima 206	
Nature	liquid
Density	1.05 ± 0.02
pH	7 ± 2
Cl^- content	< 0.1%
Na2O equivalent	<1.0%
Dry	20.2 ± 1
Dosage	0.3 - 3 kg per 100 kg of cement

3.4.1.6. Natural Fibers

Fibers are described in Chapter 3.3. Coir fibers are added to most mixes. Three different nominal fiber lengths are examined: 5 mm, 10 mm and 15 mm (Figure. 3.15). The fibers were supplied as chopped strands that were made to the individual fiber during the mixing operation (Figure. 3.16).

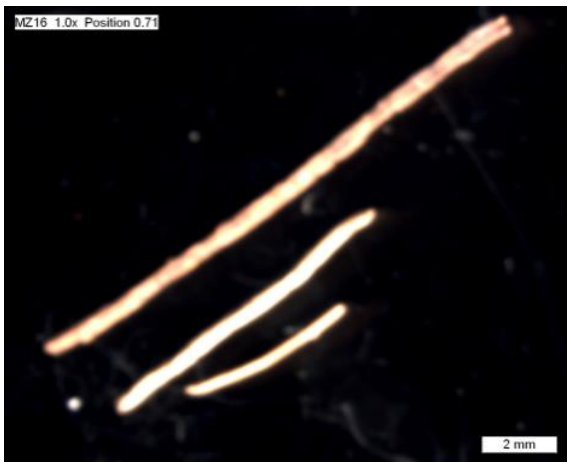

Figure 3.15. Coir Fibers Geometry


Figure 3.16. Chopped Coir Fibers

3.4.2. Mix proportion

The mix proportions are based on previous works done on cement stabilized clay blocks [Khelifi et al., 2012]. Two mixes are studied. For lower cement content, the cement proportion by mass was 10% of the total dry mix (mixture without water). For higher cement content, cement was used at a mass dosage of 20% of the dry mix. For plain mortar, the mix contained mass ratios for cement, sand and clay of 1:3:6 for low cement content. For high cement content of 2:2:6, with water-cement (W/C) ratios by mass respectively of 0.21 and 0.19.

Three lengths of coir fibers are used: 5 mm, 10 mm and 15 mm The Coir fibers contents were 2%, 3%, 4% and 5% by mass of cement.

The mix design for coir fiber cement mortar composites and water content were the same as that of plain mortar. It is well known that the W/C ratio has an influence on mortar properties, but compaction is also an important factor. The

addition of water will cause bleeding, ultimately reducing its strength in the hardened state. Reduced W/C ratio can lead to improper compaction, and then can result in less strength. Therefore, high range water-reducing admixture (HRWRA) was used to achieve good workability. The HRWRA dosage fixed at 1.5 % per weight of cement.

3.4.3. Mixing procedures

A standard Hobart mixer was used to mix the formulations. This device provides a planetary motion and variable speed drives. Its volume capacity is 5 liters by EN 196-1 for the preparation of standard cement paste or mortar. The mixer equipped with two rotation speeds 60 and 140 rpm as shown in Figure.3.17.

First of all, sand was mixed with fibers then blended at a mixer speed of 140 rpm (0.37/s) for 5 min. This step is followed by a 60 s at rest for bowl scraping. The second step consists in pouring cement and clay/kaolin and mixing the batch for 3 minutes. Then tap water was added while mixing again for 6 minutes at 280 rpm (0.74/s). The composite mix is stirred manually to disperse fibers in the matrix.

Figure. 3.17. **Hobart mixer**

3.4.4. Rheometer tests

The rheometer test is a vane test that allows to study the rheology of viscoelastic or plastic materials. It is suitable for perfect plastic materials and leads to the formation of a homogeneous stress state along the fracture surface defined by the movement of the tool.

At constant and low rotational velocity, the rheometer measures the value of the stress at break under shear and normal stress to zero on a facet of rupture. This stress is called yield stress and is usually denoted by τ_o. It is noteworthy, that the tool inserted into the mortar does not cause damage. The resistance to movement of the material induces a torque on the motor shaft. The passage of torque to shear stress is achieved by setting the time when the sum of torsions induces shear stresses acting on the sheared surfaces. This results in the relationship between torque and shear stress,

$$\tau_o = \frac{T}{B} \quad \text{..... (3.5)}$$

Where, τ_o = Shear yield stress; T = torque; B = constant dependent on the geometry. In this case, the tool is pressed into the sample to a depth corresponding exactly to the height H of the blades. Geometry sheared is that of the cylinder of height = H and a radius = R.

$$B = 2\,\pi\,R^2 H + \int_0^R 2\pi r\,dr \quad \text{..... (3.6)}$$

$$B = 2\,\pi\,R^2\left(H + \frac{R}{3}\right) \quad \text{..... (3.7)}$$

In addition, the Rheometer is used in the present work as a tool for the formulation of extrudate paste. It is based on the criteria established for cementitious material by Toutou et al. [Toutou et al., 2005]: The pastes should have a yield stress around 20 kPa.

To measure the yield stress, we use an Anton Paar Rheolab QC rheometer equipped with vane geometry as shown in Figure 3.18. The vane geometry utilized in this study consists of four blades around a cylindrical shaft. The blade height is 8.8 mm, and its diameter is 10 mm. Tests were conducted at very low speed (0.01 rad/min). At such a low shear rate, viscosity effects are negligible, and yield stress can compute from the measured torque peak value at flow onset. The experiment procedure is similar to the one used in Mahaut [Mahaut et al., 2008].

The tests are conducted at imposed strain rate. The rheometer worked like a current one but was controlled by a microcomputer: it can operate at constant

speed or constant torque. The dimensions of the tool is known, the torque values are directly converted into shear stress.

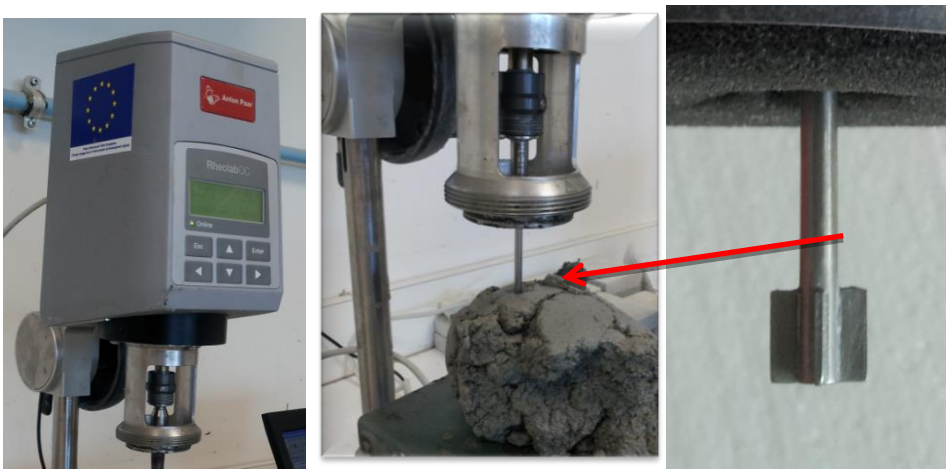

Figure 3.18. **The Anton Paar Rheolab QC Rheometer**

3.4.5. Screw Extrusion

The used extruder is a single screw extruder for horizontal extrusion Type VAVRS 50 with a Barrel diameter of 50mm and Max. Pressure rate 150 bar. The diameter of the auger is 48.5 mm. The total installed power is 4.4 kW. The device is shown in Figure.3.19.

Implementation of material flow is provided by a rotating screw in the arm commonly called cylinder extruder body. To reduce the amount of air entrained in the product formed, the vacuum pump can be easily incorporated the system,. The extruder forcing the paste flow through a die and the mix undergoes high-pressure gradient that makes its structure matrix very compact (low porosity).

The cement paste that comes out through the extruder must be simultaneously stiff enough to hold its shape through the die area and sufficiently flexible to limit the power of processing. Both conditions are fulfilled when cementitious materials exhibit an optimum yield stress of 20 kPa [Toutou et al. 2008]. Specimens of suitable dimensions are cut using a diamond cutter for mechanical testing as shown in Figure.3.20. Most care has been taken to maintain uniformity and homogeneity of the composite.

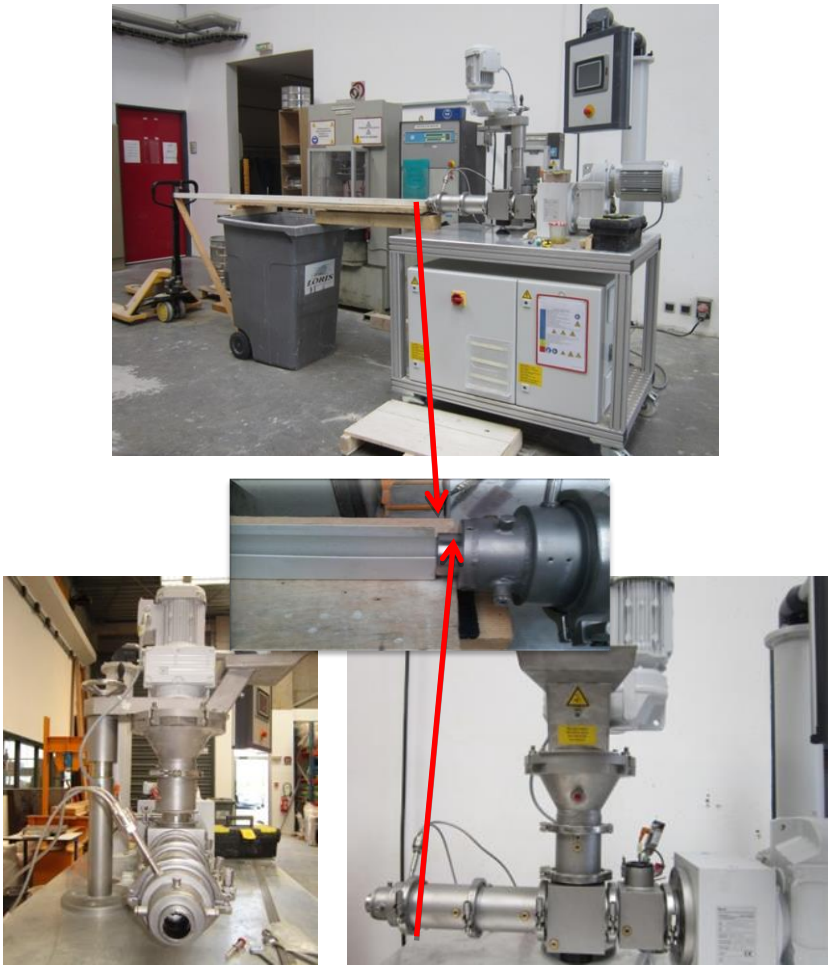

Figure.3.19. **Screw Extrusion**

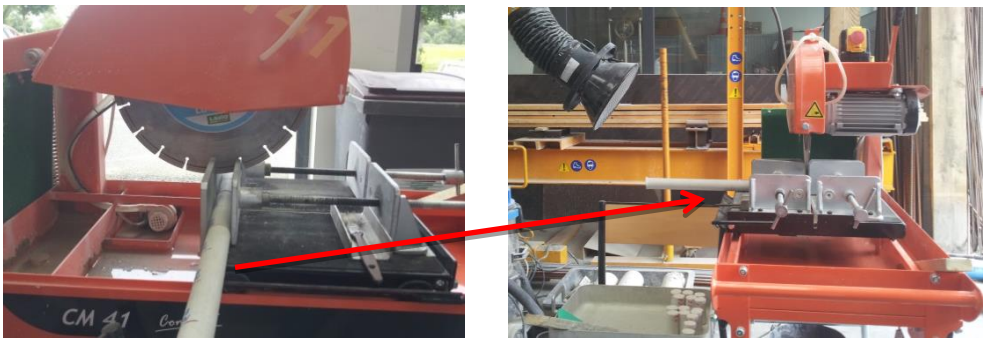

Figure.3.20. **Cutting extruded the mortar**

3.4.6. Casting procedure

The plain mortar and coir fiber-reinforced mortar composites are mixed in a mortar mixer. Fresh concrete workability was investigated immediately after the final mixing of the mortar using the rheometer. Then the mixture was poured into molds. It as shown in Figure 3.21 for the cylinder.

Figure.3.21. **Cylinder sample**

Figure.3.22. Vibrating of cylinder

The cylinder was cast by filling each mold in four layers. Each layer had frequently been compacted with 25 blows from a wood rod of 16 mm diameter before the next layer was poured, and the vibrator used. A plate vibrator is used to avoid entrapped air in the mold. Those cylinders were cast and vibrated on a vibrating table without pressure and cured in a wet chamber until the date of the test. All the samples are cured for 28 days before testing.

3.5. Fiber reinforced mortar composites at hardened state.

After a fiber tests and rheology test performed at fresh state, other experimental tests such as compressive strength, tensile splitting strength tests, and SEM observation were carried out on all of the hardened samples.

3.5.1. Specimens preparation

Preparation of the test samples is shown in Figure 3.23: mortar cylinders of 35 mm in diameter and 70 mm in height for screw extrusion were tested. Those tests are carried out for both plain and coir fiber-reinforced mortar composites for the determination of different properties of mortar/ matrix. The mix proportion of 1:3:6 and 2:2:6 by the weight of ordinary Portland cement, clay/kaolin, river sand and coir fiber were used to cast the specimens. The water/cement ratio used is 0.19. The water/cement ratio was maintained constant at all different length and volume fraction of fibers.

All samples were left in the molds for 24 hours to set at ambient temperature. They were removed from the mold and transferred into a curing in the air and immersion tank. The curing temperature was 20±1°C and humidity of approximately 50% ± 5%. The concrete mixes and the specimens are prepared by the provisions of EN196-1 standards. Then mechanical tests were carried out after 7 and 28 days of curing.

Figure.3.23. **Sample cylinder of test**

3.5.2. Water absorption.

The Samples were dried in hot air oven at 55 ^{o} C until their weight was constant.(W_i). Then, they were immersed in 50 ml distilled water. The swollen samples were wiped and weighed (W_W) after 24 hours. Then, they were dried in hot air oven at 55 ^{o} C until their weight was constant (W_f). Each sample is analyzed in four replications. The water absorption formula is as follows:

$$\text{Water absorption (WA)} = [100 \times (W_w - W_f) / (W_i)] \ (\%) \ \ldots\ldots\ldots \ (3.8)$$

3.5.3. Density tests.

The density of plain and coconut fibers reinforced mortar: The weight and volume of plain and fibers reinforced mortar were measured before the compressive strength test.

The theoretical density of composite materials in terms of the weight fraction can easily be obtained from the equations (3.9):

$$\rho_{ct} = \frac{1}{\left(\frac{Wf}{\rho f}\right) - \left(\frac{Wm}{\rho m}\right)} \qquad (3.9)$$

ρ is density and W are the weight fraction respectively. The suffix f is fiber; m is matrix and ct are the composite materials.

The actual density (ρ ce) of the composite, however, can be determined experimentally by simple water immersion technique. The volume fraction of voids (V v) in the composites is calculated using the following equation:

$$Vv = \frac{\rho\, ct - \rho\, ce}{\rho\, ct} \qquad (3.10)$$

3.5.4. Compressive tests.

Compressive strength test of plain and coir fibers mortar composites were carried out to find the modulus of elasticity, compressive strength, and finally to observe the stress-strain curves. The modulus of elasticity (E) is calculated as the ratio of stress change to strain change in the linear elastic range of the specimens. The maximum value of stress in stress–strain curves taken as the compressive strength (σ), and its corresponding strain (ε) is also noted.

The INSTRON 8803 testing machine was used to determine compression strength of the plain concrete and coir fiber cementitious composites. This machine can plot a graph of load vs. time automatically. The loading capacity of this machine is up to 500 KN. The experiment has been done using a compressive rate of 0.00015 mm sec^{-1}. Mechanical tests were performed following European standard EN 196-1 prescriptions [European standard, 2000]. The experimental compressive strength test was done in the laboratory as shown in Figure 3.24.

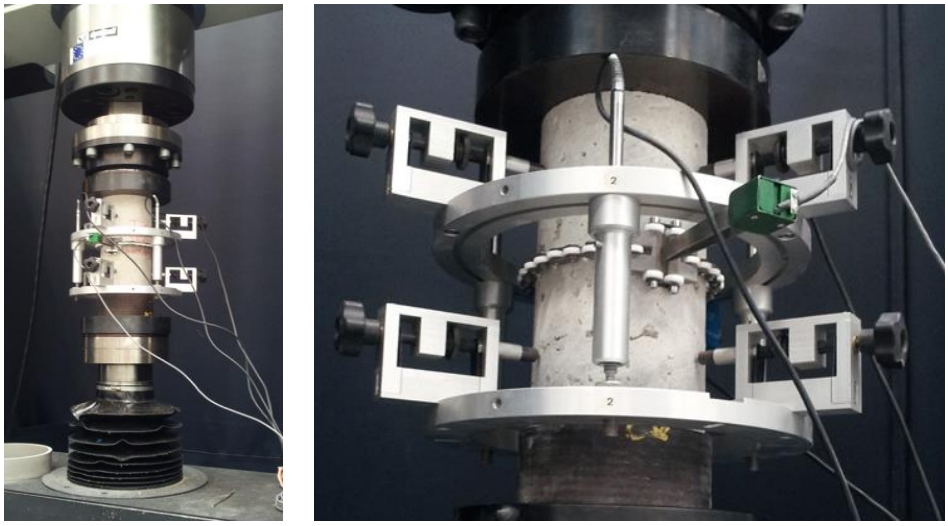

Figure.3.24**. Cylinder Axial Compression Test**

3.5.5. Tensile tests

The tensile test is performed on the Instron type 8803 (Instron, USA) testing machine at a crosshead speed of 5 mm/min, using a 50 KN load cell. The maximum load from the load-time curve of the splitting tensile strength (STS) test is taken for the calculation the tensile strength of plain/mortar and composite samples.

In splitting tensile strength test, cylinder sample exposed compressive force along the direction of the long cylinder. The resulting orthogonal tensile force causes the sample to fail in tension. The tensile splitting strength is calculated by using the following equation:

$$f\,ct = \frac{2\,F}{\pi\,L\,d} \quad \text{..... (3.11)}$$

Where *f* ct is the tensile splitting strength, in MPa, F is a maximum load of N, L is the length of the specimen in mm, d is the cross-sectional diameter, in mm.

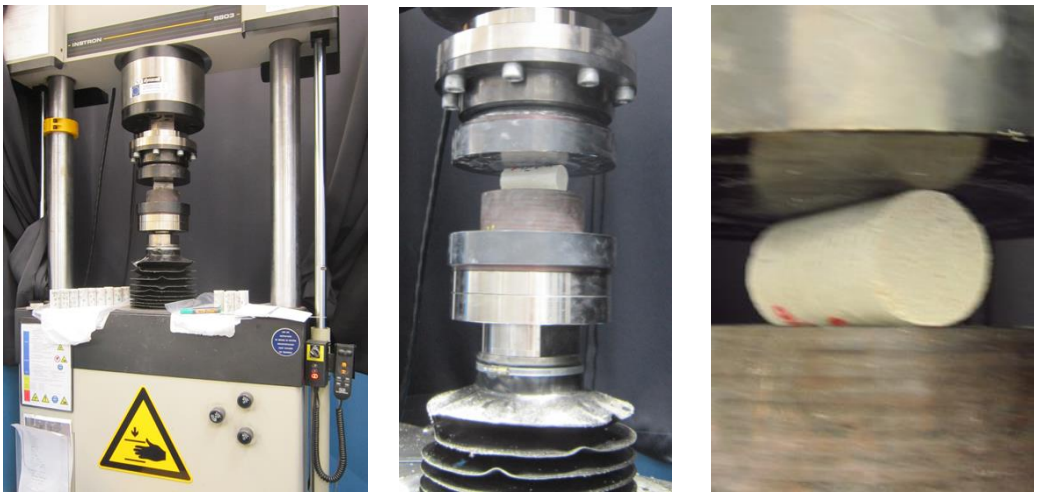

Figure.3.25**. Tensile test setup**

3.5.6. Digital image correlation

The Digital Image Correlation (DIC) system is a method for identifying the distribution and development of strain without the need for direct sample contact. the displacement of a sample of an applied speckle pattern coated on the surface is tracked on the basis of pixel distortion before converted into a measure of strain, using high-resolution image capture.

The DIC method works by correlating the digital images of surface patterns before and after straining. It consists of a three dimension digital image correlation (3D-DIC) system, sensor ARAMIS 4M, and computer. The 3D-DIC setup consists of two cameras having a max frame rate 60 Hz at a spatial resolution of 2358 x 1728 pixels, coupled with Titanar lenses of 35 mm length. Both cameras are mounted on a tripod having inbuilt spirit level to ensure horizontal level. Mechanical Testing System (MTS) Instron 8803 machine of 500 kN capacities as controlled. A typical experimental setup used in the present study as shown in Fig. 3.26.

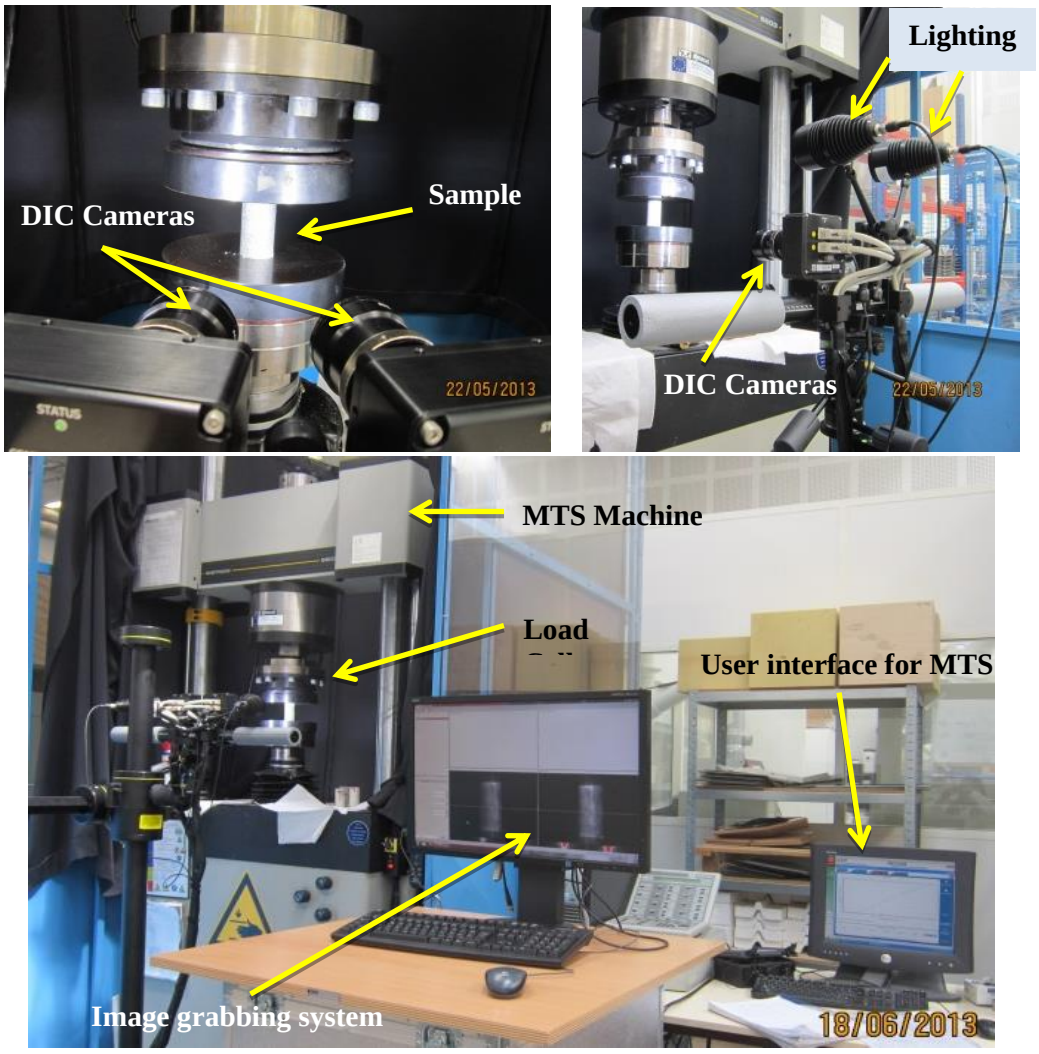

Figure.3.26. **Digital Image Correlation and Testing Setup**

In preparing the samples for DIC, a black-on-white speckle pattern was applied to the prepared surface. Random speckle patterns are made over the sample surface by spraying carbon black/titanium white colors with an airbrush

having a nozzle diameter of 0.5 mm. The test recorded images are then uploaded to the evaluation software ARAMIS and calibrated. Initial widths of the samples were measured pretest using an optical microscope. Two cameras were mounted on a tripod and profile bar then centered symmetrically about the sample position.

Uniform illumination of the specimen surface is ensured by keeping two standard halogen light sources on either side of the camera. The surface of interest is zeroed on by adjusting the focal length of both the lenses. The aperture of the lenses is adjusted to achieve a proper field of view and also to avoid saturation of the pixels in the area of view. The camera then calibrated for its position and orientation using an appropriate calibration grid plate. Cameras are connected to a workstation computer, and the images grabbed at a predefined rate.

The real-time results for multiple measurement positions the test objects surface directly transferred to the testing device, data acquisition units. Data acquisition card is used to provide an interface between MTS controller and image grabbing system for storing the required data like load and displacement values for every image being grabbed.

3.5.7. Microscopic observation.

The microscopical analysis in this study based on scanning electron microscopy (SEM), with backscattered electron image. Backscattered electron imaging is appropriate for sectioned specimens with a smooth, polished surface.

The scanning electron microscope JEOL JSM-6480LV (Figure 3. 11) used to identify the tensile fracture morphology of the coir fiber cement the mortar composite samples. The surfaces of the composite sample observed at 20 kV acceleration voltage. The composite samples mounted on stubs with silver paste. A thin film of platinum is vacuum evaporated onto them before the photomicrographs taken to enhance the conductivity of the samples, as shown in Figure 3.10.

CHAPTER.4.
PHYSICAL, MICROSTRUCTURE, THERMAL AND MECHANICAL PERFORMANCES OF COIR FIBERS

4.1. Introduction

Recently, research on green building materials becomes a way to anticipate global warming issues. Among these researchers, development of natural fibers as a concrete reinforcement is an emerging topic. The amounts of natural fibers such as coconut fiber materials are abundant in Indonesia. Coir fiber is a residual product of the copra (coconut meat) production, with volumes that exceed the needs for traditional uses like cords, brooms, Etc. Coconut fibers have the potential to be used in composite materials as reinforcement. This study deals with the description of the properties of those natural fibers from Indonesia.

The proposed methodology is to perform experiments to observe coconut fibers with and without special treatment (here a simple water washing followed by a dry stage). Mechanical properties were investigated through fibers direct tensile tests; Physical and thermal properties were studied using thermal gravimetric analysis. Finally, micro-structural properties fibers were obtained using a scanning electron microscopy (SEM).

In this research, a water washing treatment is used to modify the Indonesian coconut fiber surface. This treatment consists in a surface washing with water followed by a drying stage. No work has been reported on the treatment of Indonesian fiber surfaces. The effects of surface treatments of coconut fiber on microstructural and mechanical tensile tests of coconut fiber were investigated to assess its effectiveness.

The distribution of the tensile strength is studied, the mean and standard deviation of tensile strength is calculated following the Normal distribution and Weibull distribution resulting in the questionable benefit of applying the Weibull distribution.

4.2. Physical properties

The physical properties of any natural fiber are important to describe the mechanical strength of the fibers. Physical properties should include fiber dimensions, defects, strength, variability, crystallinity, and structure. It is important to describe the physical and mechanical properties of the fibers to optimize their potential as reinforcement in a cement matrix.

In order to optimize the efficiency of fibers in cement composites, it is necessary to carry out the treatment by washing and drying coir fiber in order to extract the substances responsible for the possibly weak interaction between fibers and cement mortar.

Treatment of fibers is done manually without any chemical additives. The present method of treatment is made through a process of washing and drying. After one day storing period in an air-conditioned room at 20°±1°C, fibers are soaked in tap water for two hours. This immersion sequence is repeated twice. Fibers are separated from dust and peat by sieving and combing. Then, fibers are cut in 5mm, 10mm, and 15mm long fiber bundles. Finally, fibers are dried in an oven at 50°C for two days. Figure 4.1 shows untreated coir fiber, and Figure 4.2 presents treated coir fiber.

Figure. 4.1. Untreated coir fiber

Figure.4.2. Treated coir fiber

4.2.1. Length of coir fiber

The natural length of coconut fibers ranges from 40-250mm. The lengths of fibers were measured using a steel ruler, and 50 pieces were randomly chosen

to find out the length distribution of coconut fiber. However, in this study, coconut fibers are cut in 5 mm, 10 mm and 15 mm fiber bundles.

4.2.2. Diameter of coir fiber

Changes in the physical properties can be due to differences in fiber morphology. Major differences in a structure such as density, cell wall thickness, length, and diameter result in different physical properties. Knowledge about diameter is important in cellulose based fiber composites as it give an indication of possible strength properties.

Treated coir fibers are cut into 40 mm long samples and their diameters are measured using an optical microscope. The cumulative distributions of fiber diameters are shown in Figure 4.3 for both treated and untreated samples. Fiber diameters distribution is modeled using an exponential based models as shown in the equation (4.1) for untreated fibers (mean square error coefficient R^2 is equal to 0.9716) and equation (4.2) for treated fiber (mean square error coefficient R^2 is equal to 0.9578).

$$D_{uff} = 77.065\, e^{0.0064\,F} \quad \ldots\ldots\ldots\ldots\ldots\ldots\ldots\ldots \quad (4.1)$$

$$D_{tf} = 55.423\, e^{0.0046\,F} \quad \ldots\ldots\ldots\ldots\ldots\ldots\ldots\ldots \quad (4.2)$$

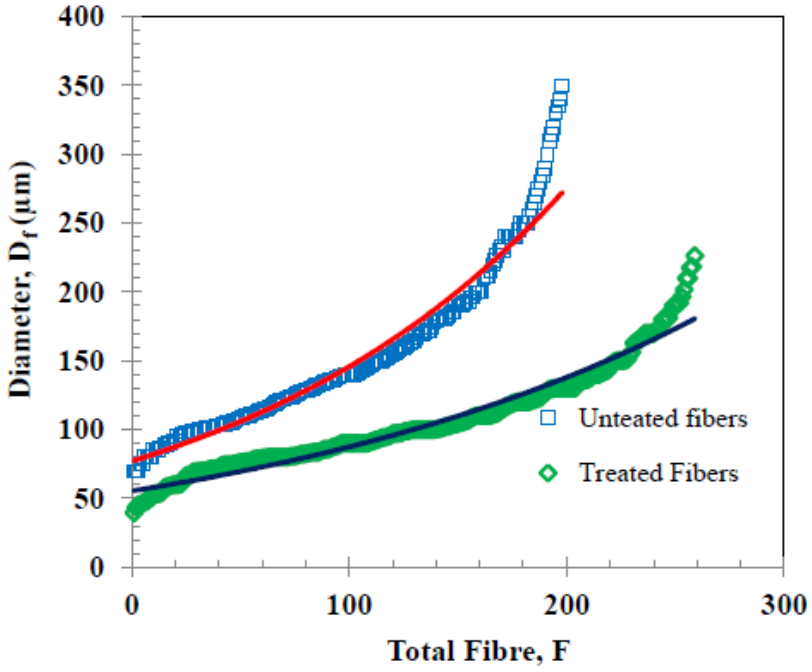

Figure.4.3. **Diameter of untreated and treated coir fiber**

The cumulative diameter distribution of fibers is modeled for composite materials with Weibull model. The cumulative distribution of the diameter of treated coir fiber is shown in Figure 4.4. The average value of fiber diameter is 106.56 µm for treated fibers with a standard deviation of 37.12 µm. The cumulative distribution of treated coir fibers diameter is described by Equation (4.3).

$$P(D_f) = 1 - \exp\left[-\left(\frac{D_f}{118.131}\right)^{3.466}\right] \quad \text{.....(4.3)}$$

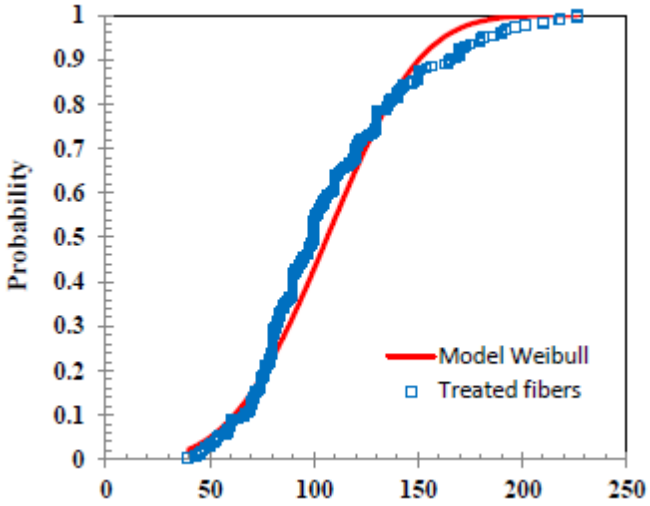

Figure.4.4. **Diameter cumulative distribution of treated coir fiber by the two-parameter Weibull**

The cumulative distribution of the diameter of untreated coir fiber is shown in Figure 4.5. The average value of fiber diameter is 154.99 µm for untreated fibers with a standard deviation of 60.13 µm. The cumulative distribution of treated coir fibers diameter is described by Equation (4.4).

$$P(D_f) = 1 - \exp\left[-\left(\frac{D_f}{118.131}\right)^{3.466}\right] \quad \text{.....(4.4)}$$

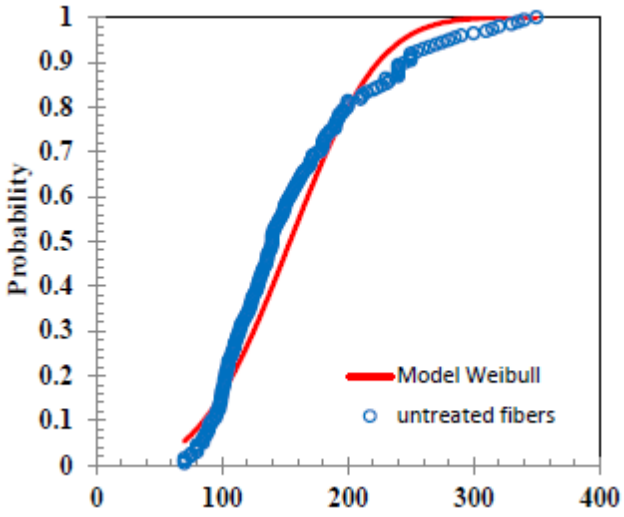

Figure.4.5. **Diameter cumulative distribution of untreated coir fiber by the two-parameter Weibull**

4.2.3. Density of coir fiber

The density of each fiber is an important parameter. For composite materials, the density of fiber has a significant effect. The weight of fiber in a composite matrix depends on the density of fiber.

The density of coir fibers was calculated using Equation (3.2).The density of untreated coir fiber is measured at 878 kg.cm^{-3}. For treated coir fibers, the density is 980 kg.cm^{-3}. . The difference between treated and untreated fibers densities can be explained by the removing of pith and low-density impurities (wax, dust) located at the surface of the fibers during the washing treatment.

Empirical equations (4.3) and (4.4).for density of untreated fiber and treated fiber are found by a numerical fitting on experimental results as shown in Figure 4.6. It can be observed that density increases with the fiber bundle length. For untreated fiber, the mean square error coefficient R^2 is equal to 0.9125,

$$\rho_{uf} = 0.1492 \ln (L_f) + 0.1339 \quad \text{(4.3)}$$

For treated fiber, the mean square error coefficient R^2 is equal to 0.9909,

$$\rho_{tf} = 0.1339 \ln (L_f) + 0.353 \quad \text{(4.4)}$$

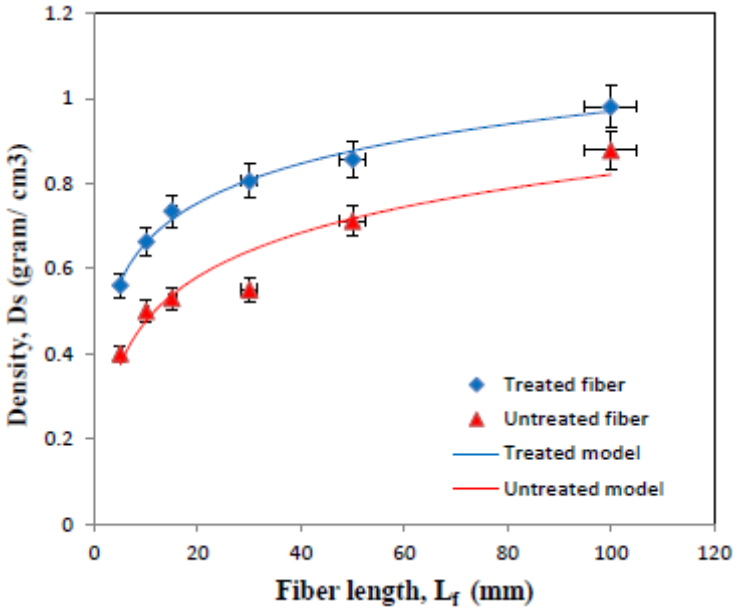

Figure.4.6. **The density of untreated and treated coir fiber versus fiber length.**

4.2.4. Water absorption of coir fiber

During the mixing and drying of matrix cement or mortar, natural fibers can absorb water and expand. The swelling of the fibers pushes away the cement matrix, at least at the micro scale. At the end of the fibers drying process, fibers have shrunk and are almost back to their original size. This phenomenon may lead to the void creation and very low-quality interfacial bonds between fibers and cement matrix. Therefore, it is necessary to measure the water absorption of fiber.

The measurements of absorption were carried out for 24 hours. Experimental data have shown that the absorption rate of water by coir fibers is maximal during the first three minutes. The absorption rate then drastically decreases. After two hours of immersion, the fibers get almost fully saturated. The absorption coefficient (ratio of the water mass over the fiber mass) is 82.4 % for treated and 120.9 % for untreated as illustrated in Figure 4.7. The amount of absorption is close to the one proposed by Savastano et al. (93.8 %) [Savastano et al., 2000].

This difference between treated and untreated fibers may be explained by the removing of dust, pith, and wax at the fiber surface. Those elements present a high specific surface that need at least to be wetted during the absorption measurement.

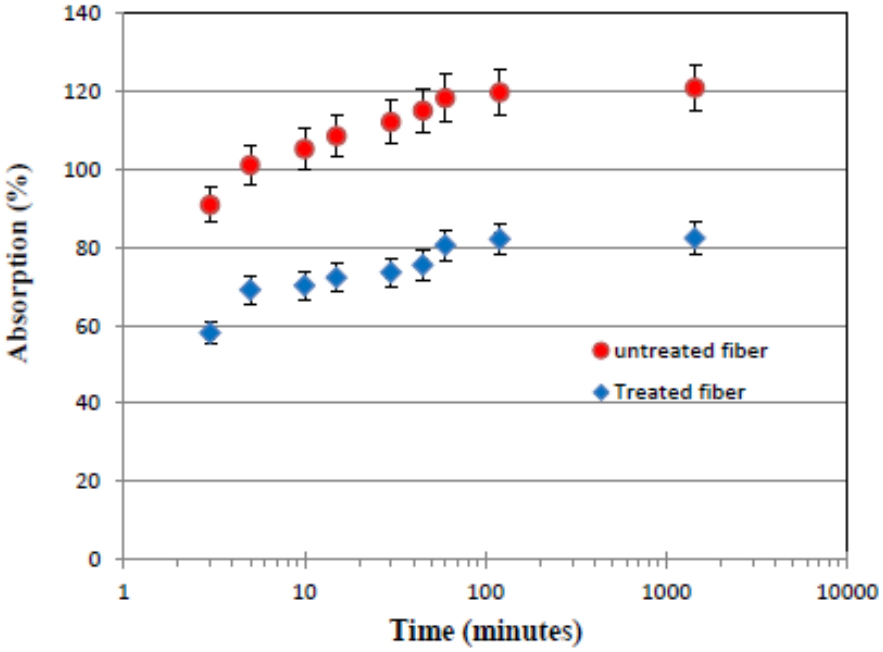

Figure.4.7. **Water absorption of coir fibers**

4.3. Microstructure analysis

The microstructure analysis was based on scanning electron microscopy (SEM), with backscattered electron image and energy dispersive spectroscopy (EDS). Examination of the fracture surface morphology of fibers and fiber surface by using these tools will provide accurate observations.

4.3.1. Surface morphological characterization

The morphology of the fiber and their diversity of size are shown to characterize coir fibers obtained after manual selection. Figure 4.8 showed the micro-optical observation of both untreated and treated coir fibers bundle. Untreated coir fibers apparently contain impurities such as wax, fatty substances and globular protrusions [Rout, 2000]. There were significant differences in the fiber morphologies after treatment compared to untreated ones.

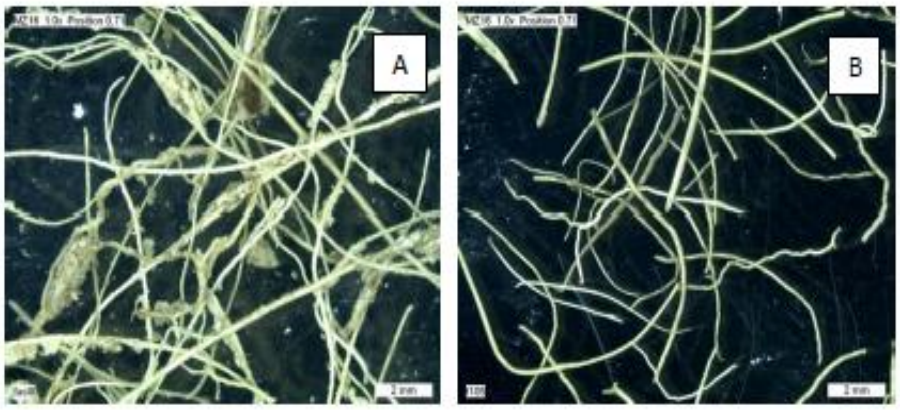

Figure.4.8. **Untreated (A) and Treated (B) of coir fibers.**

It is observed that treatment makes the fibers cleaner and reduces their surface roughness with almost all impurities removed from the fiber surface. The treatment removes wax and cuticles at the surface resulting in a smoother interface. Figure 4.9 shows the SEM micrograph of the untreated raw coir fiber bundle. The fiber surface appears to be smooth due to the presence of waxes and oil. However, the presence of pores could be seen on the surface. It shows a rough surface where hemicellulose, lignin and natural wax substances still stick on the surface [Li, Wang and Wang, 2007; Wang and Huang, 2009; Asasutjarita et al., 2009]. On the other hand, treated fiber has a clean and smooth surface as shown in Figure. 4.9. B. Longitudinal depression becomes apparent at the surface [Lumingkewas et al., 2012b]. Coir fibers have a relatively smooth surface (Figure 4.9B), which can suggest a possible poor interaction between the fibers and the matrix.

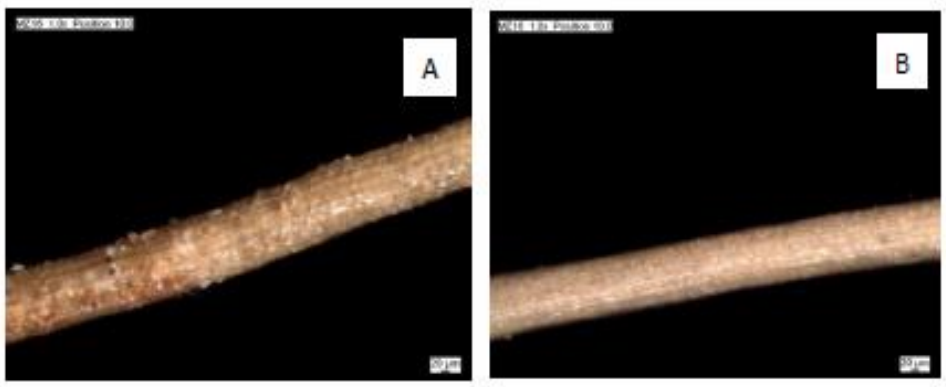

Figure.4.9**. Micro-optic of untreated (A) and treated (B) single coir fiber**

Morphology of untreated coir fiber and treated coir fiber are shown in Figure 4.10 with three different sizes magnitude (x100, x300 and x1000) using the SEM micrograph. On the surface of the untreated coir fiber, particular silica groups represented by white dots are found.

These silica crystals have formed in the locations of the interaction between the surface of the fiber and the pith of coconuts. On the other hand, the SEM micrograph of coir fiber after treatment there was a reduction in the silica particles as shown in Figure 4.25F at x1000 magnification. The removal of surface impurities on coir fibers is advantageous for fiber–matrix adhesion as it facilities both mechanical interlocking and the bonding reaction.

The morphological characterization provides useful information on the characteristics of fiber surface and internal structure, which will be helpful in predicting fiber interaction with the matrix [Castro et al., 2012].

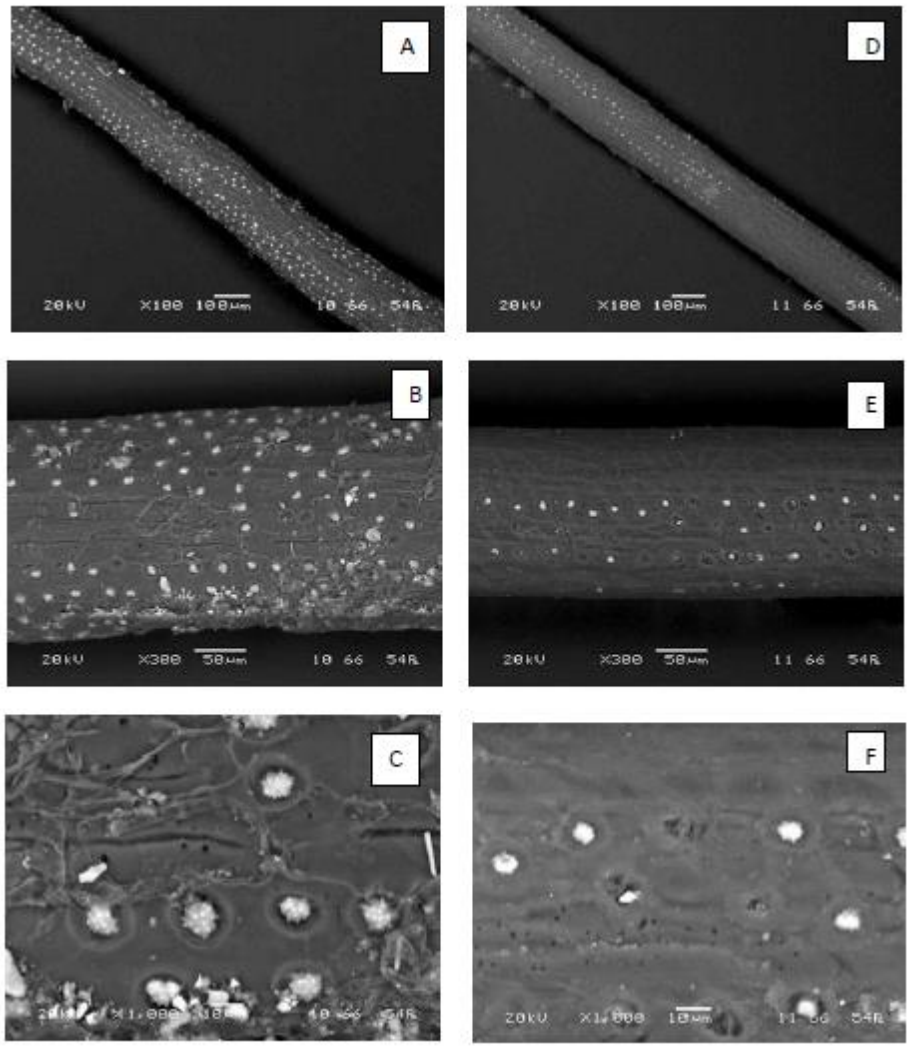

Figure.4.10. **SEM micrograph of surface untreated coir fiber (A. x100; B x300; C. x1000) and treated coir fiber (D. x100; E. x300; F. x1000).**

4.3.2. Energy dispersive spectroscopy analysis.

SEM observations on treated fibers show small white protrusions or bumps on the surface. EDS (Energy dispersive spectrometry) analysis tells us that these white bumps present dominant silica content as illustrated in figure 4.11; 4.12 [Lumingkewas et al., 2012a]. SEM observations of other white bumps with the little amount of silica are shown in Figure 4.13; 4.14. The amount of oxygen represents the largest percentage of mass for both treated and untreated fibers. The results of the chemical composition of coir fiber in the spectrum of 1 and 2 using EDS are shown in Table 4.1; 4.2. EDS analysis of the chemical elements of the white dots is shown in Figure 4.15. They mainly consist of carbon, silica and oxygen.

The natural fibers are mainly built of cellulose, hemicellulose, lignin and wax. Those elements consisted of carbon, oxygen and hydrogen elements. In the general case, high electron intensity of carbon and oxygen are detected while that of others substances like siliceous, potassium, sodium, magnesium, calcium, iron, aluminum, sulfur and phosphorus are also found in smaller quantities [Jústiz-Smith et al., 2008]. In the present case, only siliceous is found among those other elements.

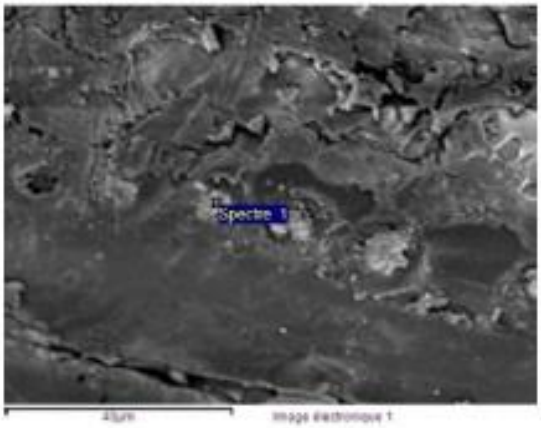

Figure.4.11. **The surface of treated fiber with the white dots spectrum 1**

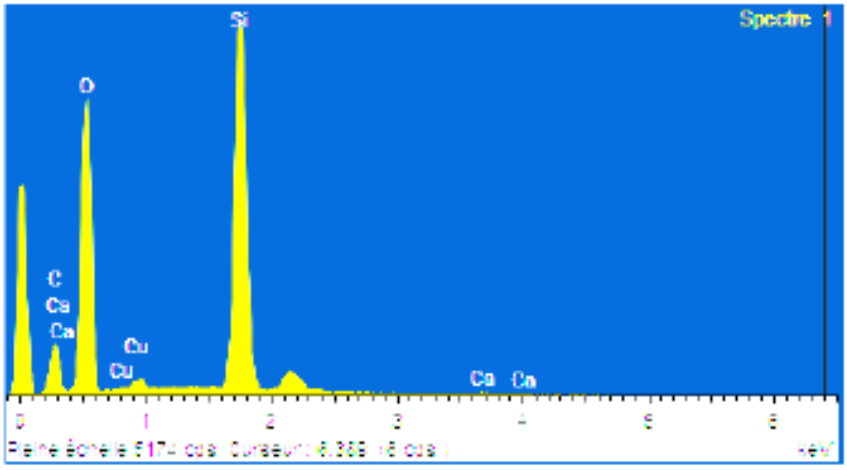

Figure.4.12. **EDS analysis of the white dots spectrum one characteristics**

Table 4.1 **Chemical composition of Coir Fibers at Spectrum one by EDS**

Element	Mass (%)
C K	20.09
O K	53.25
Si K	24.77
Ca K	0.35
Cu L	1.55
Total	100.00

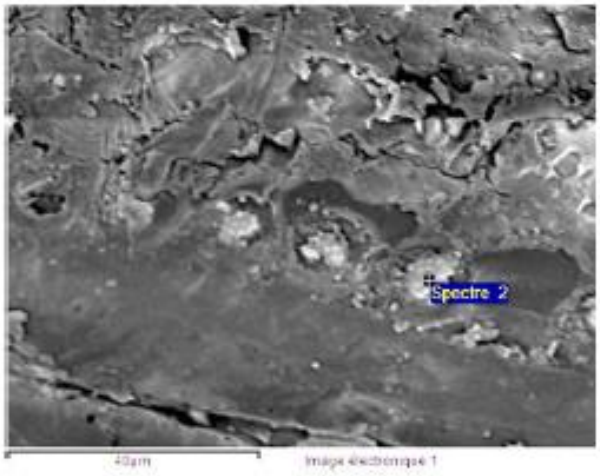

Figure.4.13. **The surface of treated fiber with the white dots spectrum 2**

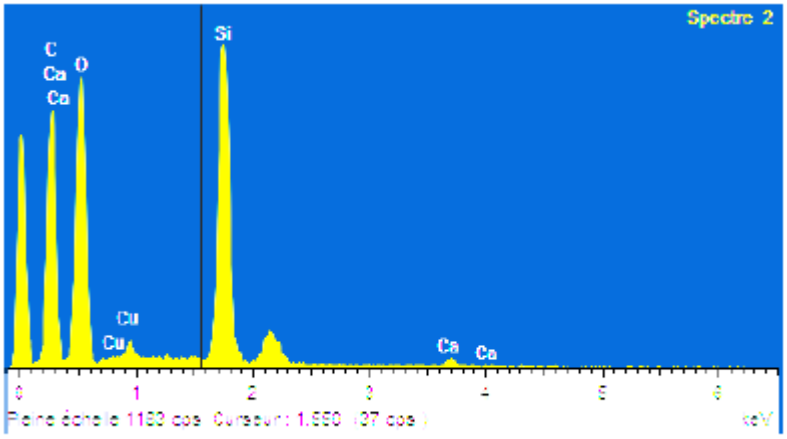

Figure.4.14. **EDS analysis of the white dots spectrum two characteristics**

Table 4.2 **Chemical composition of Coir Fibers at Spectrum two by EDS**

Element	Mass (%)
C K	44.10
O K	40.26
Si K	13.10
Ca K	0.90
Cu L	1.63
Total	100.00

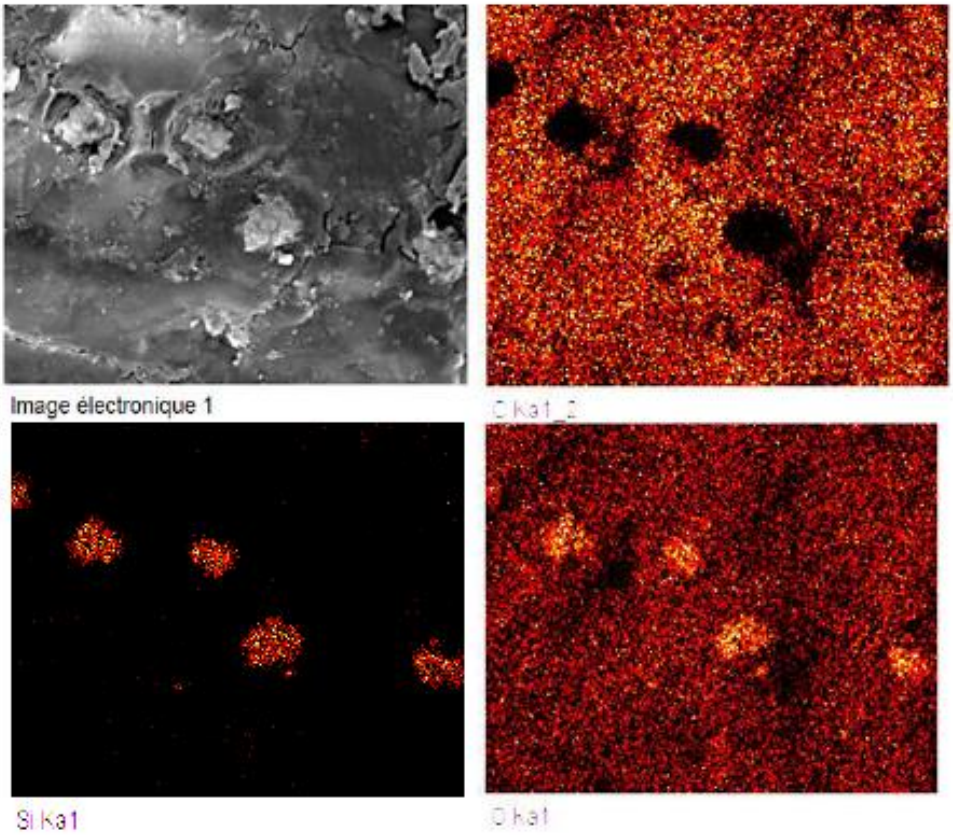

Figure.4.15. **EDS analysis of the element chemical of the white dots characteristics**

4.3.3. Fracture surfaces observations.

Scanning electron microscopy was used to examine the fracture surface and the polished surface of fibers and fractured fibers morphology as shown in Figure 4.16 for untreated coir fiber, and 4.17 treated coir fiber cross-sections. The images of the internal morphologies of the coir fibers reveal a hollow porous structure. Fiber pores are smaller after treatment. That leads to the measurement of fiber diameter nearly 20% smaller than the one of the untreated fibers (Figure 4.18).

These images show different surface morphologies. It also shows images of sections of various fibers (Figure 4.16) to characterize fibers cells and to compare them with those observed in the literature. It appears that studied fibers represent bundles of glued individual fibers (here the cells). These two images

were chosen to show the section of coir fiber at different scale magnification. The first, Figure4.16 at this scale x 100, we can see the cells of the fiber and air gap in their center.

In the second image is shown after x1000 magnification (Figure 4.17), the section of the fiber at a major scale is observed and allows seeing with more details the different cells of the fiber. We can see the wall of one of the cells of the fiber that has been extracted during the fracture of the fiber.

The fractured cross section obtained after the fiber tensile strength test is shown in Figure 4.19 using the SEM micrograph. In one fiber bundle, there are several single fibers in the form of a spiral. These spiral fibers induce large elongation at break and can explain the ductile properties of coir fiber bundles.

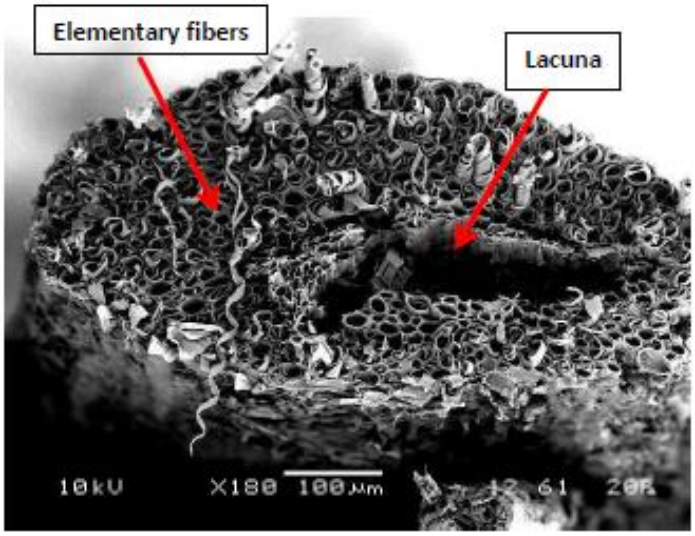

Figure.4.16. **SEM image of cross-section of a typical coir fiber at x100**

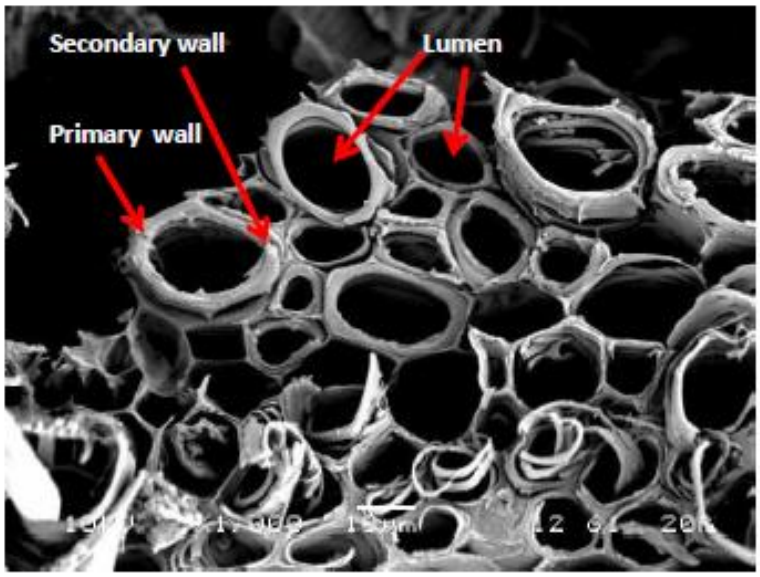

Figure.4.17. **SEM image of elementary fibers which show different lumen and cell wall of coir fiber at x 1000.**

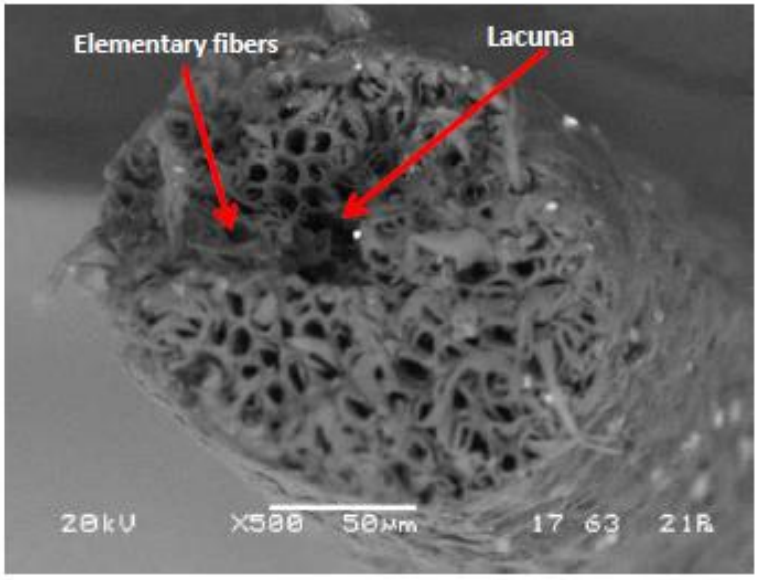

Figure.4.18. **SEM image of cross section of treated coir fiber at x500**

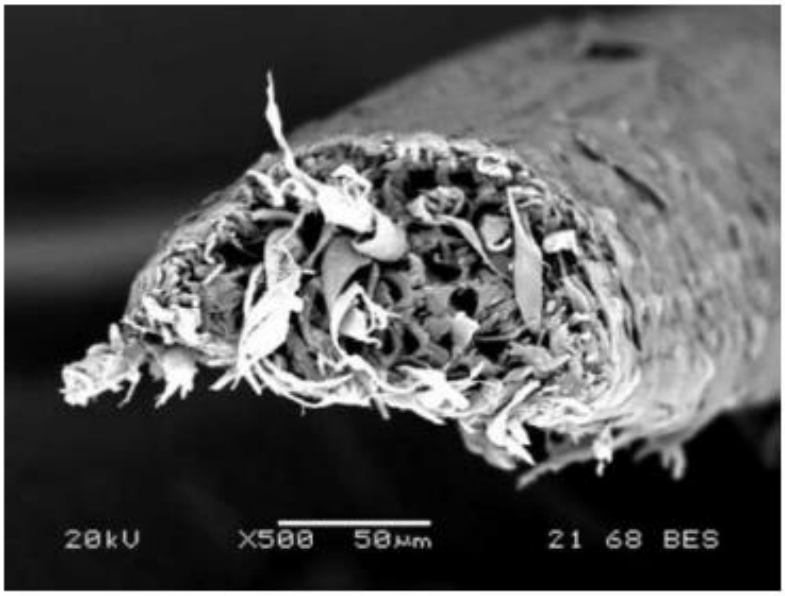

Figure.4.19. **The SEM micrograph of the cross section of treated coir fiber at x500 after tensile stress**

4.4. Thermogravimetric analysis

The results of thermogravimetric analysis (TGA) for untreated and treated coir fibers are shown in Figure 4.20and Figure 4.21. TGA curve, DGA (Derivative of TGA) curve, and Heat Flow curve result are summarized in Table 4.3.

The thermal resistance of the fiber is affected by its chemical content. Coconut fibers are characterized by higher lignin content and consequently stronger aromatic properties [Frollini, 2013]. The chemical characterization of the fibers, as expected, present three major components (known as natural fibers) which are cellulose, hemicellulose and lignin [Fengel et al., 1984]. Deviations from literature [Satyanarayana et al., 2007] could depend on several factors such as soils, weather conditions during growth and harvesting and harvesting time. Many other factors could affect the fiber composition as pre-treatment performed during harvesting or extraction of the primary product [Sousa et al., 2004].

The TGA curves of the heat is treated fibers under nitrogen atmosphere also exhibited a similar pattern than the TGA curves of untreated coir fibers

reported in the literature [Tomczak et al., 2007] and performed under an oxygen atmosphere.

Table 4.3 **Thermogravimetric results for coir fibers**

Coir fiber	Transition temperature range (°C)	Temperature of maximum rate of weight loss (°C)	Weight Loss (%)	Residual Weight (%)
Untreated	30 - 130	84.07	7.93	92.03
	130 - 280	278.45	18.36	73.67
	280 - 750	344.33	74.19	25.47
Treated	30 - 130	71.57	4.10	95.87
	130 - 750	344.17	72.13	23.74

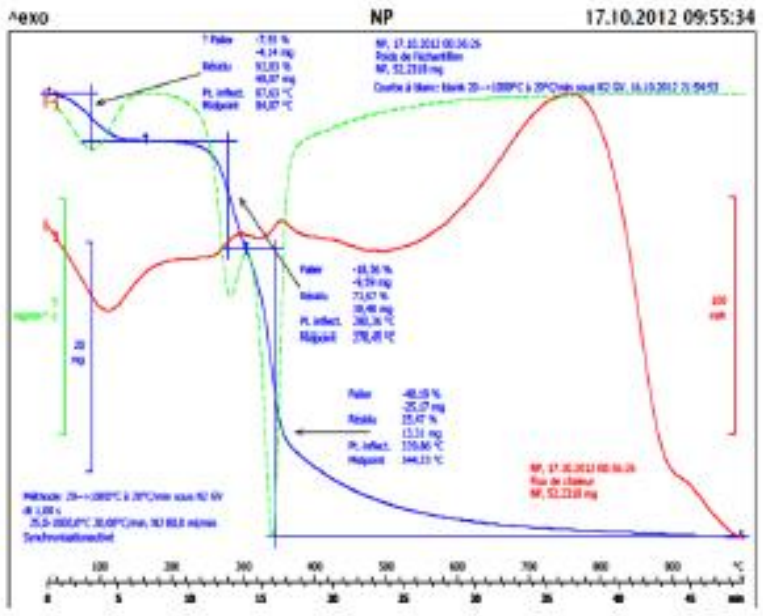

Figure 4.20 **TGA curves of the heated untreated coir fibers under nitrogen atmosphere**

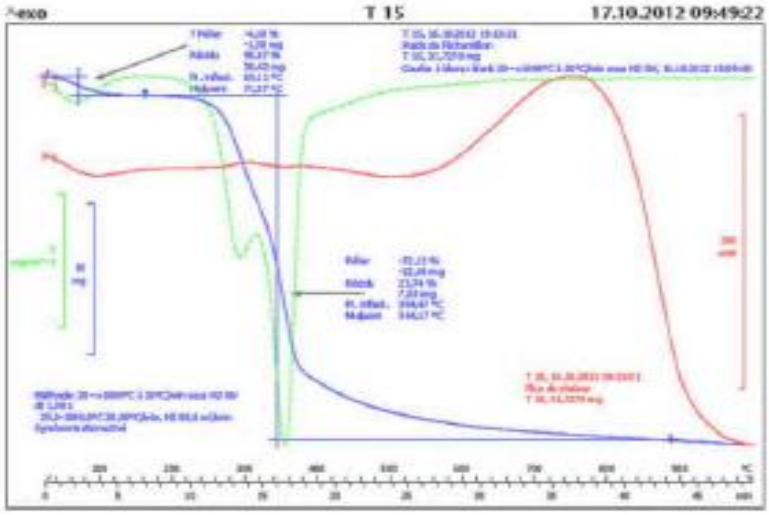

Figure 4.21 **TGA curves of the heated treated coir fibers under nitrogen atmosphere**

4.4.1. Residual weight

The initial weight loss with the temperature ranging from 30 °C to 130 °C is due to dehydration and can be considered beneficial to processing as it makes the fiber more flexible and easy to buckle [Ndazi et al., 2006]. The residual weight of coir fibers is strongly decreased for temperature ranging from 130 °C to 280 °C. Then, from 280 °C to 800 °C the residual weight slightly decreases. Figure 4.22 shows the TGA of treated and untreated coir fibers under a nitrogen atmosphere.

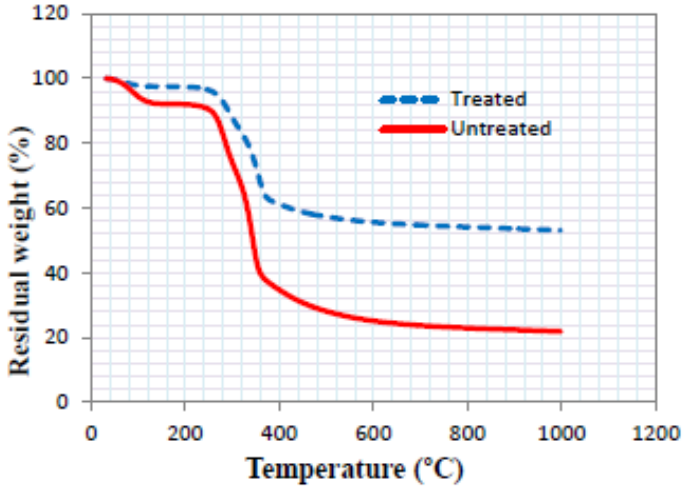

Figure 4.22. **TGA curves of the heated treated and untreated coir fibers under nitrogen atmosphere**

The increase in thermal stability has been associated with an increase in stiffness of the fiber and a decrease of amorphous hemicellulose. Condensable components responsible for the fiber plasticization can also be the reason for the large decrease in tensile strength and elongation at break, but also of the high sensitivity of the materials to temperatures and durations of heating. Thermal stability is influenced by chemical interaction within the fiber; it can be linked to the effect of the heating on the tensile properties of the fiber.

4.4.2. Derivative weight

To evaluate the thermal stability of the coir fibers, TGA is performed. Then, TGA and DGA curves are reported in Figure 4.23. TA-software is used to obtain the derivative of TGA curves (DGA).

Thermal decomposition parameters were determined from the TGA curves at a heating rate of 20 °C/min. In the present study, decomposition of the untreated coir fiber shows several stages, indicating the presence of various components that decompose at different temperatures. Due to the differences in the chemical structures of lignin, cellulose and hemicellulose they usually decompose at different temperatures. The degradation processes occur successively to water desorption, hemicellulose, cellulose, and lignin.

In this study, a small weight loss was found in the range of untreated 30 °C to 70 °C and treated 30 °C to 50 °C due to the evaporation of water or low molecular weight compounds. At approximately 50–70 °C all fibers present 2–3% of weight loss due to the absorbed water [Paiva and Frollini, 2006; Megiatto et al., 2007]. Moreover, they are thermally stable up to 130–250 °C, which can be considered to be the maximum processing temperatures because of the negligible weight loss. At higher temperatures, hemicellulose decomposition occurs at 150 °C to 280 °C followed by cellulose degradation at 280 °C to 350 °C. Lignin starts to deteriorate at approximately 350 °C to 750 °C, due to cleavage of aromatic rings and generation of several products such as water, methane, carbon monoxide and carbon dioxide [Megiatto et al., 2007]. This process occurs in a wide temperature interval due to the involved degradation of lignin with respect to cellulose and hemicellulose since lignin presents a reticulated structure [Tomczak et al., 2007].

The DGA shows that untreated coir fiber with the degradation of the cellulose component degrades at 300 °C, and lignin begins its thermal decomposition at 350 °C and persists until 750 °C. These results are similar to other natural fibers as reported in the previous article [Abraham et al., 2013].

Here the degradation of treated cellulose exhibits an upper value of 354 °C which slightly differs from the cellulose embedded in the untreated coir fibers (338 °C). This reduction in the degradation temperature is due to the presence of strong lignin–cellulose complex that exists in raw coir fiber. Raw coir fiber has a lignin content of 45–50% of weight [Abraham et al., 2013].

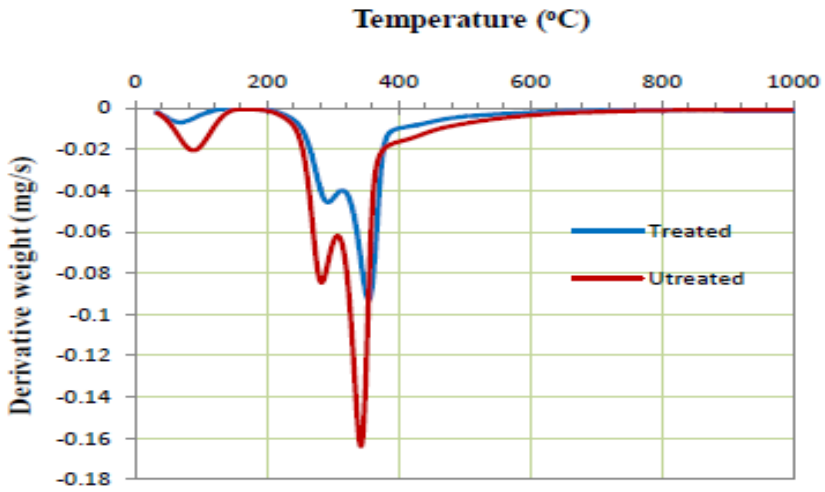

Figure 4.23. **DGA curves for the heated treated and untreated coir fibers**

4.4.3. Heat flow

Heat flow for untreated and treated coir fibers are presented in figure 4.24. Treated coir fiber heat flow is more stable than for untreated coir fiber. The transition temperature of coir fiber ranges from 30 °C to 750 °C.

The increase in thermal stability has been associated with an increase in stiffness of the fiber and loss of the amorphous hemicelluloses. On the other hand, no condensable components responsible for the fiber plasticization can also be the reason of not just considerable decrease of tensile strength and elongation at break but also of the high sensitivity of the properties to temperatures and durations of heating. Thermal stability is influenced by chemical interaction inside the fiber and can be linked to the effect of heat treatment on the tensile properties of the fiber.

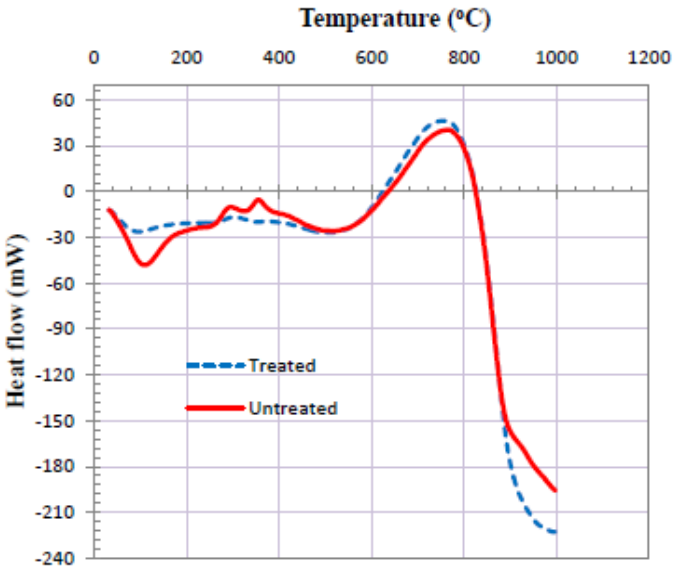

Figure 4.24. **TGA curves of the heated treated and untreated coir fibers under nitrogen atmosphere**

4.5. Mechanical properties

Means of tensile tests obtain mechanical properties carried out on single fiber bundles. They are performed to get the tensile strength, the elastic modulus (in the linear part) and the elongation at break. These values were compared for untreated and treated samples to assess the treatment influence on the mechanical properties of coir fibers.

4.5.1. Tensile strengths

Single fiber tensile properties are critical for the efficiency of fibers to be used as reinforcement in concrete composites. These fibers properties directly affect the behavior of the composites. Given mechanical properties, treated coconut fibers present better tensile strength compared to untreated ones. Typical tensile stress versus strain of coconut fiber is shown in Figure 4.25. For the tested size of 50-99 mm in diameter, differences are significant between treated and untreated fibers. Treated fibers have about 87.4% higher tensile strength and 119.4% more failure strain. Tensile test results show that fibers behavior is linear elastic until the axial strain reaches 0.03 (mm/mm). Then, the fiber behavior loses is linearity and the fibers finally broke. The strain failure value of 0.62 shows the ability of the coconut fibers to exhibit ductile behavior.

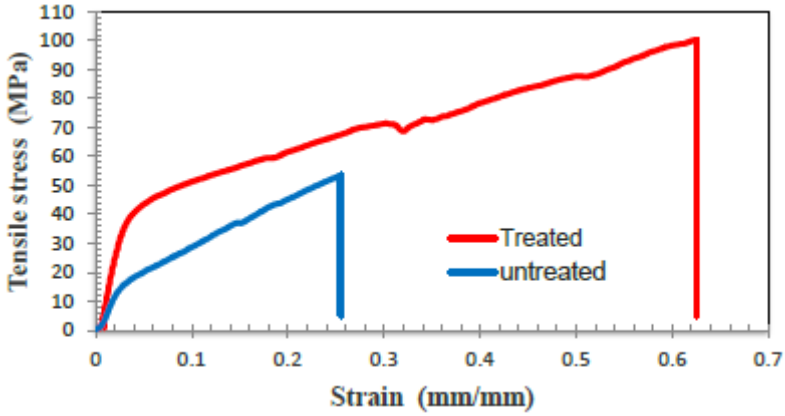

Figure 4.25. **Tensile stress vs. strain curve of the coir fiber**

Partial vanishing of wax, hemicellulose and lignin on the surface of treated fibers has led to higher fiber tensile strength [Hemsri et al., 2012]. Besides pretreatment contributed to higher strength, this partial vanishing of surface impurities allowed for a better and more homogeneous distribution of stress along the fiber diameter. It states that the coconut fibers present an extremely ductile behavior. This result has also been obtained in previous works on the same topic [Munawar et al., 2007; Li Z., 2007; Rao and Rao, 2007]. The tensile properties measured in the present work are in agreement with various earlier investigations [Romildo, 2005].

Figure 4.26 illustrates the effect of the fiber diameter on the tensile strength of coconut fibers. It can be seen that the diameter of 100-149 micrometer gives the highest tensile strength values than other diameters. That can be attributed to the fiber brittleness and defects caused by the coconut growth for diameter higher than 150 μm.

From the tensile test results for treated and untreated fibers, it appears that there is a correlation between fiber diameter and tensile strength. Equation gives formulation for untreated fibers (4.5):

$$\sigma_f = -11.429 D_f^4 + 161.68 D_f^3 - 797.32 D_f^2 + 1568.1 D_f - 845.7 \quad ..... (4.5)$$

While the formula for the treated fibers is given by equation (4.6):

$$\sigma_f = 13.2 D_f^4 + 191.83 D_f^3 - 963.7 D_f^2 + 1916.5 D_f - 1033.9 \quad .....(4.6)$$

Where σ_f is the tensile strength and D_f is the Diameter of fiber.
Figure 4.26 confirms that treatment of fibers increases the tensile strength of coconut fiber whatever the fiber diameter is.

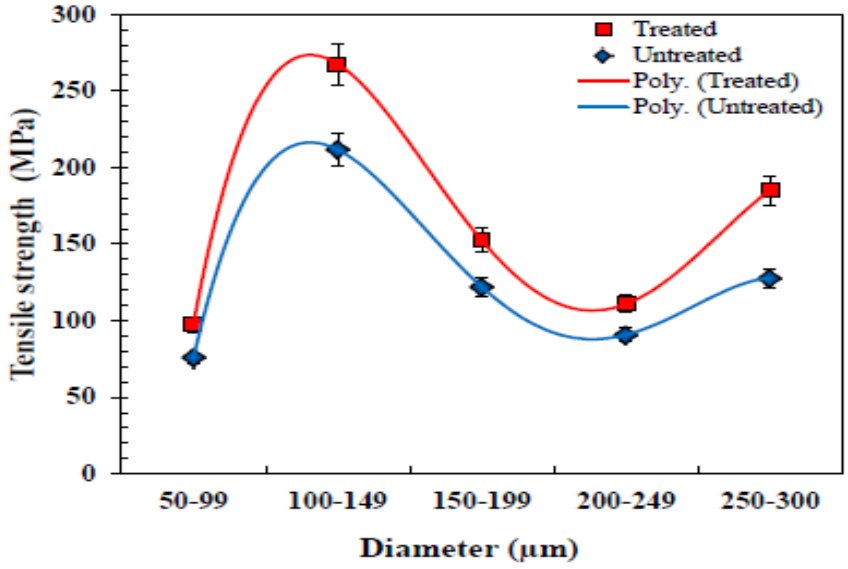

Figure.4.26**. Diameter versus Tensile strength of untreated and treated coir fibers**

4.5.2. Young's modulus

The Young's modulus is plotted in Figure 4.27 as a function of the diameter of coir fibers. The large distribution of the measuredYoung's modulus may be due to the cross section of coconut fibers are not perfectly circle, but ellipsoidal. Moduli of elasticity for the untreated fibers were found to range between 1 and3 GPa. While treated fibers exhibit elastic moduli ranging from 2 to6 GPa. These values are in the range reported in the literature for the diameter of 100-149 µm, [Tran LQN et al., 2014], [Ali M et al., 2012], [Defoirdt N et al. 2010], [Li et al., 2007], [Toledo et al., 2005].

From the tensile test results for treated and untreated fibers, it appears that there is a correlation between fiber diameter and Young's modulus. For untreated fibers, the Young modulus evolution is well described by Equation (4.7):

$$E_f = -0.1455D_f^{\,4} + 2.0252\,D_f^{\,3} - 9.8395\,D_f^{\,2} + 18.936D_f - 9.732 \quad \text{..... (4.7)}$$

While for treated fibers, the Young modulus evolution is well described by Equation (4.7):

$$E_f = 0.311\,D_f^{\,4} + 4.2982D_f^{\,3} - 20.879D_f^{\,2} + 40.685D_f - 22.29 \quad \text{.....(4.8)}$$

Where E_f is the Young's modulus and D_f is the Diameter of fiber.

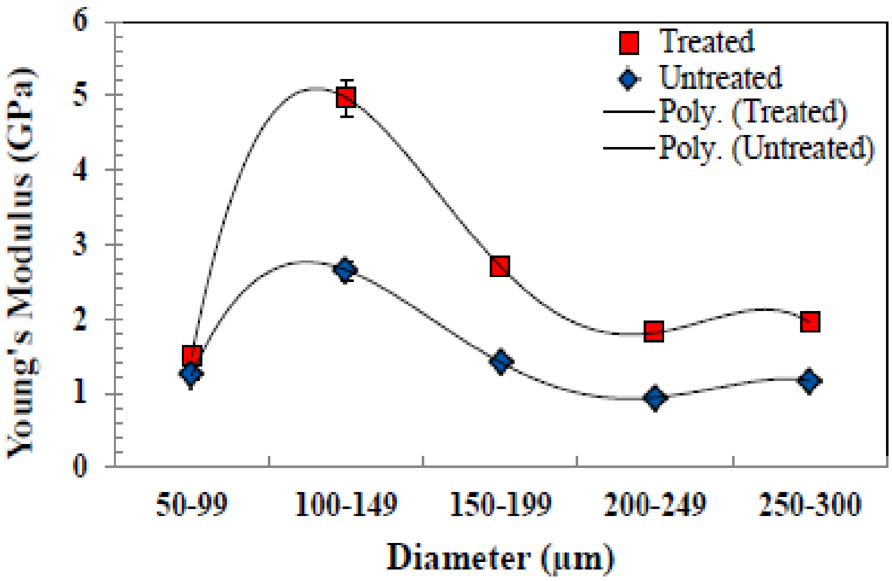

Figure.4.27**. Diameter vs. Young's modulus of coir fibers**

4.5.3. Elongation at break

The elongation at break (ε) of untreated and treated fibers versus their diameters is shown in Figure 4.28. Elongations at break of the treated fiber are higher than the untreated fibers ones for the same diameter. Also, it seems that there is a linear relationship between elongation at break and fibers diameter.

The graph in Figure 4.28 gives the evolution of elongation at break regarding the fibers diameters. This evolution of elongation at break can be written as follow for untreated fibers with $R^2 = 0.9793$:

$$\varepsilon = 10.53\ D_f + 20.23 \quad \text{...(4.9)}$$

The same type of equation can also be written for treated fibers with $R^2 = 0.9437$

$$\varepsilon = 12.059\ D_f + 26.25 \quad \text{..(4.10)}$$

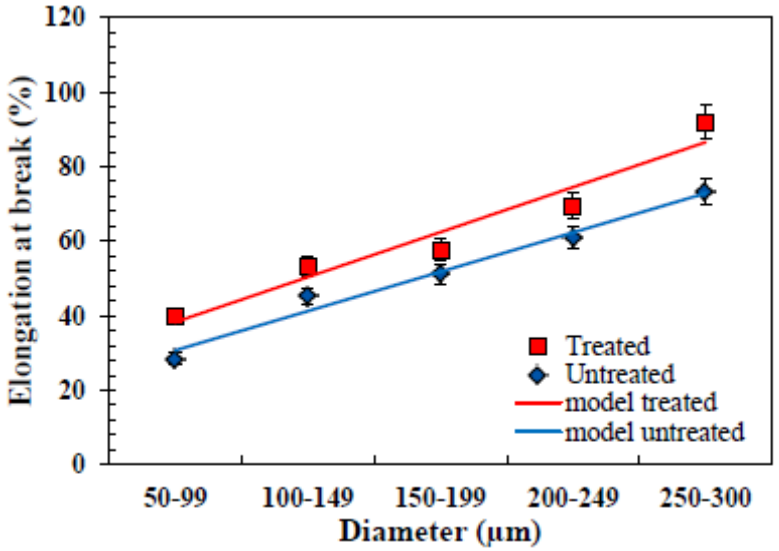

Figure.4.28**. Diameter vs. Elongation at break for coir fibers**

The mechanical properties of treated and untreated coconut coir fibers are reported in Table 4.4. It presents the results of coco fiber from other countries without reference to the size or diameter of the fibers. Indonesian coir fiber has the highest value of elongation at break. Similarly, the values of tensile strength are greater than the one of coir fiber coming from other countries.

Table 4.4 **Mechanical properties of treated and untreated coir fibers**

Properties	**Tensile strength [MPa]**	**Elongation of break [%]**	**Diameter [µm]**	**Reference**
Coir untreated	211.7	51.13	100-149	
Coir treated	267.7	62.55	100-149	
Indonesia coir	218.25	46.02	-	[Bakri, 2010]
Brazil coir	75.0	29.5	-	[Silva et al. 2000]
Indian coir	175.6	34.0	-	[Kulkarni et al. 1981]
Tanzania	68.4	21.2	-	[Ezekiela et al., 2011]

4.7. Conclusions of chapter

The conclusion shows that the treatment of coir fibers increases the tensile strength and delivers higher value to the elongation of a break than the ones of untreated fibers. Average tensile strength of treated fiber is as twice greater than the one of untreated. Based on these results, coir fiber after treatment presents an improved ductile. Indonesian coir fiber has ductile properties suitable for use as reinforcement in concrete composites with high ductility.

The treatment significantly removes impurities on the fiber surface, resulting in surface modification and improved thermal stability. TGA measurements revealed that the treatment of fibers has a positive impact on the thermal stability of the sample.

SEM observation shows that water treatment has a significant impact of on the surface of the fibers (removing impurities, decreasing the siliceous compounds content) and decreases the average diameter of the fibers. These changes in fiber structure induce an improvement of the macroscopic behavior of the fibers.

CHAPTER.5.
DESIGN, RHEOLOGY PROPERTIES, MICROSTRUCTURE, AND RHEOLOGY MODEL OF PRODUCT EXTRUDED FIBER COMPOSITES

5.1. Introduction

This study aims to obtain extruded building materials with low environmental impact. Mortar/cementitious is the basic ingredient of concrete used in this study that is made with cement, sand and clay. The mortar based materials are reinforced with natural fibers of coconut plants. The use of natural fibers and clay as raw materials are readily available locally at every place in the world. They are sustainable raw material for local construction, and their use reduces transportation, economic costs, and environmental impact.

The tested mix design is a development of the results already obtained. This study is conducted to evaluate the rheology of the coir fiber reinforced cementitious composites (CFRCC). In this section, the effects on the rheology of fiber content, fibers length and percentage of cement are studied. The cement-based materials extrusion technology to set up that is necessary to perform an adequate rheological characterization of the cement-based formulations. The rheological characterization is fundamental for the development of a new extruded product if we take into consideration some basic aspects (mix composition, cost/performances ratio, process parameters).

The process of designing a mixture of cement, sand and clay was studied for different contents of cement. The first study deals with the influence of water/cement ratio in mortar mix to ensure an extruder flow providing hardened extrudates without defects. Rheological properties of the materials were studied. According to Toutou et al. work, extrudability criterion is that the yield stress value should be at least equal to 20 kPa. [Toutou, 2005]. Moreover, mixture extrusion flow needs to be stabilized during processing; local drainage may cause surface defects. A avoid such defects, homogeneous nature of the material during extrusion should still be maintained [Perrot, 2007]. A prediction of the yield stress of coir fiber-reinforced cementitious composite is also proposed, develop the model provided by Ferec et al. [Ferec, 2014].

The final result obtained in this study is the formulation of an extrudate composite taking into accounts the effects of fiber content on the material rheology. After the examination of the fresh concrete is continued in the following chapters an examination of the hard mortar on the chapter 6. The design of composite material used to study the performance of mechanics of materials.

5.2. Mix-Design of low cement content in mortar for extrusion

The formulation of an extrudate paste is performed using a rheometer. The designed cement-based paste should be hard enough to hold its shape once extruded and soft enough to flow inside the extruder. Materials are having a yield stress of 20 kPa meet these conditions [Toutou et al., 2005]. The vane test was used to evaluate this rheological property of the mortar samples. It was carried out using a speed-controlled rheometer equipped with a four-bladed vane, measuring 8.8 mm in width and 10 mm in length. Rotation speed is controlled, and the torque is measured.

The effect of water content on the yield stress of fresh mortar containing various amounts of kaolin and cement is therefore studied to find the optimized mix design for fresh material dedicated to extrusion.

5.2.1. Mix design of an extrudable mortar.

The product development consists in investigating the feasibility of using extrusion technology to fabricate construction products. The best material water/cement ratio must be found to meet criteria of extrudability. If poor shape stability phase migration, excessively high extrusion pressure, or surface defects (usually edge tearing) were observed, the material was considered as not extrudable.

This mix design approach for each studied mixture leads to the sample extrudability. Mixes are tested with superplasticizer/High Range water Reducing Admixture (HRWRA) to reduce the water content and increase mechanical strength [Khelifi, 2013]. The superplasticizer content is1.5% by weight of cement. Different cement to clay/kaolin ratio was tested. The mass proportion of sand is 60%. For extrudate material, the ratios of cement and clay used were at maximum 40%. The material compositions of eight mix designs for the project are summarized in Table 5.1.

Table.5.1. **Mixture proportions of cement, clay, and sand**

Mixture name	Cement (%)	Clay (%)	Sand (%)
K40S60	0	40	60
C5K35S60	5	35	60
C10K40S60	10	30	60
C15K25S60	15	25	60
C20K20S60	20	20	60
C25K15S60	25	15	60
C30K10S60	30	10	60
C40S60	40	0	60

Gradually the water was added to achieve a yield stress approaching 20 kPa. The relationship between water content ensuring such yield stress with cement content is an exponential function as shown in Figure 5.1, with the following formula:

$$W/C = \alpha\, e^{-\beta C} \quad \text{..... (5.1)}$$

Where: W/C is the water/cement mass ratio in percentage, C is the cement content in percentage and α, β is coefisien regretion parametre. For this composition α = 21.532; β = 0.015.

For the composition made with 40% of cement and 60% of sand (C40S60), the amount of water content by weight of cement is W = 0.12. While the composition of 40% of Kaolin and 60% of Sand (K40S60) is the amount of water content by weight cement is W = 0.22. The water content in the clay mortar is almost twice the water contained in the cement mortar. We note that a mixture of 40% cement and 60% clay exhibiting a yield stress of 20 kPa produces a very stiff paste that does not flow under its weight.

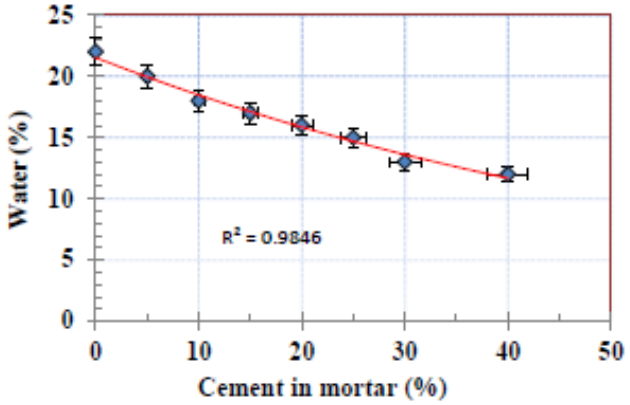

Figure.5.1**. Water content vs. cement content in mortar for a yield stress of 20 kPa**

5.2.2. The water content in clay mortar.

In this part, we study how the torque varies with water content. The mass composition of the mortar mix is made with 40% of kaolin clay and 60% of sand (K40S60). Vane test results showed that the value of the torque increases while some water decreases. Also, the time to achieve the maximum of torque increases when the water content decreases (Figure 5.2).

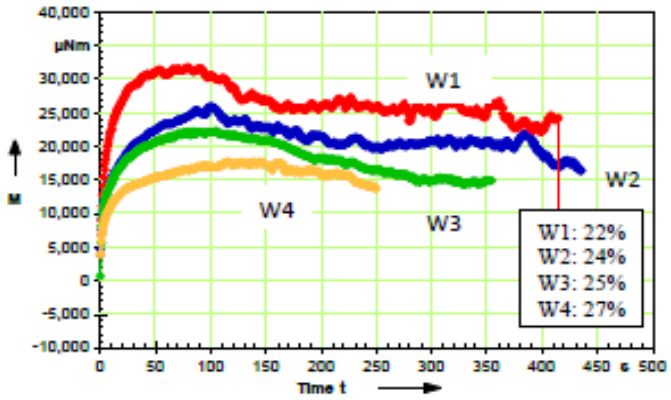

Figure. 5.2. **The torque vs. time curves for clay mortar (K40S60) containing different masses of water**

Rheological properties of the clay mortar (K40S60) showed that increasing water cement on clay will decrease the yield stress (Figure 5.3) and that the following exponential empirical relationship can describe accurately this link ($R^2 = 0.9982$):

$$\tau_{\circ} = \alpha\, e^{-\beta W} \quad \text{.....(5.2)}$$

where $\tau_{\circ}$ is the yield stress (kPa) ; W = Water (%); for K40S60 α = *324.8;* β*=0.119*

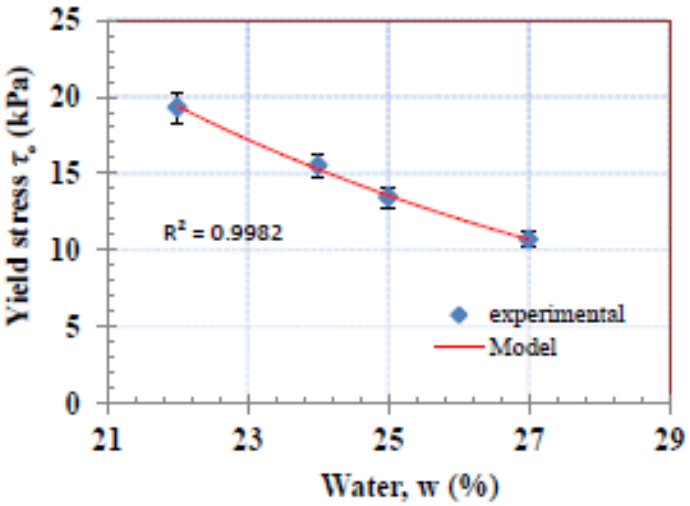

Figure. 5.3**. The yield stresses vs. water content in clay mortar**

5.2.3. Influence water content on cement mortar.

The water content of an extrudible mortar made of 40% cement and 60% sand (C40S60) in mass is searched. A yield stress of 20 kPa is found for a water content of 0.12 as shown in Figure 5.1. The surface aspect of the sample is not smooth. Also, the sample surface presents crack lines. Such aspect does not match extruded criterion on surface texture

Conditions of extruded material with a smooth surface without defects are obtained with the addition of water/cement gradually. According to rheometer tests (section 3.4.4.), a smooth surface for the composition C40S60 is obtained at water content/cement of 0.14. At this water content, the torque measured during the vane test is 20 μNm. Then, using the formula Eq. (3.5) the computed yield stress is 12 kPa.

Similarly to kaolin mortar, vane test results showed that the value of the torque increases while some water decreases. Also, the time to achieve the maximum of torque increases when the water content decreases (Figure 5.4).

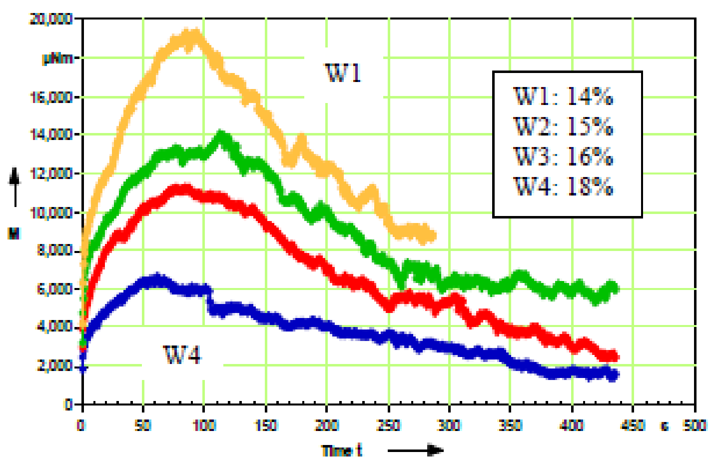

Figure. 5.4. **The torque vs. time curves for cement mortars containing different amount of water**

Rheological properties of the cement mortar (C40S60) showed that increasing water cement on clay will decrease the yield stress (Figure 5.5) and that the following exponential empirical relationship can describe accurately this link (R^2 = 0.9875):

$$\tau_{\circ} = \alpha \; e^{-\beta W} \quad \ldots\ldots\ldots\ldots\ldots\ldots\ldots\ldots\ldots\ldots\ldots\ldots\ldots\ldots \text{(5.3)}$$

Where, τ is the yield stress (kPa), W is the water content in percentage and for C40S60 α = 1238.4 ; β=0.331

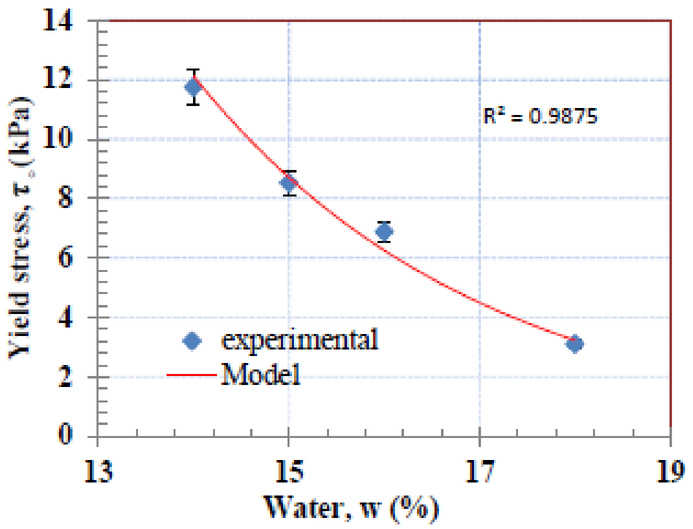

Figure. 5.5. **The yield stresses vs. water content in cement mortar**

5.2.4. The formulation of an extruded fiber reinforced composites.

Low cement content and use of local natural materials are common ways to design an environmentally friendly material. For this reason, the following two compositions (called C1 and C2) are chosen: C10K30S60 made with 10% of cement content and C20K20S60 made with 20% of cement. The yield stress of about 20 kPa was obtained for an amount of water of 0.18 by weight of cement (Figure 5.6). While C2 required a water content of 0.16 by weight of the cement to reach the targeted yield stress (Figure 5.7).

The formulation of the fiber-reinforced mortar composites consists in finding the required water content needed to achieve a 20 kPa yield stress needed for an optimized extrusion. The water content is then kept constant even for composites containing up to 5% of fibers volume content.

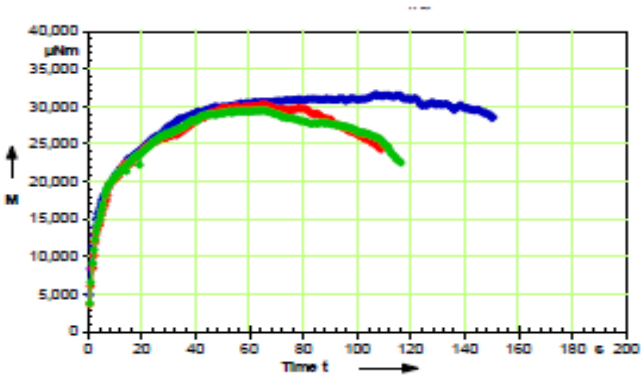

Figure. 5.6. **Torque versus time curves obtained during vane tests mix-design C1 (yield stress of 20kPa)**

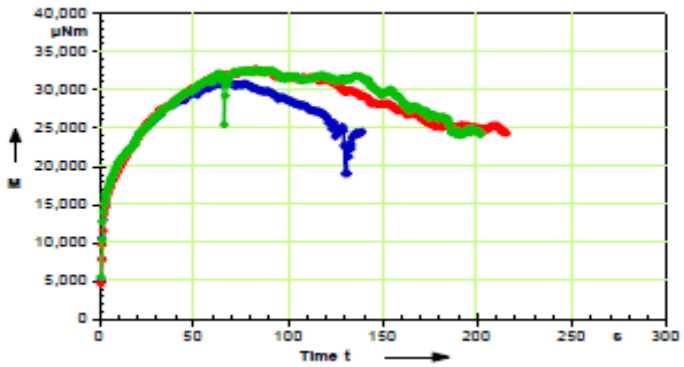

Figure. 5.7. **Torque versus time curves obtained during vane tests mix-design C2 (yield stress of 20kPa)**

During rheological vane tests measurements, torque is the important parameter recorded to compute the properties of cement mortars. This parameter is linearly linked to the material yield stress. For mix-design C1, a water content of 0.21 leads to a maximum recorded torque of 20 µNm (Figure 5.8). Such torque leads to a 13 kPa yield stress that is found to be sufficiently high to ensure stable extruded samples exhibiting surface without defect (Figure 5.9.).

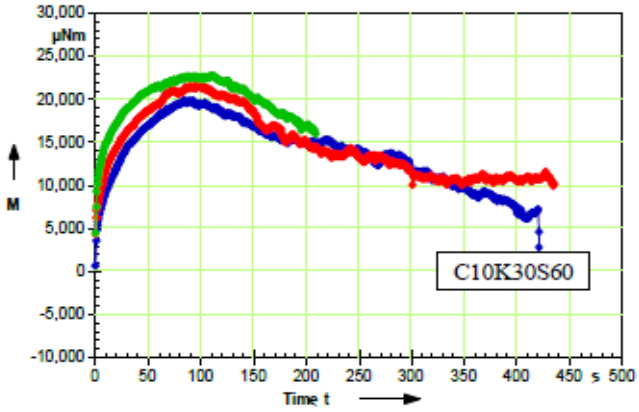

Figure. 5.8. Torque versus time curves obtained during vane tests mix-design type C1

Figure. 5.9. Surface of the extruded mortar type C1

For the mix-design C2, the same observation is made. A water content of 0.19 which leads to a yield stress of 13 kPa (20 µNm see figure 5.10) can provide extrudates which sustains gravity and presents a smooth surface without defect.

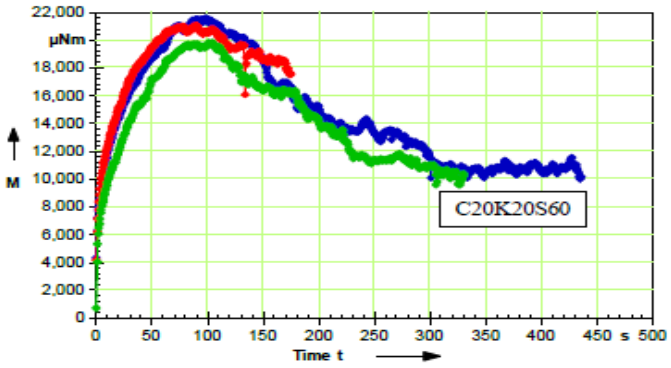

Figure. 5.10. Torque versus time curves obtained during vane tests mix-design type C2.

Figure. 5.11. Surface of the extruded mortar type C2

Figures 5.9 and 5.11 suggest that a yield stress of 13 kPa (maximum torque of 20 µNm) is enough to ensure that the extrudate can sustain gravity after extrusion. Therefore, a maximum torque of 20 µNm is targeted for the mix design procedure.

The figure showing the relationship between water content ensuring a maximum torque of 20 µNm and the cement content is plotted in Figure 5.12. The cement content is linearly decreased when the amount of water content increases. Empirical formula $R^2 = 0.9847$is able to describe this linear link:

$$W/C = \alpha - \beta * C \quad \text{..... (5.4)}$$

Where: W is the water content in percentage, C is the cement in percentage, $\alpha = 24.842$ *; $\beta=0.294$*

Figure 5.13 shows the surface aspect of extruded mortar for a paste exhibiting a yield stress of 13 kPa. We can see that the extrudate surface is smooth.

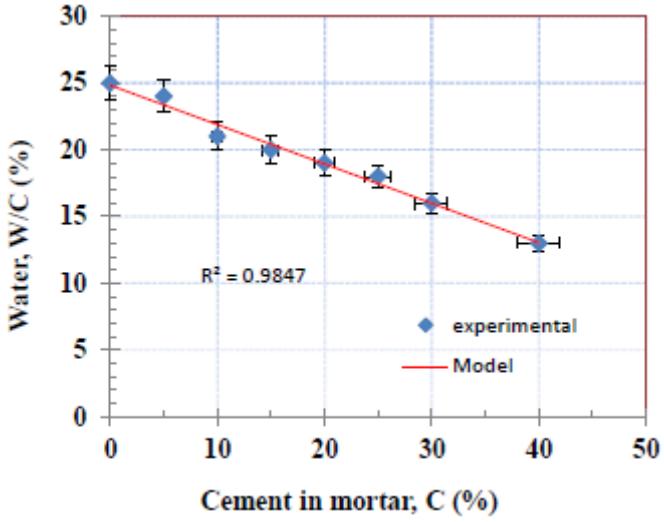

Figure. 5.12. **Water content and cement content in mortar for Torque 20 µNm**

.

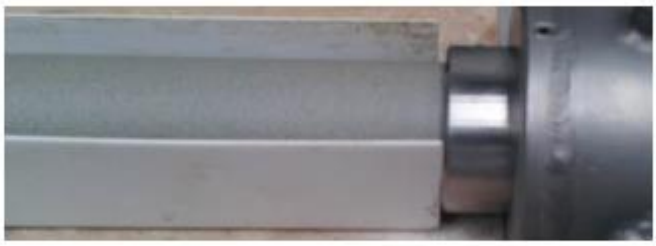

Figure. 5.13. **Surface of the extruded cement mortar**

Table 5.2**. Mix formulation of the coir fiber-reinforced fresh cement mortar for extrusion.**

Composite name	Cement (%)	Clay (%)	Sand (%)	SP (%)	Water (%)	Fiber 5mm (%)	Fiber 10mm (%)	Fiber 15mm (%)
C1-0	10	30	60	1.5	21	0		
C1-2-05	10	30	60	1.5	21	2		
C1-3-05	10	30	60	1.5	21	3		
C1-4-05	10	30	60	1.5	21	4		
C1-5-05	10	30	60	1.5	21	5		
C1-2-10	10	30	60	1.5	21		2	
C1-3-10	10	30	60	1.5	21		3	
C1-4-10	10	30	60	1.5	21		4	
C1-5-10	10	30	60	1.5	21		5	
C1-2-15	10	30	60	1.5	21			2
C1-3-15	10	30	60	1.5	21			3
C1-4-15	10	30	60	1.5	21			4
C1-5-15	10	30	60	1.5	21			5

C2-0	20	20	60	1.5	19	0		
C2-2-05	20	20	60	1.5	19	2		
C2-3-05	20	20	60	1.5	19	3		
C2-4-05	20	20	60	1.5	19	4		
C2-5-05	20	20	60	1.5	19	5		
C2-2-10	20	20	60	1.5	19		2	
C2-3-10	20	20	60	1.5	19		3	
C2-4-10	20	20	60	1.5	19		4	
C2-5-10	20	20	60	1.5	19		5	
C2-2-15	20	20	60	1.5	19			2
C2-3-15	20	20	60	1.5	19			3
C2-4-15	20	20	60	1.5	19			4
C2-5-15	20	20	60	1.5	19			5

All the ingredients are expressed as weight proportion of cement content.

Finally obtained mix designs of low cement content materials are listed in Table 5.2. Composite materials under conditions of constant water/cement content with fibers added to the mix will be then tested. Furthermore, the yield stress of fiber reinforced paste will be measured using the vane test. Compositions C1 and C2 are used to make composites reinforced with fibers. For both Composites, the water/cement (w/c) ratios are 0.21 for C1 and 0.19 for C2. Fibers lengths of 5, 10 and 15 mm; and, fiber contents of 2%, 3%, 4% and 5% (by weight of cement) have been used.

5.3. Morphologies of fresh fiber mortar composite

Analysis of the morphologies of the mortars is performed using optical microscopy. Mortars are first cured for 28 days. Samples were observed after the process of mixing and after extrusion.

Figure 5.14 shows the composite mortar after mixing with a mixer. Fiber placement does not seem to be randomly and well dispersed. Furthermore, to obtain a more compact material with fibers dispersion and forming needs to be performed by screw extrusion.

Observation of the microstructure after the mixer and cured for the fiber concentration of 2% by weight of cement is shown in Figure 5.15, the distribution of fibers in the matrix seems random. The matrix with the fiber concentration of 4% by weight of cement is also shown in Figure.5.17. Another case of fiber concentration of 3% by weight of cement can be also seen in Figure.5.16A with problems of fibers entanglement. However, after further examination, we can see

that each fiber stands alone and can be easily dispersed. As well there are holes or pores as shown in Figure.5.16B. It can be homogeneous after mortar formulations through the process of molding and extrusion processes.

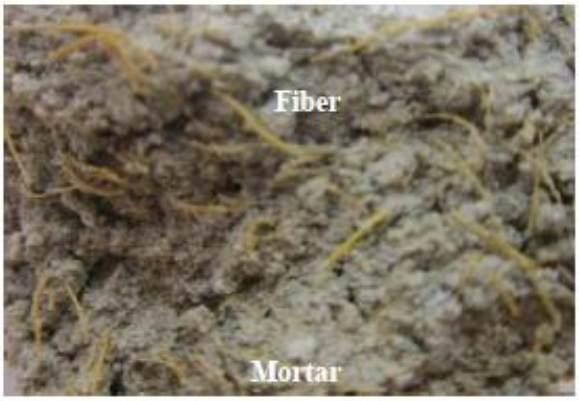

Figure. 5.14. **Morphology of fiber-reinforced cementitious composites after mixing.**

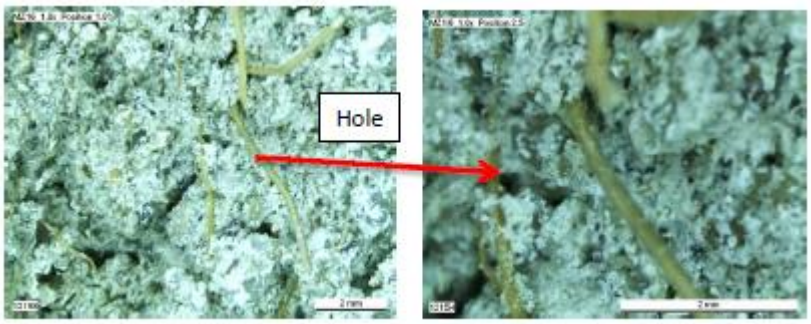

Figure. 5.15. **Morphology of fiber-reinforced cementitious composites, fiber content 2%**

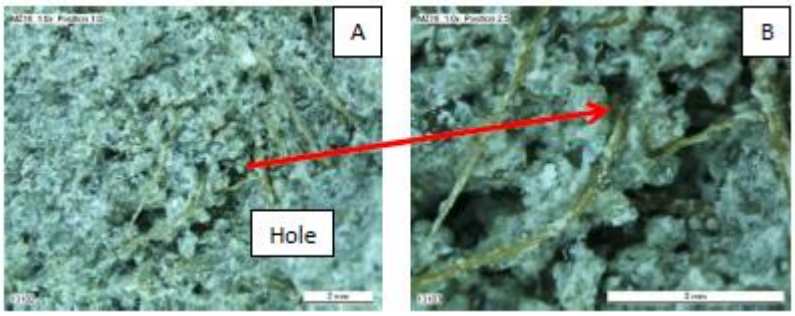

Figure. 5.16**. Morphology of fiber-reinforced cementitious composites, fiber content 3%**

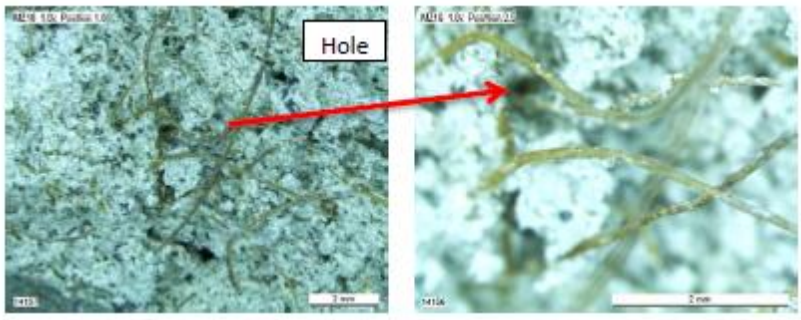

Figure. 5.17. **Morphology of fiber-reinforced cementitious composites, fiber content 4%**

Holes or pores are still visible, either in mortar formulations with low fiber content and high fiber content as shown in Figure.5.15; Figure.5.16 and Figure.5.17. Also, Interfacial microstructure of the fiber and matrix in fresh showed scattered randomly. The fiber out of the matrix indicates wrong position. That means a good adhesion between the fiber and the matrix (Figure.5.18). Similarly, the fibers are embedded in a matrix showing the presence of bonding between the fiber and the matrix (Figure.5.19). Hence, the mortar will become solid after going through the process of compaction in a mold or by screw extrusion.

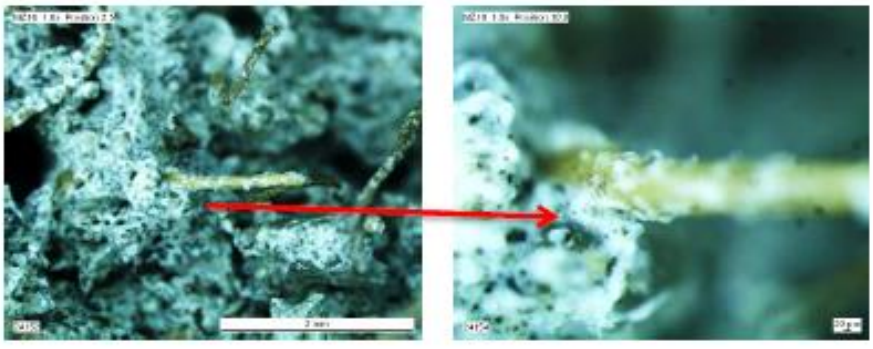

Figure. 5.18. **Microstructure adhesion of fiber out of matrix**

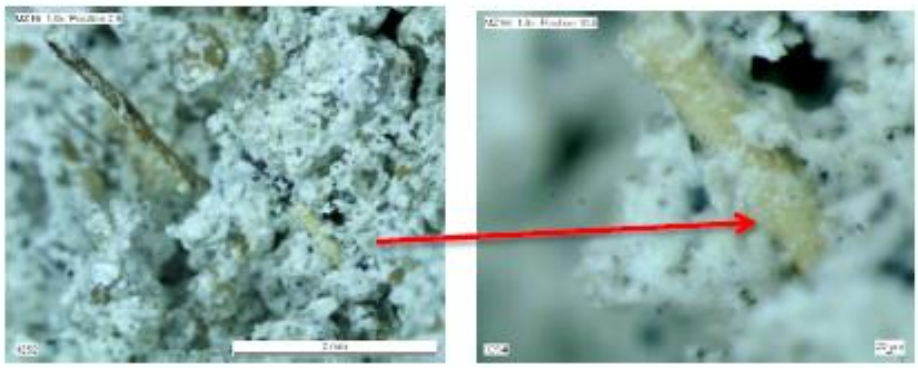

Figure. 5.19. **Microstructure adhesion of fiber embedded in a matrix**

5.4. Rheology properties of fiber mortar composite extrudability

The knowledge and understanding of material extrusion allow rheology to be used for quality control and product development. There is a need for quality control testing through rheology. It is feasible to use the current rheometer to evaluate the rheological behavior of Coir Fibers reinforced mortar composites. It is important to note that for firm paste extrusion, the yield stress is the most relevant parameter that could be used for quality extrusion control. Viscous effects remain limited due to the reliability low shear rates used in firm pastes extrusion.

The flow properties of the fresh material are a key point as fibers can move and to orient due to the concrete flow. Therefore, fibers may induce anisotropic and heterogeneous mechanical behavior that depends strongly on their dispersion and orientation state [Ferrara et al., 2011], [Kang et al., 2011], [Kuder et al., 2010], [Sanal et al., 2013]. It is well established that fiber orientation depends on both process and material rheology [Boulekbache et al., 2010], [Ozyurt et al., 2007], [Kuder et al., 2010], [Martinie et al., 2011], [Perrot et al., 2013]. The previously cited works highlight the yield stress of fiber reinforced concrete is a key parameter controlling and limiting the fibers orientation under flow. Then, some works have been carried out on the effect of fibers on the concrete rheology, [Kuder et al., 2007], [Martinie et al., 2010], [Ghanbari et al., 2009], [Kaufmann et al., 2006], [Li and Li, 2013] and on the prediction of fiber orientation during processing [Martinie et al., 2013], [Laranjeira et al., 2012] [Ferec, 2015].

Published literature on the correlation between cementitious composite rheological properties and fiber volume or dispersion has typically focused on

rigid steel fibers. It has been shown that increasing fiber volume fraction and aspect ratio decreases the workability of cementitious composite materials [Dhonde 2007], [Martinie 2010]. However, there has been no publication using natural fiber /coir fiber for cement mortar composites.

5.4.1. Fiber content and fibers length on torque

The used coir fibers i are almost produced through a process of washing and drying. Such results are obtained in the previous chapter, the used diameter ranges between 50 and 200 µm with a density of 0.86 g / cm3.

The torques recorded during vane test measurements for fresh fiber-reinforced mortar composites with different water, and fiber contents are shown in Figure 5.20 for fibers length of 5 mm, Figure 5.21 for 10 mm and Figure 5.22 for 15 mm. It can be seen that torques of all composites increase with fiber content. It is consistent with the phenomena described in a recent study [Martinie 2011] [Ferec 2015] [Feng 2013].

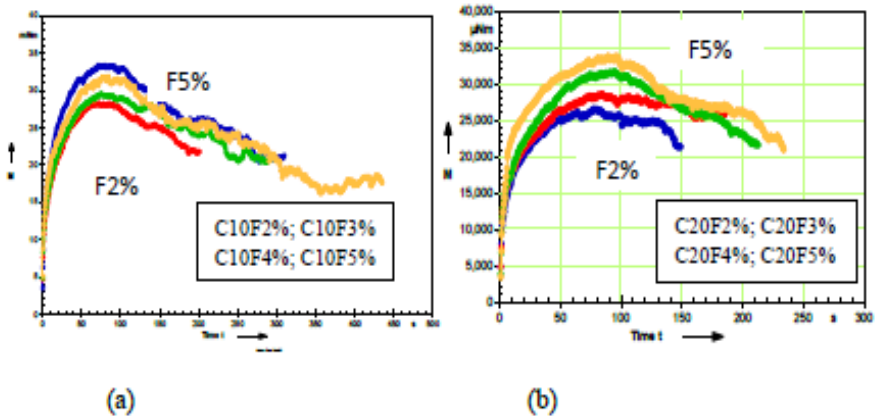

Figure. 5.20. **Torque vs. time for different fiber contents - fibers length of 5mm. (a) C1 and (b) C2**

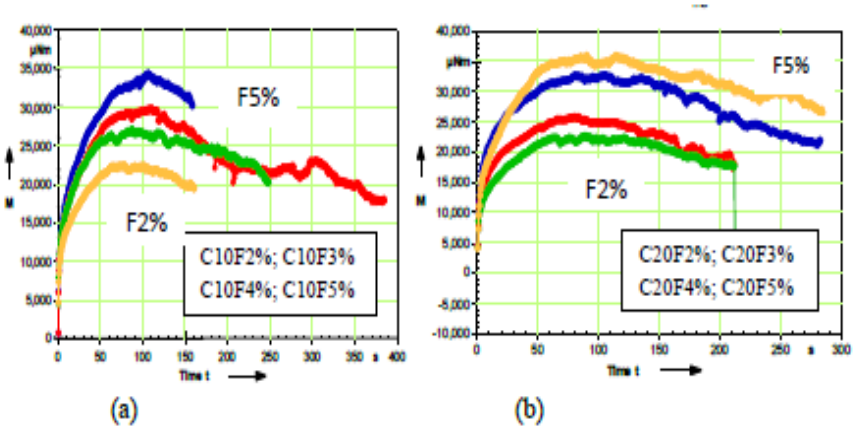

Figure.5.21.**Torque vs. time for various fiber contents - fibers length of 10mm. (a) C1 and (b) C2**

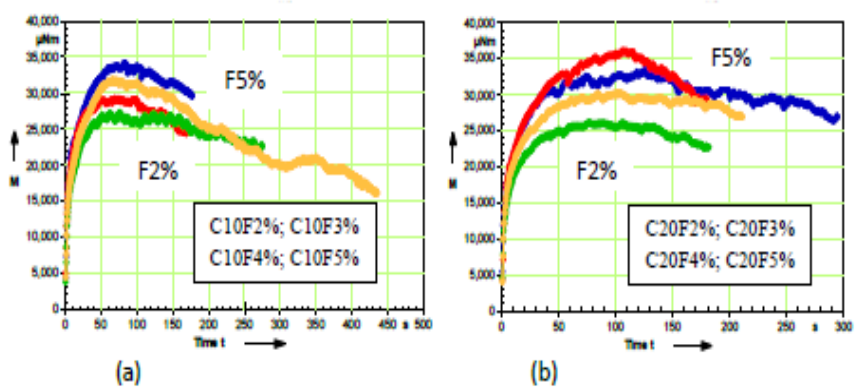

Figure.5.22.**Torque vs. time for different fiber contents - fibers length of 15mm. (a) C1 and (b) C2**

5.4.2. Fibers content and fibers length on yield stress.

The yield stress increases with fiber content and fibers length. The yield stress is plotted against the fiber content, fibers length for both types of the matrix (C1 and C2) as shown in Figure. 5.23 For fibers length of 5 mm, in Figure. 5.24 For fibers length of 10 mm and in Figure. 5.25 For fibers length of 15 mm. In general, the yield stress increases as the fiber content, and fibers length increase. This phenomenon is expected because water–solid mixture with higher water content should require a smaller shear stress to flow. In general, the yield stress for the mix-design type with a cement content of 20% (C2) is greater than the one measured with mixtures containing 10% of cement (C1). In other words, more clay content gives a lower yield stress value.

The combined effects of the fiber content and fibers length has been studied by fitting empirical relationships on experimental data fibers length. The best fitting curves with their equation and correlation coefficient R^2 value are

summarized in Table 5.3. The yield stress formulation is based on tests carried out for matrix C1, C2 and fibers length of 5 mm, 10 mm and15 mm with fiber contents of 2%, 3%, 4% and5%. The used empirical relationship can be written as follow:

$$\tau_{yc} = \alpha * e^{\beta Fc} \quad \text{..... (5.5)}$$

where: *Fc* is the fiber content (%); τ_{yc} is the yield stress (kPa); α, β are fitting parameters.

Table.5.3. **Fitting parameters values for the tested materials**

Mixture name	Fiber length (mm)	Correlation coefficient	Parameter α	Parameter β
C10K30S60 (C1)	5	0.9669	11.710	0.0928
	10	0.9967	11.983	0.1042
	15	0.9680	12.593	0.1094
C20K20S60 (C2)	5	0.9622	12.314	0.0870
	10	0.9991	12.733	0.1034
	15	0.9545	13.328	0.1073

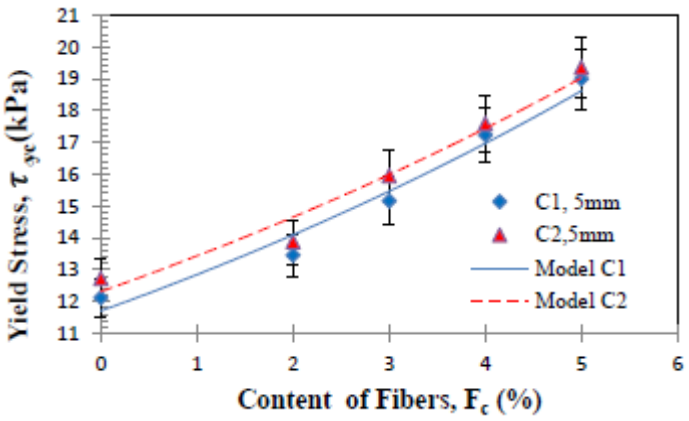

Figure. 5.23. **Yield stress vs. fibers contents for fibers length of 5mm**

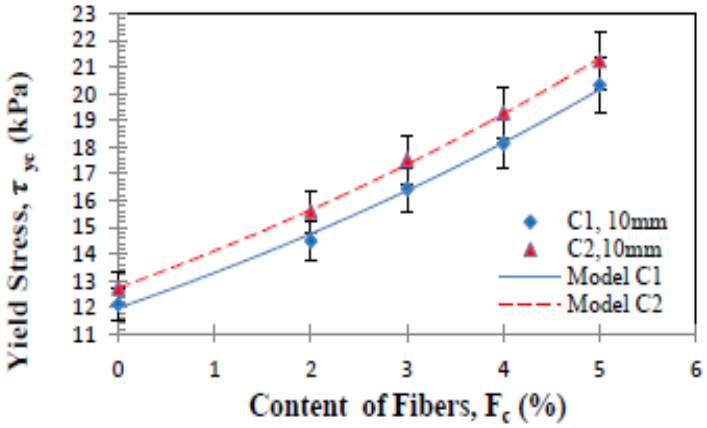

Figure. 5.24. **Yield stress vs. fibers contents for fibers length of 10mm**

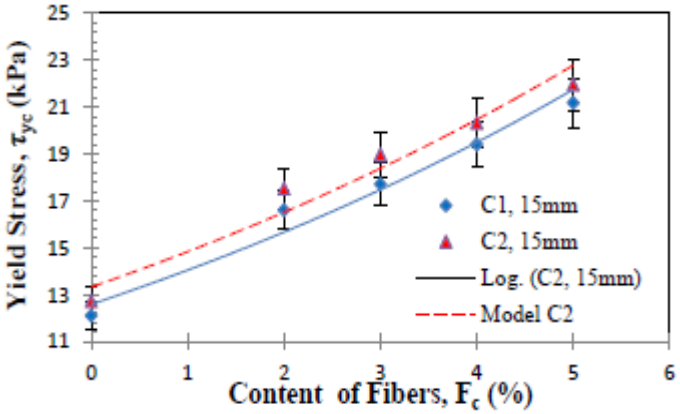

Figure. 5.25. **Yield stress vs. fibers contents for fibers length of 15mm**

The best-fit curve obtained and its equation (5.6) and R^2 value are presented in the graph for easy reading. A relatively good r^2 value of 0.99 has been achieved, indicating that the yield stress is dependent mainly on the fiber content. Nevertheless, it still appear that the yield stress is dependent not only on the fiber content but also on the fibers length.

Figures 15.26 and 15.27 show the effect of increasing the fiber content of yield stress for different fibers length (5mm, 10mm and 15 mm), respectively for matrix C1and for matrix C2. These figures show the effect on the yield stress of different fibers length. It is clear that both yield stress increase with increasing fiber content and fiber length and decreasing water/cement ratio.

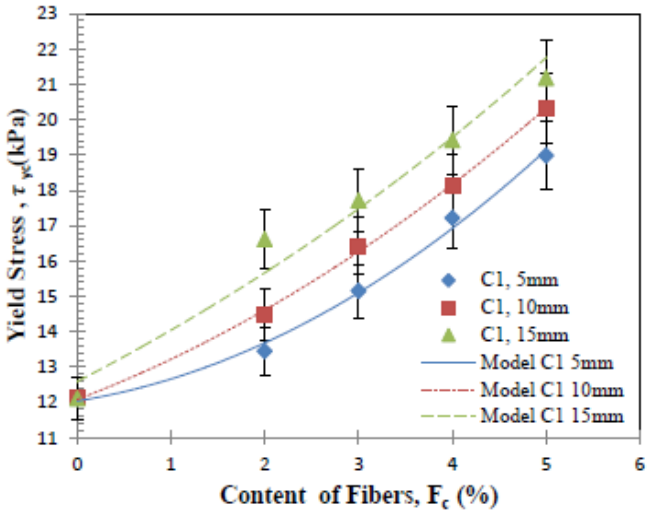

Figure. 5.26. **Relationship between the yield stress and fibers content for C1**

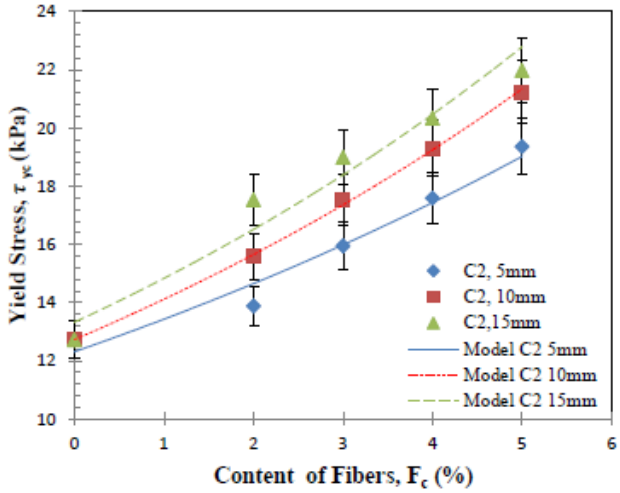

Figure. 5.27. **Relationship between the yield stress and fibers content for C2**

5.5. Rheology model

In Section 5.4, the existence of a meaningful relationship between the yield stress and the fiber content has been evidenced. In the case of properties of fresh cementitious materials, it has been shown that addition of fibers decreases the workability of the material. This effect increased with fibers volume fraction. To predict the yield stress of fiber-reinforced cementitious composites dedicated to extrusion, a physical modeling can be searched. The mortar yield stress depends on a relative yield stress that depends on the aggregate volume fraction,

fiber aspect ratio (ratio of the fibers length over the average fibers diameter) and fiber volume fraction.

Martinie et al. provide a classification of the fiber stiffness according to the ratio of concrete yield stress over elastic fiber strain. They also show that steel fibers can be considered as rigid if the deformation of the fibers due to shearing remains negligible in front of the fibers length. It is shown that the rheology model initially developed for spherical inclusions and aggregates can be adapted to fibers [Mahaut et al. 2008], [Martinie et al. 2010], [Perrot et 2013]. Férec et al. have developed a prediction model of the yield stress. For suspensions of steel fibers dispersed in kaolin paste, (a non-Newtonian fluid exhibiting a yield stress) by taking into account hydrodynamic and fiber interactions [Férec et al., 2014]. However, existing studies focus on rigid fibers, while no study has attempted to model the yield stress of suspension containing flexible fibers such as natural ones

The objective of this study is to propose a model containing adjustable parameters that are determined by fitting experimental data of yield stress values for freshly-made coir fiber-reinforced mortar composites. In a first attempt, the model developed by Ferec et al. is tested.

5.5.1. Relative yield stress as a function of the fiber factor

In this section, we focus on the relationship between the yield stress and the fiber factor (r $ø_f$). The fiber factor is a multiplication between the fiber volume fraction ($ø_f$) with the fiber aspect ratio (r). The fiber aspect ratio (r) is a ratio of the fiber length (L_f) over the fiber diameter (D_f). Relative yield stress can be plotted as a function of the fiber factor as shown in Figure 5.28 for type mix-design C1 and Figure 5.29 for mix-design C2. The background of the yield stress prediction model used here was developed from the model developed by Ferec et al., 2014 and then compared with experimental results. The presence of fiber induces an anisotropic yield stress depending on how the fiber orientation. Under a critical shear rate, the tendency of the fibers to get oriented in the flow direction is overcome by the particle-particle interactions. At higher shear rates, the hydrodynamic interactions become more important, and the fibers get oriented. The shear yield stress value for an isotropic fiber orientation state of the composite can be written as follow:

$$\tau_{yc} = \tau_{ym} + 2\, r^2 \varphi_f{}^2 B\, b_{1122}^{(0)}\, \gamma \quad \text{..... (5.6)}$$

$$b_{1122}^{(0)} = \frac{1}{12|\gamma|} \quad \text{.....(5.7)}$$

Where, $b_{1122}^{(0)}$ is a component of the isotropic orientation tensor.

The predicted relative yield stress for an isotropic fiber orientation state can obtain from Eq. (5.6) Moreover, Eq. (5.7) Moreover, written as Eq. (5.8):

$$\frac{\tau_{yc}}{\tau_{ym}} = 1 + \frac{r^2 \varphi_f{}^2 B}{6\tau_{ym}} \quad \text{..... (5.8)}$$

The relative yield stress ($\frac{\tau_{yc}}{\tau_{ym}}$) is the ratio between the yield stress of the paste containing fibers and the yield stress of the kaolin paste without any fibers.

With the addition of the rigid fibers, the relative yield stress increases with a significant enhancement at fiber factor close to 3.5. The values of the fiber factor, when this critical concentration is reached cited in the literature are between 0.2 and 2 depends on the other components in the materials tested [Banfill et al., 2006].

The results obtained with the addition of natural fiber show that the relative yield stress increases with a significant enhancement of fiber factor close to 14 for type mix-design C1 as illustrated in figure 5.28. For mix-design C2, r the relative yield stress increases with a significant enhancement of fiber factor close to 15 as shown in figure 5.29. The identification of the parameters is given in Table 5.4.

For fiber sizes of 5 mm and 10 mm, the model gives excellent results in agreement with the experimental data. However, it does not apply to a larger size (15mm). This result is the same as that produced by Ferec et al., 2014, some discrepancies observed for suspensions with fibers having an aspect ratio of larger than 30.

Table.5.4. **Parameter value of the yield stress model**

Mixture name	**Fiber length (mm)**	**Parameter B (kPa)**
C10K30S60 (C1)	5	2.20
	10	0.74
	15	0.40
C20K20S60 (C2)	5	1.59
	10	0.95
	15	0.55

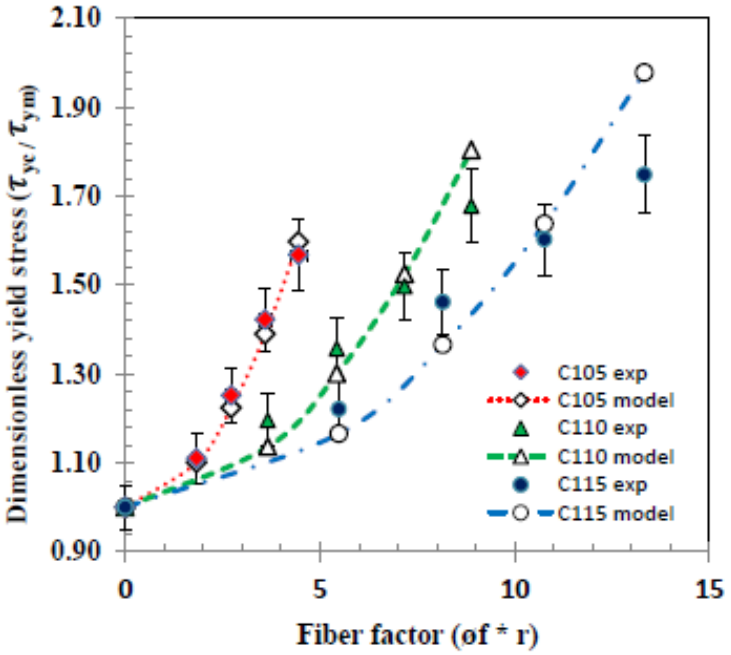

Figure. 5.28. **Relative yield stress as a function of the fiber factor** for the model predictions type C1.

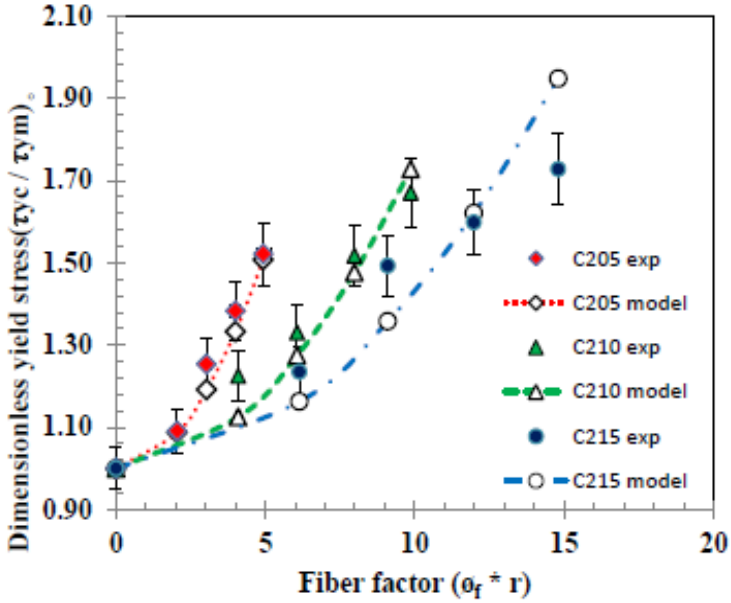

Figure. 5.29. **Relative yield stress as a function of the fiber factor** for the model predictions type C2.

5.5.2. The proposed rheological model to predict yield stress

The Ferec et al. model does not provide accurate results for the longest size. To improve the prediction ability of the model, we try to adapt the Ferec model empirically to make it suitable for all the tested fiber lengths.

Figure 5.30 dan Figure 5.31 show the experimental results along with the adapted Ferec model. We add a linear term to the Ferec model to best fit our experimental data. The Prediction model now writes:

$$\left[\frac{\tau_{yc}}{\tau_{ym}}\right] = 1 + \left[\frac{r^2(\varphi_f)^2 R}{6\tau_{ym}}\right] + \left[\frac{r\varphi_f S}{6\tau_{ym}}\right] \quad \text{..... (5.9)}$$

Fitted curves show an excellent agreement with experimental data. The value of the identified parameters is given in Table 5.5 where, the value of the parameter R decreases with the fiber aspect ratio. In contrast to the S parameter, this increases with the fiber aspect ratio.

Table.5.5. **Parameter value of modification the yield stress model**

Mixture name	Fiber length (mm)	Parameter R (kPa)	Parameter S (kPa)
C10K30S60 (C1)	5	1.8	1.55
	10	0.45	1.65
	15	0.19	1.75
C20K20S60 (C2)	5	1.4	1.5
	10	0.35	1.7
	15	0.145	1.8

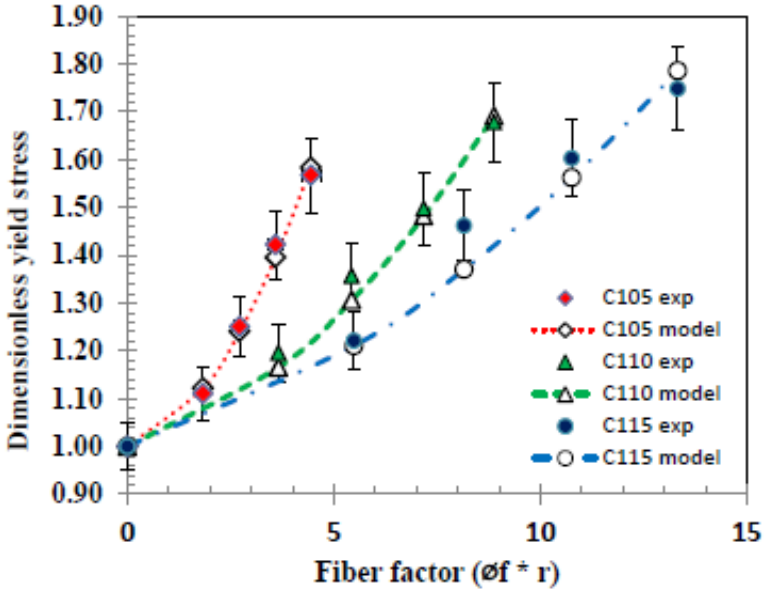

Figure. 5.30. **Relative yield stress as a function of the fiber factor** for modification the model predictions type C1.

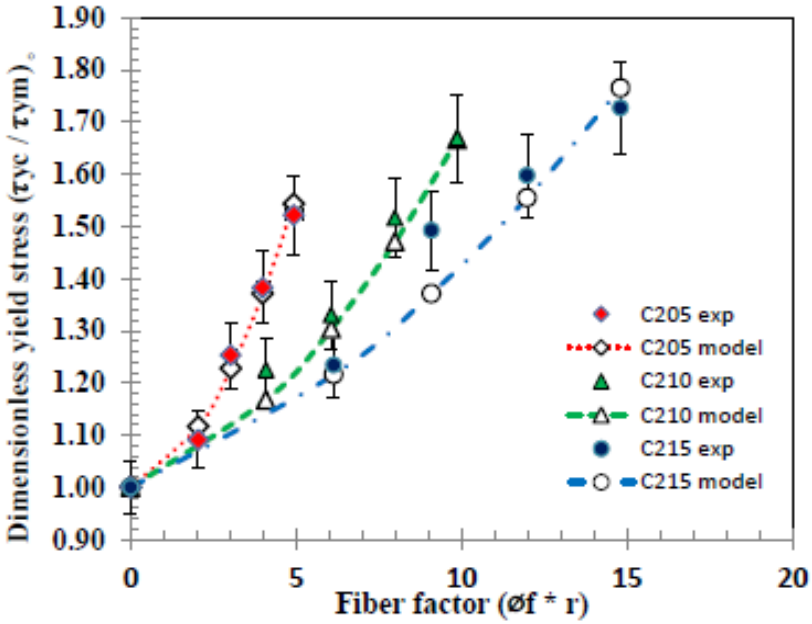

Figure. 5.31. **Relative yield stress as a function of the fiber factor** for modification the model predictions type C2.

5.5.3. Validation the rheological model.

The experimental results validate the prediction model as shown in Figure 5.32 for mix-design C1 and Figure 5.33 for mix-design C2. It is also interesting to sum up data from all experiments (C1 + C2) as shown in Figure 5.34. Table 5.6 provides parameters value of modification the yield stress model versus experimental data.

$$\tau_{Ymodel} = A * \tau_{y.exp} + B \quad \text{..... (5.10)}$$

Table.5.6. **Parameter value of modification the yield stress model**

Mixture name	Correlation coefficient	Parameter A	Parameter B
C1	0.9992	0.9982	0.0042
C2	0.9987	01.0017	0.0009
C1+C2	0.9914	0.9844	0.0361

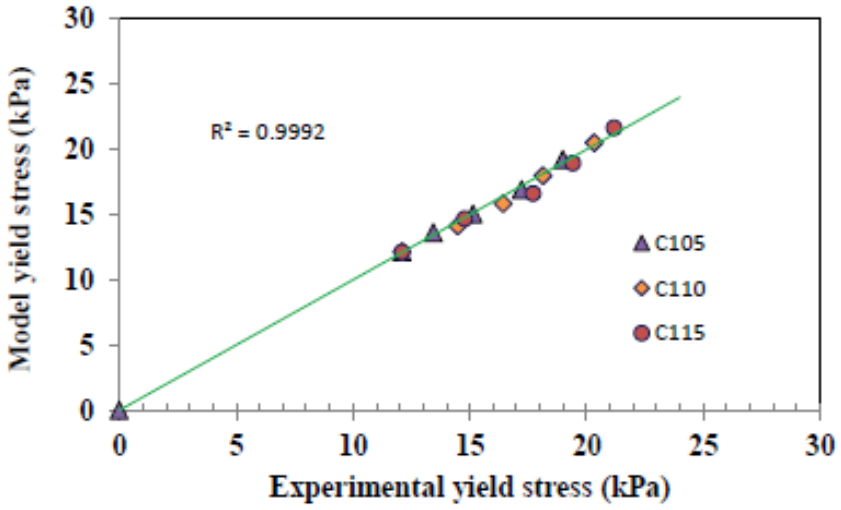

Figure. 5.32. **Model versus experimental yield stresses for type C1.**

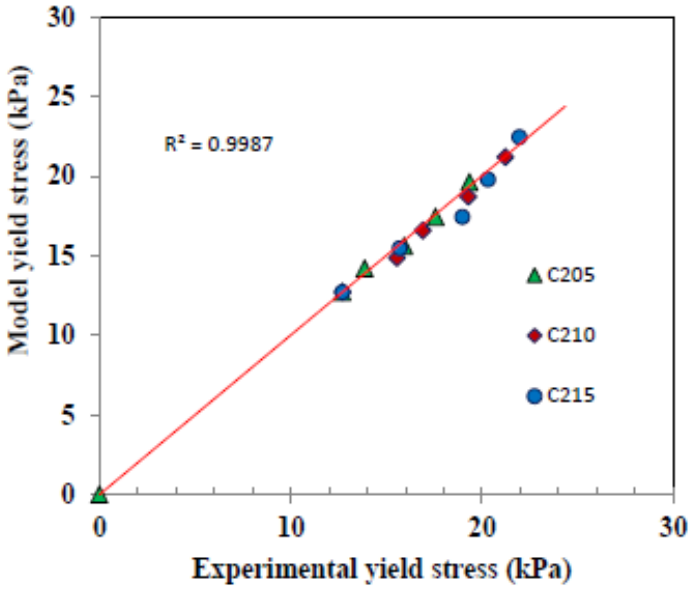

Figure. 5.33. **Model versus experimental yield stresses for type C2**

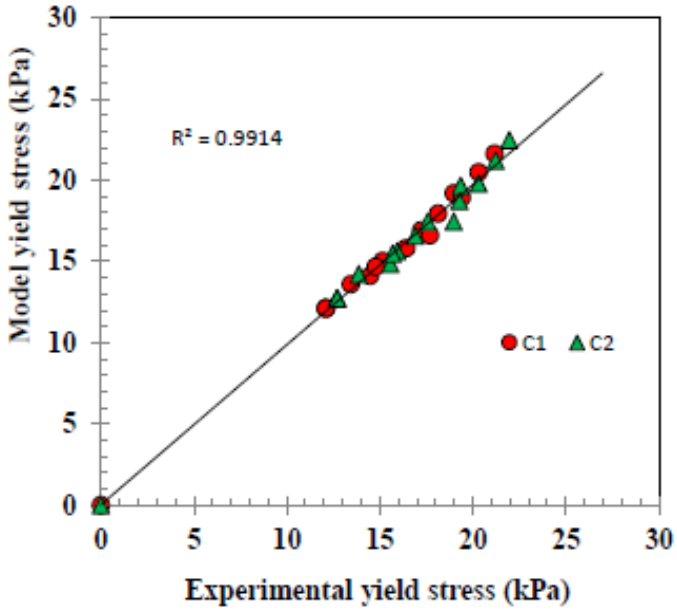

Figure. 5.34. **Model versus experimental yield stresses for type C2**

5.6. Conclusions of chapter

This present work shows that the yield stress model used for common mortar can be generalized to fiber reinforced concretes. Indeed, it predicts the evolution of the yield stress of the fiber-reinforced cementitious composite.

Rheological behaviors of cement mortar and fiber reinforced cementitious composite are presented in this chapter. The formation of clay material through extrusion produces a compact material with the surface without defects.

The rheological approach serves as an effective plain cement mortar fresh property design guide for achieving hardening properties of the fiber cement mortar composite. The rheology is important for the characteristic of fresh cement paste, grout, and mortar and concrete to perform in practical applications. It is used for the desirable properties of the hardened materials can be achieved.

The formulation of a material with low cement and from local materials that can be extruded with smooth and compact aspect has been studied. As expected, Clay absorbs more water than cement. Therefore, the amount of clay and water - cement will influence the extrusion results.

Mix design of mortar obtained from cement, clay and sand in the ratio of the weight of 10:30:60 respectively requires 18 % water - cement. As for the proportion of water - cement 20:20:60 needs a 16 % to produce the extruded material. The addition of fibers into extruded formulations requires the addition of water to obtain an extrudate mortar. To counter the loss of workability due to the addition of the selected fiber mortar mixture basic (plain mortar) without adding extra water. Furthermore, taking into account the addition of fibers up to 5 % by weight of cement, to remain in the extruded condition, for 10 % of cement formulations need a water - cement ratio of 21 %. As for the 20 % cement formulations needed water - cement ratio of 19 %.

The yield stress increases with fiber content and fibers length. The more clay content gives a lower yield stress value. Rheology models for coir fiber reinforced cementitious composites have been obtained. The model of prediction yield stress:

$$\left[\frac{\tau_{yc}}{\tau_{ym}}\right] = 1 + \left[\frac{r^2 {\varphi_f}^2 R}{6\tau_{ym}}\right] + \left[\frac{r\varphi_f S}{6\tau_{ym}}\right]$$

The model prediction shows a good agreement with the yield stress values of coir fibers reinforced cementitious composites.

The observations of the surface of the fiber cement mortar composites before extrusion are seen the small holes/ microporosity between the mortar matrix. Also, the visible concentration of fibers in the mix has not spread. That required the formation of materials using extrusion to the more evenly spread of fibers.

CHAPTER.6.
MECHANICAL PERFORMANCE, MICROSTRUCTURE, FAILURE MODE, AND MODEL OF SCREW EXTRUDED FIBER COMPOSITES USING DESTRUCTIVE TESTING METHOD

6.1. Introduction

Recently, interest in the composite in construction material has shifted towards the use of natural fibers as a reinforcement component because potential environmental benefits. The advantages of natural plant fibers, such as low abrasion, multi-functionality, low density, low cost, ready availability and relative ease of waste disposal, encourage their application in composite materials.

Almost all of the commonly available natural plant fibers that are cheap and abundant in nature. There are being used for reinforcement in combination with non-biodegradable matrix materials such as unsaturated polyester, epoxy resin, polyethylene, polypropylene and cementitious. Natural fibers have been successful in imparting to composite materials certain benefits like reduced machine wear compared with synthetic reinforcement materials and a lowering of associated health hazards.

The mechanical properties of natural cellulosic fibers are a function of several variables, the most important being the spiral angle and the cellulose content. The superior flexibility of natural fibers, when compared with that of glass fibers, enables them to bend rather than fracture during processing. The compressive parameter strength and tensile strength are very often used to quantify the quality of cementitious materials. Mechanical performance fiber reinforced cementitious represent a new generation of construction materials for the 21st century now being actively researched [Andiç-Çakir et al., 2014], [Ali M et al., 2012]. Fiber additions offer a convenient and practical means of achieving improvements in many of the mechanical properties of cement, mortar and concrete such as enhanced compressive strength and tensile strength.

In the present work, fiber composites are developed, and their mechanical properties are evaluated. The fibers used in the study included coir fiber. Cement mortar was used as the matrix. In this context, the compressive strength measured at 28 days after casting. The compressive and tensile characteristics of extruded

coir fiber reinfoced cementitious composites (CFRCC) were determined by testing a minimum of three-four cylinder specimens for each batch using the Mechanical Testing System (MTS) Instron 8803.

This investigation was carried out to evaluate the results of the mechanical performance of CFRCC under static loading. CFRCC in the present investigation is tested using screw extrusion for compressive and splitting tensile strength behavior. Stress-strain under compressive and tensile load was studied to provide insight into the behavior and failure mechanism of CFRCC composite. Effect of fiber content and fiber length evaluated to mechanical performance. To analyze the mode of failure for compression, tensile, several optical photographs were taken to study the mechanism distribution of coir fiber in cement mortar.

6.2. The aspect surface of screw extrusion.

Aspects surface of the screw extrusion process is observed. It is the relationship with the rheological results in designing composite materials. Observations were made on mortar extrusion, composite extrusion and comparing the results with the outcome of the extrusion mold.

6.2.1. Surface of extruded mortar

The results surface observations of cement mortar are shown in Figure 6.1 the surface aspects of cement mortar for 10% cement (type C1) and 20% of cement (type C2). As well as shown on the Figure 6.2 surface aspect on a cross section of the cement mortar showed results a smooth flat surface. It shows that the presence of sufficient amount of water necessary so that the material extruded material well, mentioned extrudability.

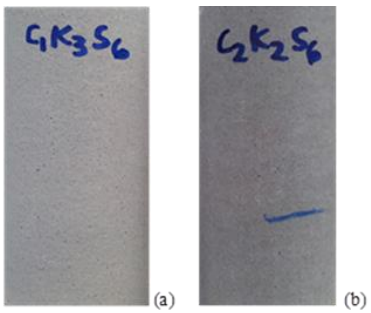

Figure. 6.1. Aspect surface cement mortar extrudability: (a) type C1, (b) type C2

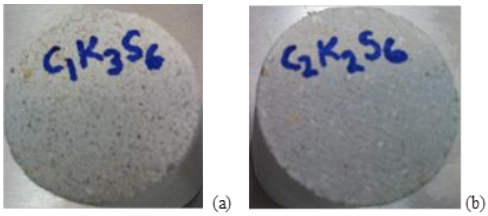

Figure. 6.2 Aspect surface of cross-section of cement mortar extrudability: (a) type C1 and (b) type C2

6.2.2. Surface of extruded composites

The extrusion results are shown in Figure 6.3 for aspect surface of CFRCC, the type C2 of 20% cement mix: (a) 2% fiber, (b) 3% fiber, (c) 4% fiber. While, the results is shown in Figure 6.4 for aspect surface of CFRCC composite type C1 of 10% cement mix: (a) 2% fiber, (b) 3% fiber, (c) 4% fiber. The both give the same result aspect surface, namely flat and smooth. It shows that the materials are extrudability.

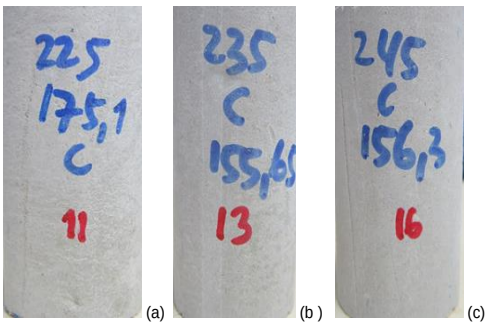

Figure. 6.3 Aspect surface of coir fiber cement clay mortar composites extrudability type C2: (a) 2% fiber, (b) 3% fiber, (c) 4% fiber.

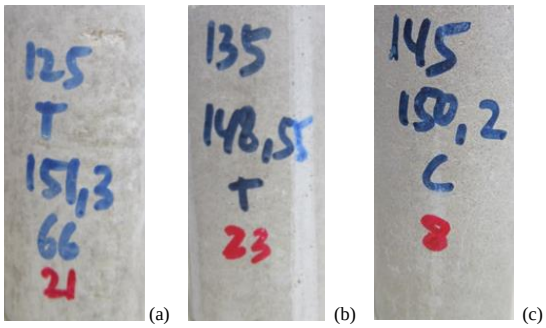

Figure. 6.4 Aspect surface of coir fiber cement clay mortar composites extrudability type C1: (a) 2% fiber, (b) 3% fiber, (c) 4% fiber.

6.2.3. Surface of mold and extrusion

The results obtained of the mold in comparison with the extrusion process as shown in Figure 6.5.The aspect surface of CFRCC composite forming using: (a) Mould and (b) Extrusion.

Although the process of formation of the test material to the mold through compaction ten layers, then compacted with ten knocks then through vibration and removed after 24 hours. The results obtained are uneven, not smooth surface defects as well as the extrusion process.

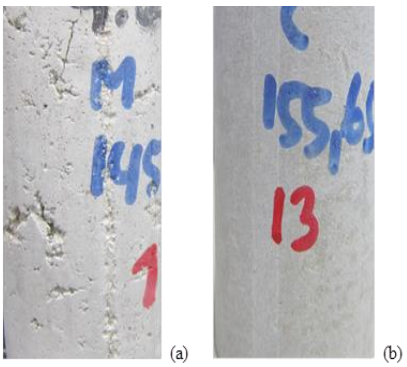

Figure. 6.5 **Aspect surface of coir fiber reinforced cementitious composites forming using: (a) Mould and (b) Extrusion**

6.3. Orientation fibers in screw extrusion.

This orientation can have significant consequences on the mechanical properties when cured, positive or negative depending on the compatibility of fiber orientation directions with solicitations. Several studies have shown the influence of fiber orientation on the behavior of material [Shah et al., 1994; Shao et al., 1997]. In the case of forming by extrusion, the fibers undergo an orientation induced by the process. The process, under the effect of shear in the shaping zone, The fibers oriented preferentially in the direction of the extrusion flow [Mobasher et al., 1998] [Akkaya et al., 2000]. Most of the time, fibers are oriented in the longitudinal direction. The ductility compared to those with fibers having random orientation [Absi et al., 1994] [Swamy et al., 1975].

The results of the observations under an optical microscope of fiber composite after going through the process extrusion after 28 days, showing the hole diminished and deployment of fiber evenly. As the visible fibers at random positions, there is a longitudinal direction and the transverse orientation of the

direction extrusion as shown in Figure 6.7 for longitudinal direction and Figure 6.8. for direction transversal. Cutting the fiber direction is longitudinal (L), and transverse (T) after extrusion is shown in Figure 6.6.

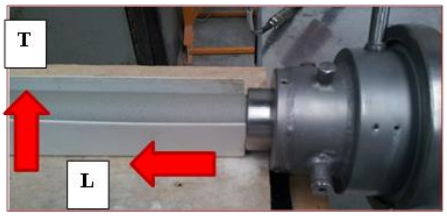

Figure. 6.6 **Direction of extrusion of fiber reinforced cementitious composites, Longitudinal (L) and Transversal (T).**

6.3.1. Longitudinal

In observation of the composite material obtained fiber direction lengthwise direction is random. The deeper observations, shown in Figure 6.7 there is a fiber cut in the transverse direction, and the fibers are embedded lengthwise.

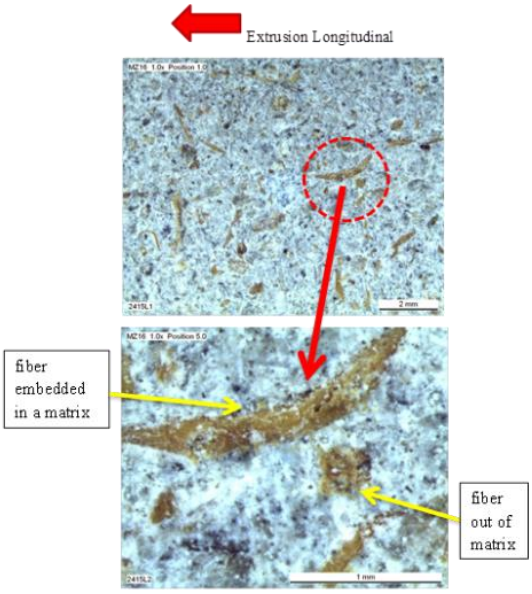

Figure. 6.7 **Morphology fiber cement mortar composites after extrusion, the longitudinal direction of extrusion (L).**

6.3.2. Transversal

Similarly, the observation of the composite material obtained in the transverse direction toward the fiber is scrambling. Deeper observations, shown in Figure 6.8 as well as on pieces lengthwise, fibers are severed in the transverse direction, and the fibers embedded lengthwise.

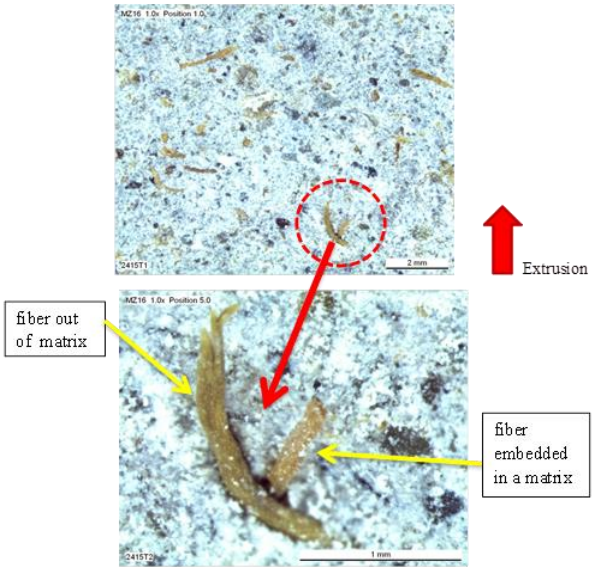

Figure. 6.8 **Morphology fiber cement mortar composites after extrusion, the transversal direction of extrusion (T).**

6.4. Mechanical performance extruded composites.

The performance of mechanics of CFRCC materials observed in the compressive stress-strain, the tensile stress-strain, and the extrusion process compared to the molding process. The experimental observations are results of stress and strain relationships.

6.4.1. Compressive stress-strain of extruded composite

Figure 6.9 shows the experimental results of the stress-strain characteristics of extruded CFRCC in typical compressive stress-strain curves of mortar and composite with a fiber length of 5 mm. The result shows that average the peak stress in the compressive strength values of wash-dry treated coir composite was 23% higher than that of the cement mortar (control sample).

Compared Andiç-Çakir et al. (2014) increase in the compressive strength values were 3.64% of the control sample for untreated coir incorporating ones and

9.00% of the control sample for alkali treated coir fiber incorporating mortars. Compared with untreated and treated an increase in compressive strength of one and a half time.

Improved performance with a compressive strength of 5 mm fiber length in the same fiber content 4% is an increasing one and a half time in the compressive strength of CFRCC materials in extrusion only with treatment by washing and drying.

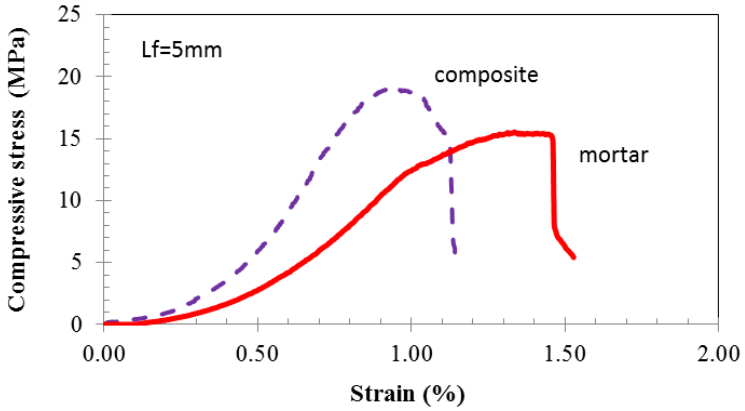

Figure. 6.9.**Typical compressive stress-strain curves mortar and composite with fiber length of 5 mm for extruded samples**

Figure 6.10 shows the experimental results of the stress-strain characteristics of extruded CFRCC in typical compressive stress-strain curves of mortar and composite with length fiber 10 mm of under forming using extrusion. It found that the peak stress of CFRCC was 30% higher than that of cement mortar. The result of the compressive strength increase of 2.3 times compared the result of Andiç-Çakir et al. (2014).

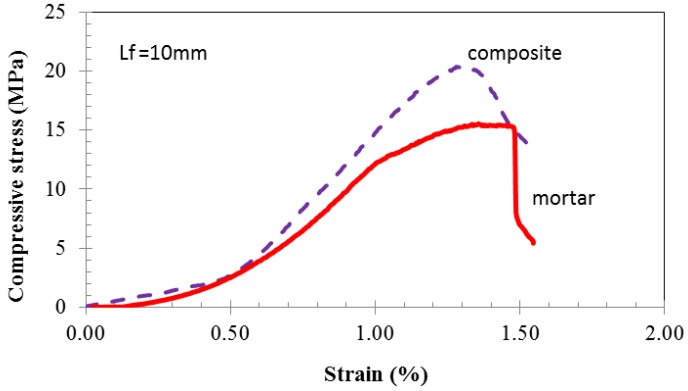

Figure. 6.10. **Typical compressive stress-strain curves mortar and composite with fiber length of 10 mm for extruded samples**

Figure 6.11 shows the experimental test results of the stress-strain characteristics of extruded CFRCC in typical compressive stress-strain curves of mortar and composite with length fiber 15 mm of under forming using extrusion. It found that the peak stress of CFRCC was 37% higher than that of cement mortar. The result of the compressive strength increase of three times compared the result of Andiç-Çakir et al. (2014).

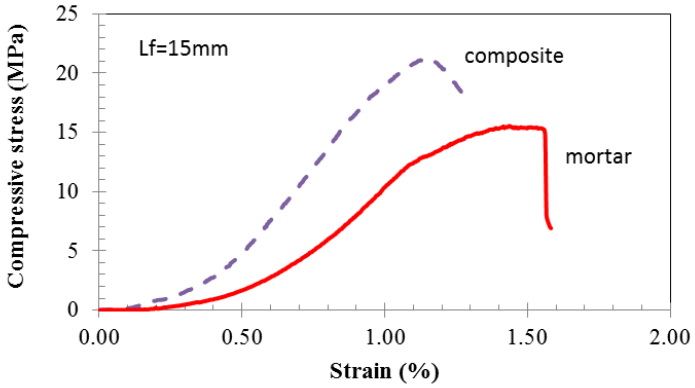

Figure. 6.11. **Typical compressive stress-strain curves mortar and composite with fiber length of 15 mm for extruded samples**

23% increased the compressive stress of CFRCC for 5mm, 30% for 10mm and 37% for 15mm fiber length, compared to cement mortar. The results obtained with the addition of fiber increased compressive stress with increasing fiber length. That is due fiber retain cracking, thus improving the behavior of materials. Compared with the results Andiç-Cakir et al. (2014) without extrusion obtained there were increased compressive stress 1.5 times of 5 mm fiber length, 2.3 times of 10 mm fiber length and 3.0 times of 15 mm fiber length for extrusion materials.

The compressive stress of the CFRCC have shown a gradual increase by increasing fiber length, and these values are higher for treated fibers when compared to untreated ones. Likewise, the extruded material provides increased compressive stress compared to the manual process.

6.4.2. Tensile stress-strain of extruded composite

Several studies have shown that the splitting tensile test is simple and reliable, giving reasonable results on resistance to direct traction compared to the bending test. Tensile strength was observed until cracks in the mortar characterize the mortar strength.

Figure 6.12 is the experimental test results of typical tensile stress-strain curves cement mortar and fiber composite with length fiber 5 mm of under

forming using extrusion. It found that the peak stress of CFRCC was 29% higher than that of cement mortar.

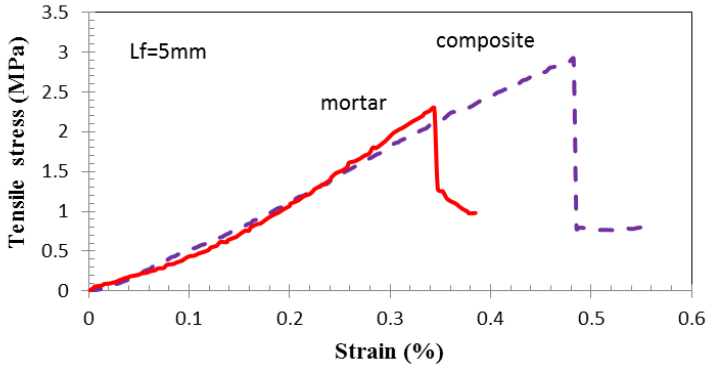

Figure. 6.12.**Typical tensile stress-strain curves mortar and composite with length fiber 5 mm of under forming using extrusion**

Figure 6.13 is the experimental test results of the stress-strain characteristics of extruded CFRCC and cement mortar with length fiber 10 mm of under forming using extrusion. The peak stress of CFRCC was 30% higher than that of cement mortar.

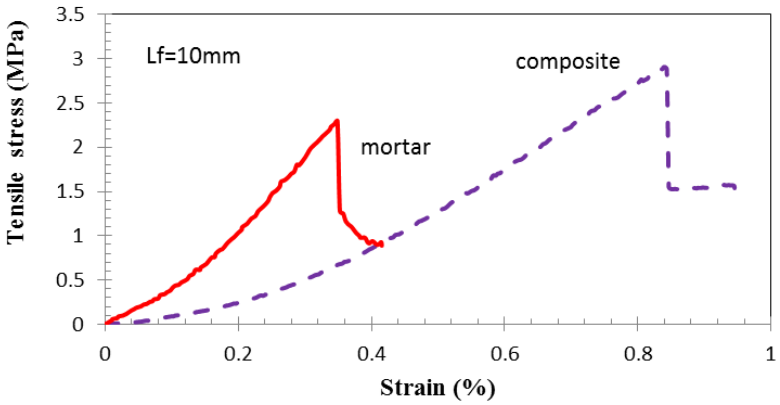

Figure. 6.13.**Typical tensile stress-strain curves mortar and composite with length fiber 10 mm of under forming using extrusion.**

Figure 6.14 is the experimental test results of typical tensile stress-strain curves cement mortar and fiber composite with length fiber 15 mm of under forming using extrusion. It found that the peak stress of CFRCC was 41% higher than that of cement mortar.

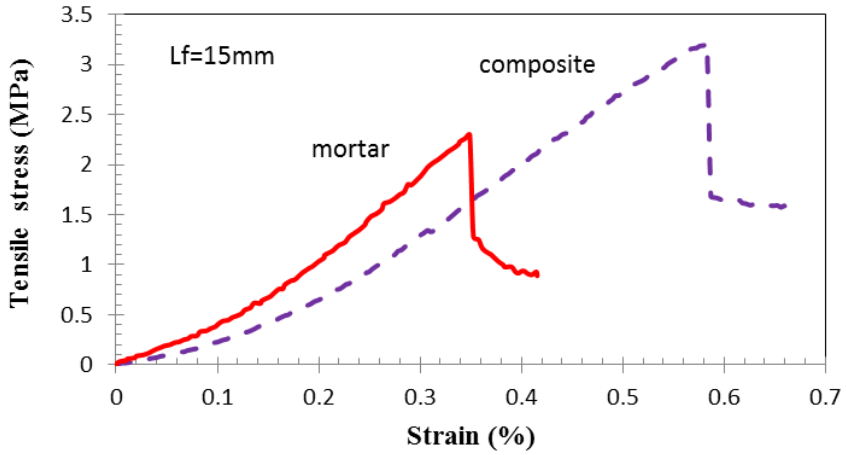

Figure. 6.14.**Typical tensile stress-strain curves mortar and composite with length fiber 15 mm of under forming using extrusion.**

29% increased the tensile stress of CFRCC for 5mm, 30% for 10mm and 41% for 15mm fiber length, compared to cement mortar. The results showed that the performance CFRCC tensile stress increases with increasing fiber length compared to cement mortar. The increase of tensile stress is higher than the increase compressive stress.

6.4.3. Stress-strain of molded and extruded sample behavior

The evolution of compressive stress of cement mortar manually processed through the molding and extrusion process is shown in Figure 6.15. In the Figure also shows a comparison between the compressive stress of the 10% cement content of type C1 and 20% cement content of type C2. The results showed that performance compressive stress can be improved through the extrusion process when compared to the manual through the molded process. It is because the compaction is done through a digital process at constant speed. Cement type C1 has a lower compressive stress of the cement type C2. It is because the content of cement.

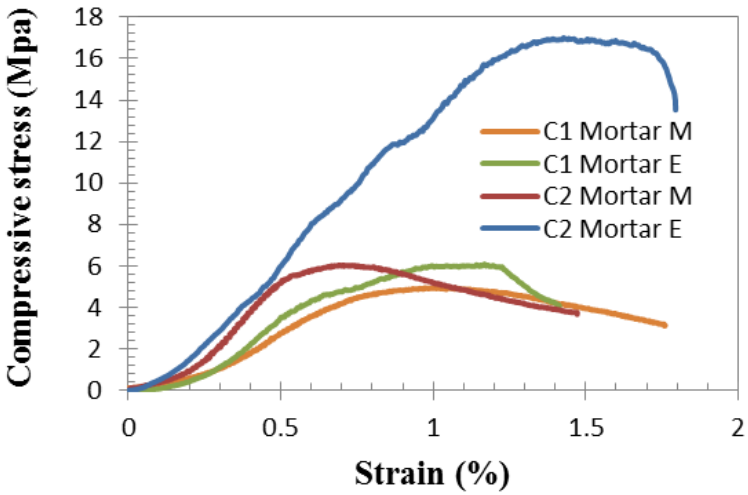

Figure. 6.15.**Mortar of typical compressive stress-strain curves under forming using mold (M) and extrusion (E) type C1 and C2**

The mean stress–strain curves for each cement mortar and fiber composite are compared and shown in Fig. 6.16. It can see clearly that the stress–strain curves of the fiber composite provide better performance than cement mortar.

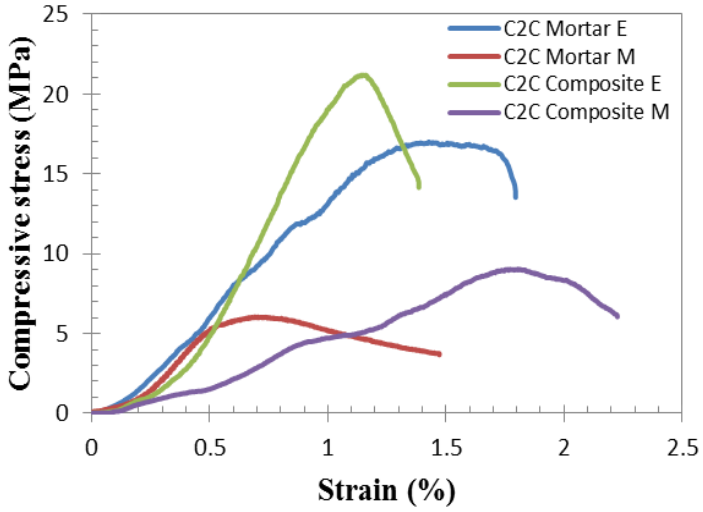

Figure. 6.16.**Mortar and composite of typical compressive stress-strain curves under forming using mold (M) and extrusion (E)**

The evolution of stress and strain in tensile strength and compressive strength are shown in the figure 6.17. Extrusion process affects the mechanical performance of materials compared to the mold that results obtained an increase of almost two times is 183% for the compressive strength while the tensile strength obtained increase in two and a half time is 257%.

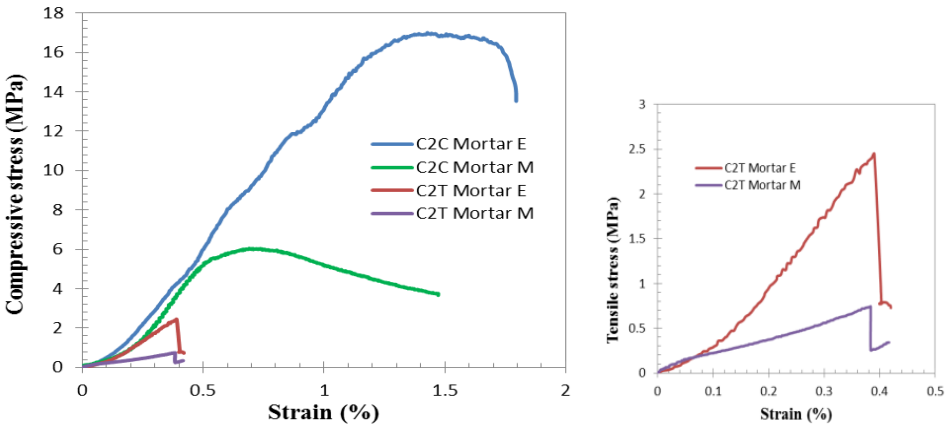

Figure. 6.17. **Compressive and tensile of stress-strain curves of mortar under forming using mold (M) and extrusion (E)**

Figure 6.15 to 6.17 gives an indication that the processes of forming by extrusion provide performance results of compressive strength, and tensile strength is better than the manual process with mold.

6.5. Failure modes.

Failure modes in extruded of cement mortar and coir fiber reinforced cementitious composites (CFRCC) are reviewed during the compression test and splitting tensile test. Observations made with photograph and micrograph

6.5.1. Failure modes in compression

The failure modes of typical compression failure modes of cement mortar type C1 without fiber: (a) extruded plain mortar; (b) after static loading shown in Figure 6.18. Moreover, the typical compression failure modes of extruded cement mortar type C2 non-fiber shown figure 6.19. Failure modes are lighter than cement mortar type C1.The mortar without fibers resulting test sample was destroyed at the top.

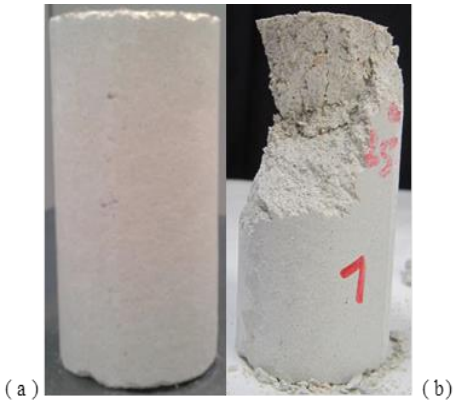

Figure 6.18.**Typical compression failure modes of cement mortar type C1 without fiber: (a) extruded plain mortar; (b) after static loading.**

Figure 6.19.**Typical compression failure modes of extruded cement mortar type C2 non-fiber: (a) plain mortar; (b) after static loading.**

The failure compression of static loading, composite 4% fiber type C1 and C2 as shown in Figure 6.20 are present the failure mode with cracked lengthwise direction unidirectional pressure and can be seen for cracks on the bottom and top surface. The detailed information on the failure modes of the coir fiber reinforced cementitious composites based on fiber content was shown in Figure 6.21. of failure compression of static loading: (a) composites 4% fiber, (b) composites 3% fiber, (c) composite 2% fiber. The crack marked has a tendency to propagate parallel to the loading direction in the mortar matrix. Fiber content increases the tendency of cracks that occur less and less. Then, it shows the strength of the fiber bond with mortar matrix.

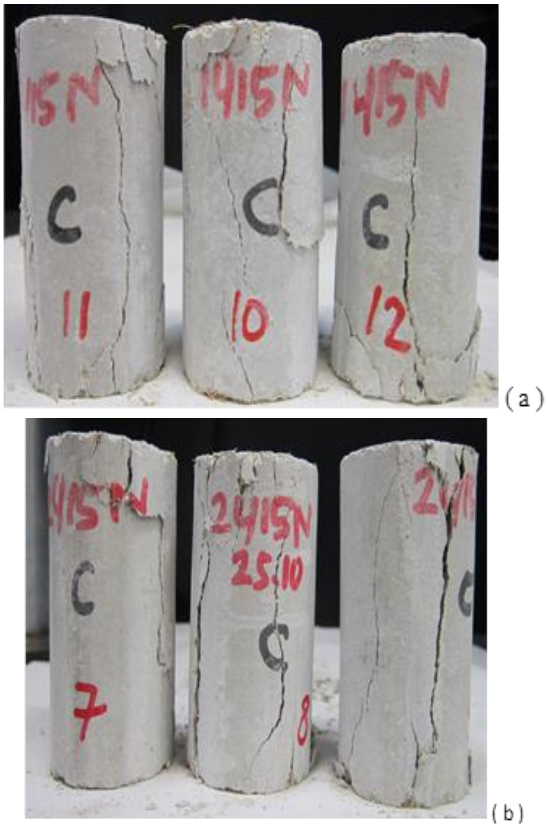

Figure 6.20.**Photograph of failure compression of static loading,** composite 4% fiber: (a) type C1 and (b) type C2

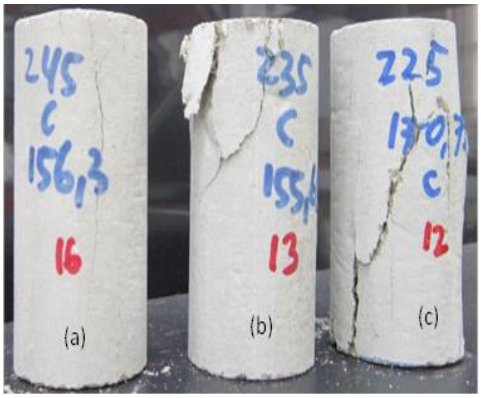

Figure 6.21.**Photograph of failure compression of static loading: (a) composites4% fiber, (b) composites 3% fiber, (c) composite 2% fiber.**

Figure 6.22 shows the bond between the fiber and matrix mortar. There are fibers that are pulled out from the mortar, fiber breaking due to the pressure, and fiber is still immersed in the mortar. It shows the direction of fibers in the mortar is random. To more clearly for coir fiber reinforced cementitious composites are

shown in Figure 6.23 composite failure after compression of static loading, for broken fiber transverse and longitudinal directions.

Figure 6.22. **Micrograph coir fiber reinforced cementitious composites, after failure compression of static loading.**

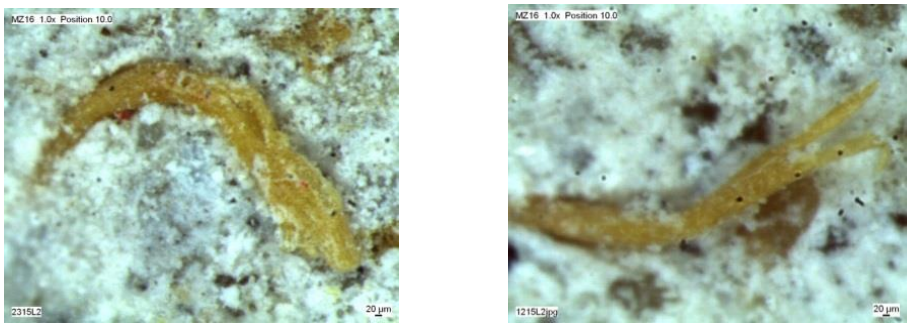

(a) (b)

Figure 6.23. **Micrograph composite after failure compression of static loading, for broken fiber.**

6.5.2. Failure modes in tension

The failure modes of typical tension failure modes under static loading: (a) cement mortar type C1 non-fiber; (b) cement mortar type C2 non-fiber is shown in Figure 6.24. The failure mode of cement mortar type C2 is more brittle than the type C1. It is influenced by the amount of cement and clay.

Typical tension failure modes under static loading of coir fiber reinforced cementitious mortar composites are shown in Figure 6.25. The existence of fiber affects the cracks that occur in the mortar. Bonding fibers to make the cement mortar tensile strength increases.

Figure 6.24.**Typical tension failure modes under static loading: (a) cementitious non-fiber type C1; (b) cementitious non-fiber type C2.**

Figure 6.25.**Typical tension failure modes under static loading of coir fiber cementitious composite.**

The detailed information on the failure modes of the coir fiber reinforced cementitious composites based on fiber content was shown in Figure 6.26. of failure modes of split tensile strength: (a)composite with 2% fiber, (b) composite 3% fiber, (c) composite 4% fiber. The crack marked has a tendency to propagate parallel to the loading direction in the mortar matrix.

Failure mode at 2% fiber content is shown in the picture 6.26a. The cracked direction parallels to the direction of loading. Cracks that occur less than the cracking that occurs in 4% fiber content in the figure 6.26b. That due to resistance tensile strength at 4% fiber content is higher than the tensile strength of 2% fiber content.

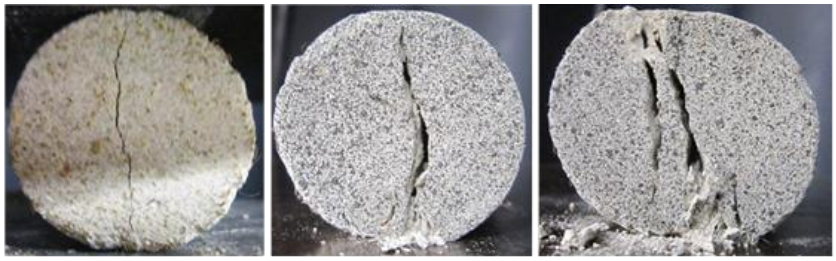

Figure 6.26.**Failure modes of split tensile strength: (a)composite with 2% fiber, (b) composite 3% fiber, (c) composite 4% fiber.**

Results cracked due to the tensile strength of coir fiber orientation to the longitudinal direction of extrusion coir fiber reinforced cementitious composites as shown in Figure 6.27. Fiber orientation looked random and disconnected and pulled out of the mortar as shown in Figure 6.28. Coir fiber reinforced cementitious composites, after the failure of static tension loading.

Figure. 6.27. **Coir fiber orientation longitudinal direction of extrusion of coir fiber cement clay mortar composites.**

Figure 6.28. **Micrograph of CFRCC composite, after the tensile failure of static loading.**

More detailed results for bonding fibers in mortar matrix as in Figure 6.29 coir fiber after the failure of static tensile loading, for broken fiber. In the picture 6.29a, had the mark of the fiber is lost, and fiber drawn out mortar. In the figure, 6.29b seemed disconnected fibers condition and seemed to mortar attached and united with the cross section of the fiber.

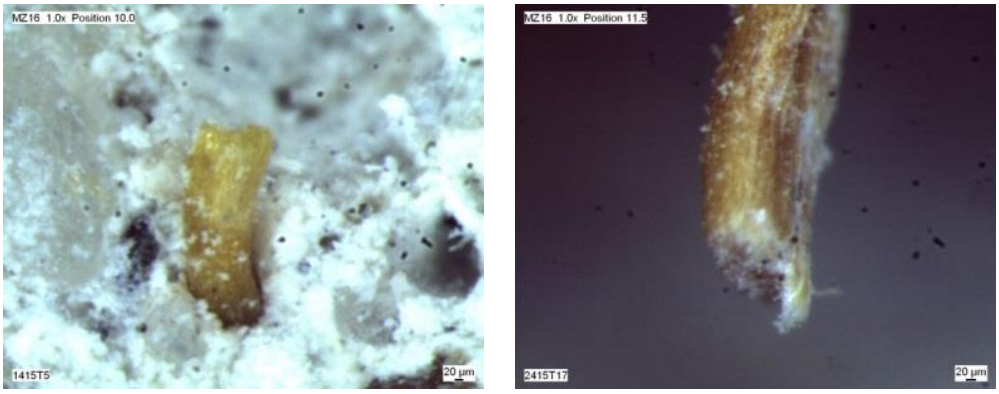

(a) (b)

Figure 6.29. **Micrograph coir fiber after the tensile failure of static loading, for broken fiber.**

.

6.6. Mechanical models

6.6.1. Compressive strength behavior

The maximum stress value of stress–strain curves is taken as compressive strength. Figure 6.30 shows the influence of fiber content on stress. The highest stress value of stress–strain curves is taken as compressive strength. The straight line is the stress of cement mortar without fiber. Compressive stress increased with fiber content.

The empirical model is developed to predict compressive stress based on a linear trend line obtained with increasing fiber content defined as shown in equation 6.1.

$$\sigma_{ci} = \alpha_i * \varphi_{fi} + \sigma_{oi} \quad \text{..... (6.1)}$$

Where: σ_{ci} is the Compressive stress (MPa); φ_{fi} is the fiber content (%); α_i is the shape parameter (MPa), σ_{oi} is reference stress parameter (MPa). The parameters values of the compressive stress versus fiber content for the tested materials is shown in Table 6.1. The compressive of CFRCC compared to cement mortar, it shown an addition of fiber can increase the compressive stress up to 41%.

Table.6.1. **Fitting parameters values of the compressive stress versus fiber content for the tested materials**

Fiber length (mm)	**Correlation coefficient**	**Parameter** α_i (MPa)	**Parameter** σ_{oi} (MPa)
5	0.9901	1.179	14.222
10	0.9783	1.624	13.639
15	0.9903	1.942	13.602

The relationship between fiber length and alpha parameter is shown defined Equation 6.2:

$$\alpha_i = (0.0763 * L_{fi} + 0.8187) \quad \text{..... (6.2)}$$

Furthermore, the models are developed to predict compressive stress based on fiber content and fiber length defined is shown in equation 6.3:

$$\sigma_{ci} = [(0.0763 * L_{fi} + 0.8187) * \varphi_{fi} + \sigma_{oi}] \quad \text{..... (6.3)}$$

where: σ_{ci} is the Compressive stress (MPa); L_{fi} is the fiber length; φ_{fi} is the fiber content (%); σ_{oi} is the reference stress parameter (MPa).

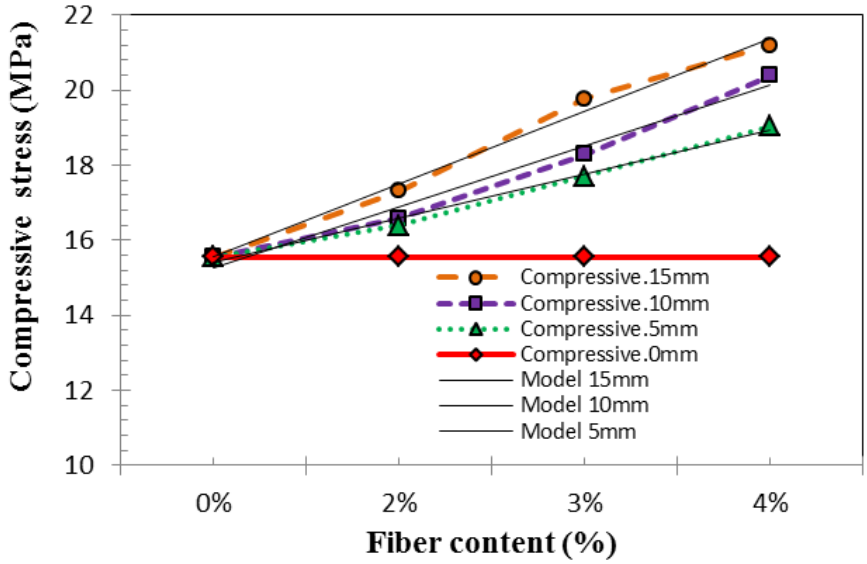

Figure. 6.30. **Effect of fiber content on compressive stress**

Figure 6.31 shows the influence of fiber length on a average maximum of stress. The fiber length of 15mm with a fiber content of 4% gives the highest value compared to cement mortar without fibers. Compressive stress increases with increasing fiber length. It is the same as for 4 cm coir fiber length the results presented by Baruah and Talukdar, (2007). However, the results obtained Ali et al. (2012) is the compressive strength decreases with increasing fiber for fiber length 2.5 cm; 5 cm; 7.5 cm. That caused by the creation of air voids because of long fibers with relatively high fiber content.

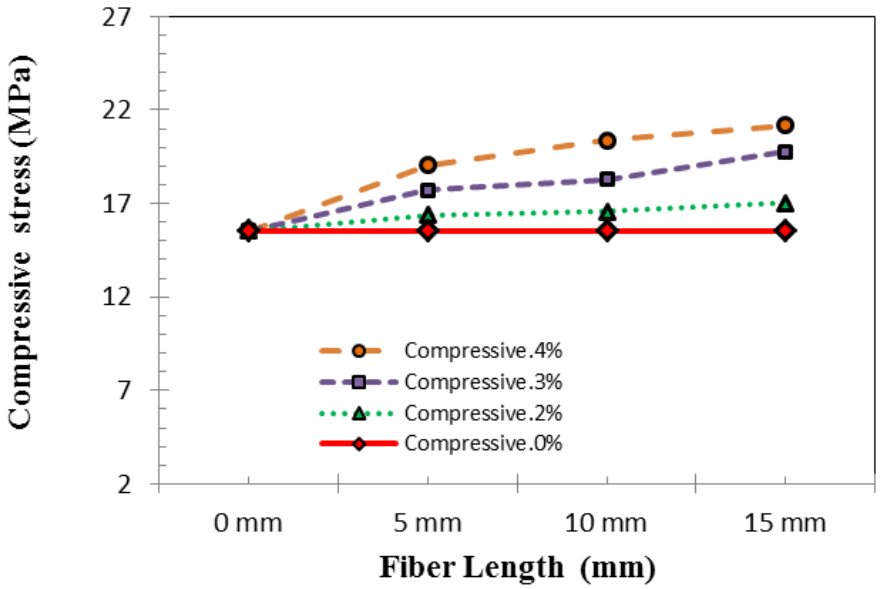

Figure. 6.31. **Effect of fiber length on compressive stress**

6.6.2. Tensile strength behavior

The effect of fiber content and fiber length on tensile stress is shown in Figure 6.32 and Figure 6.33. The tensile stress increases with higher fiber content and fiber length. The empirical model is developed to predict tensile stress is based on a linear trend line obtained with increasing fiber content as shown in equation 6.4.

$$\sigma_{ti} = \alpha_i * \varphi_{fi} + \sigma_{oi} \quad \text{..... (6.4)}$$

Where: σ_{ci} is the tensile stress (MPa); φ_{fi} is the fiber content (%); α_i is the shape parameter (MPa), σ_{oi} is reference stress parameter (MPa). The parameters values of the tensile stress versus fiber content for the tested materials as shown in Table 6.2. The tensile stress of CFRCC compared to cement mortar, an addition of fibers can increase the tensile stress up to 39%.

Table.6.2. **Fitting parameters values of the tensile stress versus fiber content for the tested materials**

Fiber length (mm)	**Correlation coefficient**	**Parameter α_i (MPa)**	**Parameter σ_{oi} (MPa)**
5	0.9654	0.216	2.032
10	0.9994	0.248	2.046
15	0.9973	0.305	2.011

The relationship between fiber length and alpha parameter is shown defined Equation 6.4:

$$\alpha_i = (0.0089 * L_{fi} + 0.1673) \quad \text{..... (6.5)}$$

Furthermore, the models are developed to predict tensile stress based on fiber content and fiber length defined is shown in equation 6.5:

$$\sigma_{ti} = [(0.0089 * L_{fi} + 0.1673) * \varphi_{fi} + \sigma_{oi}] \quad \text{..... (6.6)}$$

Where: σ_{ti} is the tensile stress (MPa); L_{fi} is the fiber length; φ_{fi} is the fiber content (%); σ_{oi} is the reference stress parameter (MPa).

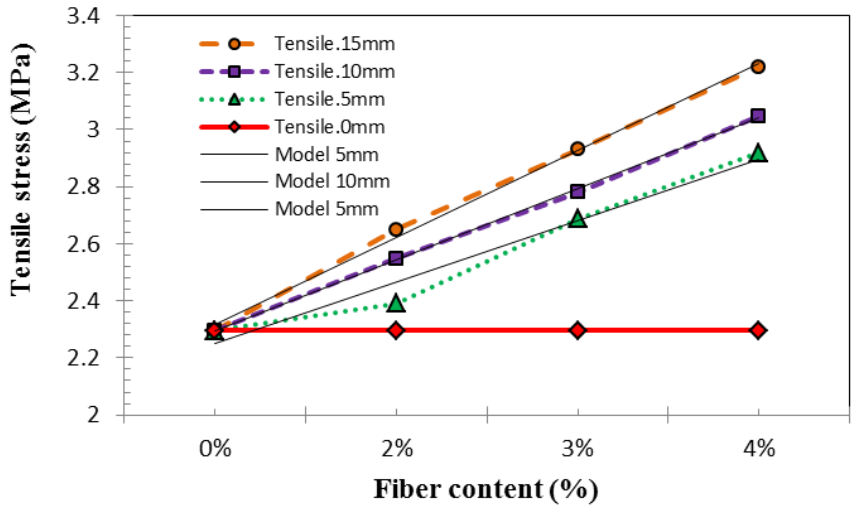

Figure. 6.32.**Effect of fiber content on tensile stress**

Figure 6.33 shows the influence of fiber length on a maximum of stress. The fiber length of 15mm with a fiber content of 4% gives the highest value compared to cement mortar without fibers. Tensile stress increases with increasing fiber length. It is the same as the results presented by Baruah and Talukdar, (2007). However, the fiber length of more than 2.5 cm the results obtained Ali et al. (2012) getting splitting tensile strength decreases with higher fiber content.

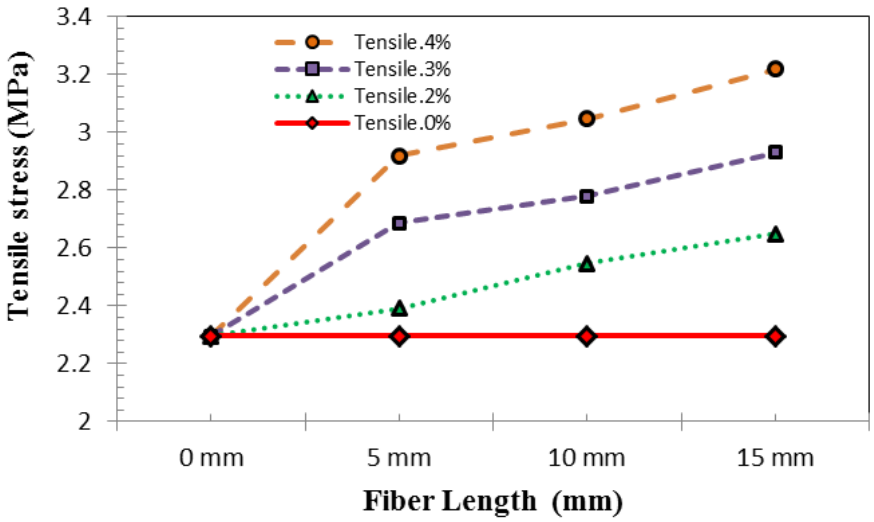

Figure. 6.33. **Effect of fiber length on tensile stress**

6.6.3. Compressive modulus behavior

Figure 6.34 shows the influence of fiber content on the static modulus of elasticity due to the compressive strength. The compressive modulus of CFM composite increased with increasing fiber content. However, the compressive modulus of CFM composites having 10 mm fibers length increasing fiber contents showed it first decreased and then increased to 4%, These values were higher than that of cement mortar. Compared to cement mortar value an addition of fibers caused about 15% increase for 5mm fibers length of the elastic modulus of CFM composite. The empirical model is developed to predict compressive modulus defined as:

$$Ec = \alpha * {\varphi_{fi}}^2 + \beta * \varphi_{fi} + \gamma \quad \text{..... (6.7)}$$

Where: *Ec* is the compressive modulus (GPa); φ_{fi} is the fiber content parameter of the values of 0, 1, 2, 3, 4 (%) , α, β , γ are fitting parameters (GPa) corresponding to fiber length. The fitting parameters values of the compressive modulus versus fiber content for the tested materials as shown in Table 6.3. The results polynomial Equation (6.7) is the same as the results obtained by Ali et al. (2012).

Table.6.3. **Fitting parameters values of the compressive modulus versus fiber content for the tested materials**

Fiber length (mm)	**Correlation coefficient**	**Parameter** α (GPa)	**Parameter** β (GPa)	**Parameter** γ (GPa)
5	0.9996	0.053	0.242	1.828
10	0.9990	0.488	-2.266	3.888
15	0.9918	0.123	-0.323	2.332

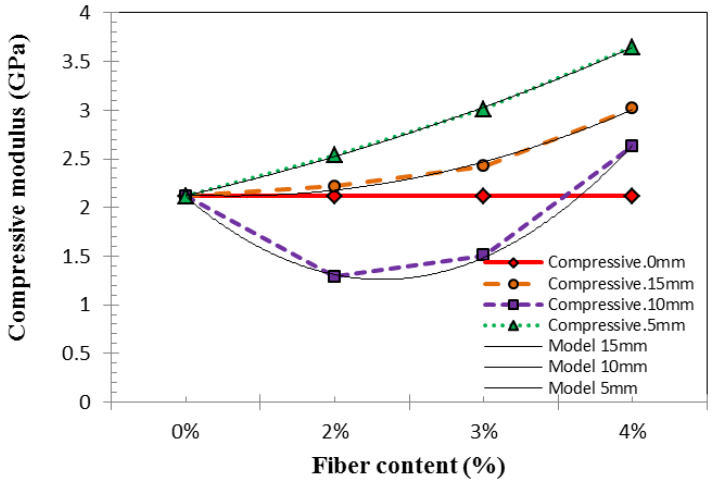

Figure. 6.34.**Effect of fiber content on compressive modulus.**

Figure 6.35 shows the influence of fiber length on the static modulus of elasticity due to the compressive strength. The elastic modulus of CFRCC having 5mm increased with increasing fibre content. However, the compressive modulus of CFRCC having 10 mm fibres length with decreasing fibre contents showed it first decreased and then increased to 4%, and these values were higher than that of cement mortar. Compared to cement mortar value, an addition of fibers caused about 72% increase for 5mm fibers length of the elastic modulus of CFRCC. The solid straight line is elastic of cement mortar.

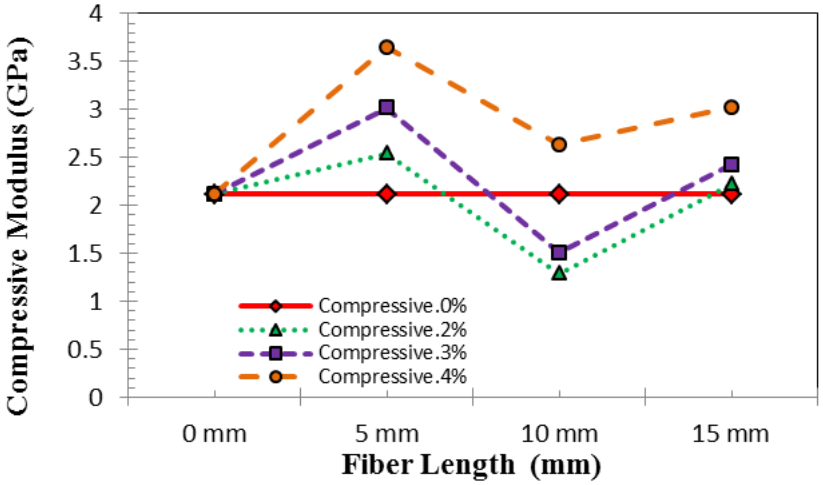

Figure. 6.35. **Effect of fiber length on compressive modulus.**

Figure 6.36, Figure 6.37 and Figure 6.38 shows the influence of fiber content on the static modulus of elasticity and the compressive stress for 5mm, 10mm and 15 mm fiber length.

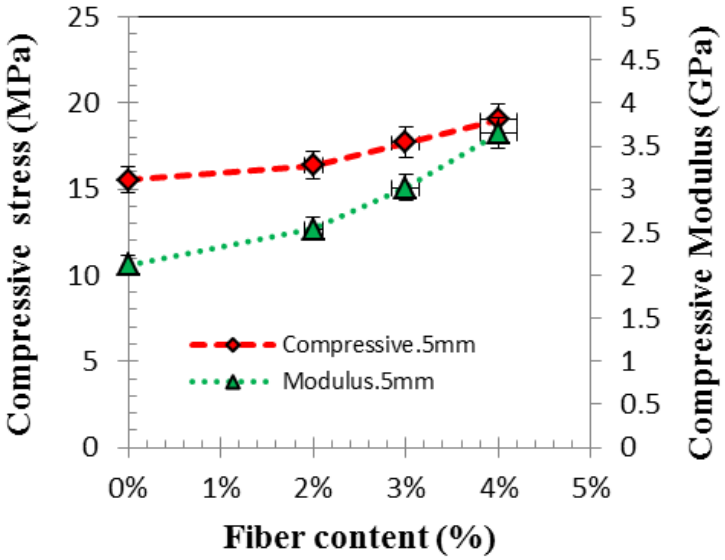

Figure. 6.36. **Effect of fiber content on compressive stress and compressive modulus for fiber length 5mm.**

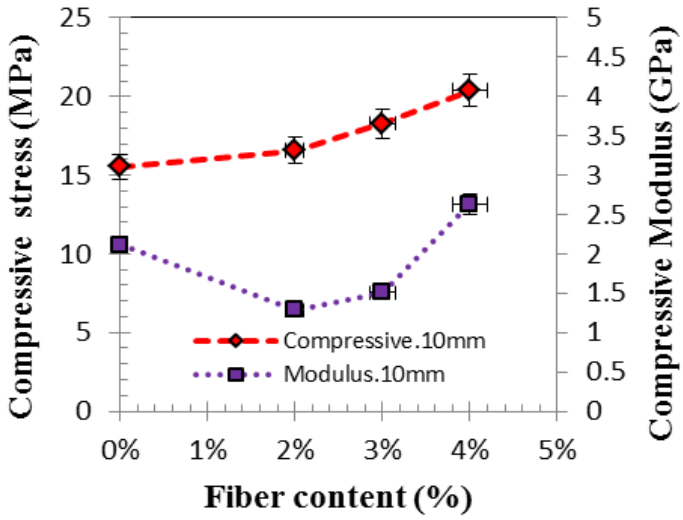

Figure. 6.37. **Effect of fiber content on compressive stress and compressive modulus for fiber length 10mm.**

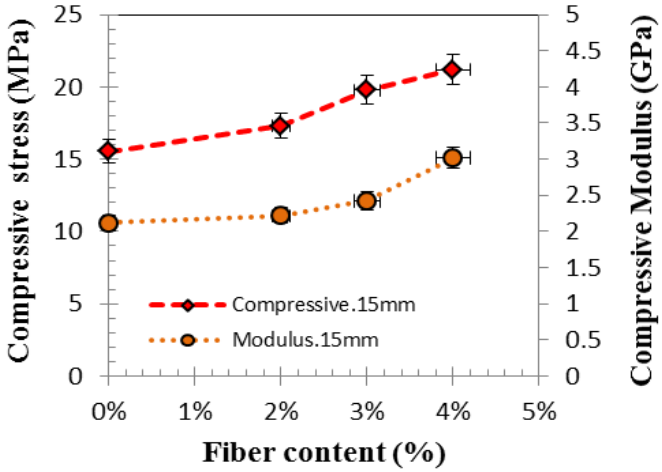

Figure. 6.38. **Effect of fiber content on compressive stress and compressive modulus for fiber length 15mm.**

Figure 6.39 shows the relationship between the compressive stress and compressive modulus on the fiber content and fiber length. The elastic modulus of CFRCC increased with increasing fibre content and increased compressive stress. That is attributed to the improvement of the fiber ability to delay the micro-crack formation and to arrest crack propagation [Sahmaran et al., 2007]. According to the research results obtained Ali et al. (2012) modulus of elasticity declined to fiber length is greater than 5cm and with added fiber.

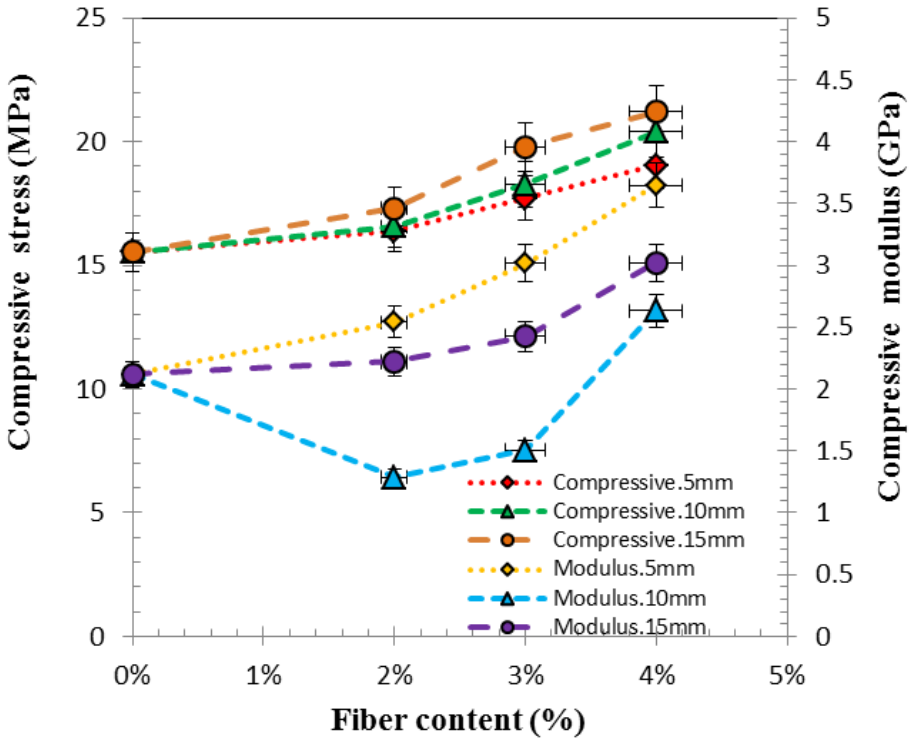

Figure. 6.39. **Effect of fiber content on compressive stress and compressive modulus**

6.6.4. Tensile modulus behavior

Figure 6.40 shows the influence of fiber content on the static modulus of elasticity due to the tensile strength. The tensile modulus of CFRCC decreased with increasing fiber content. However, a tensile modulus of CFRCC having 10 mm fibers length with increasing fiber contents showed it lowest tensile modulus than that cement mortar. Compared to cement mortar value an addition of fibers caused about 45% decrease for 10mm fibers length of the tensile modulus of CFRCC for 4% fiber content.

The empirical model is developed to predict tensile modulus of elasticity as shown in equation 6.8 and the fitting parameters values of the tensile modulus versus fiber content for the tested materials as shown in Table 6.4

$$Et = \alpha * \varphi_{fi}{}^{2} + \beta * \varphi_{fi} + \gamma \quad \text{..... (6.8)}$$

where: *Et* is the tensile modulus (GPa); φ_{fi} is the fiber content (%); α, β, γ are fitting parameters (GPa) corresponding to the fiber length.

Table.6.4. **Fitting parameters values of the tensile modulus versus Fiber content for the tested materials**

Fiber length (mm)	Correlation coefficient	Parameter α (GPa)	Parameter β (GPa)	Parameter γ (GPa)
5	0.9977	0.014	-0.141	0.956
10	0.9977	0.042	-0.328	1.107
15	0.9912	0.0004	-0.064	0.897

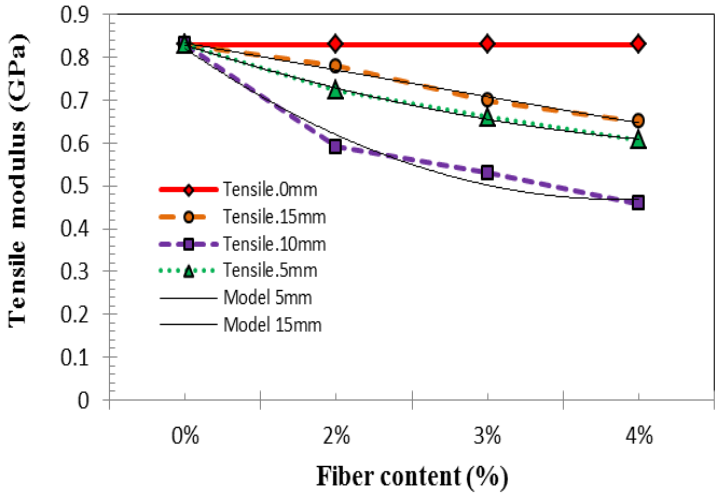

Figure. 6.40.**Effect of fiber content on tensile modulus.**

Figure 6.41 shows the influence of fiber length on tensile modulus of elasticity due to the tensile strength. The elastic modulus of fiber composite having 5mm to 15mm decreased with increasing fibre content.

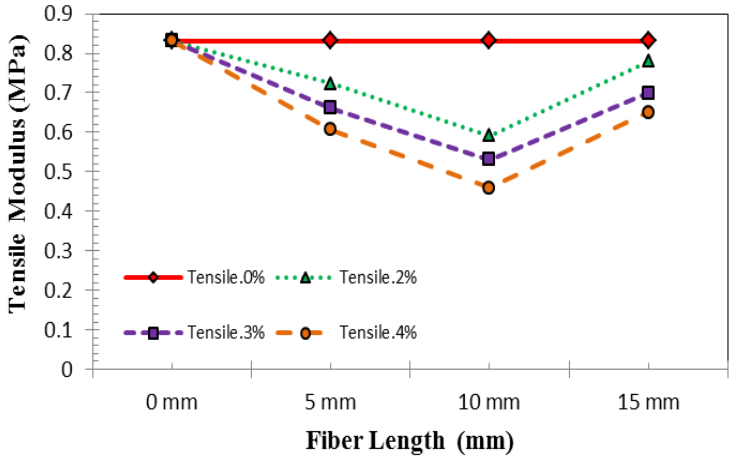

Figure. 6.41.**Effect of fiber length on tensile modulus.**

However, the compressive modulus of CFRCC having 10 mm fibres length with increasing fibre contents showed it values were lowest than that of cement mortar. Compared to cement mortar value, an addition of fibers caused about 45% decrease for 10mm fibers length of the tensile modulus of CFRCC. The solid straight line is the elastic modulus of cement mortar. Figure 6.42, Figure 6.43 and Figure 6.44 shows the influence of fiber content on tensile modulus and the tensile strength for 5mm, 10mm and 15 mm fiber length. Results showed that the increase in fiber content will increase the tensile stress, but lowers the value of the tensile modulus.

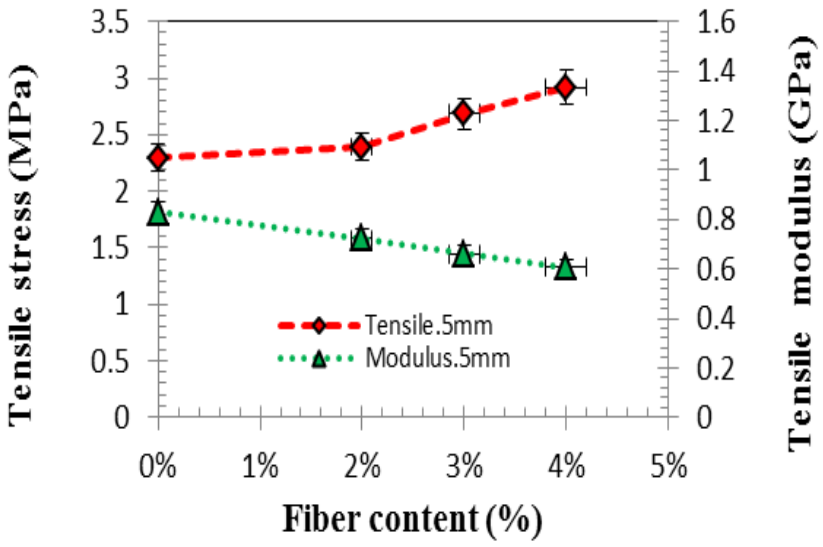

Figure. 6.42.**Effect of fiber content on tensile stress and tensile modulus for fiber length 5mm.**

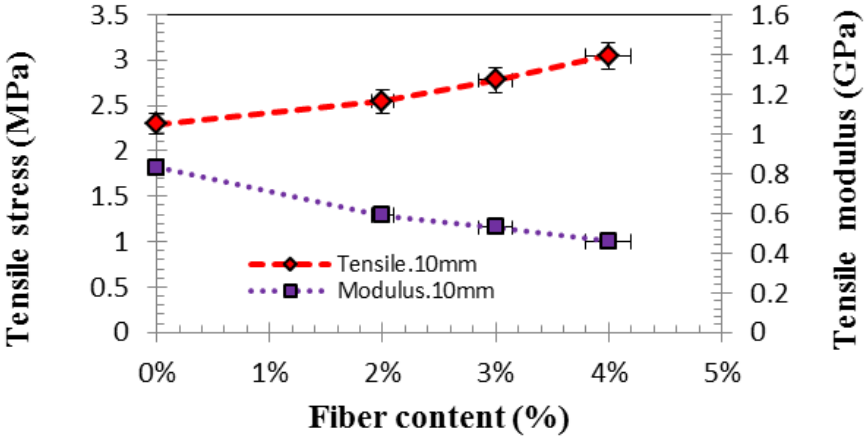

Figure. 6.43.**Effect of fiber content on tensile stress and tensile modulus for fiber length 10mm.**

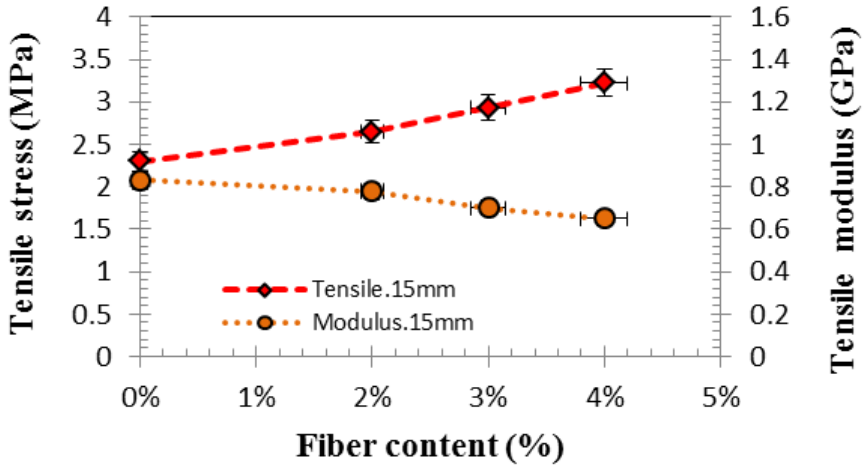

Figure. 6.44.**Effect of fiber content on tensile stress and tensile modulus for fiber length 15mm.**

Figure 6.45 shows the relationship between the tensile stress and tensile modulus on the fiber content and fiber length. The tensile modulus of CFRCC decreased with increasing fibre content and increased tensile stress. It is attributed to the improvement of the fiber ability to delay the micro-crack formation and to arrest crack propagation [Sahmaran et al., 2007].

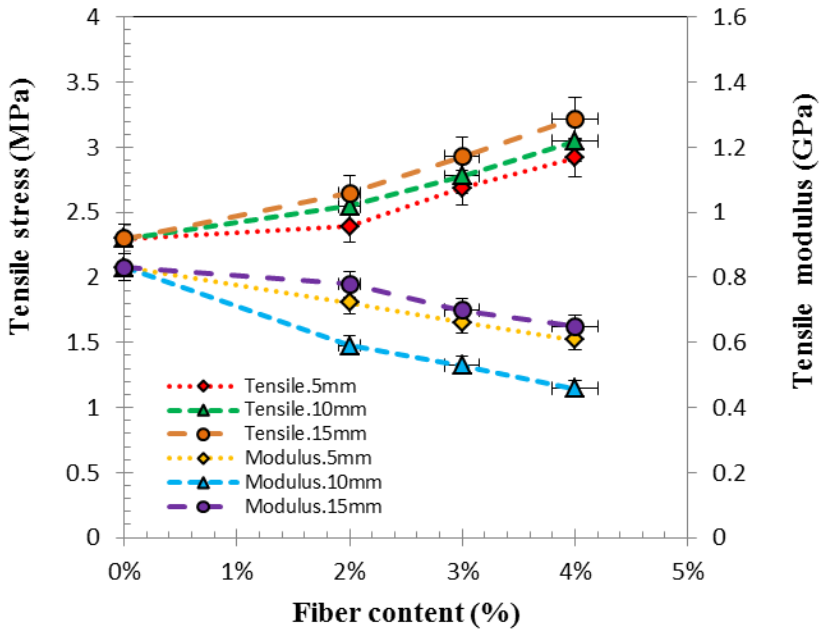

Figure. 6.45.**Effect of fiber content on tensile stress and tensile modulus**

.

6.6.5. Density behavior

Figure 6.34 and Figure 6.35 shows the effect of fiber content and length on the density of CFRCC. The solid straight line indicates the density of cement mortar. The presence of fibers content increase and the density only slightly changes. Also due to the amount of fiber, it can be justified by the effects experienced by the material in the pressure gradient during its formation. This pressure gradient matrix porosity overcomes problems caused by the fibers. However, a decrease in density could be due simply to the low mass volumes of coir fiber. The density of CFRCC decreased with higher fiber content and increased with shorter fiber length but still below the cement mortar.

The empirical model is developed to predict density as shown in equation 6.9 and the fitting parameters values of the density versus fiber content for the tested materials as shown in Table 6.5

$$\rho = \alpha * \varphi_{fi}{}^{2} + \beta * \varphi_{fi} + \gamma \quad \text{..... (6.9)}$$

where: ρ is the density (**kg**/m^3); φ_{fi} is the fiber content (%); α, β, γ are fitting parameters (kg/m^3) corresponding to the fiber length.

Table.6.5. **Fitting parameters values of the density versus fiber content for the tested materials**

Fiber length (mm)	Correlation coefficient	Parameter α (kg/m^3)	Parameter β (kg/m^3)	Parameter γ (kg/m^3)
5	0.9992	-2.907	0.545	2122.9
10	0.9866	0.409	-21.306	2142.4
15	0.9791	3.773	-47.452	2166.1

In general, the density of fiber composite in 4% fiber content decreased up to 3.9% for 15mm; 2.6% for 10mm; 2 % for 5mm as compared to that of cement mortar as shown in Figure 6.46. As well as shown in Figure 6.47, the density of fiber composite in 15mm fiber length decreased up to 3.8 % for 4% fiber content; 3.3% for 3% fiber content; 1.3% for 2% fiber content as compared to that of cement mortar.

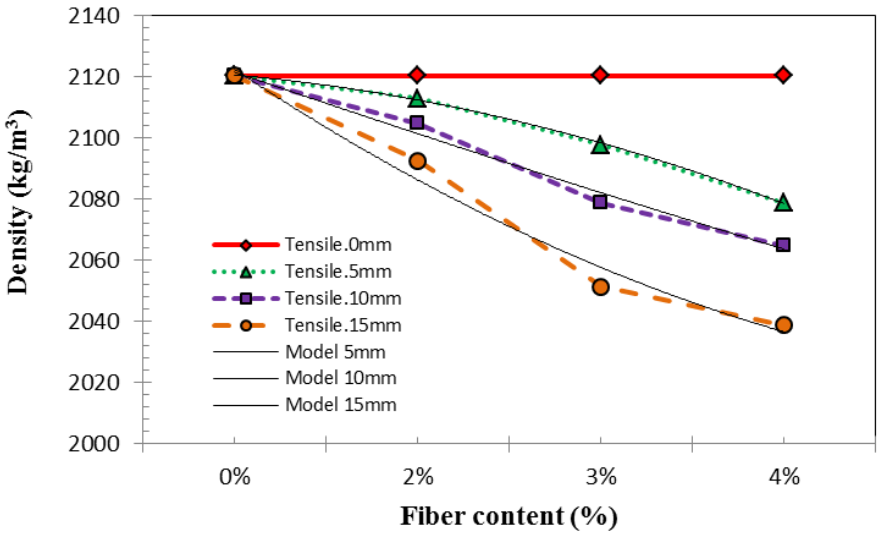

Figure. 6.46.**Effect fiber content on density**

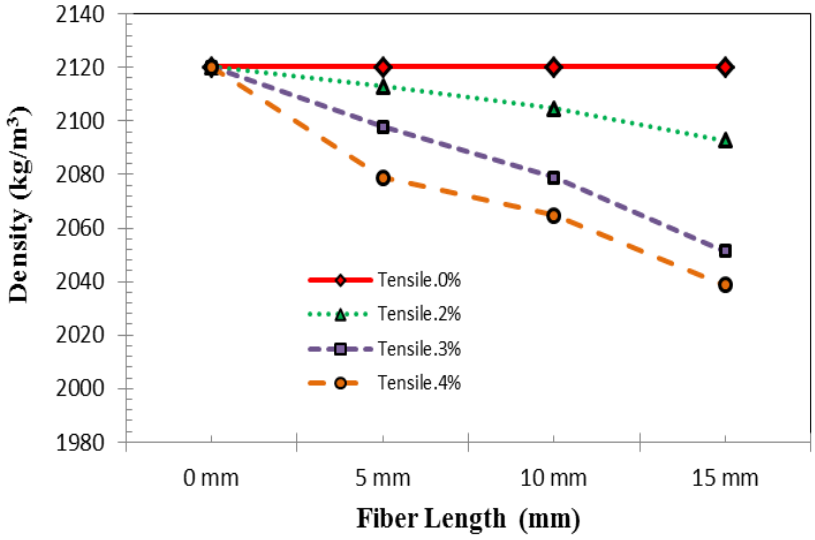

Figure. 6.47.**Effect fiber length on density**

Figure 6.48, Figure 6.49 and Figure 6.50 shows the influence of fiber content on density and the tensile strength for 5mm, 10mm and 15 mm fiber length. Results showed that the increase in fiber content will increase the tensile strength, but lowers the value of the density. Same as obtained by Ali et al. (2012) to get the density of composite decreased with higher fiber content and increased with shorter fiber length.

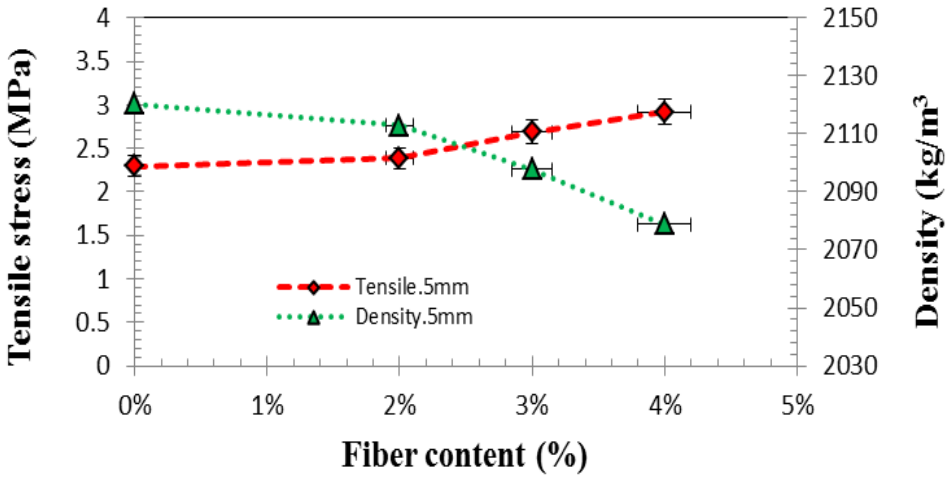

Figure. 6.48.**Effect of fiber content on tensile stress and density for fiber length 5mm.**

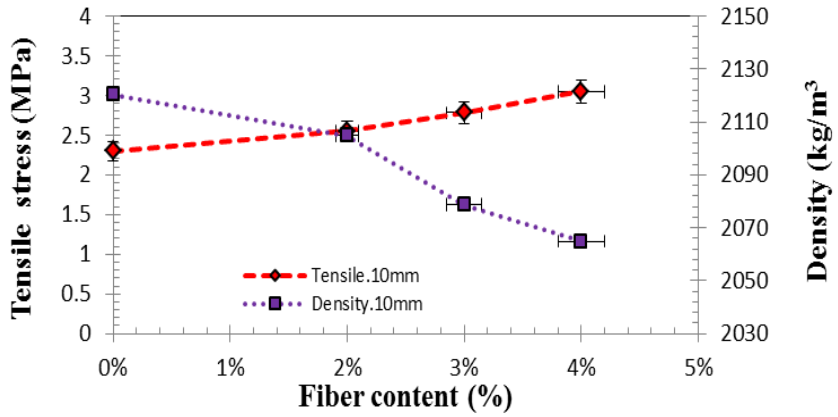

Figure. 6.49.**Effect of fiber content on tensile stress and density for fiber length 10mm.**

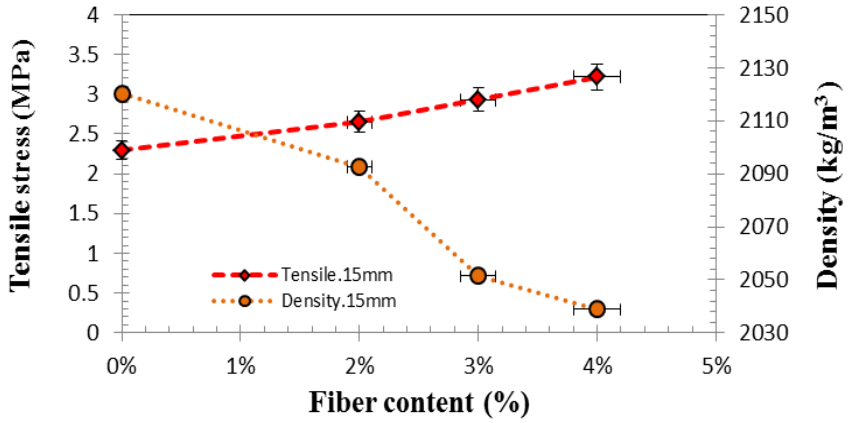

Figure. 6.50.**Effect of fiber content on tensile stress and density for fiber length 15mm.**

Effect of fiber content on density and tensile stress for fiber length are shown in Figure 6.51. Tensile stress increases with increasing fiber content while density decreases. Also, due to the amount of fiber, it can be justified by the effects experienced by the material in the pressure gradient during its formation. This pressure gradient matrix overcome porosity problems caused by the fibers. Furthermore, the density of the CFRCC decrease by an increase of fiber added, leading to an improvement in strength/weight ratio.

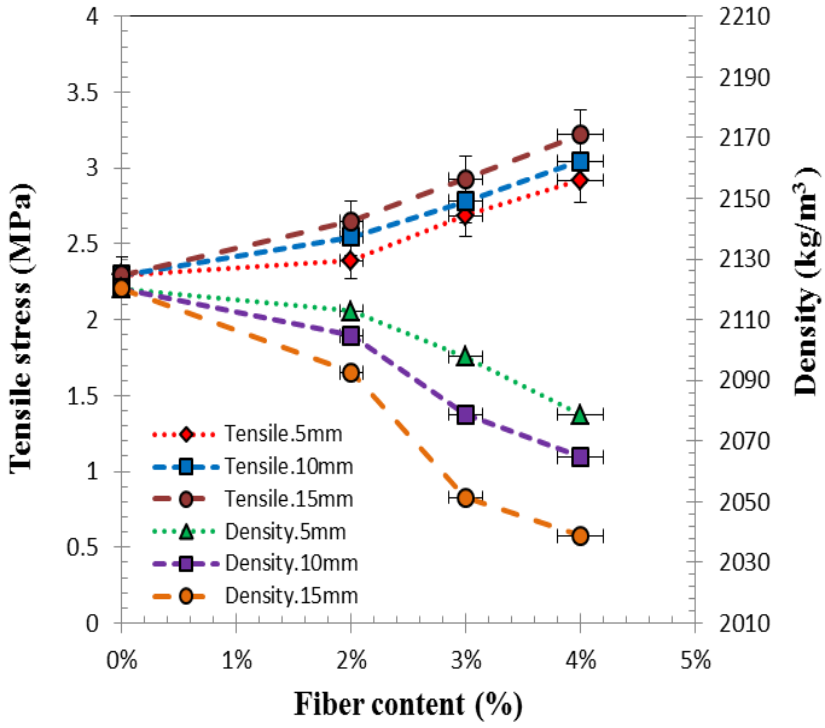

Figure. 6.51.**Effect of fiber content on tensile stress and density for fiber length.**

6.6.6. Strain Behavior

Figure 6.52 and Figure 6.53 shows he experimental test results the effect of fiber content and length on the strain of CFRCC, under forming using extrusion. The solid straight line indicates a strain of the cement mortar. Strain value increases with increasing the fiber content. The value of strain with 10mm fiber length gives a higher value than the fibers length of 15mm, and it is above the value of the strain of cement mortar.

The empirical model is developed to predict strain as shown in equation 6.10 and the fitting parameters values of the strain versus fiber content for the tested materials as shown in Table 6.6

$$\varepsilon = \alpha * {\varphi_{fi}}^2 + \beta * \varphi_{fi} + \gamma \quad \text{..... (6.10)}$$

where: ε is the tensile strain (%); φ_{fi} is the fiber content (%); α, β, γ are fitting parameters (%) corresponding to the fiber length.

Table.6.6. **Fitting parameters values of the tensile strain versus fiber content for the tested materials**

Fiber length (mm)	Correlation coefficient	Parameter α (%)	Parameter β (%)	Parameter γ (%)
5	0.9965	-0.001	0.047	0.3145
10	0.9983	-0.052	0.427	-0.0123
15	0.9705	-0.033	0.242	0.1569

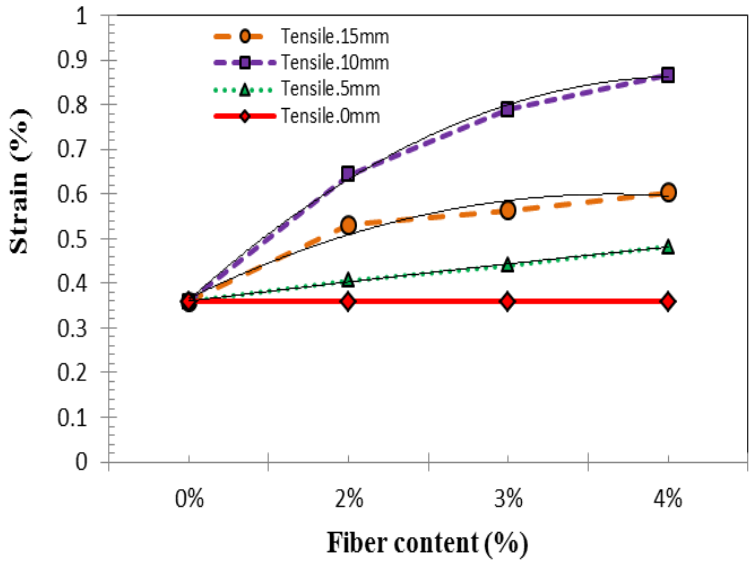

Figure. 6.52. **Effect fiber content on strain**

Figure 6.53 shows the influence fiber length on strain due to the tensile stress. The strain of CFRCC for 10 mm fiber length has a higher value than the strain at 5 mm and 15 mm fiber length. Strain value increased with increasing fibre content.

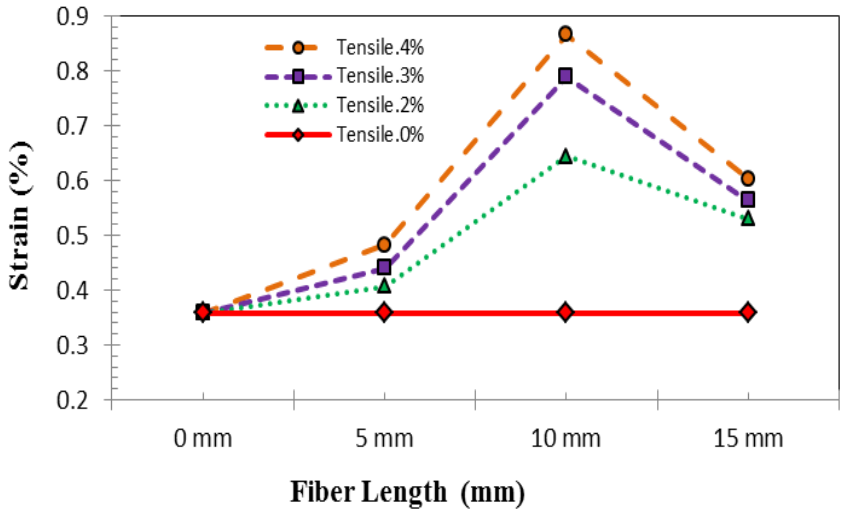

Figure. 6.53.**Effect fiber length on strain**

Effect of fiber content on strain and the tensile stress for 5mm, 10mm and 15 mm fiber length was shown in Figure 6.54, Figure 6.55 and Figure 6.56. Results showed that the increase in fiber content will increase strain and the tensile stress.

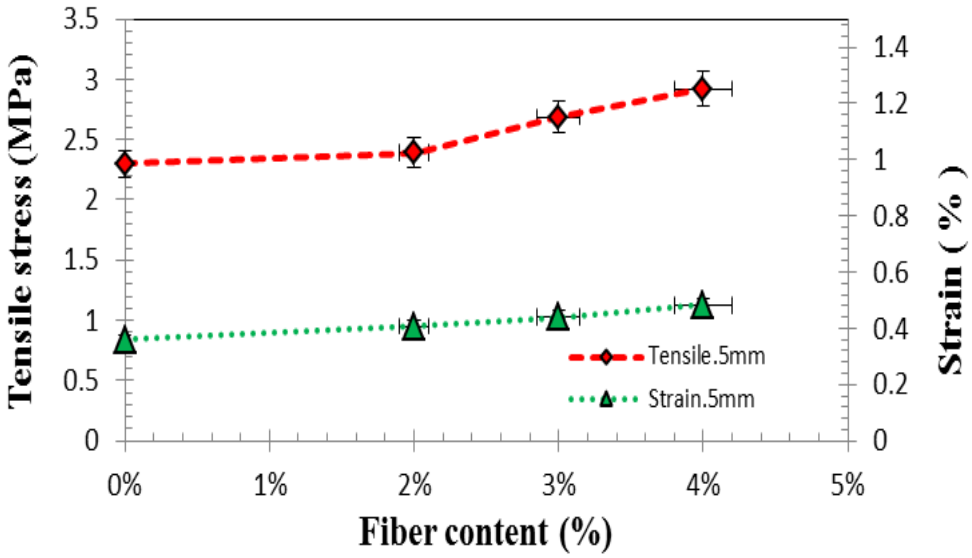

Figure. 6.54.**Effect of fiber content on tensile stress and strain for fiber length 5mm.**

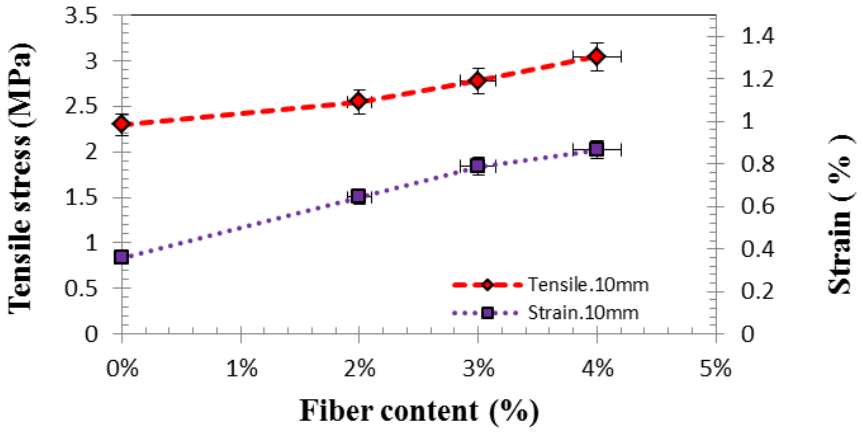

Figure. 6.55.**Effect of fiber content on tensile stress and strain for fiber length 10mm.**

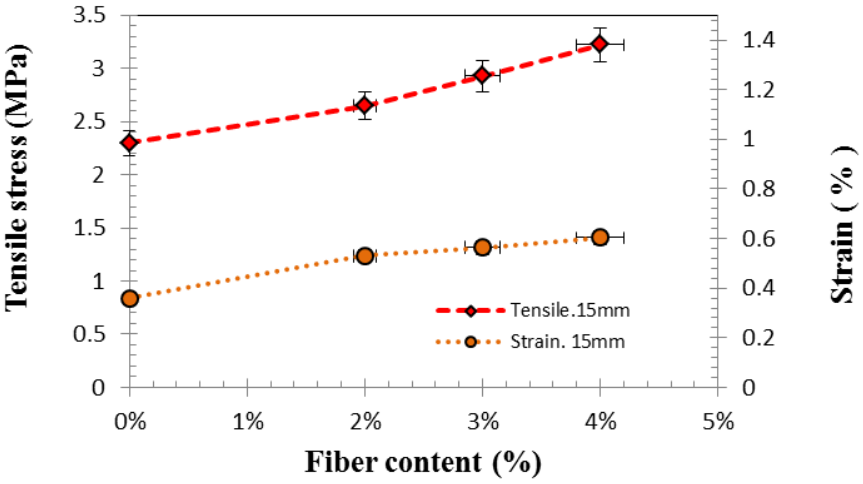

Figure. 6.56.**Effect of fiber content on tensile stress and strain for fiber length 15mm.**

Effect of fiber content on tensile stress and strain for fiber length are shown in Figure 6.57. The tensile stress and strain increase with increasing fiber content. The strain for 10mm fiber length higher strain value of the fiber length of 5mm and 15mm. The fiber length of 10mm gives a higher strain value of the fiber length of 5mm and 15mm. The increase in strain reached 142% of the strains cement mortar. While the tensile stress increased by 40% from the strain of cement mortar

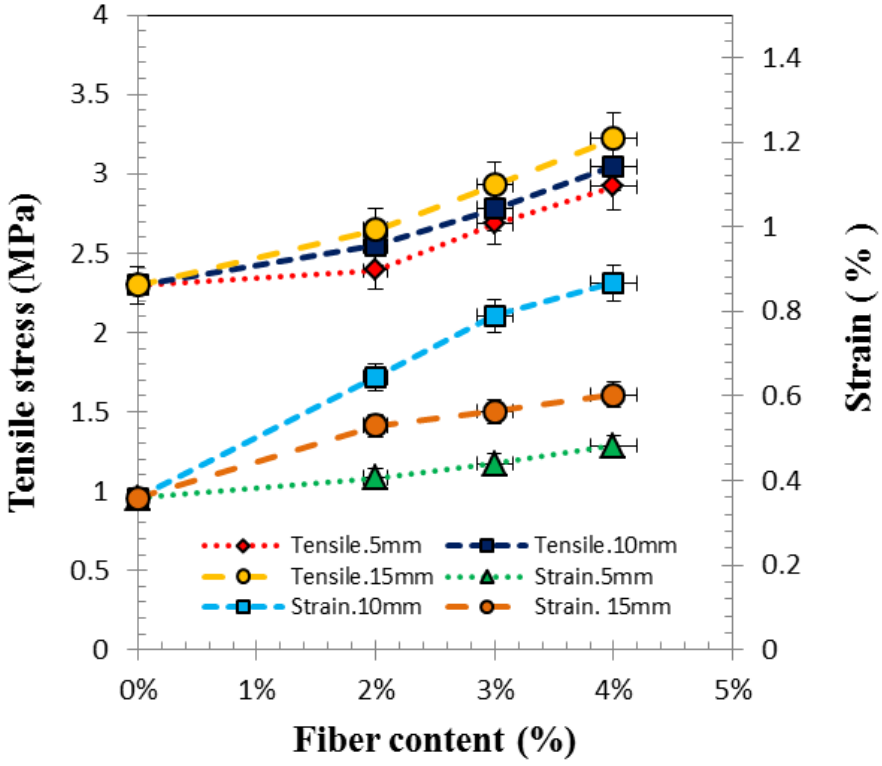

Figure. 6.57.**Effect of fiber content on tensile stress and strain for fiber length**

6.7. The conclusion of the chapter.

The performance mechanical of coir fiber reinforced cement mortar composites compared with cement mortar. Moreover, information obtained where structural composite materials are an excellent opportunity to produce components that achieve weight savings and improved properties. Fiber reinforced cementitious material can enhance by processing, such as extrusion that will improve the interfacial bond through the application of pressure.

Mechanical performance tensile and compressive strength can be improved through the process of surface treatment of fibers and after going through the extrusion process for compacting with a smooth surface result that the materials are extrudability.

Aspects surface obtained as a result of the mold in comparison with the outcome of the screw extrusion process. Mold process is uneven, not smooth surface defects as well as the extrusion process. In observation of the composite material obtained fiber direction lengthwise direction is random. The processes of

forming by extrusion provide performance results of compressive strength, and tensile strength is better than the manual process with mold.

Tensile strength and compressive strength of mortars have shown a gradual increase in increasing fiber content and fiber length. These values are higher for fiber composites when compared to cement mortar ones. The empirical model is developed to predict compressive strength and tensile strength based on a linear trend line obtained with increasing fiber content defined as:

$$\sigma_i = \alpha_i * \varphi_{fi} + \sigma_{oi}$$

The models are developed to predict compressive stress based on fiber content, and fiber length defined as:

$$\sigma_{ci} = [(0.0763 * L_{fi} + 0.8187) * \varphi_{fi} + \sigma_{oi}]$$

The models are developed to predict tensile stress based on fiber content and fiber length defined as:

$$\sigma_{ti} = [(0.0089 * L_{fi} + 0.1673) * \varphi_{fi} + \sigma_{oi}]$$

Compressive modulus of CFRCC increased with the increasing fiber content and increased compressive strength while the tensile modulus of coir fiber cement mortar composites decreased with increasing fiber content and increased tensile strength. The empirical model is developed to predict compressive modulus and tensile modulus defined as:

$$E = [\alpha * \varphi_{fi}^{2}] + [\beta * \varphi_{fi}] + \gamma$$

Density decreases with the increasing fiber content, increased the compressive strength and tensile strength. The empirical model is developed to predict density with increasing fiber content defined as:

$$\rho = [\alpha * \varphi_{fi}^{2}] + [\beta * \varphi_{fi}] + \gamma$$

The tensile strain and tensile strength increases with the increasing fiber content. The strain for 10mm fiber length has higher strain value of the fiber length of 5mm and 15mm. The empirical model is developed to predict strain with increasing fiber content defined as:

$$\varepsilon = [\alpha * \varphi_{fi}^{2}] + [\beta * \varphi_{fi}] + \gamma$$

The failure mode for mortar with cracked lengthwise direction unidirectional pressure and can be seen for cracks on the bottom and top surface. The mortar without fibers resulting test sample destroyed at the top. The failure mode for composites that the crack marked has a tendency to propagate parallel to the loading direction in the mortar matrix. Fiber content increases the tendency of cracks that occur less. It shows the strength of the fiber bond with mortar matrix.

CHAPTER.7.
MICROMECHANICS, MICROSTRUCTURE, DAMAGE AND MODELS OF SCREW EXTRUDED FIBER COMPOSITES USING NONDESTRUCTIVE TESTING METHOD

7.1. Introduction

In this section, the following deals with characteristic, damage, micromechanics and modeling of the cement mortar and coir fiber reinforced cementitious composite mortar (CFRCC) using digital image correlation (DIC), nondestructive method. Results of the microstructural examination, using an optical microscope and scanning electron microscope (SEM). It is shown that the shape of the pore, the distribution and orientation of coir fiber determines the compressive and tensile behavior of the composite. In the present investigation, the maximum compressive and tensile strengths are observed for composite containing coir fiber and hence the discussion based on this composition. The compressive parameter strength and tensile strength are very often used to quantify the quality of cementitious materials.

7.2. Mechanical characteristics of fiber composite behavior

The mechanical properties of extruded cement mortar and extruded CFRCC obtained from the DIC technique are presented in this section. Compressive strength and tensile strength are processed with Aramis -3D software. The specimen used cylindrical for compressive and splitting tensile test.

7.2.1. Compressive strength behavior

The axial deformation of cement mortar and fiber composite was recorded using DIC method. The strain of the front surface of the fiber composite measured with the DIC system by stacking images obtained at different stages of loading. The stress–strain curves measured by MTS and DIC method showed good agreement as displayed and compared in Figure 7.1 for cement mortar and Figure 7.2 for fiber composite.

The axial strain at the beginning introduced due to the vertical deformation. The cement mortar that did not contain coarse aggregates exhibited the almost uniform deformation before the peak load.

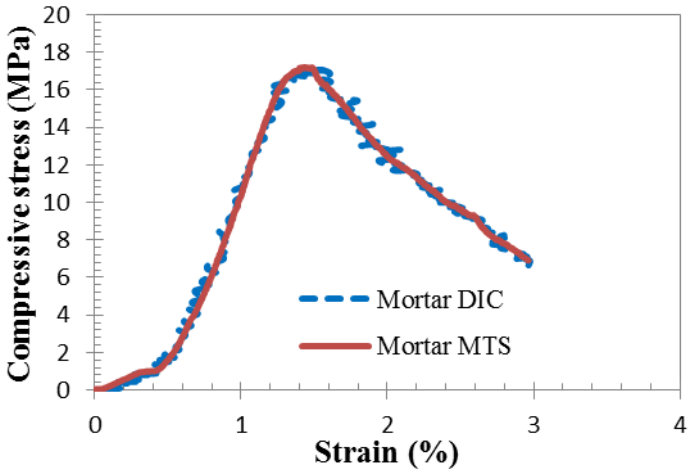

Figure. 7.1. **Typical compressive stress – strain curves of cement mortar using MTS and DIC**

The peak load from the compressive strength showed a lower value in the cement mortar compared to the fiber composite. It indicates that the stiffness of cement mortar appears relatively lower than those of fiber composite. However, the cement mortar having the strain higher than the CRFCC, because the cement mortar have a long time for failure and due to effect clay in a mortar.

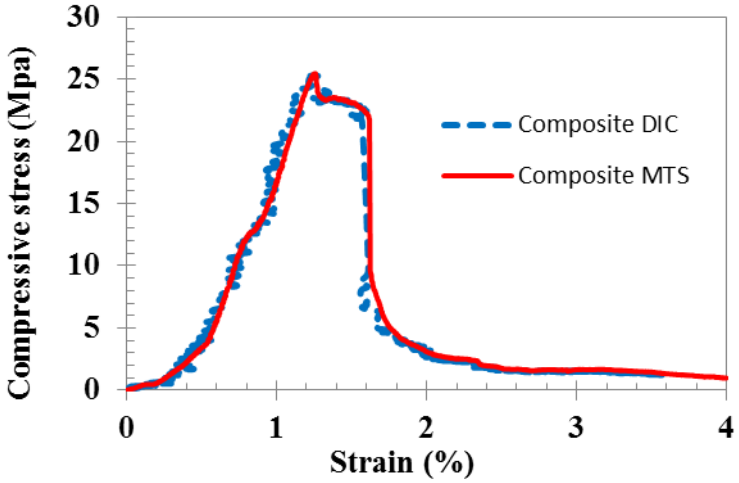

Figure. 7.2. **Typical compressive stress – strain curves of fiber composite using MTS and DIC**

When compared to the fiber composite then cement mortar as shown in Figure 7.3. Stress value of the fiber composite higher than the cement mortar.

That is because of the contribution of fiber strength. However, the strain of the cement mortar is greater than the fiber composite for compressive strength testing.

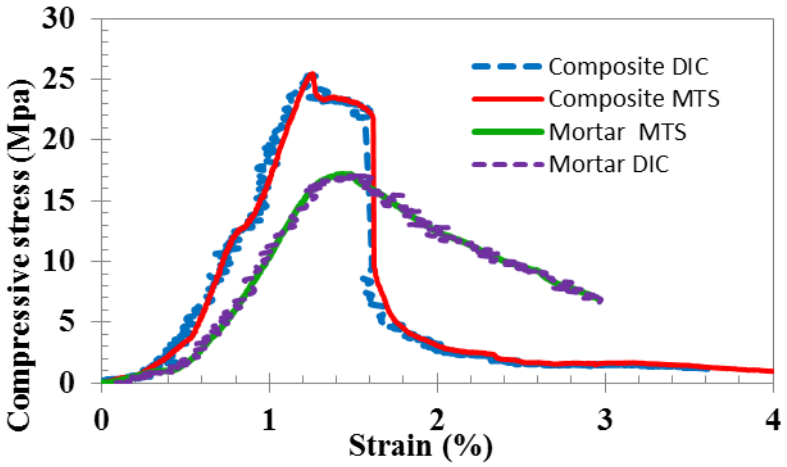

Figure. 7.3. **Typical compressive stress – strain curves of fiber composite using MTS and DIC**

7.2.2. Tensile strength behavior

Observation of the tensile strength through the splitting tensile strength measurement using the MTS contact method and by DIC no contact method as shown in Figure 7.4 and Figure. 7.5. show approximately equal results.

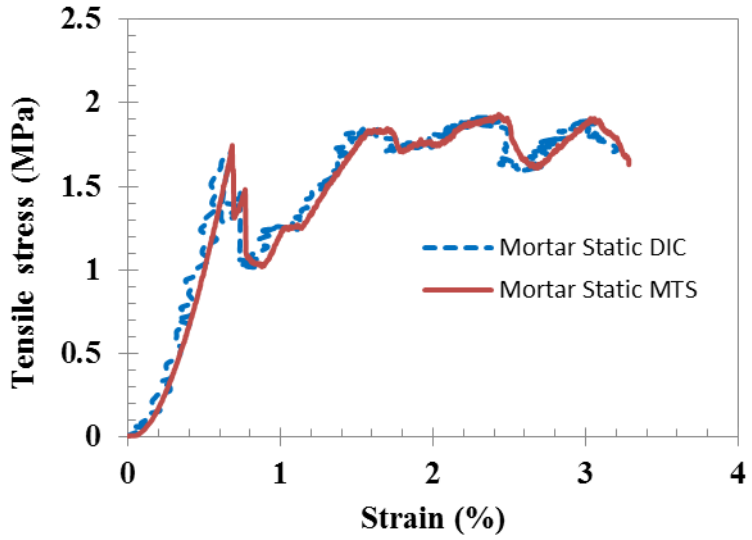

Figure. 7.4. **Typical split tensile stress – strain curves of cement mortar using MTS and DIC**

The load value can retain by the CFRCC is twice that of the load obtained by cement mortar. That is because in the case of cement mortar cracks in the matrix. However, cracks occur in the CFRCC material after the defense of the fiber. Also, when viewed from a failure of the CFRCC materials have nearly twice the time of the failure of the cement mortar. Thus, the addition fibers made of ductile properties for CFRCC materials.

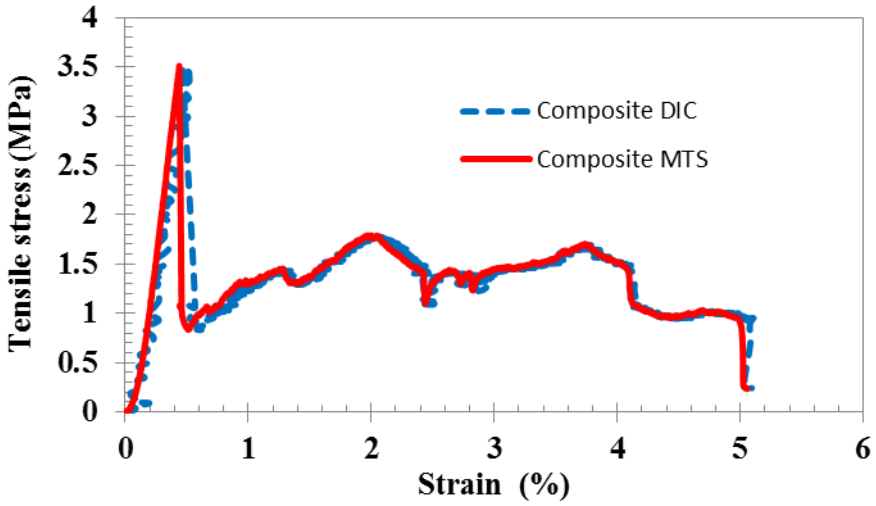

Figure. 7.5. **Typical split tensile stress – strain curves of fiber composite using MTS and DIC**

Figure 7.6 shows the stress value of the fiber composite is higher than the cement mortar. As well as strain value of composite after the peak load has higher strain than the strain of the cement mortar. The CFRCC strain reached 5% while on cement mortar reaches 3%. That is due to the effect of the strength of the fiber that is ductile.

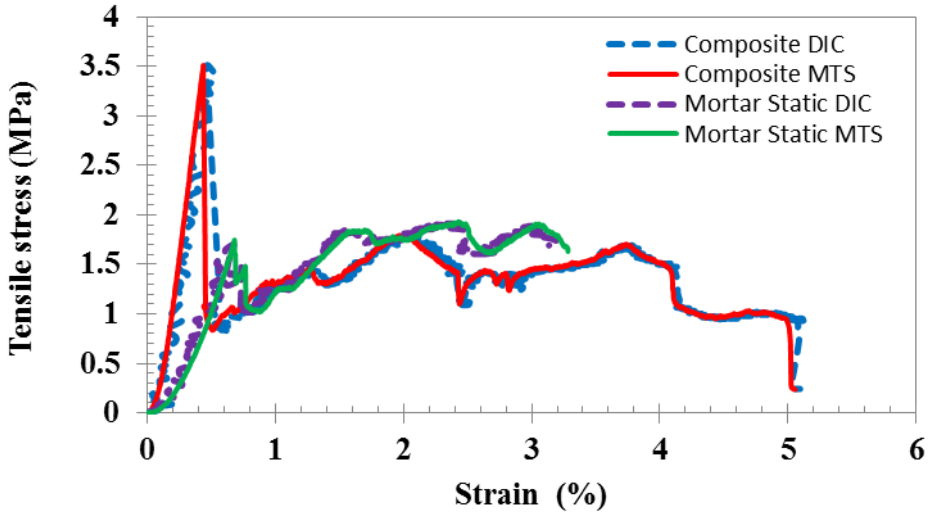

Figure. 7.6. **Typical split tensile stress – strain curves of fiber composite using MTS and DIC**

7.3. Damage Evolution.

Digital Image Correlation (DIC) are used to investigate the damage processes of cement mortar and CFRCC under compressive strength and tensile strength. Strain and displacement were computed to analyze the initial cracks and propagation during loading.

The compressive and tensile characteristics of extruded CFRCC were determined by testing a minimum of three-cylinder specimens for each batch using the Mechanical Testing System (MTS) and the Digital Image Correlation (DIC). The accuracy of displacement and strain measurements obtained. DIC technique depends on the quality of speckle pattern, surrounding vibrations, lighting, out-of-plane displacements and specimen height used for strain computations. [Shah et Chandra Kishen, 2011]. The displacement contour maps obtained from the DIC system can show detailed crack patterns. On the other hand, the small strain concentrations distribution can provide information about the micro cracks initiation and development [Van Mier, 2008]

On the contrary, the deformations in the fiber composite and cement mortar which stemmed from the growth of microcracks and failure of interfacial bonds show continuous increase through the whole pre-peak range. Hence, the failure processes in these specimens started from a very early loading stage and developed gradually with the increase of loading. During the pre-peak loading phase, the lateral deformation of fiber composite was more evident than that of cement mortar. It indicates that there are more micro cracks in the fiber composite than cement mortar within the pre-peak loading range.

We will now describe the strain and displacement distribution of CFRCC composite obtained from DIC method at different stages of loading and the strain contour maps obtained from DIC measurement system at four phases are elastic, inelastic, plastic and failure.

7.3.1. the compressive strength of extruded composites

The evolution of the compressive behavior of extruded CFRCC can divide into four phase (elastic, inelastic, softening and failure).

7.3.1.1 Elastic stage

Figure.7.7. Shows the evolution of apparent normal strain in the elastic region during the compression for fiber composite. It shows typical displacement and strain distribution contour. During this stage, reaching 30% of the maximum loading no cracks has occurred.

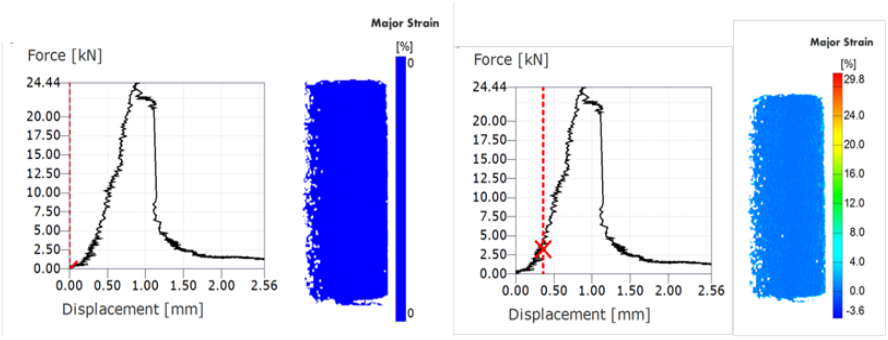

Figure. 7.7. **Evolution of apparent normal strain during the compression at the elastic region for fiber composite.**

7.3.1.2 Inelastic

Figure . 7.8. Presents the strain distribution contour of CFRCC at the inelastic region, 30%-100% of peak loading. At this stage, initial microcracks occurred in 50% of the maximum load. Cracks spread following the spread of cracks to the highest load of 100%; Fiber began to pull out from the matrix and then disconnected. With the increase of loading, the cracks did not uniformly develop on the specimen surface, which locally concentrated and grew vertically.

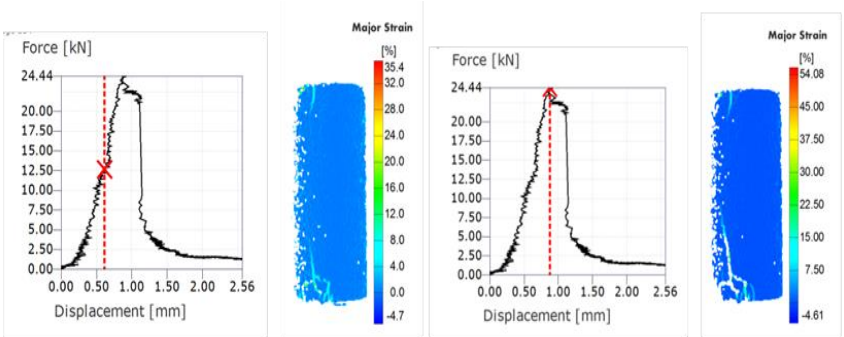

Figure. 7.8. **Evolution of apparent normal strain during the compression during inelasticity phase for fiber composite.**

7.3.1.3 Softening stage

In the softening region, fibers worked up at 20% after the peak load. In this conditions, basic cement mortar failure occurs, fibers are pulled out, broken, and the matrix collapsed, as shown in Figure 7.9. It is observed that a crack initiated at the peak load and propagated in the loading direction at the post-peak range. The main crack propagated almost over the whole height of the sample test.

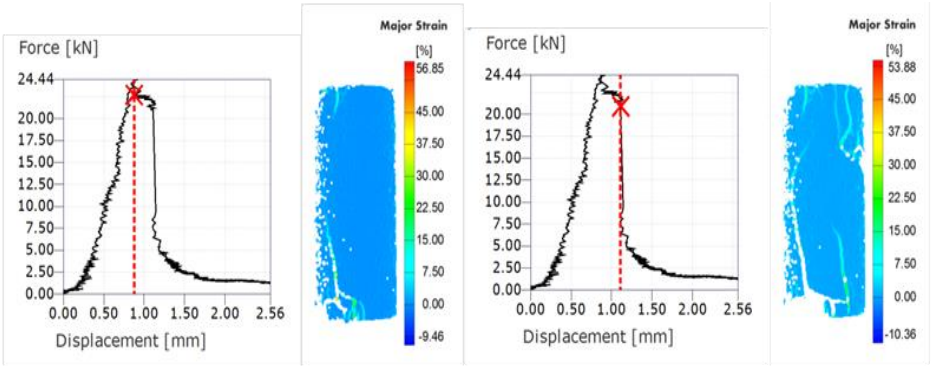

Figure. 7.9. **Evolution of apparent normal strain at selected points during the compression at inelastic after peak load for fiber composite.**

7.3.1.4 Failure

After softening phase, the global failure occurs to crack propagates along the direction of loading and then load drop and sample failure. Although, the sample is still standing thanks to the remaining bridges of fibers into the matrix.

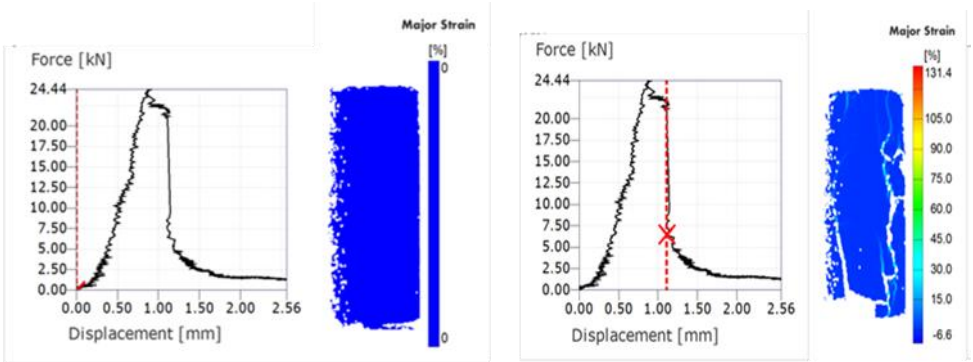

Figure. 7.10. **Evolution of apparent normal strain at selected points during the compression at failure for fiber composite**

7.3.2. Composites extruded on tensile strength

The evolution of the damage by the splitting test in quasi -static loading can be divided into three phases: elastic, failure and post failure. The initial crack occurs after the peak load

7.3.2.1 Elastic

Figure.7.11. It shows the evolution of apparent normal strain in the elastic region. It shows typical displacement and strain distribution contour. In this region, no cracks occur.

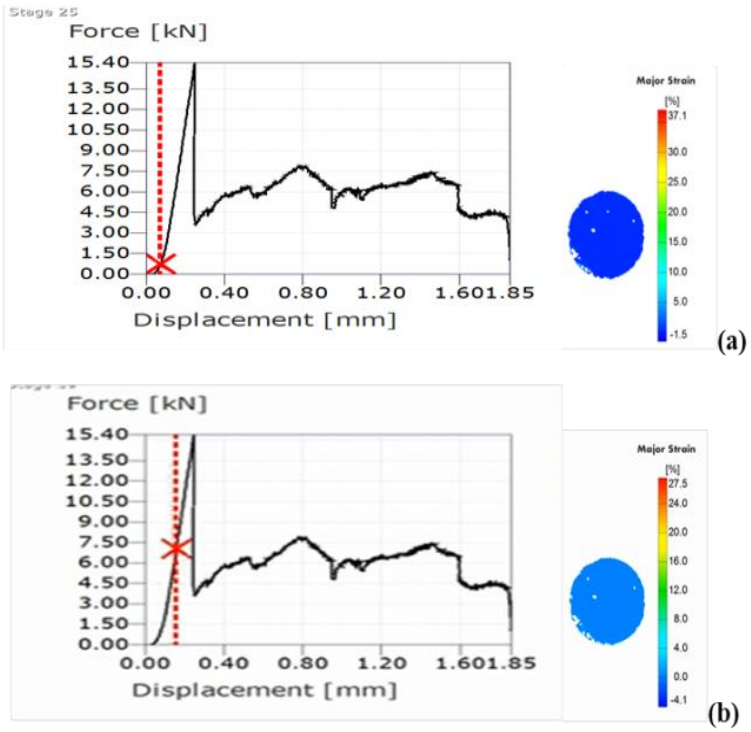

Figure. 7.11. **Evolution of apparent average strain during the splitting tension static loading at elastic for fiber composite.**

7.3.2.2 Peak load

Figure 7.12. Shows the strain distribution at the peak load. Initial crack is instantaneous along the diameter and corresponds to the load drop. In this condition, a tensile strength between the fiber composite and cement mortar matrix occurs until leading to the fiber pull-out and breakage. The failure

processes of fiber composite under tensile strength showed a linearly elastic behavior until peak. The fiber composite showed better post-peak behavior than cement mortar.

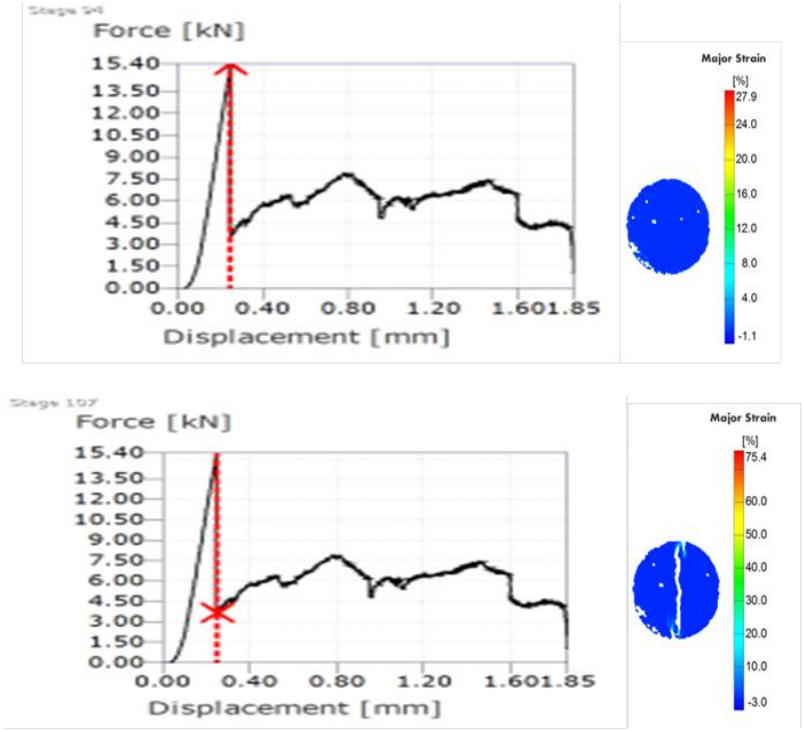

Figure. 7.12. **Evolution of apparent average strain during the splitting tension at peak load for fiber composite.**

7.3.2.3 Post-failure stage

Figure 7.13. Presents damage evolution after peak load and load drop until 55% of peak load. In this region, cracks propagated and then fiber pulled out from the matrix and broke up. It first occurred in the middle of the outer side of the top and bottom. Failure occurs when the center of the crack has reached the top of the sample loading location.

The tensile of the CFRCC has a value of the displacement of the one and half time of the compressive. Also, the residual strength 50% of the maximum load after load peaks. This condition of the CFRCC is suitable for application to the pavement and drainage pipelines.

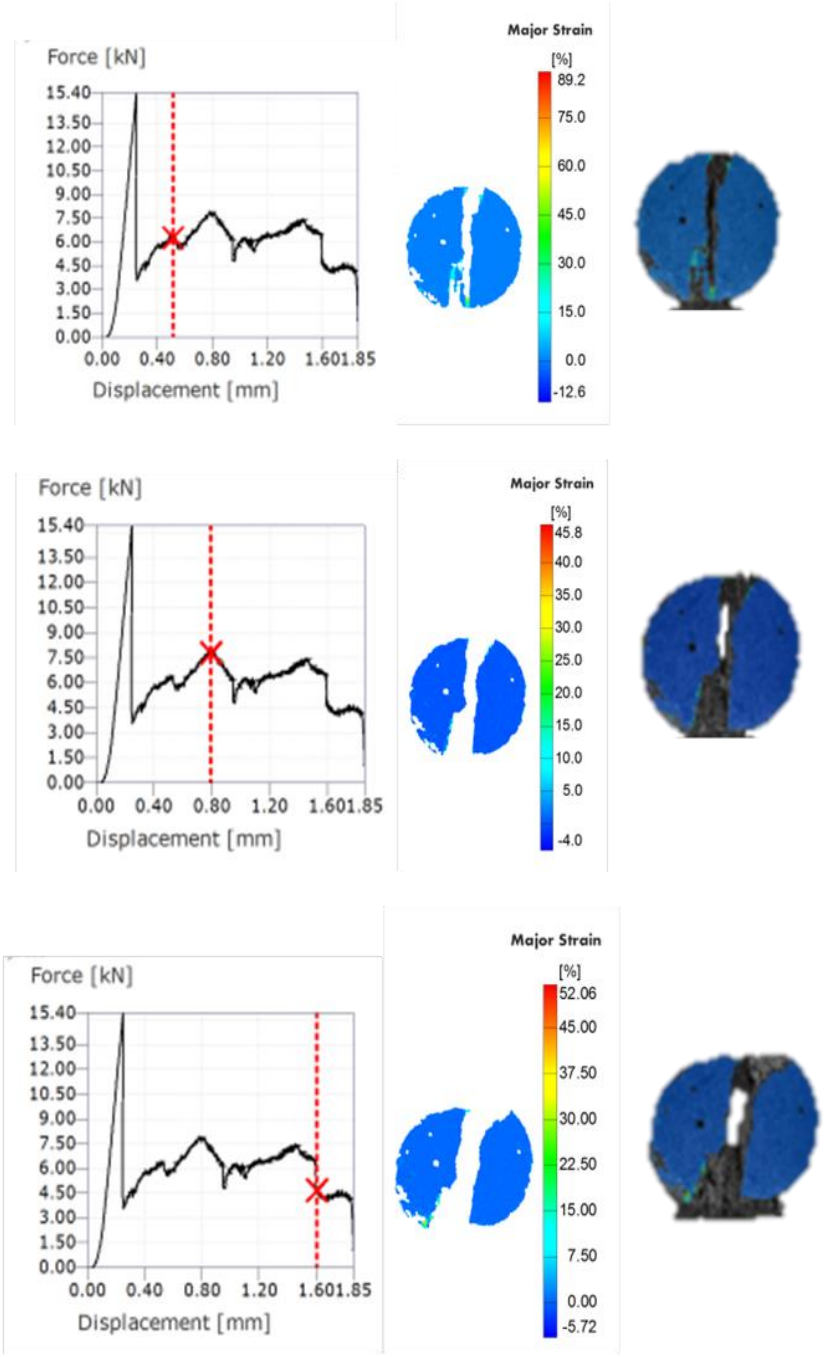

Figure. 7.13. **Evolution of apparent normal strain during the splitting tension at plastic for fiber composite**

7.4. Microstructure

The microstructure was observed using the scanning electron micrographs (SEM). It showed void formation on the mortar surface at the fracture surface; fiber fracture were also seen in the crack growth direction and interfacial transition zone.

7.4.1. Fractography

Fractography of extruded CFRCC after failure under static loading produced by SEM given in Figure. 7.14. It is showing the existence of apparent voids due to the fiber pull-out detected despite the existence of certain partial bonding between large microfibers and mortar matrices. In general, the fault occurs inside, after the resistance of the fiber. Some of the fibers appear to break up, there is a strong attachment to the fiber and mortar. Noticeably, the crack growth came from the direction of loading and then surrounds the fiber.

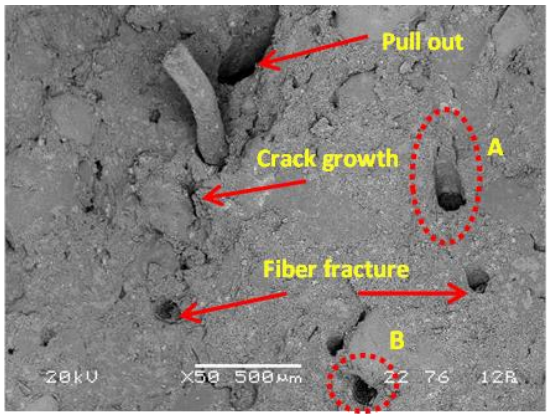

Figure.7.14. **Fracture surface under static loading on splitting tensile of extruded CFRCC of SEM micrograph (50x magnification).**

Furthermore, after a 200x magnification, as shown in Figure 7.15. SEM showed after the break up of coconut fiber resistance between fiber and matrix. Thus breaking occurs in the mortar after the withdrawal of the fiber. The growth of small cracks is also observed in the mortar surface zone. The CFRCC strength is partially bearded by the bond between the fiber and the mortar.

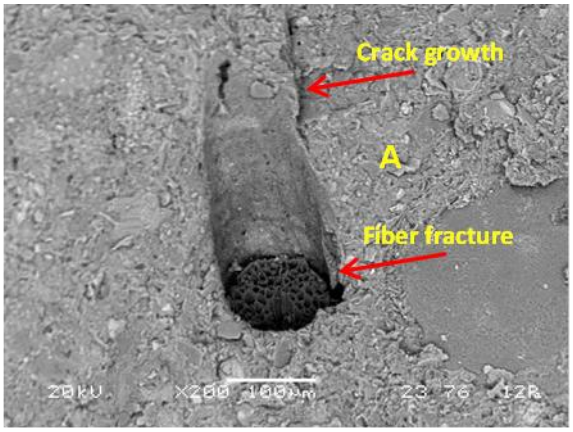

Figure.7.15. **SEM micrograph (200x magnification) of the fracture surface under static loading of extruded CFRCC**

There is also a broken fiber surface evenly with the mortar, as illustrated in figure 7.16. After a 500x magnification that looks broken fiber regularly, without any part of the fiber cells out of the fiber.

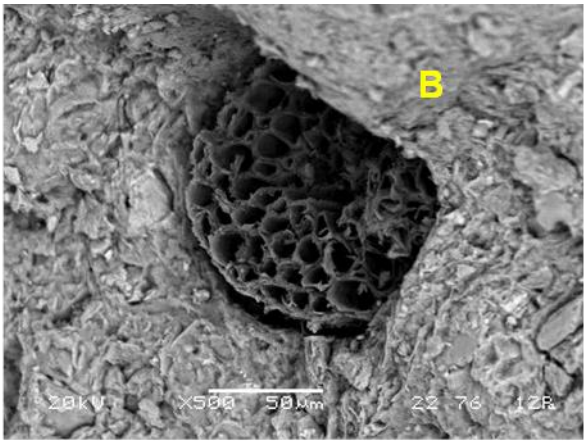

Figure.7.16. **SEM micrograph (500x magnification) of the fracture surface under static loading of extruded CFRCC**

Also, the conditions are shown in Figure 7.17 disconnected fiber, which previously occurred due to the withdrawal of ductile fibers. At the end of the fiber, show the fiber cells fused due to strain.

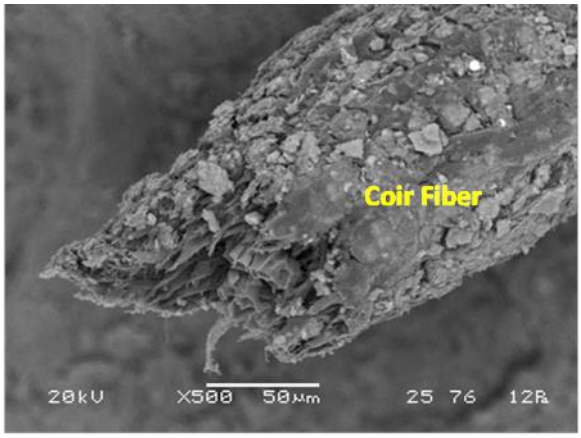

Figure.7.17. **SEM micrograph (500x magnification) of the fiber fracture under static loading of extruded CFRCC**

7.4.2. Interfacial transition zone.

Figure 7.18 shows the relationship between fibers and mortar after the failure of the CFRCC. The interfacial transition zone (ITZ) of CFRCC under static loading by SEM 500x magnifications is shown in figure 7.18. It shows the micro cracks in the mortar and gap which exist at the fiber-mortar interfacial zone.

As the test results in the failure processes of the CFRCC shown, bond cracks first appeared around the weak interfacial transition zone and then propagated into the mortar regions. Moreover, the micro cracks locations, sizes, and shapes in the interfacial transition zone were influenced by the relative strength of the mortar matrix. As a result, the observable cracks appeared at both the old interfacial transition zone and new interfacial transition zone. Also, the cracks development of fiber composite depends on the relative strength of fiber and mortar. When the force of the fiber is weaker than that of mortar, the cracks probably go through the fiber in CFRCC. It implies that the relative strength significantly influences the failure mode of CFRCC.

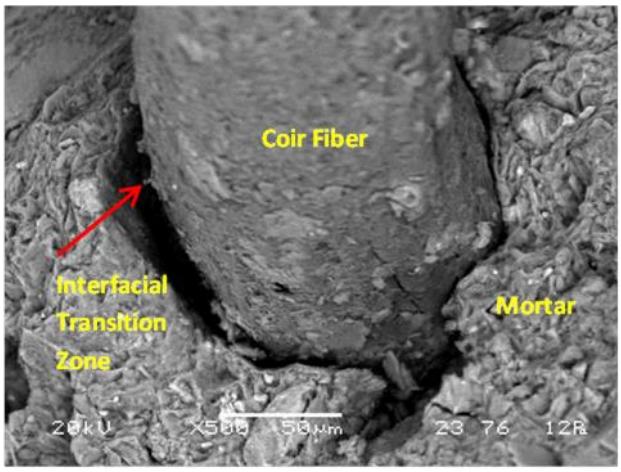

Figure.7.18. **SEM micrograph (500x magnifications) of the fracture surface of CFRCC after static loading.**

Meanwhile, fiber embedded in the mortar after failure in the interfacial transition zone of CFRCC under static loading by SEM 500x magnifications is shown in figure 7.19. It shows that the matrix and the fibers are strongly bonded. In general, the microstructure studies suggest that a strong bond exists between the fiber and the matrix /mortar.

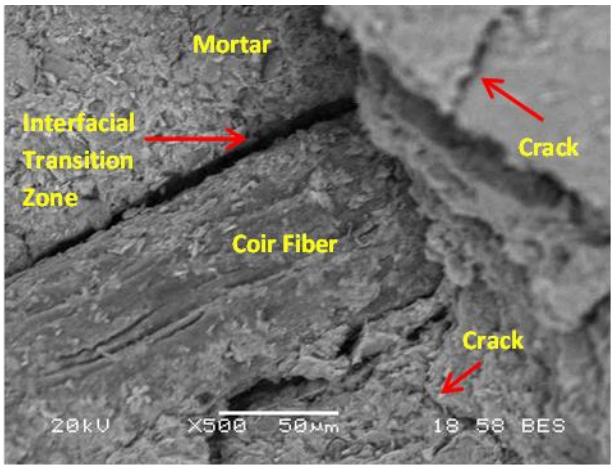

Figure.7.19. **SEM micrograph (500x magnifications) of the fracture surface of CFRCC after static loading.**

7.5. Micromechanical models.

An analytical approach based on micromechanical models is proposed. The analytical approach using the rule of the mixture (ROM) is a micro-mechanical based approach used for approximate estimation of CFRCC properties. It base on an assumption that a fiber composite property is the volume weighted average of its constituent properties, fiber, and mortar. Micromechanical models permit to study the tensile strength and compressive strength of the composite material. The analytical model approach confronted with the experimental results.

7.5.1. Micromechanical models for tensile strength.

For fiber composite materials in which the reinforcement fiber is subject to much higher stresses ($\sigma_f >> \sigma_{m,}$) than the matrix and there is a redistribution of the load. Theoretical calculations of the tensile strength in the longitudinal direction were conducted using the rule of mixtures (the two contributions assuming $\varphi_m + \varphi_f = 1$, i.e. no voids or other inclusions):

$$\sigma_{tc} = \sigma_{tm} \ (1-\varphi_f) \ + \sigma_f \ \varphi_f \quad \ldots\ldots\ldots\ldots\ldots\ldots \quad (7.1)$$

where, σ_{tc} is tensile strength of composites (MPa), σ_{tm} is tensile strength of mortar (MPa), σ_f is tensile strength of fiber (MPa), and φ_f is fiber volume fraction (described in equation (7.2) and (7.3)).

$$\varphi_f = \frac{v_f}{v_f + v_m} \quad \ldots\ldots\ldots\ldots\ldots\ldots\ldots\ldots \quad (7.2)$$

$$\varphi_f = \frac{w_f}{w_f + \left(\frac{\rho_f}{\rho_m}\right)(1-w_f)} \quad \ldots\ldots\ldots\ldots\ldots\ldots \quad (7.3)$$

Modified rule of the mixture is often used to predict the strength of short fiber composites [Shao and Bernd, 1996]. This method considered two other factors that will affect the properties of composite materials which is fiber orientation and fiber length. Hence, it is also applied to estimate the performance of the specimens too. The equation (7.1) for tensile strength applied to fiber composites The formulas are given equation (7.4.).

$$\sigma_{tc} = \sigma_{tm} \ (1 - \varphi_f) + \eta_L \ \eta_O \ \sigma_f \ \varphi_f \quad \ldots\ldots\ldots\ldots\ldots\ldots\ldots\ldots \quad (7.4)$$

Where, η_L is the fiber length distribution factor (η_L =1 for fibers longer than about 10mm), and η_o is the fiber orientation distribution factor (η_O =0.2 for fibers random 3D).

The experimental tensile strength results were obtained by carried out splitting tensile strength test by DIC and MTS. the comparison made between The ROM value using equations (7.4) and experimental value to evaluate the validity of the theoretical outcome. The tensile strength of CFRCC using equation (7.4) need calibration coefficient for fiber content (C_f) to signification with experimental. The results obtained for φ_f = 0.04 is C_f =0.45; for φ_f = 0.06 is C_f =0.55; for φ_f = 0.08 is C_f =0.85. For CFRCC using equation (7.4), proposed tensile strength fiber composite models with calibration coefficient for fiber content (C_f) is modified rule of mixture (MROM) as shown in Equation (7.5):

$$\sigma_{tc} = C_f \eta_L \eta_O \sigma_f \varphi_f + \sigma_{tm} (1 - \varphi_f) \quad \ldots\ldots\ldots\ldots\ldots\ldots\ldots\ldots (7.5)$$

Figure 7.20 showed the predicted and experimental tensile strength of different fiber volume fraction. The tensile strength value of CFRCC by MROM is less approaching the experiments value. R-square value = 0.8626 can be expressed following equation (7.6):

$$\sigma_{tc} = 18.129\ \varphi_f + 1.7664 \ldots\ldots\ldots\ldots\ldots\ldots\ldots\ldots (7.6)$$

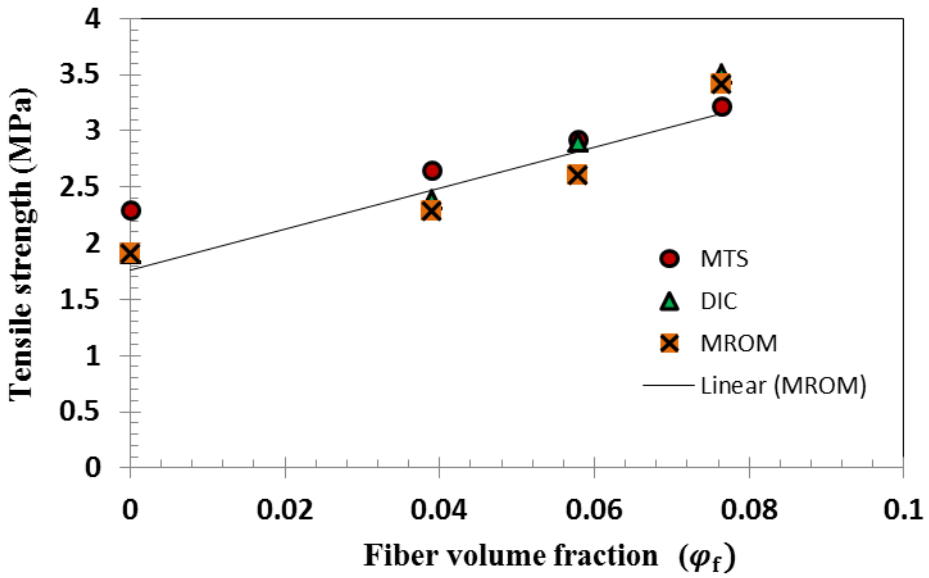

Figure. 7.20. **The tensile strength versus fiber volume fraction.**

Summerscales et al.,(2011),(2013) proposed for the elasticity modulus that a fiber diameter distribution factor should be included in ROM. Virk et al., (2012) also proposed the fiber area correction factor for elasticity modulus. The law

states that the composite tensile strength (σ_{tc}) should account for both the tensile strength of the cement mortar/plain matrix (σ_m) and the tensile strength of fiber (σ_f), wich is a contribution from the fibers (length L_f , diameter d_f and fiber volume fraction φ_f). Taking into account the ratio of fiber (L_f / d_f), the proposed models development Equation (7.5) as follows Equation (7.7):

$$\sigma_{tc} = C_f \eta_l \eta_o (L_f / d_f) \varphi_f \sigma_f + \sigma_{tm} (1 - \varphi_f) \quad \ldots\ldots\ldots\ldots\ldots\ldots (7.7)$$

The results have been obtained relationship of tensile strength (σ_{tm}) to compressive strength (σ_{cm}) of cement mortar in this study proposed as shown in Equation (7.9):

$$\sigma_{tm} = 0.532\sqrt{\sigma_{cm}} \quad \ldots\ldots\ldots\ldots\ldots\ldots\ldots (7.8)$$

By entering equation (7.8), the proposed models of equation (7.7) can be expressed:

$$\sigma_{tc} = C_f \eta_l \eta_o (L_f / d_f) \varphi_f \sigma_f + 0.532\sqrt{\sigma_{cm}} (1 - \varphi_f) \quad \ldots\ldots\ldots\ldots\ldots\ldots (7.9)$$

The tensile strength results obtained with the proposed models equation (7.9) for signification with experimental results. The results of the CFRCC obtained for φ_f = 0.04 is C_f =0.11; for φ_f = 0.06 is C_f =0.075; for φ_f = 0.08 is C_f =0.07.

The results comparison tensile strength of fiber composite between the experimental results (MTS method and DIC method) with the proposed modified the rule of mixture (MROM) (Equation (7.5)) and proposed model (Equation (7.9)) as shown in Figure 7.21.

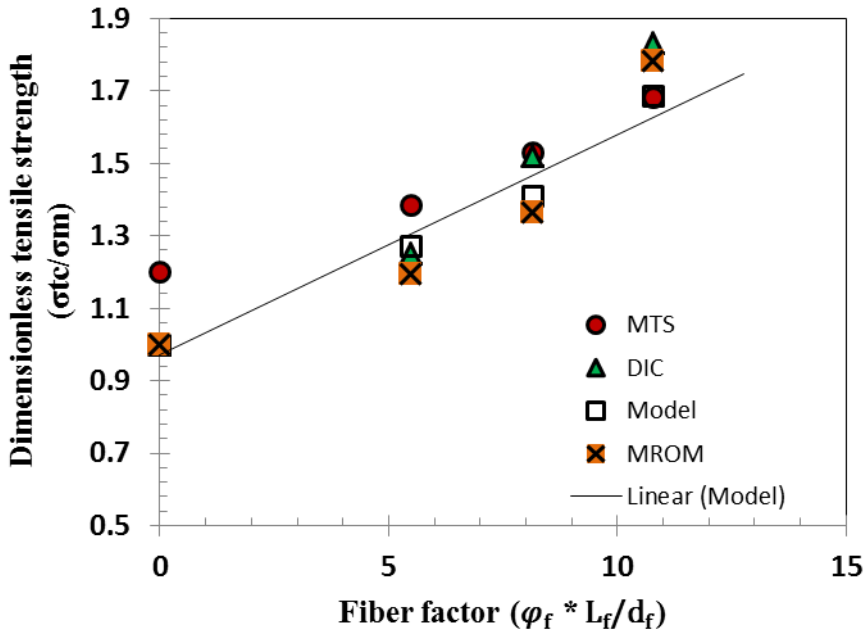

Figure. 7.21. **Relative tensile strength as a function of the fiber factor for modification the model predictions.**

For fiber factor versus relative tensile strength of CFRCC is shown in Figure 7.21 the following equations are proposed equation (7.10):

(R-square value = 0.9645) $$\frac{\sigma_{tc}}{\sigma_{tm}} = 0.061\left(\frac{L_f}{d_f}\varphi_f\right) + 0.9703 \quad \text{.....} \quad (7.10)$$

To change σ_{tm} it can show as follows equation (7.11):

$$\sigma_{tc} = 0.0325\left(\frac{L_f}{d_f}\varphi_f\right)\sqrt{\sigma_{cm}} + 0.5162\sqrt{\sigma_{cm}} \quad \text{.....} \quad (7.11)$$

Equation (7.10) is in good agreement with the relative tensile strength test data shown in Figure. 7.21. For different values.

The tensile strength of CFRCC is observed from experimental and model is shown in Figure 7.20-21, increased with volume fraction φ_f irrespective of the mix type, a similar observation were done on Portland cement based fiber composites (Tasse ST and Lubell AS, 2014).

7.5.2. Micromechanical models for compressive strength

Observation and analysis of the model of the compressive strength of the CFRCC based micromechanical model is a rule of the mixer. It is as has been done to produce a compressive strength composite model. The compressive strength of a composite (σ_{cc}) material can normally be predicted using the standard rule-of-mixtures in the longitudinal direction were conducted using the rule of mixtures models is shown in equation (7.12):

$$\sigma_{cc} = \sigma_{cm}\, \varphi_m + \sigma_f\, \varphi_f \quad \ldots\ldots\ldots\ldots\ldots\ldots\ldots\ldots\ldots\ldots \quad (7.12)$$

Theoretical calculations of the compressive strength in the longitudinal direction were conducted using the rule of mixtures (the two contributions assuming $\varphi_m + \varphi_f = 1$, i.e. no voids or other inclusions):

$$\sigma_{cc} = \sigma_{cm}\, (1 - \varphi_f) + \sigma_f\, \varphi_f \quad \ldots\ldots\ldots\ldots\ldots\ldots\ldots\ldots \quad (7.13)$$

where, σ_{cc} is the compressive strength of composites (MPa), σ_{cm} is the compressive strength of mortar (MPa), σ_f is compressive strength of fiber (MPa), and φ_f is fiber volume fraction.

Modified rule of the mixture is often used to predict the strength of short fiber composites [Shao and Bernd, 1996]. This method considered two other factors that will affect the properties of composite materials which is fiber orientation and fiber length. Hence, it is also applied to estimate the performance of the specimens too. The equation (7.13) for compressive strength applied to fiber reinforced composites The formulas are given equation (7.4.).

$$\sigma_{cc} = \sigma_{cm}\, (1 - \varphi_f) + \eta_L\, \eta_O\, \sigma_f\, \varphi_f \quad \ldots\ldots\ldots\ldots\ldots\ldots\ldots\ldots\ldots\ldots \quad (7.14)$$

Where, η_L is the fiber length distribution factor (η_L =1 for fibers longer than about 10mm), and η_o is the fiber orientation distribution factor (η_O =0.2 for fibers random 3D).

The experimental compressive strength results were obtained by carried out compressive strength test by DIC and MTS. The comparison is made between The ROM value using equations (7.14) and experimental value to evaluate the validity of the theoretical result. The compressive strength of fiber composite using equation (7.14) need calibration coefficient for fiber content (C_f) to signification with experimental. The results obtained for φ_f = 0.04 is C_f =0.45; for φ_f = 0.06 is C_f =2.5; for φ_f = 0.08 is C_f =4.5. For CFRCC using equation (7.14),

proposed compressive strength fiber composite models with calibration coefficient for fiber content (C_f) is modified rule of mixture (MROM) as shown in Equation (7.15):

$$\sigma_{cc} = C_f \eta_L \eta_O \sigma_f \varphi_f + \sigma_{cm} (1 - \varphi_f) \quad \text{..... (7.15)}$$

Figure 7.22 showed the predicted and experimental tensile strength of different fiber volume fraction. The compressive strength value of CFRCC by MROM is less approaching the experiments value. R-square value = 0.8006 can be expressed following equation (7.16):

$$\sigma_{cc} = 84.4\ \varphi_f + 15.034 \quad \text{..... (7.16)}$$

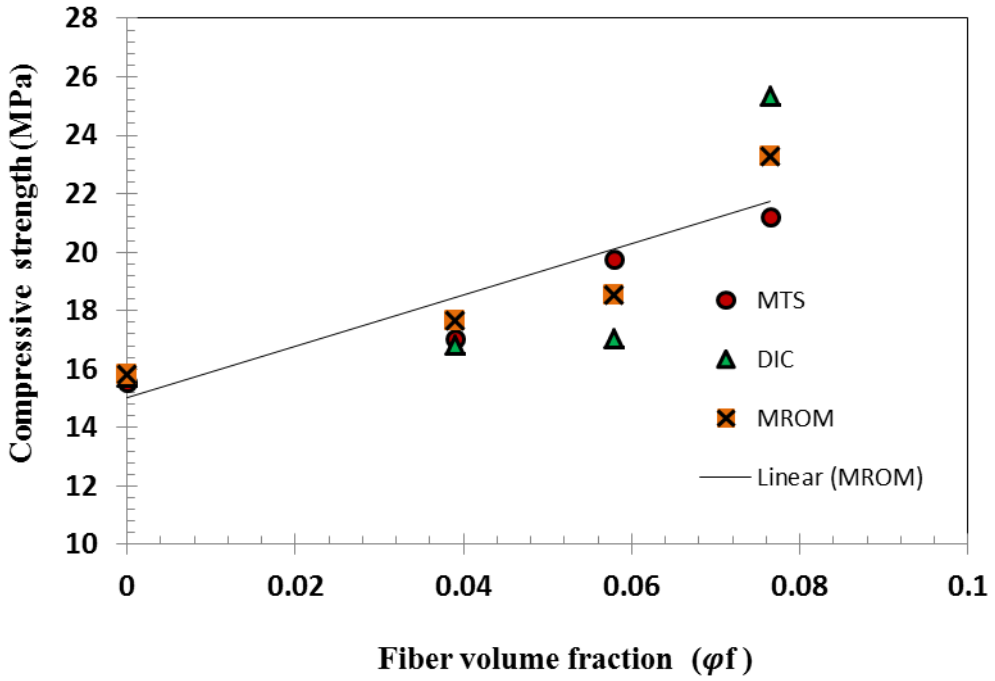

Figure. 7.22. **The compressive strength versus fiber volume fraction.**

Summerscales et al.,(2011),(2013) proposed for the elasticity modulus that a fiber diameter distribution factor should be included in ROM. Virk et al., (2012) also proposed the fiber area correction factor for elasticity modulus. The law states that the composite compressive strength (σ_{cc}) should account for both the tensile strength of the cement mortar / plain matrix (σ_{cm}) and the fiber, wich is a contribution from the fibers (length L_f , diameter d_f and fiber volume fraction φ_f). Taking into account the ratio of fiber (L_f / d_f), the proposed compressive strength fiber composite models development Equation (7.15) as follows Equation (7.17):

$$\sigma_{cc} = C_f \eta_l \eta_o (L_f / d_f) \varphi_f \sigma_f + \sigma_{cm} (1 - \varphi_f) \quad \text{..... (7.17)}$$

The compressive strength results obtained with the proposed models equation (7.17) for signification with experimental results. The results of the CFRCC obtained for φ_f = 0.04 is C_f =0.45; for φ_f = 0.06 is C_f =0.40; for φ_f = 0.08 is C_f =0.35.

The results comparison compressive strength of fiber composite between the experimental results (MTS method and DIC method) with the proposed models is modified the rule of mixture (MROM) is Equation (7.15) and developed MROM is proposed model be Equation (7.17) as shown in Figure 7.23.

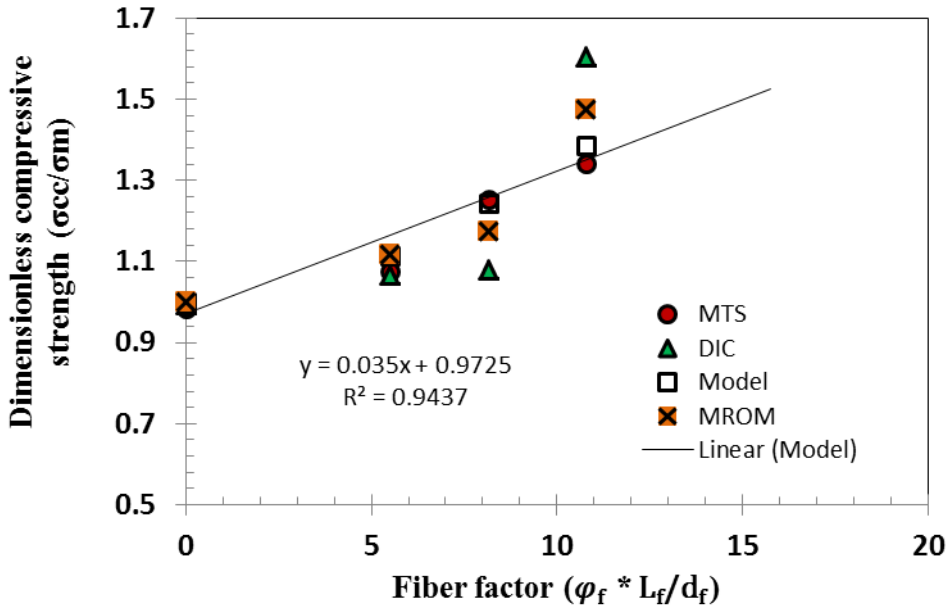

Figure. 7.23. **Relative compressive strength versus the fiber factor for modification the model predictions.**

For fiber factor versus relative compressive strength of CFRCC is shown in Figure 7.23 the following equations are proposed equation (7.30):

(R-square value = 0.9437) $$\frac{\sigma_{cc}}{\sigma_{cm}} = 0.035\left(\frac{L_f}{d_f}\varphi_f\right) + 0.9725 \quad \text{..... (7.18)}$$

Equation (7.18) is in good agreement with the relative tensile strength test data shown in Figure. 7.23. For different values.

It is observed from Figure 7.22-23 that compressive strength increased with increases in volume fraction irrespective of the mix type. A similar observation as Portland cement based fiber composites (Tasse ST and Lubell AS, 2014).

7.5.3. Comparison between models and experimental results

Two analytical approaches namely the standard rule of the mixture and developed model of the CFRCC properties were proposed. Analytical approaches were compared with experiment data from the MTS and the DIC results. They are presented in Table 7.1 for tensile strength and Table 7.2 for compressive strength. It shows the theoretical tensile strength values calculated from the modified rule of mixtures model and developed the model, along with the experimental values using MTS and DIC. Experimental strength values of composites with fiber contents of 2%, 3%, and 4% were approximately 95% of the analytical model.

It can be observed from the table that the model results are closer to the experimental for the case of tensile strength and compressive strength. For tensile strength, the experimental and analytical results for MTS and MROM do not compare very well. However, proposed model, MROM, and the experimental result of DIC compare very well. Unlike the case with the compressive strength, the experimental and analytical results are much closed.

Table.7.1. **Comparison tensile strength of fiber composite properties obtained from experiment and analytical model.**

Parameters **Tensile strength for composite** σ_{tc}	**Values tensile strength (MPa)**			
	Experiment		Analytical model	
	MTS	DIC	Modified Rule of mixture (MROM)	Proposed model
Cement Mortar	2.2966	1.9116	1.9116	1.9116
Fiber composite 2% fiber content	2.6483	2.3886	2.2808	2.4323
Fiber composite 3% fiber content	2.9293	2.9037	2.6066	2.6966
CFM Composite 4% fiber content	3.2198	3.5019	3.4098	3.2235

Table.7.2. **Comparison compressive strength of fiber composite properties obtained from experiment and analytical model.**

Parameters the compressive strength of the composite σ_{cc}	**Values compressive strength (MPa)**			
	Experiment		Analytical model	
	MTS	DIC	Modified Rule of mixture (MROM)	Proposed model
Cement Mortar	15.5451	15.7201	15.7990	15.7990
Fiber Composite 2% fiber content	17.0220	16.8334	17.6483	17.6182
Fiber Composite 3% fiber content	19.7809	17.0555	18.5463	19.6612
CFM Composite 4% fiber content	21.1966	25.3200	23.2966	21.8812

Validation is done with the relationship between the experimental and analytic models. Figure 7.24 showing $y = 0.9611x + 0.0216$, $R^2 = 0.992 \cong 1$ and Figure 7.25 showing $y = 0.9803x + 0.0117$, $R^2 = 0.9987 \cong 1$ respectively for tensile strength and compressive strength are shows the same correlation approach.

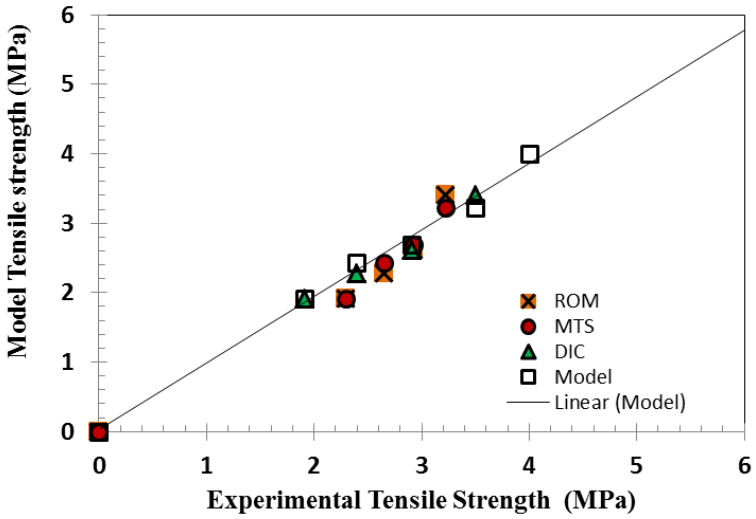

Figure. 7.24. **Model versus experimental tensile strength for the CFRCC**

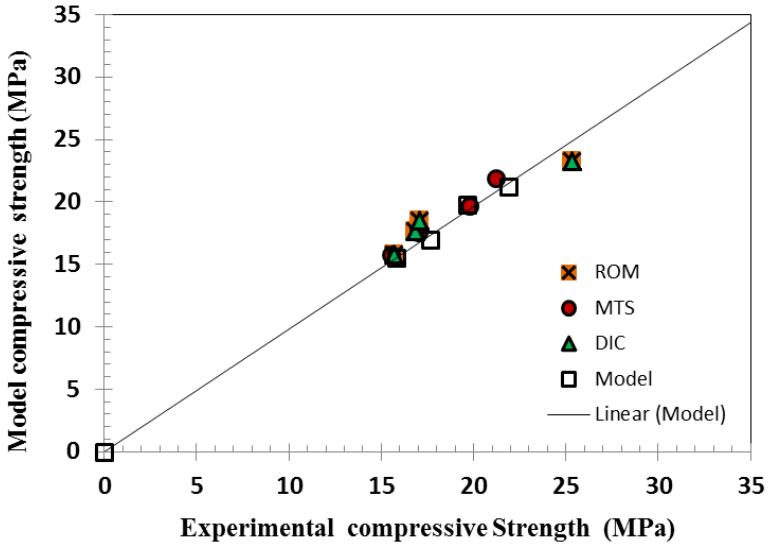

Figure. 7.25. **Model versus experimental compressive strength for the CFRCC**

7.6. Conclusions of chapter

The study results indicate that the discrepancy between the tensile strength of coir fiber and mortar matrix significantly influences the mechanical properties and crack patterns of the composites materials. The findings in this investigation are useful to improve the mechanical properties of CFRCC by optimizing the mix proportion with extrusion.

It found that the damage process is related to the relative strength of fiber and mortar matrix. The observation implies that the propagations of microcracks are different between composites and plain mortar. The compressive strength and tensile strength results all indicated that the fiber failure mode was predominantly by fracture fiber rather than pull out, even for the shortest fibers in use in this study.

The global cracks developed along the loading direction for all the cement-based materials. For cement mortar, the first crack appeared surface mortar and then propagated into the mortar region to the load direction. In fiber composite, the initial cracks occurred around interfacial transition zone and propagated across the mortar region connecting with each other. Understanding of the differences in the failure processes between cement mortar and fiber composite can provide insights into the failure mechanism of concrete. It can use

to improve the mechanical properties of concrete through optimization of the mixture proportions.

A micromechanical analytical model of the fiber composite is developed based on the micromechanics. Based on the analysis, the following conclusions can be obtained. Developed new rules of the mixture have proposed which introduce additional length and diameter fiber parameters. The models proposed for fiber composite is the tensile strength and compressive strength of the mechanical properties. The model proposed in this paper accepts micromechanical parameters of fiber and mortar; it can be used to predict the tensile strength and compressive strength of fiber composite.

The general model prediction defined as:

$\sigma_{cc} = C_f \eta_l \eta_o (L_f / d_f) \varphi_f \sigma_f + \sigma_{cm} (1- \varphi_f)$ (for compressive strength)

$\sigma_{tc} = C_f \eta_l \eta_o (L_f / d_f) \varphi_f \sigma_f + 0.532\sqrt{\sigma_{cm}} (1- \varphi_f)$ (for tensile strength)

The analytical model is developed to predict tensile strength of the CFRCC defined as:

$$\sigma_{tc} = 0.0325 \left(\frac{L_f}{d_f} \varphi_f \right) \sqrt{\sigma_{cm}} + 0.5162 \sqrt{\sigma_{cm}}$$

The analytical model is developed to predict compressive strength of the CFRCC defined as:

$$\sigma_{cc} = 0.035 \left(\frac{L_f}{d_f} \varphi_f \right) \sigma_{cm} + 0.9725 \, \sigma_{cm}$$

The develop rule of the mixture models was successfully used to relate the tensile strength and compressive strength with fiber volume and length The experimental result demonstrates the validity of the proposed model is agreement close. The DIC results and MTS result compared with the models destructive testing results; they compared very well.

CHAPTER.8.
GENERAL CONCLUSIONS AND FURTHER RESEARCH

8.1. Conclusions.

This study developed new fiber composite materials for a structural element of the screw extruded with the local materials that are cement, clay, sand and coir fiber, which can use for building construction. It was designed to investigate the properties of coir fiber, cement mortar, and composites on fresh state and hardened state using MTS and DIC testing method. Also, it observed the microstructure by SEM and developed analytical models for the yield stress of rheology, mechanical and micromechanical.
The related conclusions are summarized as follows:

A. Physical, mechanical performances, and microstructure of coir fibers

1. The treatment of coir fibers increases the tensile strength and delivers higher value to the elongation of a break than the ones of untreated fibers. Average tensile strength of treated fiber is as twice greater than the one of untreated. Based on these results, coir fiber after treatment presents an improved ductile. Indonesian coir fiber has ductile properties suitable for use as reinforcement in concrete composites with high ductility.
2. The treatment significantly removes impurities on the fiber surface, resulting in surface modification and improved thermal stability. TGA measurements revealed that the treatment of fibers has a positive impact on the thermal stability of the sample.
3. SEM observation shows that water treatment has a significant impact of on the surface of the fibers (removing impurities, decreasing the siliceous compounds content) and decreases the average diameter of the fibers. These changes in fiber structure induce an improvement of the macroscopic behavior of the fibers.

B. Design, rheology properties, microstructure and rheology model of product extruded composites.

1. This present work shows that yield stress model used for common mortar can be generalized to fiber reinforced concretes. Indeed, it is the evolution of the yield stress of fiber-reinforced cementitious composite.
2. Rheological behaviors of mortar and composites reinforced with fibers are presented. The formation of cement clay material through extrusion produces a compact material with the material surface without defects.

3. The rheological approach is an effective design guide of fresh cement mortar to achieve hardening properties of the composite. The rheology is important for the characteristic of fresh cement mortar performing in practical applications. It is used for achieving the desirable properties of the hardened materials
4. The formulation of a material with low cement and from local materials that can extrude with smooth and compact is studied. Clay absorbs more water than cement. Therefore, the amount of clay and water/cement ratio is added to the mortar will influence the extrusion results.
5. Mix design mortar obtained from cement, clay and sand in the ratio of the weight of 1:3:6 respectively require 18 % water/cement. As for the proportion of 2:2:6 it need a 16 % water/cement to produce the extruded material.
6. The addition of fibers into extruded formulations, the calculation, required the addition of water/cement ratio, to obtain an extruded mortar well and to counter the loss of workability due to the addition of the selected fiber into mortar mixture basic (plain mortar) without adding extra water.
7. The addition of fibers up to 5 % by weight of cement, to remain in the extruded condition, for 10 % of cement formulations need water/cement ratio of 21 %. As for the 20 % cement formulations needed water/cement ratio of 19 %.
8. Rheology properties show that the value of the torque increases with decreasing amount of water and the yield stress increases with fiber content and fiber length.
9. Rheology models for CFRCC composites have been obtained. The model rheology of prediction yield stress is as follows:

$$\left[\frac{\tau_{yc}}{\tau_{ym}}\right] = 1 + \left[\frac{r^2(\varphi_f)^2 R}{6\tau_{ym}}\right] + \left[\frac{r\varphi_f S}{6\tau_{ym}}\right]$$

   The model predictions the yield stress show good agreement with the yield stress values experiment.

10. The SEM observations of the CFRCC before extrusion was the small holes and not spread between the mortar and fibers, due need extrusion in order to fiber spread more evenly and compact between fiber and mortar.

C. Mechanical performance, microstructure, and models of screw extruded composites using destructive testing method

1. The performance mechanical of the CFRCC compared with cement mortar is presented. Fiber reinforced cementitious composite can enhance by processing, such as extrusion, which improve the interfacial bond through the application of pressure.

2. Aspects surface is obtained as a consequence of the mold in comparison with the outcome of the screw extrusion process. Mold process is uneven, not smooth surface defects compare than the extrusion process.
3. The SEM observation of the composite material obtained fiber direction lengthwise direction is random.
4. The processes of forming by extrusion provide performance results of compressive strength, and tensile strength that is better than the manual process with mold.
5. Tensile strength and compressive strength of mortars have shown a gradual increase in increasing fiber content and fiber length. These values are higher for CFRCC composites when compared to cement mortar ones.
6. The empirical model is developed to predict compressive strength and tensile strength based on a linear trend line obtained with increasing fiber content defined as:

   $\sigma_i = \alpha_i * \varphi_{fi} + \sigma_{oi}$
7. The models are developed to predict compressive stress based on fiber content, and fiber length defined as:

   $$\sigma_{ci} = [(0.0763 * L_{fi} + 0.8187) * \varphi_{fi} + \sigma_{oi}]$$
8. The models are developed to predict tensile stress based on fiber content and fiber length defined as:

   $$\sigma_{ti} = [(0.0089 * L_{fi} + 0.1673) * \varphi_{fi} + \sigma_{oi}]$$
9. Compressive modulus of CFRCC increased with the increasing fiber content and increased compressive strength while the tensile modulus of coir fiber cement mortar composites decreased with increasing fiber content and increased tensile strength.
10. The empirical model is developed to predict compressive modulus and tensile modulus defined as:

    $$E = [\alpha * {\varphi_{fi}}^2] + [\beta * \varphi_{fi}] + \gamma$$
11. Density decreases with the increasing fiber content, increased the compressive strength and tensile strength. The empirical model is developed to predict density with increasing fiber content defined as:

    $$\rho = [\alpha * {\varphi_{fi}}^2] + [\beta * \varphi_{fi}] + \gamma$$
12. The tensile strain and tensile strength increases with the increasing fiber content. The strain for 10mm fiber length has higher strain value of the fiber length of 5mm and 15mm. The empirical model is developed to predict strain with increasing fiber content defined as:

    $$\varepsilon = [\alpha * {\varphi_{fi}}^2] + [\beta * \varphi_{fi}] + \gamma$$
13. The failure mode for the mortar with cracked lengthwise direction unidirectional pressure can be seen for cracks on the bottom and top surface. The mortar without fibers results in test sample destroyed at the top. The failure mode for composites that the crack marked has a tendency to propagate parallel to the

loading direction in the mortar matrix. Fiber content increases the tendency of cracks that occur less. It shows the strength of the fiber bond with mortar matrix.

14. The proposed analytical model for CFRCC composite was found to fit closely the experimental data points of the stress-strain curve and hence, can use in the prediction of stress-strain characteristics for concrete structures.

D. Micromechanical, damage evolution, microstructure, and models of screw extruded composites using nondestructive testing method

1. The study results indicate that the discrepancy between the tensile strength of coir fiber and mortar matrix significantly influences the mechanical properties and crack patterns of the composites materials. The findings in this investigation are useful to improve the mechanical properties of CFRCC by optimizing the mix proportion with extrusion.
2. It found that the damage process is related to the relative strength of fiber and mortar matrix. The observation implies that the propagations of microcracks are different between composites and plain mortar. The compressive strength and tensile strength results all indicated that the fiber failure mode was predominantly by fracture fiber rather than pull out, even for the shortest fibers in use in this study.
3. The global cracks developed along the loading direction for all the cement-based materials. For cement mortar, the first crack appeared surface mortar and then propagated into the mortar region to the load direction. In fiber composite, the initial cracks occurred around interfacial transition zone and propagated across the mortar region connecting with each other. Understanding of the differences in the failure processes between cement mortar and fiber composite can provide insights into the failure mechanism of concrete. It can be used to improve the mechanical properties of concrete through optimization of the mixture proportions.
4. A micromechanical analytical model of the fiber composite is developed based on the micromechanics. Based on the analysis, the following conclusions can be obtained. Developed new rules of the mixture have proposed which introduce additional length and diameter fiber parameters. The models proposed for fiber composite is the tensile strength and compressive strength of the mechanical properties. The model proposed in this paper accepts micromechanical parameters of fiber and mortar; it can be used to predict the tensile strength and compressive strength of fiber composite.
5. The general model for prediction compressive defined as:

$$\sigma_{cc} = C_f \eta_l \eta_o (L_f / d_f)\ \varphi_f\ \sigma_f + \sigma_{cm} (1 - \varphi_f)$$

6. The general model for prediction tensile defined as:

$$\sigma_{tc} = C_f \eta_l \eta_o (L_f / d_f)\ \varphi_f\ \ \sigma_f + \ 0.532\sqrt{\sigma_{cm}}\ (1- \varphi_f\ )$$

7. The analytical model is developed to predict tensile strength of the CFRCC defined as:

$$\sigma_{tc} = 0.0325 \left(\frac{L_f}{d_f} \varphi_f \right) \sqrt{\sigma_{cm}} \ + 0.5162 \sqrt{\sigma_{cm}}$$

8. The analytical model is developed to predict compressive strength of the CFRCC defined as:

$$\sigma_{cc} = 0.035 \left(\frac{L_f}{d_f} \varphi_f \right) \sigma_{cm} \ + \ 0.9725\ \sigma_{cm}$$

9. The develop rule of the mixture models was successfully used to relate the tensile strength and compressive strength with fiber volume and length The experimental result demonstrates the validity of the proposed model is agreement close. The DIC results and MTS results compared with the models, they compared very well.

8.2. Further Research.

Although, the findings important and the model that has been obtained from the development of new materials in this research, further research is still needed to be done for more specific characteristics based on this research. The following are the recommendations for future work:

1. Develop a program of research with the same experimental test that can be performed and developed using different natural fibers (such as bamboo fiber, rice fiber, fiber banana leaves) and mortar of different materials.
2. Develop research use fiber treatment with chemicals and refinement of methods of treatment.
3. Develop an investigation on the effect of fiber on the thermal response, cyclic load to composite materials.
4. Further investigation of the post-failure analysis using DIC to understand the damage mechanisms of CFRCC composite material.
5. Study the simulation models to predict the mechanical properties and cracks with finite element method.

6. Apply the results of the research conducted on the construction material products, such as an ingredient in the manufacture of panel buildings, pavement, drainage pipes, mortar for concrete, and brick.

REFERENCES

[1] [CDIAC, 2003] Carbon Dioxide Information Analysis Center. (2003). Trends on Line – a Compendium of Data on Global Change. Available on the web at http://cdiac.esd.ornl.gov/ftp/ndp030/global00.ems

[2] [CDIAC, 2010] Carbon Dioxide Information Analysis Center. (2010). Trends on Line – a Global Fossil- Fuel CO2 Emissions. Available on the web at http://cdiac.esd.ornl.gov/trends/emis/tre_glob_2010.html

[3] [Olivier et al., 2012] Jos G.J. Olivier, Greet Janssens-Maenhout, Jeroen A.H.W. Peters. (2012) Trends in global CO2 emissions 2012 report, PBL Netherlands Environmental Assessment Agency The Hague/Bilthoven

[4] [Habert & Roussel.,2009] G. Habert, N. Roussel, (2009).Study of two concrete mix-design strategies to reach carbon mitigation objectives, Cement and Concrete Composites, 31:397-402.

[5] [Jan et al., 2004]. E.G. Jan, van Dam, J.A. Martien, van den Oever, W. Teunissen, R.P. Edwin, Keijsers, G. Aurora, Peralta,(2004), Process for production of high density/high performance binderless boards from whole coconut husk, part 1: Lignin as intrinsic thermosetting binder resin, Ind. Crops Prod. 19, 207– 216.

[6] [Rodrígueza et al. 2011]. N.J. Rodrígueza, M. Yá˜nez-Limónb, F.A. Gutiérrez-Micelia, O. Gomez-Guzmanc, T.P. Matadamas-Ortizd, Luicita Lagunez-Riverad, J.A. Vazquez Feijood, (2011), Assessment of coconut fibre insulation characteristics and its use to modulate temperatures in concrete slabs with the aid of a finite element methodology, Energy and Buildings 43 ,1264–1272

[7] [Mohanty et al. 2000] Mohanty AK., Misra M, Hinrichsen G Biofibres. (2000), Biodegradable polymers and biocomposites: An overview, Macromolecular Materials & Engineering 276/277:1–24

[8] [CAPPI, 2008]. Center for Agricultural Policy Prosperity Initiative.,(2008), Small-scale Review of Coconuts, Prosperity Initiative.

[9] [Munawar et al., 2007]. Munawar Sasa Sofyan, Kenji Umemura, Shuichi Kawai, (2007), Characterization of the morphological, physical, and mechanical properties of seven nonwood plant fiber bundles, J Wood Sci 53:108–113. The Japan Wood Research Society 2006 DOI 10.1007/s10086-006-0836-x

[10] [Kulkarni et al, 1981] A.G. Kulkarni, K.G. Satyanarayana, K. Sukumaran, P. K. Rohatgi. (1981). Mechanical behaviour of coir fibres under tensile load, Journal Of Materials Science 16: 905—914

[11] [Satyanarayana. KG et al., 1982].K. G. Satyanarayana, C. K. S. Pillai, K. Sukumaran, (1982). Structure property studies of fibres from various parts of the coconut tree, Journal Of Materials Science 17: 2453-2462

[12] [Noguera P et al., 2003] Patricia Noguera, Manuel Abad, Rosa Puchades, Angel Maquieira, and Vicente Noguera. (2003). Influence of Particle Size on Physical and Chemical Properties of Coconut Coir Dust as Container Medium, Communications In Soil Science And Plant Analysis Vol. 34, Nos. 3 & 4, Pp. 593–605

[13] [Rahman MM & Khan MA, 2007]. M. Mizanur Rahman, Mubarak A. Khan, (2007), Surface treatment of coir (Cocos nucifera) fibers and its influence on the fibers' physico-mechanical properties, Composites Science and Technology 67: 2369–2376

[14] [Jústiz-Smith CA et al., 2008]. Nilza G. Jústiz-Smith, G. Junior Virgo, Vernon E. Buchanan, (2008), Potential of Jamaican banana, coconut coir, and bagasse fibres as composite materials, Materials characterization, 59:1273–1278.

[15] [Defoirdt N et al., 2010]. Nele Defoirdt, Subhankar Biswas, Linde De Vriese, Le Quan Ngoc Tran, Joris Van Acker, (2010) Assessment of the tensile properties of coir, bamboo and jute fibre, Composites: Part A 41:588–595

[16] [Muensri P et al., 2011]. Pakanita Muensri a, Thiranan Kunanopparat b,⇑, Paul Menut c, Suwit Siriwattanayotin, (2011), Effect of lignin removal on the properties of coconut coir fiber/wheat gluten biocomposite, Composites: Part A 42:173–179

[17] [Ngesa et al., 2011]. Ezekiela Ngesa, Bwire Ndazia, Christian Nyahumwa, Sigbritt Karlsson, (2011), Effect of temperature and durations of heating on coir fibers, Industrial Crops and Products 33:638–643.

[18] [Saw SK et al., 2011]. Sudhir Kumar Saw, Gautam Sarkhel, Arup Choudhury, (2011), Surface modification of coir fibre involving oxidation of lignins followed by reaction with furfuryl alcohol: Characterization and stability, Applied Surface Science 257: 3763–3769.

[19] [Arsène1 et al., 2004] Marie-Ange Arsène, Holmer Savastano Jr., Seyed M. Allameh, Khosrow Ghavami, Wole O. Soboyejo. (2004). Cementitious Composites Reinforced With Vegetable Fibers,…….

[20] [Arsène1 et al., 2007] M.-A. Arsène, A. Okwo, K. Bilba, A. B. O. Soboyejo & W. O. Soboyejo (2007): Chemically and Thermally Treated Vegetable Fibers for Reinforcement of Cement-Based Composites, Materials, and Manufacturing Processes, 22:2, 214-227

[21] [Kuder & Shah, 2010] K.G. Kuder, S.P. Shah, (2010). Processing of high-performance fiber-reinforced cementbased composites, Construction and Building Materials, 24: 181-186.

[22] [Filho et al., 2000] Filho RDT, Scrivener K, England GL, Ghavami K. Durability of alkali sensitive sisal and coconut fibres in cement mortar composites. Cement and Concrete Composites 2000;22:127–143.

[23] [Savastano et al. 2003]. Savastano Jr., H.; Warden, P.G.; Coutts, R.S.P. (2003). Potential of Alternative Fibre Cements as Building Materials for Developing Areas. Cement and Concrete Composites, vol. 25, p. 585-592

[24] [Tolêdo Filho et al., 2003] R.D. Tolêdo Filho, K. Ghavami, G.L. England, K. Scrivener., (2003). Development of vegetable fibre-mortar composites of improved durability, Cement and Concrete Composites, 25:185-196.

[25] [Khelifi et al. 2012] H. Khelifi, A. Perrot, T. Lecompte, G. Ausias, (2012). Design of clay/cement mixtures for extruded building products. Materials and Structures. DOI 10.1617/s11527-012-9949-4.

[26] [Qian et al. 2003] X. Qian, X. Zhou, B. Mu, Z. Li, (2003). Fiber alignment and property direction dependency of FRC extrudate, Cement and Concrete Research, 33(10):1575-1581.

[27] [Perrot et al. 2009a] A. Perrot, D. Rangeard, Y. Mélinge, P. Estellé, C. Lanos (2009). Extrusion criterion for firm cement-based materials, Applied Rheology, 19: 96-98

[28] [Peled & Shah, 2003] A. Peled, S.P. Shah, (2003) Processing effects in cementitious composites: extrusion and casting, Journal of materials in civil engineering 15(2): 192-199.

[29] [Perrot et al. 2009b]. Perrot A, Melinge Y, Estelle P, Lanos C (2009) Vibroextrusion: a new forming process for cement-based materials. Adv Cem Res 21(3):125–133

[30] [De Larrard & Sedran, 2002] F. De Larrard, T. Sedran, (2002). Mixture-proportioning of high-performance concrete, Cement and Concrete Research, 32: 1699-1704.

[31] [Faruk.O et al.,2012] Biocomposites reinforced with natural fibers: 2000–2010, Progress in Polymer Science (2012;37(11): 1552-1596

[32] [Brandt 2008] Brandt A. Fibre reinforced cement-based (FRC) composites after over 40 years of development in building and civil engineering. Compos Struct 2008;86:3–9.

[33] [Azuma et al. 2009] Azuma K, Uchiyama I, Chiba Y, Okumura J. Mesothelioma risk and environmental exposure to asbestos: past and future trends in Japan. Int J Occup Environ Health 2009;15:166–72.

[34] [Ramakrishna et Sundararajan 2005a] Ramakrishna G, Sundararajan T (2005a). Impact strength of a few natural fibre reinforced cement mortar slabs: A comparative study. Cement Concrete Compos., 27(5): 547-553.

[35] [Li and Wang, 2007]. Li Z, Wang L, Wang X. (2007). Cement composites reinforced with surface modified coir fibers. J. Comp. Mat., 41(12): 1445-1457

[36] [Asautjarit et al..2007] Asasutjarit C, Hirunlabh J, Khedari J, Charoenvai S, Zeghmati SB, Shin CC. (2007). Development of coconut coir-based lightweight cement board. Construction Building Materials;21:277–88.

[37] [Toledo Filho et al.,2005] R.D. Toledo Filho, K. Ghavami, M.A. SanjuÃ¡n, G.L. England, (2005). Free, restrained and drying shrinkage of cement mortar composites reinforced with vegetable fibres, Cement and Concrete Composites, 27:537-546.

[38] [Rao, 2007] Rao KMM, Rao KM (2007). Extraction and tensile properties of natural fibres: Vakka, date, and bamboo. Compos. Struct., 77(3): 288-295.

[39] [Li Z et al. 2006] Li Z, Wang X, Wang L. Properties of hemp fibre reinforced concrete composites. Composites Part A 2006;37:497–505.

[40] [Fernandez et al., 2002], Fernandes, E.M., Correlo, V.M., Mano, J.F., Reis, R.L., Novel cork-polymer composites reinforced with short natural coconut fibres: Effect of fibre loading and coupling agent addition, Composites Science and Technology (2013), doi: http://dx.doi.org/10.1016/j.compscitech.2013.01.021

[41] [Reis 2006] Reis J.(2006) Fracture and flexural characterization of natural fibre-reinforced polymer concrete. Construction Building Materials 20:673–678.

[42] [Paramasivan et al. 1984] Paramasivan, P, Nathan GK and Das Gupta NC. Coconut Fiber Reinforced Corrugated Slabs, Int. J. Cement Composites and Lightweight Concrete, 1984; 6(1): 19-27.

[43] [Ramakrishna et Sundararajan 2005a] Ramakrishna G, Sundararajan T (2005a). Impact strength of a few natural fibre reinforced cement mortar slabs: A comparative study. Cement Concrete Compos., 27(5): 547-553.
[44] [Li et al., 2007] Li Z, Wang L, Wang X. (2007). Cement composites reinforced with surface modified coir fibers. J. Comp. Mat., 41(12): 1445-1457
[45] [Heinze T, Fischer K, 2005] Heinze T, Fischer K, editors. Cellulose and cellulose derivatives. John Wiley & Sons Inc; 2005. ISBN: 13: 978-3-52731326-6.
[46] [Summerscales.J et al., 2010] John Summerscales, Nilmini P.J. Dissanayake, Amandeep S. Virk, Wayne Hall,(2010), A review of bast fibres and their composites. Part 1 – Fibres as reinforcements, Composites: Part A 41:1329–1335
[47] [John et al. 2005] John VM, Cincotto MA, Sjotrom C, Agopyan V, Oliveira CTA. Durability of slag mortar reinforced with coconut fibre. Cem Concr Compos 2005;27:565–74.
[48] [Mohanty et al. 2000] Mohanty AK., Misra M, Hinrichsen G Biofibres, Biodegradable polymers and biocomposites: An overview, Macromolecular Materials & Engineering 2000;276/277:1–24
[49] [Faruk.O et al.,2012] Biocomposites reinforced with natural fibers: 2000–2010, Progress in Polymer Science (2012;37(11): 1552-1596
[50] [Hattallia et al. 2002] Hattallia S, Benaboura A, Ham-Pichavant F, Nourmamode A, Castellan A. Adding value to alfa grass (Stipa tenacissima L.) soda lignin as phenolic resins. 1. Lignin characterization. Polymer Degradation and Stability 2002;76:259–64.
[51] [Hoareau et al. 2004] Hoareau W, Trindade WG, Siegmund B, Castellan A, Frollini E. Sugar cane bagasse and curaua lignins oxidized by chlorine dioxide and reacted with furfuryl alcohol: characterization and stability. Polymer Degradation and Stability 2004;86:567–657
[52] [Rowell 2008] Rowell RM. Natural fibres: types and properties. In: Pickering K, editor. Properties and performance of natural-fibre composites. Cambridge, UK: Woodhead Publishing; 2008; 3–66.
[53] [Pacheco et Jalali 2011] Pacheco-Torgal F, Jalali S. Cementitous building materials reinforced with vegetable fibres: a review. Construction and Building Materials 2011; 25(2):575–581.
[54] [Savastano et al. 2003b]. Savastano H, Warden P, Coutts R. Mechanically pulped sisal as reinforcement in cementitious matrices. Cement Concrete Composites 2003;25:311–9.
[55] [Sawsen et al., 2015]. Chafei Sawsen, Khadraoui Fouzia, Boutouil Mohamed, Gomina Moussa, (2015). Effect of flax fibers treatments on the rheological and the mechanical behavior of a cement composite, Construction and Building Materials 79:229–235.
[56] [Savastano et al. 2003a]. Savastano Jr., H.; Warden, P.G.; Coutts, R.S.P. (2003). Potential of Alternative Fibre Cements as Building Materials for Developing Areas. Cement and Concrete Composites, vol. 25, p. 585-592.
[57] [Jústiz-Smith CA et al., 2008]. Nilza G. Jústiz-Smith, G. Junior Virgo, Vernon E. Buchanan, (2008), Potential of Jamaican banana, coconut coir, and bagasse fibres as composite materials, Materials characterization, 59:1273–1278.

[58] [Wang W and Huang, 2009] Wang W, Huang G. (2009). Characterisation and utilization of natural coconut fibres composites. Mater, 30(7):2741–4.
[59] [APCC, 2006].APCC (2006) Coconut Statistical Yearbook. Asia and Pacific Coconut Community, Jakarta, Indonesia.
[60] [APCC, 2008]. APCC (2008) Coconut Statistical Yearbook. Asia and Pacific Coconut Community, Jakarta, Indonesia.
[61] [Jorg Mussig, 2010] Jorg Mussig, (2010). Industrial Applications of Natural Fibres Structure, Properties and Technical Applications Edited by, Edition first published, John Wiley & Sons, Ltd.
[62] [Dam et al., 2002] J.E.G. van Dam, (2002). Coir Processing Technologies, Food and Agriculture Organization of the United Nations and the Common Fund for Commodities.
[63] [Asautjarita et al..2009] Asasutjarita C, Charoenvai S, Hirunlabh J, Khedari J. (2009). Materials and mechanical properties of pretreated coir-based green composites. Composites: Part B, 40:633–637.
[64] [Ayrilmis et al. 2011] Ayrilmis N, Jarusombuti S, Fueangvivat V, Bauchongkol P, White RH., Coir fiber reinforced polypropylene composite panel for automotive interior applications Fibers and Polymers 2011;12: 919–926
[65] [Ali M., 2012] Majid Ali. (2012). Natural fibres as construction materials, Journal of Civil Engineering and Construction Technology, Vol. 3(3), pp. 80-89.
[66] [Satyanarayana. KG et al., 1982].K. G. Satyanarayana, C. K. S. Pillai, K. Sukumaran, (1982). Structure property studies of fibres from various parts of the coconut tree, Journal Of Materials Science 17: 2453-2462
[67] [Khedari et al..2004] Khedari J, Nankongnab N, Hirunlabh J, Teekasap S. New low-cost insulation particle boards from mixture of durian peel and coconut coir. Build Environ 2004;39(1):59–65.
[68] [Le Digabel et al. 2006]. Le Digabel F, Averous L. Effects of lignin content on the properties of lignocellulose-based biocomposites. Carbohydr Polym 2006;66(4):537–45.
[69] [Ramakrishna et Sundararajan 2005b] Ramakrishna G, Sundararajan T (2005b). Studies on the durability of natural fibres and the effect of corroded fibres on the strength of mortar. Cement Concrete Composites, 27(5): 575-582.
[70] [Rowell 2002].
[71] [Abraham E et al., 2013] Abraham E, Deepa B, Pothen LA., Cintil J, Thomas S, John MJ, Anandjiwal R, Narine SS.(2013). Environmental friendly method for the extraction of coir fibre and isolation of nanofibre. Carbohydrate Polymers, 92(15): 1477–1483
[72] [Aziz et al. 1981] Aziz. MA, Paramasivam P, and Lee. SL. Prospects of Natural Fiber Reinforced Concretes in Construction, Int. J. Cement Composites and Lightweight Concrete 1981; 3(2): 123-132.
[73] [Malkapuram et al. 2008] Malkapuram R, Kumar V, Yuvraj SN. Recent development in natural fibre reinforced polypropylene composites. J Reinf Plast Comp 2008;28(10):1169–89
[74] [Ghavami et.al. 1999] Ghavami K, Filho R, Barbosa P. Behaviour of composite soil reinforced with natural fibers. Cement Concrete Compos 1999; 21:39–48.

[75] [Martinie et al. 2010] Martinie L, Rossi P, Roussel N. Rheology of fiber reinforced cementitious materials: classification and prediction, Cement Concrete. Research 2010;40:226–234.

[76] [Sedan et al., 2008]. D. Sedan, C. Pagnoux, A. Smith, T. Chotard, (2008), Mechanical properties of hemp fibre reinforced cement: Influence of the fibre/matrix interaction, Journal of the European Ceramic Society 28:183–192

[77] [Ali M et al. 2013] Ali M, Li X, Chouw N, 2013, Experimental investigations on bond strength between coconut fibre and concrete, Materials & Design, 44: 596–605

[78] [Baruah et Talukdar 2007] Baruah P, Talukdar S. A comparative study of compressive, flexural, tensile and shear strength of concrete with fibres of different origins. Indian Concr J 2007;81(7):17–24.

[79] [Li et al, 2004] Z. Li, X. Zhou, B. Shen. (2004). Fiber-cement extrudates with perlite subjected to high temperatures, Journal of Materials in Civil Engineering, 221-229.

[80] [Filho et al., 2000] Filho RDT, Scrivener K, England GL, Ghavami K. Durability of alkali sensitive sisal and coconut fibres in cement mortar composites. Cement and Concrete Composites 2000;22:127–143.

[81] [Awwad et al., 2012]. Awwad E, Mabsout M, Hamad B, Farran MT, Khatib H. Studies on fibrereinforced concrete using industrial hemp fibres. Constr Build Mater 2012;35:710–7.

[82] [Khedari et al..2002] Khedari J, Suttisonk B, Pratintong N, Hirunlabh J. New lightweight composite construction materials with low thermal conductivity. Cement Composite 2002;23:65–70.

[83] [Asautjarita et al..2007] Asasutjarit C, Hirunlabh J, Khedari J, Charoenvai S, Zeghmati SB, Shin CC. (2007). Development of coconut coir-based lightweight cement board. Construction Building Materials;21:277–88.

[84] [Rodrígueza et al. 2011]. N.J. Rodrígueza,∗, M. Yá˜nez-Limónb, F.A. Gutiérrez-Micelia, O. Gomez-Guzmanc, T.P. Matadamas-Ortizd, Luicita Lagunez-Riverad, J.A. Vazquez Feijood, (2011), Assessment of coconut fibre insulation characteristics and its use to modulate temperatures in concrete slabs with the aid of a finite element methodology, Energy and Buildings 43 ,1264–1272

[85] [Riande E, 2000] Riande E, Diaz-Calleja R, Prolongo M, Masegosa R, Salom C. Polymer Viscoelasticity: stress and strain in practice. Marcel Dekker, Inc.; 2000.

[86] [George et al. 2001]. George J, Sreekala MS, Thomas S. A review of interface modification and characterization of natural fibre reinforced plastic composites. Polymer Engineering Science41(9):1471–85.

[87] [Mu et al. 1999] Mu B, Li Z, Chui SNC, Peng J. Cementitious Composite manufactured by extrusion technique. Cement Concrete Research 1999;29:237–240

[88] [Peled et Shah 1999] Peled A, Shah SP. Processing effects in cementitious composites: extrusion and casting. J Material Civil Engineering 1999;29:237–240.

[89] [Perrot et al. 2009] A. Perrot, D. Rangeard, Y. Mélinge, P. Estellé, C. Lanos (2009). Extrusion criterion for firm cement-based materials, Applied Rheology, 19: 96-98

[90] [Perrot A et al. 2007] Perrot A, Lanos C, Mélinge Y, Estellé P, (2007). Mortar physical properties evolution in extrusion flow, Rheologica Acta;46(8):1065-1073
[91] [Toutou and Roussel, 2006] T. Toutou, N. Roussel, (2006). Multi scale experimental study of concrete rheology: from water scale to gravel scale, Materials and Structures, 39:189-199
[92] [Lecompte 2012] T. Lecompte, A. Perrot, V. Picandet, H. Bellegou, S. Amziane, Cement-based mixes: Shearing properties and pore pressure, Cement and Concrete Research, 42 (2012) 139- 147.
[93] [Perrot et al. 2006 b] A. Perrot, C. Lanos, P. Estellé, Y. (2006b). Melinge, Ram extrusion force for a frictional plastic material: model prediction and application to cement paste, Rheologica Acta, 45: 457-467.
[94] [Perrot et al. 2006 b] A. Perrot, C. Lanos, P. Estellé, Y. (2006b). Melinge, Ram extrusion force for a frictional plastic material: model prediction and application to cement paste, Rheologica Acta, 45: 457-467.
[95] [Toutou 2002] Z. Toutou, (2002). Rhéologie des suspensions concentrées: évaluation des conditions dextrudabilté, Thèse de doctorat, INSA de Rennes.
[96] [Shao and Moras. 2002] Y. Shao, S. Moras, Strength, toughness and durability of extruded cement boards with unbleached kraft pulp, Cement and Concrete Research, Special Publication. 2002; 206:439-452
[97] [Mu et al..2000] B. Mu, Z. Li, J. Peng, Short fiber-reinforced cementitious extruded plates with high percentage of slag and different fibers, Cement and Concrete Research, 30 (2000) 1277-1282.
[98] [Li and Wang, 2001] V.C. LI, Y. Wang, Tensile strain-hardening behavior of ployvinum alcohol and engineered cemdntitious composites, Material Journal, 98 (2001) 483-492.
[99] [Shao et al. 2001] Y. Shao, J. Qiu, S.P. Shah, Microstructure of extruded cement-based fiberboard, Cement, and Concrete Research. 2001; 31: 1153-1161.
[100] [Qian et al. 2003] X. Qian, X. Zhou, B. Mu, Z. Li, (2003). Fiber alignment and property direction dependency of FRC extrudate, Cement and Concrete Research, 33(10):1575-1581.
[101] [Akkaya et al. 2000c] Y. Akkaya-c, J.D. Picka, S.P. Shah, (2000). Spacial disribution of aligned short fiber in cement composites, Journal of Engineering Mechanics, 12:272-279.
[102] [Akkaya et al. 2000c] Y. Akkaya-c, J.D. Picka, S.P. Shah, (2000). Spacial disribution of aligned short fiber in cement composites, Journal of Engineering Mechanics, 12:272-279.
[103] [Akkaya et al. 2000b] Y. Akkaya-b, A. Peled, S.P. Shah, (2000). Parameters related to fiber length and processing in cementitious composite, Materiels and Structures, 33:515-524.
[104] [Peled & Shah, 2003] A. Peled, S.P. Shah, (2003) Processing effects in cementitious composites: extrusion and casting, Journal of materials in civil engineering 15(2): 192-199.
[105] [Habert & Roussel.,2009] G. Habert, N. Roussel, (2009).Study of two concrete mix-design strategies to reach carbon mitigation objectives, Cement and Concrete Composites, 31:397-402.

[106] [Huntzinger et Eatmon. 2009] Huntzinger DN, Eatmon TD. A life-cycle assessment of Portland cement manufacturing: comparing the traditional process with alternative technologies, Journal of Cleaner Production 2009;17:668–67
[107] [Mahaut 2008] F. Mahaut, S. MokÃ©ddem, X. Chateau, N. Roussel, G. Ovarlez, Effect of coarse particle volume fraction on the yield stress and thixotropy of cementitious materials, Cement, and Concrete Research, 38 (2008) 1276-1285.
[108] [Savastano et al. 2000]. Savastano Jr H, Warden G, Coutts P.(2000). Brazilian waste fibers as reinforcement for cement-based composites, Cement Concrete Composites, 22: 379–84.
[109] [Castro, 2012] Castro, D.O., Ruvolo Filho, A., Frollini, E., (2012). Materials prepared from biopolyethylene and curaua fibers: composites from biomass. Polym. Test. 31, 880–888.
[110] [Frollini et al., 2013] Frollini E., N. Bartoluccia, L. Sisti, A. Celli. (2013). Poly(butylene succinate) reinforced with different lignocellulosic fibers. Industrial Crops and Products 45: 160– 169
[111] [Fenge et al., 1984] Fengel, D., Wegener, G., de Gruyter, W., (1984). Wood: Chemistry, Ultrastructure, Reactions. Wiley, Berlin and New York.
[112] [Satyanarayan et al., 2007] Satyanarayana, K.G., Guimaraes, J.L., Wypych, F., (2007). Studies on lignocellulosic fibers of Brazil. Part I: source, production, morphology, properties and applications. Compos. Part A: Appl. Sci. Manuf. 38, 1694–1709.
[113] [Tomczak et al., 2007] Tomczak, F., Demetrio, T.H., Satyanarayana, K.G., (2007). Studies on lignocellulosic fibers of Brazil part II: Morphology and properties of brazilian coconut fibers. Composite. Part A 38, 1710–1721
[114] [Ndazi et al., 2006] Ndazi, B., Tesha, J.V., Bisanda, E.T.N., (2006). Some opportunities and challenges of producing bio-composites fromnon-woodresidues. Journal Material Scince. 41, 6984–6990.
[115] [EN 206-1, 2000] EN 206-1: Concrete—Part 1: Specification, performance, production and conformity,2000.
[116] [Hemsri et al., 2012] Hemsri Sudsiri, Kasia Grieco, Alexandru D.Asandei, Richard S. Parnas. (2012) Wheat gluten composites reinforced with coconut fiber, Composite Part A 43:1160-1168.
[117] [Romildo et al., 2005] Romildo D.T.F, Khosrow G, Miguel A. Sanju, G.L, (2005). Free, restrained and drying shrinkage of cement mortar composites reinforced with vegetable fibres, Cement & Concrete Composites,(27):537–546
[118] Tran LQN et al., 2014
[119] [Defoirdt N et al., 2010]. Nele Defoirdt, Subhankar Biswas, Linde De Vriese, Le Quan Ngoc Tran, Joris Van Acker, Assessment of the tensile properties of coir, bamboo and jute fibre, Composites: Part A 41 (2010) 588–595
[120] [Joffe, 2009].
[121] [Toutou et al. 2005] Toutou Z, Roussel N, Lanos C The squeezing test, A tool to identify firm cement based material's rheological behaviour and evaluate their extrusion ability. Cemet Concrete Research 2005;35:1891–1899
[122] [Kuder & Shah, 2010] K.G. Kuder, S.P. Shah, (2010). Processing of high-performance fiber-reinforced cementbased composites, Construction and Building Materials, 24: 181-186.

[123] [Martinie et Roussel 2011] Martinie L, Roussel N. Simple tools for fiber orientation prediction in industrial practice, Cement and Concrete Research 2011;41:993–1000
[124] [Perrot et al., 2013], A. Perrot, T. Lecompte, P. Estelle, S. Amziane, (2013), Structural build-up of rigid fiber reinforced cement-based materials, Materials and Structures (2013) 46:1561–1568
[125] [Dhonde et al., 2007] H.B. Dhonde, Y.L. Mo, T.T.C. Hsu, J. Vogel, Fresh and Hardened Properties of Self-Consolidating Fiber-Reinforced Concrete, Materials Journal, 104 (2007) 491-500.
[126] [Férec et al., 2015], J. Férec, A. Perrot, G. Ausias, (2015), Toward modeling anisotropic yield stress and consistency induced by fiber in fiber-reinforced viscoplastic fluids, Journal of Non-Newtonian Fluid Mechanics 220:69-76
[127] [Banfill 2006] P.F.G. Banfill, G. Starrs, G. Derruau, W.J. McCarter, T.M. Chrisp, Rheology of low carbon fibre content reinforced cement mortar, Cement, and Concrete Composites, 28(2006) 773-780.
[128] [Akkaya et al. 2000a] Y. Akkaya-a, A. Peled, J.D. Picka, S.P. Shah, (2000). Effect of sand addition on the properties of fiber reinforced composites, Material Journal, 97:393-400.
[129] [Andiç-Çakir et al., 2014], Ozge Andic-Cakir, Mehmet Sarikanat, Hikmet Bahadir Tufekci, Cihan Demirci, Umit Halis Erdog˘an, (2014), Physical and mechanical properties of randomly oriented coir fiber–cementitious composites, Composites: Part B 61: 49–54
[130] [Summerscales et al.,2011], Summerscales J, Hall W, Virk AS. (2011), A fibre diameter distribution factor (FDDF) for natural fibre composites. J Mater Sci;46(17):5876–80.
[131] [Summerscales et al.,2013], John Summerscales, Amandeep Virk, Wayne Hall, (2013), A review of bast fibres and their composites: Part 3 – Modelling, Composites: Part A 44 (2013) 132–139
[132] [Summerscales et al.,2010], Summerscales J, Dissanayake N, Hall W, Virk AS. A review of bast fibres and their composites. Part 2: Composites. Compos A: Appl Sci Manuf 2010;41(10): 1336–44.
[133] [Summerscales et al.,2010], Summerscales J, Dissanayake N, Hall W, Virk AS. A review of bast fibres and their composites. Part 1: Fibres as reinforcements. Compos A: Appl Sci Manuf October 2010;41(10):1329–35.
[134] [Tasse ST and Lubell AS, 2014]. S.T. Tassew, A.S. Lubell, (2014), Mechanical properties of glass fiber reinforced ceramic concrete, Construction and Building Materials 51: 215–224
[135] [Achour et al. 2008] T. Achour, T. Lecompte, M. Ben-Ouezdou, R. Mensi, (2008). Tensile strength and elastic modulus of calcareous concrete: application to Tunisians mixtures, Materials and Structures, 41:1427-1439.
[136] [Akcaya and Tasdemir, 2012] Akcaya B, Tasdemir MA. (2012). Mechanical behaviour and fibre dispersion of hybrid steel fibre reinforced self-compacting concrete, Construction and Building Materials, 28(1):287-293
[137] [ASTM D3822, 2007] ASTM D3822. 2007, Standard test method for tensile properties of single textile fibers;
[138] [Al Rim et al., 1999] K. Al Rim, A. Ledhem, O. Douzane, R.M. Dheilly, M. Queneudec, (1999). Influence of the proportion of wood on the thermal and mechanical performances of clay-cement-wood Composites, Cement and Concrete Composites, 21:269-276.

[139] [ASTM C 1018-85] ASTM C 1018-85: Standard test method for flexural toughness and fiber crack strength of fiber reinforced concrete (using beam with third-point loading), 1990.
[140] [Bahar 2004] R. Bahar, M. Benazzoug, S. Kenai, Performance of compacted cement-stabilised soil, Cement and Concrete Composites, 26 (2004) 811-820.
[141] [Banfill 2006] P.F.G. Banfill, G. Starrs, G. Derruau, W.J. McCarter, T.M. Chrisp, Rheology of low carbon fibre content reinforced cement mortar, Cement, and Concrete Composites, 28(2006) 773-780.
[142] [Barnes and Nguyen, 2001] H.A. Barnes, Q.D. Nguyen, (2001), Rotating Vane rheometry-a review, Journal of Non-Newtonian Fluid Mechanics, 98: 1-14.
[143] [Baruah et Talukdar 2007] Baruah P, Talukdar S. A comparative study of compressive, flexural, tensile and shear strength of concrete with fibres of different origins. Indian Concr J 2007;81(7):17–24.
[144] [Bledzki et al. 2010] Bledzki AK, Mamun AA, Volk J. Barley. Husk and coconut shell reinforced polypropylene composites: the effect of fibre physical, chemical and surface properties. Composites Science and Technology 2010;70:840–6.
[145] [Bourmaud et Baley, 2009] Bourmaud A, Baley C. Rigidity analysis of polypropylene/vegetal fibre composites after recycling Polymer Degradation and Stability 2009;94: 297–305
[146] [Brandt 2008] Brandt A. Fibre reinforced cement-based (FRC) composites after over 40 years of development in building and civil engineering. Compos Struct 2008;86:3–9.
[147] [Burgueno et al., 2004] Burgueno R, Quagliata MJ, Mohanty AK, Mehta G, Drzal LT, Misra M. Load-bearing natural fiber composite cellular beams and panels. Composites Part A: Applied Science and Manufacturing, 2004;.35:645–56.
[148] [Burgueno et al., 2005a], Burgueno R, Quagliata MJ, Mohanty AK, Mehta G, Drzal LT, Misra M. Hierarchical cellular designs for load-bearing biocomposite beams and plates. Materials Science and Engineering A 2005;390: 178–87.
[149] [Burgueno et al., 2005b], Burgueno R, Quagliata MJ, Mohanty AK, Mehta G, Drzal LT, Misra M. Hybrid biofiber-based composites for structural cellular plates. Composites Part A: Applied Science and Manufacturing 2005;36:581–93.
[150] [CDIAC, 2003] Carbon Dioxide Information Analysis Center. (2003). Trends on Line – a Compendium of Data on Global Change. Available in the web at http://cdiac.esd.ornl.gov/ftp/ndp030/global00.ems
[151] [CDIAC, 2010] Carbon Dioxide Information Analysis Center. (2010). Trends on Line – a Global Fossil- Fuel CO2 Emissions. Available in the web at http://cdiac.esd.ornl.gov/trends/emis/tre_glob_2010.html
[152] [Chain 2002] T.W. Chain, D.G. Baird, An evaluation of a squeeze flow rheometer for the rheological characterization of a filled polymer witha yield stress, Rheologica Acta, 41 (2002) 245-256.
[153] [Chateau 2008] X. Chateau, G. Ovarlez, K.L. Trung, Homogenization approach to the behavior of suspensions of non-colloidal particles in yield stress fluids, Journal of Rheology 52 (2008) 489-506.
[154] [Chow et al., 2007], Chow CPL, Xing XS, Li RKY, (2007), Moisture absorption studies of sisal fibre reinforced polypropylene composites. Composites Science and Technology 67(2):306–13.
[155] [Colak 2006] A. Colak, A new model for the estimation of compressive strength of Portland cement concrete, Cement and Concrete Research, 36 (2006) 1409-1413.
[156] [CAPPI, 2008]. Center for Agricultural Policy Prosperity Initiative.,(2008), Small-scale Review of Coconuts, Prosperity Initiative.
[157] [Cucchiara2004] C. Cucchiara, L. La Mendola, M. Papia, Effectiveness of stirrups and steel fibres as shear reinforcement, Cement and Concrete Composites, 26 (2004) 777-786.

[158] [Damtoft et al., 2008] J.S. Damtoft, J. Lukasik, D. Herfort, D. Sorrentino, E.M. Gartner, Sustainable development and climate change initiatives, Cement and Concrete Research, 38 (2008) 115-127.
[159] [De Larrard & Sedran, 2002] F. De Larrard, T. Sedran, (2002). Mixture-proportioning of high-performance concrete, Cement and Concrete Research, 32: 1699-1704.
[160] [Deng et al., 2007] Z. Deng, J. Li, Tension and impact behaviors of new type fiber reinforced concrete, Computers and Concrete, 4 (2007) 19-31.
[161] [Dhonde et al., 2007] H.B. Dhonde, Y.L. Mo, T.T.C. Hsu, J. Vogel, Fresh and Hardened Properties of Self-Consolidating Fiber-Reinforced Concrete, Materials Journal, 104 (2007) 491-500.
[162] [Dhonde et al., 2008b] H.B. Dhonde, Y.L. Mo, T.T.C. Hsu, J. Vogel, Fresh and hardened properties of self-consolidating fiber-reinforced concrete, Material Journal, 104 (2008b) 491-500.
[163] [Ding et al., 2008] Y. Ding, S. Liu, Y. Zhang, A. Thomas, The investigation on the workability of fibre cocktail reinforced self-compacting high performance concrete, Construction and Building Materials, 22 (2008) 1462-1470.
[164] [Domanti et al., 2000] A.T.J. Domanti, J. Bridgwater, Surface Fracture in Axisymmetric Paste Extrusion: An Experimental Study, Chemical Engineering Research and Design, 78 (2000) 68-78.
[165] [Domanti et al., 2002] A.T.J. Domanti, D.J. Horrobin, J. Bridgwater, An investigation of fracture criteria for predicting surface fracture in paste extrusion, International Journal of Mechanical Sciences, 44 (2002) 1381-1410.
[166] [Ezekiela et al. , 2011]Ezekiela Ngesa, Bwire Ndazia, Christian Nyahumwa, Sigbritt Karlsson, (2011), Effect of temperature and durations of heating on coir fibers, Industrial Crops and Products 33 (2011) 638–643.
[167] [EN 206-1, 2000] EN 206-1: Concrete—Part 1: Specification, performance, production and conformity,2000.
[168] [EN 197-1, 2011] EN 197-1: Part 1: Composition, specifications and conformity criteria for common cements, 2011.
[169] [Espert et al., 2004] Espert, A., Vilaplana, F., Karlsson, S., 2004. Comparison of water absorption in natural cellulosic fibres from wood and one-year crops in polypropylene composites and its influence on their mechanical properties. Composites Part A 35, 1267–1276.
[170] [Estellé 2012] P. Estellé, C. Lanos, High torque vane rheometer for concrete: Principle and validation from rheological measurements, Applied Rheology, 22 (2012).
[171] [Estellé 2004] P. Estellé, C. Lanos, Z. Toutou, C. Servais, Squeeze flow of sticking viscoplastic fluids: Direct identification of behaviour parameters by an equivalent flow curve, 16thInternational Congress on Rheology, Seoul, 2004
[172] [Ferrara 2007] L. Ferrara, Y.-D. Park, S.P. Shah, A method for mix-design of fiber-reinforced self-compacting concrete, Cement and Concrete Research, 37 (2007) 957-971.
[173] [Ferraris 2001] C.F. Ferraris, K.H. Obla, R. Hill, The influence of mineral admixtures on the rheology of cement paste and concrete, Cement, and Concrete Research, 31 (2001) 245-255.
[174] [Filho et al., 2000] Filho RDT, Scrivener K, England GL, Ghavami K. Durability of alkali sensitive sisal and coconut fibres in cement mortar composites. Cement and Concrete Composites 2000;22:127–143.
[175] [Flatt 2004] R.J. Flatt, Towards a prediction of superplasticized concrete rheology, materials, and Structures, 37 (2004) 289-300.
[176] [Flatt 2001] R.J. Flatt, Y.F. Houst, A simplified view on chemical effects perturbing the action of superplasticizers, Cement and Concrete Research, 31 (2001) 1169-1176.

[177] [Frollini et al., 2013] Frollini E., N. Bartoluccia, L. Sisti, A. Celli. (2013). Poly(butylene succinate) reinforced with different lignocellulosic fibers. Industrial Crops and Products 45: 160– 169
[178] [George et al. 2001]. George J, Sreekala MS, Thomas S. A review of interface modification and characterization of natural fibre reinforced plastic composites. Polymer Engineering Science41(9):1471–85.
[179] [Geiker 2002] M.R. Geiker, M. Brandl, L.N. Thrane, D.H. Bager, O. Wallevik, The effect of measuring procedure on the apparent rheological properties of self-compacting concrete, Cement and Concrete Research, 32 (2002) 1791-1795.
[180] [Geethamma et al. 2005]. Geethamma VG, Kalaprasad G, Groeninckx G, Thomas S. Dynamic mechanical behavior of short coir fiber reinforced natural rubber composites. Composites Part A: Applied Science and Manufacturing 2005;36:1499–506.
[181] [Gruber 2001] K.A. Gruber, T. Ramlochan, A. Boddy, R.D. Hooton, M.D.A. Thomas, Increasing concrete durability with high-reactivity metakaolin, Cement and Concrete Composites, 23 (2001) 479-484.
[182] [Grünewald 2001] S. Grünewald, J.C. Walraven, Parameter-study on the influence of steel fibers and coarse aggregate content on fresh properties of self-compacting concrete, Cement and Concrete Research, 31 (2001) 1793-1798.
[183] [Haque et al., 2009] Haque M, Hasan M, Islam M, Ali M. Physico-mechanical properties of chemically treated palm and coir fiber reinforced polypropylene composites. Bioresource Technology 2009;100:4903–6.
[184] [Hemsri et al., 2012] Hemsri Sudsiri, Kasia Grieco, Alexandru D.Asandei, Richard S. Parnas. (2012) Wheat gluten composites reinforced with coconut fiber, Composite Part A 43:1160-1168.
[185] [Hill et Khalil. 2000a] Hill CAS, Khalil HPSA. The effect of environmental exposure upon the mechanical properties of coir or oil palm fiber reinforced composites, Journal of Applied Polymer Science 2000;77:1322.
[186] [Hill et Khalil. 2000b] Hill CAS and Khalil HPS. A Effect of fiber treatments on mechanical properties of coir or oil palm fiber reinforced polyester composites, Journal of Applied Polymer Science 2000b;78:1685.
[187] [Ikai et al. 2010] Ikai S, Reicher J, Rodrigues A, Zampieri V. Asbestos-free technology with new high toughness polypropylene (PP) fibers in air-cured Hatschek process. Constr Build Mater 2010;24:171–80.
[188] [Islam et al., 2012], Islam MN, Rahman MR, Haque MM, Huque MM. (2010), Physicomechanical properties of chemically treated coir reinforced polypropylene composites. Composites Part A: Applied Science and Manufacturing 41:192–8.
[189] [Jan et al., 2004]. E.G. Jan, van Dam, J.A. Martien, van den Oever, W. Teunissen, R.P. Edwin, Keijsers, G. Aurora, Peralta,(2004), Process for production of high density/high performance binderless boards from whole coconut husk, part 1: Lignin as intrinsic thermosetting binder resin, Ind. Crops Prod. 19, 207– 216.
[190] [Jayasekara 2010] C. Jayasekara, N. Amarasinghe, *Coir – Coconut Cultivation, Extraction and Processing of Coir* - Industrial Applications of Natural Fibres: Structure, Properties and Technical Applications, (2010)
[191] [Jarny et al, 2005] S. Jarny, N. Roussel, S. Rodts, F. Bertrand, R. Le Roy et P. Coussot,(2005). Rheological behavior of cement pastes from MRI velocimetry, Cement and Concrete Research, 35:1873-1881.
[192] [Kadlecek 02] V. Kadlecek, S. Modry, V.J. Kadlecek, Size effect of test specimens on tensile splitting strength of concrete: general relation, Materials and Structures, 35 (2002) 28-34.
[193] [Kawamura 2011] M. Kawamura, Y. Kasai, Mix design and strength of soil–cement concrete based on the effective water concept, Materials and Structures, 44 (2011) 529-540.

[194] [Kellenberger et Althaus. 2009] Kellenberger D, Althaus HJ. Relevance of simplifications in LCA of building components, Building and Environment 2009;44:818–825.
[195] [Khedari.J.et al.2009] Khedari J, Watsanasathaporn P, Hirunlabh J. Development of fibre-based soil–cement block with low thermal conductivity, Cement Concrete Comp. 2009; 27:111–116.
[196] [Khedari et al..2002] Khedari J, Suttisonk B, Pratintong N, Hirunlabh J. New lightweight composite construction materials with low thermal conductivity. Cement Composite 2002;23:65–70.
[197] [Khokhar 2010] M.I.A. Khokhar, E. Roziere, P. Turcry, F. Grondin, A. Loukili, Mix design of concrete with high content of mineral additions: Optimisation to improve early age strength, Cement and Concrete Composites, 32 (2010) 377-385.
[198] [Kuder 2007] K.G. Kuder, N. Ozyurt, E.B. Mu, S.P. Shah, Rheology of fiber-reinforced cementitious materials, Cement and Concrete Research, 37 (2007) 191-199.
[199] [Kunanopparat T, 2008a] Kunanopparat T, Menut P, Morel M-H, Guilbert S. Plasticized wheat gluten reinforcement with natural fibers: effect of thermal treatment on the fiber/matrix adhesion. Composites Part A 2008;39(12):1787–92.
[200] [Kunanopparat T, 2008b] Kunanopparat T, Menut P, Morel M-H, Guilbert S. Reinforcement of plasticized wheat gluten with natural fibers: from mechanical improvement to deplasticizing effect. Composites Part A 2008;39(5):777–85.
[201] [Kulkarni et al, 1981] A.G. Kulkarni, K.G. Satyanarayana, K. Sukumaran, P. K. Rohatgi. (1981). Mechanical behaviour of coir fibres under tensile load, Journal Of Materials Science 16: 905—914
[202] [Langlet2007] T. Langlet, E. Aamr-Daya, A. Benazzouk, R.M. Dheilly, M. Quéneudec, The suitability of utilising flax by-product materials for lightweight cement composites, Construction and Building Materials, (2007).
[203] [Lucinda, 2012], Lucinda Broad , 2degrees20 July 2012 China now producing as much CO2 per person as Europe https://www.2degreesnetwork.com/groups/energy-carbon-management/resources/china-now-pro
[204] [Li 2002] V.C. LI, Large volume, high-performance applications of fibers in civil engineering, Journal of Applied Polymer Science 83 (2002).
[205] [Li 2003] Z. Li, Z. Ding, Property improvement of Portland cement by incorporating with metakaolin and slag, Cement and Concrete Research, 33 (2003) 579-584.
[206] [Li et al. 2004] Li Z, Wang L, Wang X. Flexural characteristics of coir fibre reinforced cementitious composites. Fibers Polym 2004;7(3):286–94.
[207] [Liu W, 2004]. Liu W, Mohanty AK, Askeland P, Drzal LT, Misra M. Influence of fiber surface treatment on properties of Indian grass fiber reinforced soy protein based biocomposites. Polymer 2004;45(22):7589–96.
[208] [Lumingkewas RH et al., 2013a]. Riana H.Lumingkewas, Heru Purnomo, Gilles Ausias, Dedi Priadi, Thibaut Lecompte, Arnaud Perrot, Tensile Characteristics of Coconut Fibers Reinforced Mortar Composites, Advanced Materials Research Vol. 651 (2013) pp 269-273 doi:10.4028/www.scientific.net/AMR.651.269
[209] [Lumingkewas RH et al., 2013b]. Riana H Lumingkewas, Gilles Ausias, Thibaut Lecompte, Arnaud Perrot, Irwan Katili, Heru Purnomo, Sigit P Hadiwardoyo, Effect of Fibers Content on the Tensile Properties of Coconut Fibers Reinforced Cement Mortar Composites, Advanced Materials Research Vol. 742 (2013) pp 92-97 doi:10.4028/www.scientific.net/AMR.742.92
[210] [Lumingkewas RH et al., 2012a]. Riana.H.Lumingkewas, H.Purnomo, G.Ausias, T.Lecompte, A.Perrot, D.Priadi, I. Katili. (2012a). Properties of Indonesian coconut fibers, Third International Conference on Natural Polymers, Bio-Materials their blends and Gels, Kerala, India.
[211] [Lumingkewas RH et al., 2012b]. Riana.H.Lumingkewas, G.Ausias, T.Lecompte, A. Perrot, I.Katili, H.Purnomo, (2012b). Microstructural properties of natural coconut

fibers-based green mortar composite. Journee de Doctorant de l'Ecole Doctorale SICMA UBS, Lorient, France.

[212] [Mohammadi 2008] Y. Mohammadi, S.P. Singh, S.K. Kaushik, Properties of steel fibrous concrete containing mixed fibres in fresh and hardened state, Construction and Building Materials, 22 (2008) 956-965.

[213] [Mora 2007] Mora E. Life cycle, sustainability and the transcendent quality of building materials. Build Environ 2007;42:1329–34

[214] [Muensri P et al., 2011]. Pakanita Muensri, Thiranan Kunanopparat, Paul Menut, Suwit Siriwattanayotin, (2011), Effect of lignin removal on the properties of coconut coir fiber/wheat gluten biocomposite, Composites: Part A 42:173–179

[215] [Naaman 2003] A.E. Naaman, Engineered steel fiber with optimal reinforcement properties properties for reinforcement of cement composites, Journal of Addvanced Concrete Technology, 1 (2003) 901-916.

[216] [Nehdi 2004] M. Nehdi, M.A. Rahman, Estimating rheological properties of cement pastes using various rheological models for different test geometry, gap and surface friction, Cement and Concrete Research, 34 (2004) 1993-2007.

[217] [Noguera P et al., 2003] Patricia Noguera, Manuel Abad, Rosa Puchades, Angel Maquieira, and Vicente Noguera. (2003). Influence of Particle Size on Physical and Chemical Properties of Coconut Coir Dust as Container Medium, Communications In Soil Science And Plant Analysis Vol. 34, Nos. 3 & 4, Pp. 593–605, 2003

[218] [Olivier et al., 2012] Jos G.J. Olivier, Greet Janssens-Maenhout, Jeroen A.H.W. Peters. (2012) Trends on global CO2 emissions 2012 report, PBL Netherlands Environmental Assessment Agency The Hague/Bilthoven.

[219] [Paiva and P Frollini, 2006] aiva, J.M.F., Frollini, E., (2006). Unmodified and modified surface sisal fibers as reinforcement of phenolic and lignophenolic matrices composites thermal analyses of fibers and composites. Macromol. Mater. Eng. 291, 405–417.

[220] [Park 2005] C.K. Park, M.H. Noh, T.H. Park, Rheological properties of cementitious materials containing mineral admixtures, Cement and Concrete Research, 35 (2005) 842-849.

[221] [Peled et Shah 1999] Peled A, Shah SP. Processing effects in cementitious composites: extrusion and casting. J Material Civil Engineering 1999;29:237–240.

[222] [Pereira 2005] C. Pereira, F.C. Jorge, J.M.F. Ferreira, Adsorption of cations from a cement suspensiononto lignocellulosic substrates and its influence on cement setting, Journal of Wood Chemistry and Technology 25 (2005) 231-244.

[223] [Pereira 2006] C. Pereira, F.C. Jorge, M. Irle, J.M. Ferreira, Characterizing the setting of cement when mixed with cork, blue gum, or maritime pine, grown in Portugal I: temperature profiles and compatibility indices, Journal of Wood Science 52 (2006) 311-317.

[224] [Perrot 2012a] A. Perrot, T. Lecompte, H. Khelifi, C. Brumaud, J. Hot, N. Roussel, Yield stress and bleeding of fresh cement pastes, Cement and Concrete Research, 42 (2012a) 937-944.

[225] [Perrot et al. 2009] A. Perrot, D. Rangeard, Y. Mélinge, P. Estellé, C. Lanos (2009). Extrusion criterion for firm cement-based materials, Applied Rheology, 19: 96-98

[226] [Perrot et al. 2009]. Perrot A, Melinge Y, Estelle P, Lanos C (2009) Vibroextrusion: a new forming process for cement-based materials. Adv Cem Res 21(3):125–133

[227] [Perrot 12b] A. Perrot, D. Rangeard, Y. Mélinge, F. Micaelli, P. Estellé, C. Lanos, Use of ram extruder as a combined rheo-tribometer to study the behaviour of high yield stress fluids at low strain rate, Rheologica Acta, 51 (2012b) 743-754.

[228] [Picandet 11] V. Picandet, D. Rangeard, A. Perrot, T. Lecompte, Permeability measurement of fresh cement paste, Cement and Concrete Research, 41 (2011) 330-338.

[229] [Rabideau 10] B.D. Rabideau, P. Moucheront, F.o. Bertrand, S.p. Rodts, N. Roussel, C.Lanos, P. Coussot, The extrusion of a model yield stress fluid imaged by MRI velocimetry, Journal of Non-Newtonian Fluid Mechanics, 165 (2010) 394-408.

[230] [Rahman MM & Khan MA, 2007]. M. Mizanur Rahman, Mubarak A. Khan, (2007), Surface treatment of coir (Cocos nucifera) fibers and its influence on the fibers' physico-mechanical properties, Composites Science and Technology 67 (2007) 2369–2376

[231] [Ramakrishna et Sundararajan 2005b] Ramakrishna G, Sundararajan T (2005b). Studies on the durability of natural fibres and the effect of corroded fibres on the strength of mortar. Cement Concrete Composites, 27(5): 575-582.

[232] [Ramires, 2010] Ramires, E.C., Megiatto Jr., J.D., Gardrat, C., Castellan, A., Frollini, E., 2010a. Biobased Composites from glyoxal–phenolic resins and sisal fibers. Bioresour. Technol.101, 1998–2006.

[233] [Richard et Cheyrezy. 1995] Richard P and Cheyrezy MH. Composition of reactive powder concrete. Cement Concrete Research 1995;25(7):1501–1511.

[234] [Rosa MF et al., 2009] Rosa MF, Chiou B-S, Medeiros ES, Wood DF, Williams TG, Mattoso LHC, et al. Effect of fiber treatments on tensile and thermal properties of starch/ethylene vinyl alcohol copolymers/coir biocomposites. Bioresour Technol 2009;100(21):5196–202.

[235] [Rout et al., 2000] Rout J, Tripathy SS, Nayak SK, Misra M, Mohanty AK. (2000). Scanning electron microscopy study of chemically modified coir fibers. *Journal Appied Polymer Science*, 79(7):1169–77.

[236] [Roussel 2012] N. Roussel, G. Ovarlez, S. Garrault, C. Brumaud, The origins of thixotropy of fresh cement pastes, Cement and Concrete Research, 42 (2012) 148-157.

[237] [Roussel 07] N. Roussel, The LCPC BOX: a cheap and simple technique for yield stress measurements of SCC, Materials and Structures, 40 (2007) 889–896.

[238] [Roussel 06c] N. Roussel, C. Lanos, Z. Toutou, Identification of Bingham fluid flow parameters using a simple squeeze test, Journal of Non-Newtonian Fluid Mechanics, 135 (2006c) 1-7.

[239] [Rozman HD,2000] Rozman HD, Tan KW, Kumar RN, Abubakar A, Mohd Ishak ZA, Ismail H. The effect of lignin as a compatibilizer on the physical properties of coconut fiber– polypropylene composites. Eur Polym J 2000;36(7):1483–94.

[240] [Sanjuan & Filho, 1998]. M.A. Sanjua´n and R.D. Tolêdo Filho, (1998), Effectiveness Of Crack Control At Early Age On The Corrosion Of Steel Bars In Low Modulus Sisal And Coconut Fibre-Reinforced Mortars, Cement and Concrete Research, Vol. 28, No. 4, pp. 555–565.

[241] [Savastano Jr 2009] H. Savastano Jr, S.F. Santos, M. Radonjic, W.O. Soboyejo, Fracture and fatigue of natural fiber-reinforced cementitious composites, Cement, and Concrete Composites, 31 (2009) 232-243.

[242] [Saw SK et al., 2011]. Sudhir Kumar Saw, Gautam Sarkhel, Arup Choudhury, (2011), Surface modification of coir fibre involving oxidation of lignins followed by reaction with furfuryl alcohol: Characterization and stability, Applied Surface Science 257: 3763–3769.

[243] [Schartzentruber 2000] A. Schartzentruber, C. Catherine, La méthode du Mortier de Béton Equivalent (MBE): Un nouvel outil daide à la formulation de bétons adjuvantés Materials and Structures, 33 (2000) 475-482.

[244] [Shah 2008] V.P. Shah, D.C. Debella, R.J. Ries, Life cycle assessment of residential heating and cooling systems in four regions in the United States, Energy and Buildings, 40 (2008) 503-513.

[245] [Silva et al., 2000] Silva, G.G., De Souza, D.A., Machado, J.C., Hourston, D.J., (2000). Mechanical and thermal characterization of native brazilian coir fiber. J. Appl. Polym. Sci. 76, 1197–1206.

[246] [Silva 2010] F.v.d.A. Silva, R.D.T. Filho, J.o.d.A.M. Filho, E.d.M.R. Fairbairn, Physical and mechanical properties of durable sisal fiber-cement composites, Construction and Building Materials, 24 (2010) 777-785.
[247] [Tolêdo Filho et al., 2003] R.D. Tolêdo Filho, K. Ghavami, G.L. England, K. Scrivener., (2003). Development of vegetable fibre-mortar composites of improved durability, Cement and Concrete Composites, 25:185-196.
[248] [Tolêdo Filho et al., 2000] Tolêdo Filho RD, Scrivener K, England GL, Ghavami K.(2000) Durability of alkali-sensitive sisal and coconut fibres in cement mortar composites. Cement Concrete Compos 22:127–43.
[249] [Thomason, 2013] J.L. Thomason. (2013). On the application of Weibull analysis to experimentally determined single fibre strength distributions, Composites Science and Technology 77 (2013) 74–80
[250] [Tregger et al., 2010] N.A. Tregger, M.E. Pakula, S.P. Shah, (2010). Influence of clays on the rheology of cement pastes, Cement and Concrete Research, 40: 384-391.
[251] [Vilmar et al., 2010] Vilmar Barbosa Jr., Elaine Cristina Ramires, Ilce Aiko Tanaka Razera, Elisabete Frollini, Biobased Composites from tannin–phenolic polymers reinforced with coir fibers, Industrial Crops and Products 32 (2010) 305–312.
[252] [Venkatarama Reddy 11] B.V. Venkatarama Reddy, P.P. Kumar, Cement stabilised rammed earth. Part A: compaction characteristics and physical properties of compacted cement stabilized soils, materials and Structures, 44 (2011) 681-693.
[253] [Voigt 06] T. Voigt, T. Malonn, S.P. Shah, Green and early age compressive strength of extruded cement mortar monitored with compression tests and ultrasonic techniques, Cement and Concrete Research, 36 (2006) 858-867.
[254] [Wie et Gu. 2009].Wie W, Gu H. Characterisation and utilization of natural coconut fibres composites. *Materials and Design* 2009;30:2741–4.
[255] [Wilson 2012] D.I. Wilson, S.L. Rough, Paste engineering: Multi-Phase Materials and multiphase flows, The Canadian Journal of Chemical Engineering, 90 (2012) 277–289.
[256] [Weibull, 1939] W. Weibull, A statistical theory of strength of materials, Royal Swedish Institute for Engineering Research 153 (1939) 1–45.
[257] [Weibull, 1951] W. Weibull, A statistical distribution function of wide applicability, Journal of Applied Mechanics–Transactions of the Asme 18 (1951) 253.
[258] [Yahia and Khayat, 2001] A. Yahia, K.H. Khayat, Analytical models for estimating yield stress of highperformance pseudoplastic grout, Cement, and Concrete Research, 31 (2001) 731-738.
[259] [Yammine et al., 2008] J. Yammine, M. Chaouche, M. Guerinet, M. Moranville, N. Roussel, From ordinary rhelogy concrete to self compacting concrete: A transition between frictional and hydrodynamic interactions, Cement and Concrete Research, 38 (2008) 890-896.
[260] [Yan and Chouw, 2013], Libo Yan, Nawawi Chouw,(2013) Experimental study of flax FRP tube encased coir fibre reinforced concrete composite column, Construction and Building Materials, 40: 1118-1127
[261] [Zaman et al.,2002] A.A. Zaman, R. Tsuchiya, B.M. Moudgil, (2002). Adsorption of a Low-Molecular- Weight Polyacrylic Acid on Silica, Alumina, and Kaolin, Journal of Colloid and Interface Science, 256:73-78.
[262] [Zhang, 2006] Z.B. Zhang, J. Zhang, (2006). Experimental study on relationship between shrinkage strain and environmental humidity of concrete, Journal of Building Materials, 9:720- 723.
[263] [Zhou and Li, 2005] X. Zhou, Z. Li, (2005) Characterizing rheology of fresh short fiber reinforced cementitious composite through capillary extruder, Journal of Materials in Civil Engineering, 28-35.
[264] Shao, Y. F. and Bernd, L. (1996) Effects of Fibre Length and Fibre Orientation Distributions on The Tensile Strength of short-Fibre-Reinforced Polymers. *Composites Science and Technology*. Volume (56): 1179-1190.

[265] Blumentritt, B. F., VU, B. T. and Cooper, S. L., "Mechanical properties of Discontinuous Fiber Reinforced Thermoplastics. II. Random-in-Plane Fiber Orientation", Polymer Engineering and Science, Vol. 15, No. 6, 1975, p.428-436.

[266] USGS (2014) Cement Statistics and Information, and other commodities. US Geological Survey. Internet: http://minerals.usgs.gov/minerals/pubs/commodity/ cement/mcs-2014-cemen.pdf

[267] [Olivier et al., 2013]Olivier, J.G.J., Janssens-Maenhout, G., Muntean, M. and Peters, J.A.H.W. (2013) Trends in global CO2 emissions: 2014 Report. PBL Netherlands Environmental Assessment Agency, The Hague; European Commission, Joint Research Centre (JRC), Institute for Environment and Sustainability (IES). Internet: http://www.pbl.nl/sites/default/files/cms/publicaties/ pbl-2013-trends-in-global-co2-emissions-2013- report-1148.pdf.

.

APPENDICES
International Journal And Proceeding Published

1. **Riana H.Lumingkewas**, Heru Purnomo, Gilles Ausias, Dedi Priadi, Thibaut Lecompte, Arnaud Perrot, Tensile Characteristics of Coconut Fibers Reinforced Mortar Composites, Advanced Materials Research Vol. 651 (2013) pp 269-273 © (2013) Trans Tech Publications, Switzerland, doi:10.4028/www.scientific.net/AMR.651.269

2. **Riana H Lumingkewas**, Gilles Ausias, Thibaut Lecompte, Arnaud Perrot, Irwan Katili, Heru Purnomo, Sigit P Hadiwardoy. Effect of Fibers Content on the Tensile Properties of Coconut Fibers Reinforced Cement Mortar Composites, Advanced Materials Research Vol. 742 (2013) pp 92-97 © (2013) Trans Tech Publications, Switzerland, doi:10.4028/www.scientific.net/AMR.742.92

3. **Riana Lumingkewas**, Gilles Ausias, Thibaut Lecompte, Arnaud Perrot, IrwanKatili, HeruPurnomo, Microstructural Properties Of Natural Coconut Fibers-Based Green Mortar Composites, Proceeding, Journée des doctorants de l'école doctorale Santé Information Communication Matière et Mathématiques (SICMA). Université Européenne de Bretagne. Lorient, France, September, 13th, 2012.

4. **Riana H. Lumingkewas,** Heru Purnomo, Gilles Ausias, Thibaut Lecompte, Arnaud Perrot, Dedi Priadi, IrwanKatili. Properties Of Indonesian Coconut Fibers For Cement-Based Materials Reinforcement, Proceeding, Third international conference on natural polymers, biopolymers,biomaterials, their composites, blends, IPNs, Polyelectrolytes and Gels : macro to nano scales (ICNP-2012). Kottayam, Kerala, India. October 26, 27 &28, 2012.

5. **Riana H.Lumingkewas**, Heru Purnomo, Gilles Ausias, Dedi Priadi, Thibaut Lecompte, Arnaud Perrot, Tensile Characteristics of Coconut Fibers Reinforced Mortar Composites, Proceeding, International Conference Engineering Material (ICEM 2012) Singapore, Singapore, December 30-31, 2012.

6. **Riana H Lumingkewas**, Gilles Ausias, Thibaut Lecompte, Arnaud Perrot, Irwan Katili, Heru Purnomo, Sigit P Hadiwardoyo, Effect of Fibers Content on the Tensile Properties of Coconut Fibers Reinforced Cement Mortar Composites, Proceeding, International Conference on Civil, Materials and Environmental Sciences, Vancouver, Canada, April 17-18, 2013.

7. Heru Purnomo, Dedi Priadi, **Riana H Lumingkewas**, Strength Improvement of Early Age Unfired Soil-Lime Bricks, International journal, Advanced Materials Research Vol. 689 (2013) pp 299-303.

8. Heru Purnomo, Dedi Priadi, Gilles Ausias, Thibaut Lecompte, **H. Riana Lumingkewas,** Arnaud Perrot, Effect of Coconut Fibers Addition to early Age Unfired Soil-Lime Bricks Strength, International Journal, Key Engineering Materials.Vol.594-595 (2014) pp 471-476

ABSTRAK

Name : Riana Herlina LUMINGKEWAS
Study Program: Civil Engineering
Title: Development Of Materials For Construction With Low Environmental Impact Made With Low Content Of Cement And With Natural Fibers.

Tujuan dari disertasi ini adalah memberikan kontribusi pada bidang bahan bangunan untuk industri konstruksi, dengan mengembangkan penelitian tentang bahan bangunan terbarukan yang ramah lingkungan. Bahan dibuat dengan sedikit semen dan menggunakan bahan-bahan lokal seperti tanah liat dan limbah serat alam. Pembentukan melalui proses teknologi ekstrusi. Tujuan jangka panjang untuk menemukan bahan-bahan baru bangunan ramah lingkungan terbuat dari bahan lokal untuk meningkatkan kualitas kinerja, mempercepat pembangunan dan mengurangi biaya konstruksi.

Studi pertama dilakukan pemeriksaan sifat fisik, mekanik, termal dan mikro-struktur serat alam dari sabut kelapa yang banyak tersedia di Indonesia. Kemudian, ditinjau perbandingan serat sabut kelapa yang melalui perawatan dan tidak dirawat. Selanjutnya, mengembangkan model Weibull untuk mendapatkan model kekuatan tarik serat tunggal sabut kelapa. Studi kedua, merancang formula bahan komposit serat sabut kelapa diperkuat semen dan lempung untuk dapat dibentuk melalui proses teknologi ekstruksi spiral. Setelah itu, pengujian rheologi digunakan rheometer untuk memeriksa dampak serat pada perilaku semen yang distabilkan dengan pasta tanah liat. Lalu, dianalisa untuk diperoleh model prediksi tegangan luluh bahan komposit. Studi ketiga, memeriksa kinerja produk ekstrusi secara mekanik, menggunakan metode destruktif dengan sistem pengujian mekanik (MTS) dan menggunakan metode pengujian non destruktif dengan korelasi citra digital (DIC). Lalu, dikembangkan model mekanikal dan mikromekanikal serat komposit. Untuk mendapatkan karakterisasi komponen mikro pengujian dengan Scanning Electron Microscope (SEM). Evolusi kegagalan dan kerusakan bahan diamati retak mikro.

Hasil yang diperoleh dari studi ini, kinerja serat dapat ditingkatkan melalui perawatan serta didapatkan model kekuatan tarik serat tunggal. Selanjutnya, didapatkan formula produk ekstrusi bahan mortar serat komposit yang dapat diekstruksi tanpa cacat pada permukaan. Diperoleh juga model reologi untuk memprediksi tegangan luluh serat komposit. Penambahan serat sabut kelapa meningkatkan kekuatan tekan dan tarik dibandingkan tanpa serat. Evolusi Kegagalan dan kerusakkan bahan serat komposite lebih tangguh dari pada bahan normal. Didapat pula model mekanikal akibat efek serat dan model mikromekanikal tekan dan tarik dari serat komposit. Model yang dihasilkan dibandingkan dengan hasil data eksperimen MTS dan DIC, memberikan hasil adanya kesesuaian. Bahan bangunan yang dihasilkan merupakan bahan ramah lingkungan, daktail dan sangat cocok untuk bangunan di daerah gempa.

.

Kata kunci: *serat alam, rheology, ekstrusi, mekanikal, mikrostruktur, damage, DIC.*

RESUME

Name : Riana Herlina LUMINGKEWAS
Study Program : Civil Engineering
Title : Développement de matériaux pour la construction à faible impact environnemental Fait à faible teneur en ciment et de fibres naturelles

Le but de cette thèse est de contribuer au domaine des matériaux de construction pour l'industrie de la construction, en développant la recherche sur les matériaux de construction renouvelables qui sont respectueux de l'environnement. Matériaux fabriqués avec un peu de ciment et en utilisant des matériaux locaux tels que l'argile et des déchets de fibres naturelles. Formation dans le processus de la technologie d'extrusion. Objectif à long terme de trouver de nouveaux matériaux de construction respectueux de l'environnement à partir de matériaux locaux pour améliorer la qualité de la performance, d'accélérer le développement et de réduire les coûts de construction.

La première étude a examiné la structure de microphysique, mécanique, thermique et de fibres naturelles de noix de coco qui est largement disponible en Indonésie. Puis, en termes de rapport en fibres de coco et que grâce à un traitement non traités. En outre, le développement de modèles de Weibull pour obtenir des modèles d'une seule résistance à la traction de la fibre de coco. La deuxième étude, la formule conçue de coco matériaux composites de ciment renforcés de fibres et de l'argile doit être formée par un processus de technologie de l'extrusion en spirale. Après cela, le test rhéologique rhéomètre utilisé pour examiner l'incidence sur le comportement de la pâte de ciment de fibres stabilisé avec de l'argile. Ensuite, analysé pour obtenir des modèles prédictifs de la limite d'élasticité des matériaux composites. La troisième étude, inspecter les performances du produit d'extrusion mécanique, en utilisant destructrice système de test mécanique (MTS) et en utilisant des méthodes d'essais non destructifs avec corrélation d'image numérique (DIC). Ensuite, développé des modèles micromécaniques des fibres mécaniques et composites. Pour obtenir la caractérisation des tests micro composants par microscope électronique à balayage (MEB). L'évolution de l'échec et de dommages matériels observé microfissures.

Les résultats obtenus de cette étude, la performance de la fibre peut être améliorée par un traitement et ont obtenu un seul des modèles de résistance à la traction de la fibre. En outre, les produits d'extrusion de la formule mortier obtenu des matériaux composites de fibres peuvent être extrudés sans défauts sur la surface. Aussi obtenu modèles rhéologiques pour prédire le rendement des composites de fibre de contrainte. Ajout de la fibre de coco augmente la résistance à la compression et à la traction que sans fibres. L'évolution de défaillance et de la destruction du matériel de fibre composite est plus résistant que le matériau normal. De même dérivé des effets de modèles et des modèles de micromécanique robinet de fibres et traînée de composites de fibres mécaniques. Le modèle résultant est comparé avec les résultats des données expérimentales MTS et DIC, donnant les résultats de leur pertinence. Le matériau de construction qui en résulte est des matériaux écologiques, ductiles et très approprié pour les bâtiments dans les zones sismiques

Mots-clés: *fibres de coco, extrusion, rhéologie, mécaniques, dommage, micromécanique.*

ABSTRACT

Name : Riana Herlina LUMINGKEWAS
Study Program: Civil Engineering
Title: Development of Environmentally Friendly Materials for Construction Made With Low Content of Cement and With Natural Fibers

The purpose of this study is to contribute to the field of building materials on concrete technology for the construction industry, by developing research on renewable building materials that are environmentally friendly. Materials are made with low cement and using local materials such as clay, sand, and waste natural fiber, formation through the process of extrusion technology. The long-term goal is finding new green building materials of natural fiber reinforced cementitious composite to improve the quality of performance, speed up the building and reduce construction costs.

The first study examined the physical, mechanical, thermal and microstructure of natural fibers of coir fiber that is widely available in Indonesia. Then, in terms of coir fiber ratio treated and untreated. The second study, designed the formulation of coir fiber reinforced cementitious composite materials to formed through a process of the screw extrusion technology. After that, rheological testing rheometer used to examine the behavior of fiber cement paste stabilized with clay. Then, it analyzed to derive predictive models of the yield stress of fiber reinforced cementitious composite materials. The third study, inspect mechanical extrusion product performance, using Mechanical Testing System (MTS) and using non-destructive testing methods with Digital Image Correlation (DIC). Then, develop mechanical models and micromechanical models. To get the characterization of micro-components are testing by Scanning Electron Microscope (SEM).

The results obtained from this study, the performance of coir fiber can be improved through treatment. Furthermore, the formula obtained extrusion products coir fiber cementitious composite materials can extrude without defects on the surface. Also, it obtained rheological models to predict the yield stress. The addition of coir fiber increases the compressive strength and tensile strength than the normal concrete. Similarly, it obtained mechanical models of the fiber effects and micromechanical models of compressive strength and tensile strength of the fiber cementitious composite. The resulting model compared with experimental data results of MTS and DIC, are giving significant results.

Keywords: *coir fibers, extrusion, rheology, mechanical, micromechanical.*